Chem

BULLETIN

OF THE

CHEMISTRY HALL LIBRARY

CHEMICAL SOCIETY OF JAPAN

Vol. 32 No. 11 November 1959

OHIO STATE UNIVERSITY
JAN 21 1960
LIBRARY

CONTENTS

General and Physical

T. HAMAMURA: The Kinetic Study of Surface-chemical Reactions at Extremely Low Pressures. IV. The Thermal Reaction between Water Vapor and a Tungsten Filament. Part IV. 1180
H. MATSUO: Crystallinity Studies of Polychlorotrifluoroethylene by the Infrared Method. II. Kinetics of the Crystallization 1184
Y. TSUZUKI, S. MOTOKI and K. MIGITA: Ultraviolet Absorption Spectra of Substituted Phenylureas 1189
S. HIROTA and M. TAKADA: Analysis of Non-Newtonian Flow by Falling-Sphere Method. .1191
S. YAMASHITA: Spectrophotometric Study of the Iodine-Complexes of *cis*- and *trans*-Stilbene.1212
Y. KINOSHITA, I. MATSUBARA and Y. SAITO: The Crystal Structure of Bis(glutaronitrilo)-copper(I) Nitrate. 1216
Y. KINOSHITA, I. MATSUBARA, T. HIGUCHI and Y. SAITO: The Crystal Structure of Bis-(adiponitrilo)copper(I) Nitrate 1221
A. KUBOYAMA: π-Electronic Structure of *o*-Quinones 1226
M. NAKAGAKI: Behavior of Surface Active Molecules at an Interface. II. Statistical Thermodynamics of Monolayers of Rod-Like Molecules 1231
R. FUJISHIRO and K. KIMURA: Dielectric Constants of Binary Mixtures; 1,2-Dichloroethane and Nonpolar Solvents. 1237
A. AIHARA: Estimation of the Energy of Hydrogen Bonds Formed in Crystals. I. Sublimation Pressures of Some Organic Molecular Crystals and the Additivity of Lattice Energy.1242
K. ARAKAWA: Stress Relaxation of Thermo-Reversible Gels. Polyvinyl Alcohol—Congo Red—Water System 1248
H. TADOKORO: Infrared Studies of Polyvinyl Alcohol by Deuteration of its OH Groups. . .1252
T. TANAKA: Heats of Combustion and Formation of Lower Members of Methyl- and Ethyl-methoxypolysiloxanes 1258
K. HIROTA, K. FUEKI, K. SHINDO and Y. NAKAI: Studies on the State of Formic Acid Adsorbed on Silica and Alumina by a Combined Method of Nuclear Magnetic Resonance and Infrared Absorption 1261
T. UKAJI: The Molecular Structure of the Monomer and the Dimer of Acrylic Acid. . . .1266
T. UKAJI: The Molecular Structure of the Monomer and the Dimer of Methacrylic Acid. . .1270
T. UKAJI: The Molecular Structure of Methyl Acrylate and Methyl Methacrylate 1275

(*Continued on inside cover*)

Published by the Chemical Society of Japan

THE CHEMICAL SOCIETY OF JAPAN

(NIPPON KAGAKUKAI)

Founded in 1948

Successor to the former Chemical Society of Japan founded in 1878 and to the Society of Chemical Industry, Japan founded in 1898.

OFFICERS

Munio KOTAKE, *President*, Osaka University, Osaka
Jurô HORIUTI, *Vice-President*, Hokkaido University, Sapporo
Teiji ICHIKAWA, *Vice-President*, Hiroshima University, Hiroshima
Eiichi IWASE, *Vice-President*, Institute of Physical and Chemical Research, Tokyo
Kenichi YAMAMOTO, *Vice-President*, Waseda University, Tokyo

BULLETIN OF THE CHEMICAL SOCIETY OF JAPAN

Editor: Yoshiyuki URUSHIBARA, The University of Tokyo, Tokyo
Assistant Editor: Saburo NAGAKURA, The University of Tokyo, Tokyo
Editorial Board:

Toshio ANDO	Kei MATSUZAKI	Tadao SHIBA
Genjiro HAZATO	Koji NAKANISHI	Osamu SIMAMURA
Kenichi HONDA	Shigeo OKUMURA	Tadashi SUEHIRO
Isao ICHISHIMA	Kazuo SAITO	Kenzi TAMARU
Masaji KUBO	Naoyasu SATA	Takeo WATASE
Hisao KUROYA	Tetsuro SEIYAMA	Tsuneo YOSHINO

(*Continued from outside cover*)

Analytical and Inorganic

S. MISUMI and Y. IDE: Polarographic Studies on the Rare Earths. II. Europium. 1159
S. TOBISAWA: Magnetochemical Investigation on Thermal Decomposition of Silver Oxide. .1173
A. NAKAHARA: The Preparation and Properties of *N*-Salicylideneglycinato-aquo-copper(II), Sodium *N*-Salicylideneglycylglycinato-cuprate(II) and Related Compounds 1195
G. YAMAGUCHI and H. YANAGIDA: Study on the Reductive Spinel—A New Spinel Formula AlN-Al_2O_3 instead of the Previous One Al_3O_4 1264

Organic and Biological

T. OKUDA: Aminosäure-Synthese aus Nitromalonester. IV. Eine neue Synthese von Tryptophan mit Hilfe der Alkylierung des Indols mit 1,1,5,5-Tetracarbalkoxy-1,5-dinitro-3-azapentan 1165
M. YAMAGUCHI: Total Synthesis of Isorenieratene. 1171
R. UEHARA: Polymerization of Methyl Methacrylate Initiated by Phenylazo *p*-Tolyl Sulfone 1199
M. NAKAZAKI and S. ISOE: Synthesis of 3,6-Dimethyl-2,3-dihydro-1*H*-cyclopent[*a*]anthracene. A Possible Dehydrogenation Product of Anthranoid Rearrangement Product of Steroids.1202

Short Communications

K. TANAKA: The Glass Transition Temperatures of Various Kinds of Polyethylenes. . . .1279
K. WATANABE: Studies on Organic Catalytic Reactions. I. 1280
Y. NISHIZAWA: The New Synthetic Method of β-Acetyl-butyrolactone 1282

Polarographic Studies on the Rare Earths. II. Europium

By Seizo MISUMI and Yasushi IDE

(Received March 22, 1959)

Europium has the stable dipositive oxidation state similar to samarium and ytterbium among the rare earth elements. It is also clearly recognized that this intermediate dipositive oxidation state exists during the reduction process of the tripositive europium ions on dropping mercury electrode and this fact has already been studied by some investigators. Laitinen and Taebel[1], and also Noddack and Brukl[2] obtained only a single wave having the half-wave potential of −0.77 V. vs. S. C. E. in acidic solution and −0.67 V. vs. S. C. E. in neutral solution. On the other hand, Holleck[3] obtained double wave for europium. Namely, the half-wave potential of the first wave was −0.78 V. vs. S. C. E. and that of the second wave, −2.14 V. vs. S. C. E. with lithium chloride as the supporting electrolyte, and −0.82 V. and −2.14 V. vs. S. C. E. respectively when with tetramethylammonium iodide. Many other polarographic studies on the europium complexes with various complex-forming agents were reported by Holleck[4], Onstott[5] and Vlček[6].

In this paper, the authors have reported the behaviors of europium ion in the process of reduction on the dropping mercury electrode. The reduction waves were studied in detail under various conditions, especially in order to know the electrode reactions.

Experimental

All current-voltage curves were recorded by the Yanagimoto photographic polarograph PEL-Model 3 Type. All potentials were corrected and referred to saturated calomel electrode (S. C. E). The capillary used had the flowing weight of mercury, m=0.789 mg./sec. at the height of 58.5 cm. (corr.) Hg and the drop time, t=5.20 and 3.10 sec./drop at the applied potentials of −0.8 V. and −2.0 V. vs. S. C. E. respectively (the factor $m^{2/3}\,t^{1/6}$ was from 1.021 to 1.135 $mg^{2/3}\,sec^{-1/2}$ in the same potential range). pH value of the solution was measured with the Hitachi glass electrode pH meter EHM-1 Type for micro amount. All experiments were carried out in a thermostat of 25.0±0.1°C.

Europium solution was prepared by dissolving pure europium oxide (Eu_2O_3: more than 99.9%), purified with ion exchange resin. The concentration of the stock solution was 0.01 M/l. Lithium chloride and lithium perchlorate used as supporting electrolytes were guaranteed grade pure Shikajirushi. The concentrations of these stock solutions were 1 mol./l. The gelatin solution used as maximum suppressor, was prepared freshly in every experiment.

To the sample solution of europium, certain quantities of the supporting electrolyte and of gelatin were added to be the final concentrations, 0.1 M/l. and 0.01%, respectively. And then a micro amount of 0.01 N sulfuric acid was added to prevent the hydrolysis of the aquo europium ion and to adjust pH at the same time. The total volume of the solution was made up to 5 ml. with distilled water. The concentration of europium ion was in the range from 0.5 to 1.6 mM/l. and pH of the solution was varied from 2.75 to 3.90. Dissolved oxygen was removed by passing purified nitrogen gas through the solution for at least 20 min. Then polarograms were recorded.

Results and Discussion

1) The Reduction Wave of Aquo Tripositive Europium Ion. — Typical reduction waves of aquo tripositive europium ion are shown in Fig. 1. At pH less than 3.9, three stepped waves were obtained and the first and the third waves are due to the

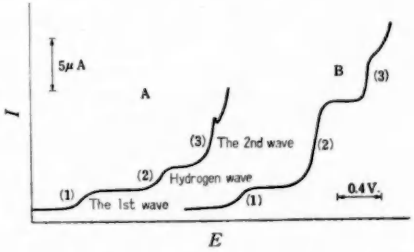

Fig. 1. The reduction waves of europium. Eu^{3+} ion: 1.104 mM in 0.1 M LiCl and 0.01% gelatin medium. pH: A=3.50, B=3.05.

CHEMISTRY HALL LIBRARY

1) H. A. Laitinen and W. A. Taebel, *Ind. Eng. Chem., Anal. Ed.*, **13**, 825 (1941).
2) W. Noddack and A. Brukl, *Angew. Chem.*, **50**, 362 (1937).
3) L. Holleck, *Z. Naturforsch.*, **2b**, 81 (1947).
4) L. Holleck and D. Eckardt, *Z. Elektrochem.*, **59**, 202 (1955).
5) E. I. Onstott, *J. Am. Chem. Soc.*, **74**, 3773 (1952).
6) A. A. Vlček, *Collection Czechoslov. Chem. Communs.*, **20**, 1507 (1955).

TABLE I. DEPENDENCE OF LIMITING CURRENTS OF THE FIRST AND THE SECOND WAVES ON THE HEIGHTS OF THE MERCURY COLUMN

h cm.	h_{corr} cm.		i_l, μA		$i_l/\sqrt{h_{corr}}$	
	$h_{1.corr}$	$h_{2.corr}$	i_{l_1}	i_{l_2}	$i_{l_1}/\sqrt{h_{1.corr}}$	$i_{l_2}/\sqrt{h_{2.corr}}$
40	38.4	38.1	1.60	3.29	0.258	0.535
50	48.4	48.1	1.79	3.62	0.257	0.522
90	58.5	58.1	1.94	3.97	0.254	0.521

(Eu^{3+} ion: 1.023 mM in 0.1 M LiCl and 0.01% gelatin medium, pH: 3.10)

reduction of aquo europium ion and the second wave is the hydrogen wave. In this paper hereafter, the first step is called "the first wave" and the third step "the second wave" of europium.

Owing to the variation in pH and the concentration of europium, the differences between the forms of the reduction waves were indicated. From the polarograms obtained, the following results were derived as the common characteristics, i. e., 1) at pH more than 3.2, independent of concentration, the second wave had a small maximum, but as the pH decreased, this maximum usually disappeared; 2) at pH less than 2.7, a well defined second wave could not be obtained. It is supposed that the large diffusion current of the hydrogen wave probably disturbed the second wave. The effect of various supporting electrolytes on the forms of the reduction waves were rather small and negligible, giving polarograms of similar types.

2) Dependence of Limiting Current of the First and the Second Waves on the Pressure of Dropping Mercury and Influence of Temperature on the Diffusion Current. — The relation between limiting currents and various heights of the mercury column is shown in Table I. The results obviously indicate the fact that the limiting current is proportional to the square root of the height of the mercury column, corrected for the back pressure. Accordingly, the limiting current is diffusion controlled.

The temperature coefficient of the half-wave potential of the first wave at 20~30°C, was 0.4 mV./deg. and that of the limiting current 1.9%/deg., which would be expected in the case of diffusion controlled process for the reduction of tripositive ion.

3) Reversibility. — The reduction waves were analyzed by logarithmic plot. The results are shown in Table II. As the reciprocal slope of the first wave was nearly constant, the average value 0.087 V., in the range of pH 3.50 to 2.75, the first reduction wave was irreversible and due to one electron transfer. The value of $\alpha_1 n_1$, was about 0.68 on the average. The transfer coefficient α was equal to 0.68 if the number of electrons associated with the electrode reaction was assumed to be one (α is a transfer coefficient in the equation of potential on irreversible wave, $E = E_{1/2} - \boldsymbol{RT}/\alpha n\boldsymbol{F} \cdot \ln(i/i_d - i)$. The plots of E against $\log(i/i_d - i)$ indicated an almost straight line. The reciprocal slope of the second wave decreased gradually with decrease of pH and approached a constant value, about 0.030 and the value of $\alpha_2 n_2$ increased reversely up to about 2.0. The plots of E against $\log(i/i_d - i)$ for the second wave indicated the slightly curved line near a pH about 3.50, but with decrease of pH it approached a straight line. Therefore, it is considered that the electrode reaction of the second wave was irreversible or quasi-reversible and according to the decrease of pH, it approached the reversible wave and the reaction was accompanied with two electron transfer. Many investigators have reported the reduction process of aquo tripositive europium ion as reversible except Vlček[6] who suggested that it was irreversible. The results in this experiment were also in good agreement with those of Vlček's report on the confirmation of irreversibility in the reduction process of the aquo europium ion.

TABLE II. THE RECIPROCAL SLOPE OF E VS. $\log(i/i_d - i)$ AND THE VALUE OF αn

pH	Reciprocal slope, V.		$\alpha_1 n_1$	$\alpha_2 n_2$
	1st wave	2nd wave		
3.50	0.087	0.045	0.63	1.3
3.15	0.085	0.045	0.78	1.7
3.05	0.086	0.034	0.69	1.7
2.95	0.087	0.030	0.68	2.0
2.75	0.090	0.030	0.66	2.0
(Eu^{3+} ion: 1.104 mM in 0.1 M LiCl and 0.01% gelatin medium)				
2.90	0.090	0.048	0.65	1.2
2.80	0.082	0.036	0.71	1.6
(Eu^{3+} ion: 1.000 mM in 0.1 M $LiClO_4$ and 0.01% gelatin medium)				

The oxidation wave of aquo dipositive europium ions (Eu^{2+} aq.), which were obtained by the reduction of aquo tripositive europium ions (Eu^{3+} aq.) with John's reductor, was studied. The half-wave potential of the oxidation wave of aquo dipositive europium ions was −0.292 V. vs. S. C. E. at pH 2.55 and this value did not coincide with the half-wave potential of the reduction wave of aquo tripositive europium ions under the same conditions. Thus, from this fact, the electrode reaction of the first wave was shown evidently to be irreversible (the potential difference of anodic and cathodic waves was about 0.440 V.).

4) The Effects of Variation in pH Value on the Reduction Waves.—The results of variation in pH value are shown in Table III, by which the effects on half-wave potentials and diffusion currents were studied. Both the half-wave potential of the first wave $(E_1)_{1/2}$ and the second wave $(E_2)_{1/2}$ shifted all to the more negative side as pH values were decreased. The extent of the shift for the first wave was somewhat greater especially in the range of pH 3.50 to 3.15 than at pH less than 3.15. This fact is probably due to the existence of various hydroxo europium complex ions, produced by hydrolysis of aquo europium complex ions in each step of variation in pH of solution, owing to the basicity of europium. The diffusion currents were independent of pH, almost constant at the same concentration in the range of pH, given in Table III.

5) The Effects of Variation in Concentration on the Reduction Wave.—In the various concentrations of europium ion, i. e., 0.552, 1.104 and 1.656 mM/l. at the constant pH (adjusted to ca. 2.95), the reduction waves were recorded. These effects of variations in concentrations of europium ions on half-wave potentials and diffusion currents were studied. Results are shown in Table IV.

The half-wave potentials of the first and the second wave, $(E_1)_{1/2}$ and $(E_2)_{1/2}$, were constant, independent of concentrations. The diffusion current of the first wave i_d, increased proportionally to concentration and thus the ratio i_{d_1}/c (c : concentration of europium ion) indicated constant value too, i. e., there exists a linear relationship between diffusion current and concentration, which can be used for determination of europium. Especially, since in the potential range where the first wave of tripositive europium ion appears, the reduction waves of all other rare earth ions are absent, it is possible to determine polarographically the contents of europium in a mixture of several kinds of rare earth elements. The diffusion current constant of the first wave, I_{d_1}, was also constant. The diffusion current of the second wave, i_{d_2}, however, increased anomalously with the increase of the concentration and the value of the ratio i_{d_2}/c and the diffusion current constant of the second wave, I_{d_2}, decreased gradually

TABLE III. THE EFFECTS OF VARIATION IN pH ON HALF-WAVE POTENTIAL, DIFFUSION CURRENT AND DIFFUSION CURRENT CONSTANT

pH	Half-wave potential V. vs. S. C. E.		Diffusion current μA		Diffusion current constant	
	$(E_1)_{1/2}$	$(E_2)_{1/2}$	i_{d_1}	i_{d_2}	I_{d_1}	I_{d_2}
3.50	−0.731	−1.948	1.94	3.97	1.55	3.43
3.15	−0.760	−1.958	1.98	3.89	1.58	3.40
3.05	−0.762	−1.967	1.95	3.92	1.56	3.42
2.95	−0.767	−1.971	1.94	3.95	1.55	3.44
2.75	−0.771	−1.975	2.00	3.99	1.60	3.45

(Eu^{3+} ion: 1.104 mM in 0.1 M LiCl and 0.01% gelatin medium)

TABLE IV. THE EFFECTS OF VARIATION IN CONCENTRATION OF EUROPIUM ION ON HALF-WAVE POTENTIALS AND DIFFUSION CURRENTS

Concn. of Eu^{3+} ion mM	Half-wave potential V. vs. S. C. E.		Diffusion current μA		i_d/c		Diffusion current constant	
	$(E_1)_{1/2}$	$(E_2)_{1/2}$	i_{d_1}	i_{d_2}	i_{d_1}/c	i_{d_2}/c	I_{d_1}	I_{d_2}
0.552	−0.761	−1.972	0.99	2.33	1.79	4.22	1.59	4.10
1.104	−0.767	−1.971	1.94	3.99	1.76	3.58	1.55	3.44
1.659	−0.764	−1.976	2.94	5.07	1.78	3.42	1.58	3.55

(pH: 2.95, 0.1 M LiCl, 0.01% gelatin)

with rise of concentration. These anomalies may be attributed to precipitation or adsorption of the basic substances of europium on the electrode surfaces.

6) The Effects by the Kinds of Anions Contained in the Supporting Electrolytes.—The reduction process of aquo europium ion on dropping mercury electrode, often depends on its ionic states. These ionic states show considerably different dependence upon the kinds of electrolytes dissolved in the solution. Therefore, the kinds of supporting electrolytes added, are frequently able to cause remarkably different results to the reduction wave. Particularly, by the anion species of supporting electrolytes and further by the differences of their concentrations, the reversibility of the electrode reaction and the rate-determining step are influenced. From this standpoint, under the same conditions, by varying the anion species of the supporting electrolytes, the effects on the reduction waves were studied. The results are shown in Table V.

At the same concentration, somewhat large effects by the species of anions in the supporting electrolytes on the reduction wave could be seen as shown in Table V. Although pH was not kept strictly the same, the trend of the effects on the reduction wave could be seen. The half-wave potential of the second wave shifted to the more negative side in the order of $I^- < Cl^- < ClO_4^-$. Since the ionic strength was kept always constant, the half-wave potential should have the same value under the same conditions, but owing to the kinds of the anion species the different values were indicated. It is considered that the aquo europium ion forms the halogeno aquo complex ion with halogen ion, which takes part in the electrode reaction. However, as the perchlorate ion is the anion which does not form complex generally with the metal ions, it is also considered that the aquo europium ion exists in the same ionic state (single ion) in the solution with lithium perchlorate as the supporting electrolyte. If the halogeno aquo europium complex ion exists in the solution with the halides as the supporting electrolytes, it is known that this complex ion becomes more reducible than the aquo europium ion (single ion) and as the results of the electrode reaction approaches the reversible one from the irreversible. These facts were recognized from the reciprocal slope and the half-wave potential in this experiment. That is to say, in the presence of the halogen ions, the half-wave potential of the second wave shifted to the positive side and the reversibility increased at the same time. The value of the diffusion current constant of the first wave, I_{d_1}, was nearly constant in the case of the halide ions, but in the case of the perchlorate ions, the diffusion current constant of the second wave, I_{d_2}, was greater, which means the irreversible reaction. Thus, the aquo complex ion (single ion) is more difficult to be reduced than the halogeno aquo complex ion. This fact

TABLE V. EFFECTS OF THE VARIOUS ANION SPECIES OF THE SUPPORTING ELECTROLYTES ON THE REDUCTION WAVES

Supporting electrolytes 0.1 M	Concn. of Eu^{3+} ion mM	pH	Half-wave potential V. vs. S. C. E.		Diffusion current constant		Reciprocal slope, V.	
			$(E_1)_{1/2}$	$(E_2)_{1/2}$	I_{d_1}	I_{d_2}	1st wave	2nd wave
LiI	1.000	3.15	−0.635	−1.965	1.56	3.44	0.089	0.034
LiCl	1.023	3.10	−0.766	−1.967	1.55	3.47	0.082	0.030
$LiClO_4$	1.000	2.90	−0.733	−2.048	1.58	4.18	0.090	0.048

(Concn. of gelatin: 0.01%)

TABLE VI. EFFECTS OF THE CONCENTRATION OF THE SUPPORTING ELECTROLYTES ON THE REDUCTION WAVE

Concn. of LiCl M	Half-wave potential V. vs. S. C. E.		Diffusion current constant, μA		Reciprocal slope, V.	
	$(E_1)_{1/2}$	$(E_2)_{1/2}$	I_{d_1}	I_{d_2}	1st wave	2nd wave
0.1	−0.766	−1.967	1.55	3.47	0.092	0.035
0.2	−0.768	−1.960	1.48	3.42	0.088	0.037
0.5	−0.767	−1.953	1.57	3.51	0.096	0.034
0.7	−0.750	−1.954	1.52	3.30	0.103	0.037

(Concn. of the gelatin: 0.01%, concn. of Eu^{3+} ion: 1.000 mM, pH: 3.10)

was in good agreement with the values of the reciprocal slopes for the second waves.

The results concerning the variation in the concentration of lithium chloride as supporting electrolyte are given in Table VI, in which effects of the chloride ion on the reduction wave are shown.

The half-wave potential of polarography is generally represented by the term containing activity coefficients and diffusion coefficients. If either the activity coefficient or the diffusion coefficient is varied, the half-wave potential will probably indicate a different value. With increasing oncentratoins of total electrolytes the activity coefficient tends to decrease and as the result, the half-wave potential is likely to shift to the more negative potential. Moreover the stability of halogeno aquo europium complex ion is thermodynamically greater than the aquo europium ion and the negative shift will probably take place.

But, on the contrary, as shown in the results of Table VI, there can be seen a tendency for the half-wave potential to shift apparently to the more positive side according to the increase of the concentration of litnium chloride as the supporting electrolyte. At the concentration of 0.5 to 0.7 mmol., the extent of the shift was considerably great. With the increase of chloride ions, the increased chloro aquo complex ions caused the overpotentials to decrease and this large decrease in this overpotential, i. e., the easiness of reduction, outweighed the shift in the equilibrium relation. Thus the half-wave potential seems to shift apparently to the more positive side. In spite of these facts, the value of the reciprocal slope increased with the increase of the concentration of lithium chloride, that is, the irreversibility in the electrode reaction increased too.

7) The Effects of Concentration of Gelatin as Maximum Suppressor, on the Reduction Wave. — By the variation in concentration of gelatin from 0 to 0.05%, the effects on the reduction waves were studied. With the increase of the concentration of gelatin, the half-wave potentials of both the first and the second waves shifted to the more negative side respectively and the values of the reciprocal slopes increased. At pH less than 3.2, without gelatin, a large maximum appeared in the second wave, but with the increase of concentration of gelatin added as maximum suppressor, the maximum decreased gradually and, when 0.01% concentration of gelatin was added, it disappeared completely. At pH more than 3.2, even at concentration of gelatin 0.01%, the maximum could be seen slightly.

8) The Electrode Reduction and the Relation between Reduction Process and Electronic Structure of Aquo Europium Ion.—The reduction of aquo europium ion on dropping mercury electrode, proceeds irreversibly or quasi reversible as described in section 3. In the equation of the current-voltage curve for the irreversible reaction, $E=E_{1/2}-0.0591/\alpha n\cdot\log(i/i_d-i)$ $(0<\alpha<1)$, it was derived that n_1 was equal to 1 and n_2 to 2, by using the results given in Table II. Consequently, the electrode reaction for the first wave was one electron change and that for the second wave two electrons. As the limiting current was diffusion controlled, with Ilkovic's equation, the following relation could be held theoretically between diffusion currents of the first wave and of the second wave, i. e., $i_{d_1} : i_{d_2}=1 : 2$. Therefore, the ratio of the diffusion current constants for the first and the second wave, $I_{d_1} : I_{d_2}= 1 : 2$ is obtained.

The experimental average values of diffusion current constants were as follows, namely, $(I_{d_1})_{av}=1.57$ and $(I_{d_2})_{av}=3.46$. Hence, the ratio $(I_{d_1})_{av} : (I_{d_2})_{av}=1 : 2.2$ was obtained, which was in fairly good agreement with the value of the theoretical ratio. Thus, it is considered that the electrode reaction in the reduction of aquo tripositive europium ion proceeds as follows:

The first wave,

$$Eu^{3+}\,aq.+\ e^- \rightarrow Eu^{2+}aq.$$

The second wave,

$$Eu^{2+}\,aq.+\ 2e^- \rightarrow Eu^0$$

For the rate determining steps of the irreversible electrode reaction, the following main factors are supposedly considered.

a) The overpotential required for dehydration of the coordinated water molecules.

b) The stepwise dissociation of the aquo complex ion.

c) The overpotential required for the changes of the inner electronic configuration (in some $(n-2)f$ orbitals).

d) The stability in the oxidation state of the aquo complex ion.

e) The others.

The results of the irreversible reduction process of the aquo curopium complex ion at the dropping mercury electrode, was

TABLE VII. POLAROGRAPHIC REDUCTION (ELECTRON TRANSFER AND ELECTRONIC CONFIGURATION)

Electrode reaction	Electronic configuration (Oxidized form) 1st wave	(Reduced form) 2nd wave	
Eu^{3+} aq. → Eu^{2+} aq. Irreversible	$f^6s^2p^6d^0d^0d^0[d^2sp^3]+e^-$		
		→ $f^6s^2p^6d^1d^0d^0[d^2sp^3]$	(2 step electron transfer)
		→ $f^7s^2p^6d^0d^0d^0[d^2sp^3]+2e^-$	
Eu^{2+} aq. → Eu^0 Irreversible			→ $f^7s^2p^6d^1d^1d^0[d^2sp^3]$
			→ $f^7s^2p^6s^2$—ligand

(Eu: $4f^75s^25p^66s^2$)

in good agreement with the conclusions of Vlček's rule[7], concerning the mechanism of the electron transfer by polarographic reduction. The dipositive stable oxidation state of europium is already known in solution. As Vlček pointed out, the true two step reduction wave as *f*-transition element was seen for the aquo europium complex ion. Generally, the rate of the electrode reaction is determined always by the slowest of the processes and the change by the electron transfer in reduction processes may always have a tendency to produce the most stable electronic configuration. The aquo europium complex ion is assumed to have simply the coordination number 6 and to be $Eu(H_2O)_6^{3+}$ complex ions. The probable relation between electron transfer and electronic configuration is shown in Table VII.

Summary

The double reduction waves of pure aquo tripositive europium ion, under various conditions, at dropping mercury electrode were studied. The effects of the variations in pH, the concentration of europium ion, the anion species of supporting electrolytes, and the concentration of gelatin as maximum suppressor, etc. were examined. The electrode reaction of the first wave was irreversible and one electron reduction, and that of the second wave was the irreversible or quasi reversible two electrons reduction. The half-wave potentials of the first wave and the second wave at pH 2.95 were as follows.

$(E_1)_{1/2}$: −0.767 V. vs. S. C. E.

$(E_2)_{1/2}$: −1.971 V. vs. S. C. E.

where concentration of Eu^{3+} ion: 1.104 mM in 0.1 M LiCl and 0.01% gelatin medium.

The authors wish to thank the Ministry of Education for the financial support given to this research.

Department of Chemistry
Faculty of Science
Kyushu University
Hakozaki, Fukuoka

7) A. A. Vlček, *Collection Czechoslov. Chem. Communs.*, **20**, 894 (1955).

Aminosäure-Synthese aus Nitromalonester. IV[1]. *Eine neue Synthese von Tryptophan mit Hilfe der Alkylierung des Indols mit 1, 1, 5, 5-Tetracarbalkoxy-1, 5-dinitro-3-azapentan**

Von Tôru OKUDA

(Eingegangen am 25. März 1959)

Seitdem Hopkins und Cole[2] zum erstenmal im Jahre 1901 Tryptophan aus dem Caseinhydrolysat isolierten, sind bisher zahlreiche Untersuchungen über die synthetische Darstellung dieser Aminosäure gemacht worden, von denen nur die praktischen im folgenden angeführt seien: (1) Umsetzung von Gramin mit Acylaminomalonestern[3-5], Nitroessigester[6] bzw. Nitromalonester[7]; (2) Umsetzung von Indol mit Dialkylaminomethyl-acylaminomalonestern[8]; (3) Fischer-Indol-Ringschluß des aus Acetamino-malonester, Acrolein und Phenylhydrazin dargestellten Phenylhydrazons[9]; (4) reduzierende Aminierung von α-Keto-β-(3-indolyl)propionsäure[10]; (5) Decarboxylierung von 2-Carboxytryptophan, welches von γ-Butyrolacton[11], Acetessigester[12] bzw. α-Ketoglutarsäure[13] abgeleitet wird; (6) Addition von Indol zu α-Acetaminoacrylsäure[14]. Es bleibt trotzdem noch die einfachere Synthese dieser Aminosäure in besserer Ausbeute wünschenswert.

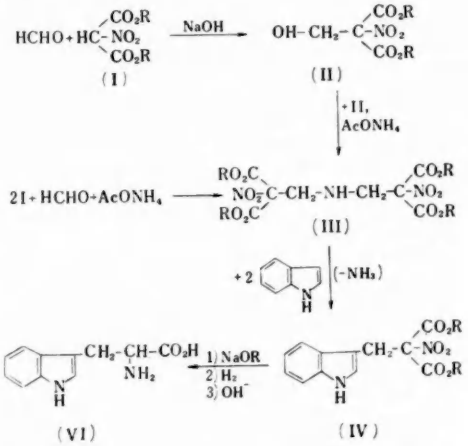

Wie das oben angegebene Reaktionsschema zeigt, stellt die vorliegende Arbeit eine neue Synthese des Tryptophans dar, in der, Nitromalonester als Ausgangsstoff dient. In früheren Mitteilungen haben wir über Synthesen von Ornithin[15], Prolin[16], Glutaminsäure-γ-semialdehydacetal[16] und Glutaminsäure[1] aus dem gleichen Ester (I) berichtet.

Wie schon zitiert, haben Weisblat und Lyttle ein Verfahren zur Darstellung des Tryptophans mittels Nitromalonesters entdeckt[7], indem sie zunächst I in siedendem Toluol mit Gramin zur Reaktion brachten und anschließend das Kondensationsprodukt reduzierten und verseiften.

Unsere Synthese geht auch von dem gleichen Nitromalonester (I) aus, aber, wie aus dem Reaktionsschema ersichtlich ist, unterscheidet sich dieser von dem von ihnen entdeckten Verfahren darin, daß bei uns eine bisher unbekannte, neuartige Alkylierungsreaktion mittels 1,1,5,5-Tetracarbalkoxy-1,5-dinitro-3-azapentans (III), einer Art bis-substituierten Amins, welches durch eine Mannich-Reaktion von Nitromalonester (I), Formaldehyd und Ammoniak gewonnen wird, angewandt ist.

Mannich-Reaktion von Nitromalonester mit Formaldehyd und Ammoniak. — Durch Einwirkung von wässriger Formaldehyd-

* Auszugsweise vorgetragen an der XI. Versammlung der Japanischen Chemischen Gesellschaft, Tokio, 4. April 1958.

1) III. Mitteil.: T. Okuda, Dieses Bulletin, **32**, 931 (1959).

2) F. G. Hopkins und S. W. Cole, *Proc. Roy. Soc. (London)*, **68**, 21 (1901); *J. Physiol.*, **27**, 418 (1902).

3) E. E. Howe, A. T. Zambito, H. R. Snyder und M. Tishler, *J. Am. Chem. Soc.*, **67**, 38 (1945).

4) H. Hellmann, *Z. physiol. Chem.*, **284**, 163 (1949).

5) N. F. Albertson, S. Archer und C. M. Suter, *J. Am. Chem. Soc.*, **67**, 36 (1945).

6) D. A. Lyttle und D. I. Weisblat, ebenda, **69**, 2118 (1947).

7) D. I. Weisblat und D. A. Lyttle, ebenda, **71**, 3079 (1948).

8) A. Butenandt und H. Hellmann, *Z. physiol. Chem.*, **284**, 168 (1949).

9) O. A. Moe und D. T. Warner, *J. Am. Chem. Soc.*, **70**, 2763 (1948).

10) S. Sakurai, *J. Biochem. (Tokio)*, **44**, 47 (1957).

11) H. Plieninger, *Chem. Ber.*, **83**, 268 (1950).

12) B. Hegedüs, *Helv. Chim. Acta*, **29**, 1499 (1946).

13) S. Sakurai und Y. Komachiya, nicht veröffentlicht.

14) H. R. Snyder und J. A. MacDonald, *J. Am. Chem. Soc.*, **77**, 1257 (1955).

15) S. Akabori, Y. Izumi und T. Okuda, *J. Chem. Soc. Japan, Pure Chem. Sec. (Nippon Kagaku Zasshi)*, **77**, 490 (1955).

16) T. Okuda, Dieses Bulletin, **30**, 358 (1957).

Lösung auf Nitromalonester (I) in Gegenwart einer katalytischen Menge Natronlauge als Kondensationsmittel konnten wir Hydroxymethyl-nitromalonsäure-dimethylester (IIa) als weiße Kristalle vom Schmp. 90~91°C und den Äthylester (IIb) als farblose Flüssigkeit vom Sdp $_{1\ mm}$. 120~125°C in guten Ausbeuten erhalten. Versuche, α-Carbalkoxy-α-nitro-β-(3-indolyl)-propionsäureester (III) direkt durch Umsetzung von Indol mit Hydroxymethyl-nitromalonester (II) oder mit dessen acetyliertem Derivate darzustellen, waren alle ohne Erfolg, was uns einen andern Weg einschlagen ließ.

Kürzlich haben Feuer und Mitarb.[17] sowie Fränkel und Mitarb.[18] gefunden, daß 2,2-Dinitroalkanole, die aus *gem*-Dinitroparaffinen und Formaldehyd gewonnen wurden, unter Bildung von Bis-(2,2-dinitroalkyl)-aminen mit Ammoniak in wässriger Essigsäure-Lösung kondensieren.

Auch für die Mannich-Reaktion von Hydroxymethyl-nitromalonester (II) mit Ammoniak galten die Bedingungen, unter denen Bis-(2,2-dinitroalkyl)-amine dargestellt wurden. Wenn man also II mit 2 Mol. Ammoniumacetat in Wasser auf etwa 60°C behandelte, so erhielt man leicht das Kondensationsprodukt. Anderseits gelang es uns, auch durch Versetzung von Nitromalonester (I) mit Ammoniumacetat und Formaldehyd das gleiche Mannich-Kondensationsprodukt direkt zu gewinnen.

Im Jahre 1903 erhielten Ulpiani und Mitarb.[19] durch Umsetzung von Ammoniumsalz des *aci*-Nitromalonsäure-diäthylesters mit einem großen Überschuß von Formaldehyd ein kristallinisches Produkt vom Schmp. 46°C, das vermutlich mit dem von uns dargestellten als identisch anzusehen ist. Sie gaben aber aus falschen experimentellen Daten die Formel VII an. Bald darauf wurde diese

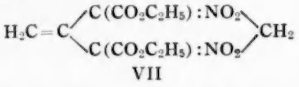

VII

auf Grund der ebullioskopischen und kryoskopischen Molekulargewichtsbestimmung derart korrigiert, daß dieser Verbindung statt der Formel VII wohl eher die Formel IIIb zukommen sollte[20].

Zur endgültigen Entscheidung der

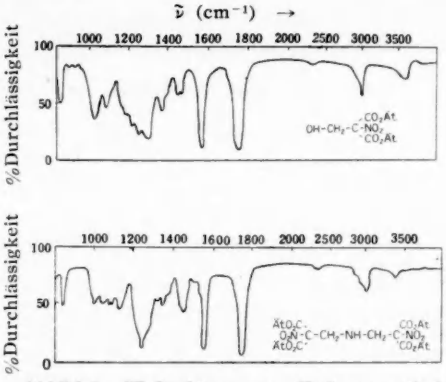

Abbild 1. IR-Spektren von Hydroxymethyl-nitromalonsäure-diäthylester (IIb) und 1,1,5,5-Tetracarbäthoxy-1,5-dinitro-3-azapentan (IIIb). (in Flüssigkeit)

Konstitution des Kondensationsprodukts, dessen Formel trotz der Battagliaschen Berichtigung im Beilsteins Handbuch mit dem Wort "vielleicht" aufgeschrieben ist[21], wiederholten wir die Elementaranalyse und die Molekulargewichtsbestimmung nach der Rast-Methode und konnten dabei bestätigen, daß die von Battaglia angegebene Formel III als ein bis-substituierten Amin richtig ist. Die Struktur von III ergibt sich auch aus folgenden Befunden: das Infrarot-Spektrum (Abbild. 1) zeigt lediglich eine NH-Bande (3300 cm^{-1}), aber keine NH_2-Doppelbande (3300~3500 cm^{-1}).

Alkylierung des Kohlenstoffatoms in β-Stellung von Indol mit 1,1,5,5-Tetracarbalkoxy-1,5-dinitro-3-azapentan. — An der Molekularstruktur von 1,1,5,5-Tetracarbalkoxy-1,5-dinitro-3-azapentan (III) ist anzunehmen, daß durch die Einflüsse der Carbalkoxyl- und Nitro-Gruppen, welche elektronenanziehend wirken können, an beiden Enden des Moleküls die Bindungen zwischen dem mittelständigen Stickstoffatom und den benachbarten Kohlenstoffatomen aufgelockert genug seien, um sich unter gewissen Bedingungen abzuspalten. Es wäre daher denkbar, das Ziel der Substitution eines Wasserstoffatoms von nucleophilen oder potentiell nucleophilen Verbindungen durch Dicarbalkoxy-nitroäthyl-Gruppe $\left(\begin{matrix}RO_2C\\O_2N\\RO_2C\end{matrix}\!\!>\!C\!-\!CH_2-\right)$ mittels dieses bis-substituierten Amins anzustreben.

Es ist wohl bekannt, daß im allgemeinen

17) H. Feuer, G. B. Bachman und W. May, *J. Am. Chem. Soc.*, **76**, 5124 (1954).
18) M. B. Fränkel und K. Klager, ebenda, **79**, 2953 (1957).
19) C. Ulpiani und E. Pannain, *Gazz. chim. ital.*, **33I**, 379 (1903).
20) A. Battaglia, ebenda, **38I**, 356 (1908).
21) "Beilsteins Handbuch der Organischen Chemie", 2. Band, Julius Springer, Berlin (1920), S. 597.

die *C*-Alkylierungsreaktion von *H*-aciden Verbindungen mittels tertiärer Mannich-Basen oder quartärer Ammoniumsalze in Anwesenheit von Natriumhydroxyd als Kondensationsmittel mit Erfolg durchgeführt werden kann[22].

Aber bisher ist unseres Wissens keine Literaturangabe über die *C*-Alkylierungsreaktion mittels sekundärer Aminen bekanntgeworden.

Bei den Vorversuchen beobachteten wir, daß beim Erhitzen von Indol und 1,1,5,5-Tatracarbalkoxy-1,5-dinitro-3-azapentan (III) in Xylol unter Stickstoff-Strom auf 130~140°C die Entwicklung des Ammoniaks eintrat. Diese und andere Versuche, die hintenan beschrieben sind, deuten auf die Umsetzung von 2 Mol. Indol mit 1 Mol. Azapentan (III) unter Abspaltung von 1 Mol. Ammoniak hin (s. das Reaktionsschema).

Beim Arbeiten mit äquivalenten Mengen von beiden Reagenzien war jedoch die Entwicklungsmenge des Ammoniaks ziemlich gering (etwa 50% d. Theorie), was uns zur Bestimmung optimaler Bedingungen auf dieser Reaktionsetappe veranließ. In Tabelle I sind einige typische Versuchsergebnisse mit verschiedenen Molenverhältnissen von Indol zu Azapentan (III) in An- oder Abwensenheit von Kondensationsmitteln zusammengestellt.

TABELLE I. VERGLEICH DER AMMONIAKENTWICKLUNGSMENGE BEI DER ALKYLIERUNG VON INDOL MIT AZAPENTAN UNTER VERSCHIEDENEN BEDINGUNGEN

Mol.-Verhältnis von Indol zu III	Lösungsmittel	Katalysator	Reaktionsdauer Std	Ausb. %
2	Xylol	kein	4	45
2	Xylol	K_2CO_3	2	6
2	kein	kein	5	52
5	Xylol	kein	8	89
4	Xylol	kein	6	84

Die Kurven auf Abbild. 2 zeigen Einflüsse von Molenverhältnissen auf die Ammoniakentwicklung ohne Zusatz von einem Katalysator.

Wie aus Tabelle I und Abbild. 2 ersichtlich ist, sind die befriedigenden Ausbeuten (über 80% d. Theorie) durch Verwendung von über 4 Mol. Indol zu 1 Mol. Azapentan (III) erreicht worden**. Hierbei ist auch berichtenswert, daß die Anwesenheit einer

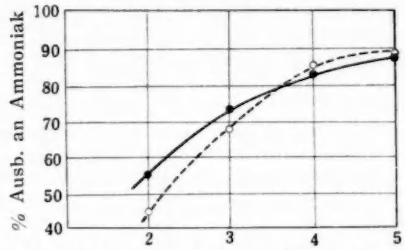

Abbild. 2. Einfluß des Molenverhältnisses von Indol zu Azapentan auf die Ammoniakentwicklung.
—●— IIIa, ---○--- IIIb

katalytischen Menge Alkali die Entwicklung von Ammoniakgas erheblich verhinderte, während die Abwesenheit des Lösungsmittels wenigstens auf die Gasentwicklung keinen wesentlichen Einfluß ausübte.

Das Kondensationsprodukt (IV) war zwar nicht zur Kristallisation zu bringen, sondern immer als zähflüssiges Öl zu erhalten, dessen Konstitution jedoch durch die weiteren Umsetzungen gesichert wurde.

Eine von den günstigen Voraussetzungen für Gelingen dieser Alkylierungsreaktion scheint die bereits erwähnte Auflockerung der *N*-*C*-Bindungen im alkylierenden Amin (III) zu sein. Zugleich dürfte dabei eine sterische Assistenz[23] eine Rolle spielen, die dem großen Umfang der Amino-Gruppe zuzuschreiben ist. Auch die Flüchtigkeit des dabei abgespalteten Ammoniaks begünstigt vermutlich den Verlauf der Reaktion; denn das Kondensationsprodukt (IV) ist gegen Alkali sehr empfindlich.

Auch in Gegenwart von Indol wurde die Eliminierung einer Carbalkoxy-Gruppe von IV mit Natriumalkoholat ebenso[7] bequem

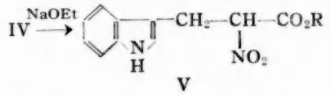

V

durchgeführt. Bei Zugabe von Eiswasser in das Reaktionsgemisch ging das entstandene Natriumsalz des *α-aci*-Nitro-*β*-(3-indolyl)propionsäureester (V) in wässrige

22) Vgl. J. H. Brewster und E. L. Eliel, "Organic Reactions", Vol. VII, John Wiley & Sons, Inc., New York (1953), S. 99.

** Unter ähnlichen Bedingungen wurden Phenol und Azapentan zur Reaktion gebracht, wobei heftige Ammoiakgasentwicklung beobachtet wurde. Die Chromatographie einer Probe des Hydrolysats ergab, daß es Tyrosin und wahrscheinlich 2-Oxyphenylalanin enthält. Die Reaktion wurde präparativ nicht weiter untersucht, zeigt aber an, daß sich auch Phenol in *o*- und *p*-Stellung alkylieren läßt.

23) G. L. Shoemaker und R. W. Keown, *J. Am. Chem. Soc.*, **76**, 6374 (1954).

Schicht über, während das an der Alkylierungsreaktion nicht beteiligte Indol in ätherischer Schicht zurückblieb, womit das Ziel der Trennung von V aus Indol einfach erreicht werden konnte. Der beim Ansäuern der Natriumsalz-Lösung gewonnene, freie Nitroester (V) wurde unter Druck hydriert. Die Gesamtausbeute an Tryptophan, bezogen auf Nitromalonester (I), war 50～60%.

Beschreibung der Versuche

Hydroxymethyl-nitromalonsäure-dimethylester (IIa).—Ein Gemisch von 8.5 g (0.105 Mol, 3.15 g Formaldehyd) 37 proz. Formalin und 17.7 g (0.1 Mol) Nitromalonsäure-dimethylester in 20 ccm Methanol wurde in Gegenwart von 0.5 ccm 1 N NaOH unter gelindem Rühren 2 Stdn auf 40°C erwärmt. Dabei entstand anfangs eine klare gelbliche Lösung, aus der sich im Verlauf der Reaktion weiße Kristalle des Kondensationsproduktes abschied. Nach Erkalten wurde die Reaktionsmischung mit 200 ccm eisgekühltem Wasser verdünnt und über Nacht im Eisschrank stehengelassen. Man saugte die Kristalle ab, wusch mit wenig kaltem Wasser und trocknete. Die Ausbeute an Hydroxymethyl-nitromalonsäure-dimethylester (IIa) vom Schmp. 83～84°C betrug 20.5 g (nahezu quantitativ). Der durch Umkristallisation aus Methanol-Wasser analysenrein erhaltene Ester schmolz bei 92～93°C.

$C_6H_9O_7N_2$(207.1) Ber. C 34.37 H 4.38 N 6.76
Gef. C 34.59 H 4.21 N 6.37

Hydroxymethyl-nitromalonsäure-diäthylester (IIb).—Ein Gemisch von 82.0 g (0.4 Mol) Nitromalonsäure-diäthylester, 34 g (12.6 g Formaldehyd, 0.42 Mol) 37% Formalin in 60 ccm Methanol wurde in Gegenwart von 3 ccm 1 N Natronlauge unter Schüttelung 3 Stdn auf 35～45°C erwärmt. Nach Erkalten und Neutralisierung des als Kondensationsmittel verwendeten Natriumhydroxyds mit Salzsäure wurde die gelblich klare Lösung in 500 ccm Eiswasser gegossen, wobei sich ein Öl ausschied. Die obere wässrige Schicht wurde dreimal mit je 200 ccm Benzol extrahiert. Die Auszüge und das ausgeschiedene Öl wurden vereinigt, die benzolische Lösung wurde mit Wasser gewaschen und auf Natriumsulfat getrocknet. Nach dem Abdampfen des Benzols destillierte man *i. Vak.* den Rückstand. 83 g Hydroxymethyl-nitromalonsäure-diäthylester(IIb) wurden als farblose Flüssigkeit vom Sdp 1 mm. 120～125°C erhalten. Ausbeute 94%.

$C_8H_{13}O_7N$(235.2) Ber. C 40.85 H 5.57 N 5.96
Gef. C 40.77 H 5.57 N 5.93

Banden im IR-Spektrum bei: 3554 cm^{-1} (—OH); 1755 cm^{-1} (>C=O); 1572 cm^{-1} ($—NO^2$) (s. Abbild. 1).

Acetoxymethyl-nitromalonsäure-diäthylester.—11 g (0.047 Mol) Hydroxymethyl-nitromalonsäure-diäthylester (IIb) wurden in Gegenwart einer katalytischen Menge *p*-Toluolsulfonsäure mit 20 ccm Acetanhydrid 30 Min zum Sieden erhitzt. Nach dem Einengen des Reaktionsgemisches erhielt man durch Vakuumdestillation die acetylierte Verbindung als farblose Flüssigkeit. Sdp 1 mm. 123～127°C. Ausbeute 12 g.

$C_{10}H_{15}O_8N$(277.2) Ber. C 43.32 H 5.45 N 5.05
Gef. C 43.32 H 5.74 N 4.84

1, 1, 5, 5-Tetracarbomethoxy-1, 5-dinitro-3-azapentan (IIIa).—25.4 g (0.2 Mol) Nitromalonsäure-dimethylester (Ia) wurden in einer Lösung von 23.1 g (0.3 Mol) Ammoniumacetat in 120 ccm Wasser auf 40°C gelöst, dann zu dieser Lösung wurden 17 g (6.2 g Formaldehyd, 0.21 Mol) 37% Formalin schnell hinzugefügt. Bald darauf begann sie sich unter Wärmeentwicklung zu trüben. Nach 20 minutigem Erwärmen bei 40°C ließ man das Gemisch im Eisschrank 2-3 Tage stehen, wobei die anfangs ölige Substanz kristallinisch erstarrte. Man saugte die Kristalle ab, wusch mit eiskaltem Wasser und trocknete. Für die Weiterverarbeitung wurde das so erhaltene Präparat ohne besondere Reinigung verwendet. Ausbeute 35～38 g (88～96% d. Theorie) Das aus Äther-Petroläther umkristallisierte 1, 1, 5, 5-Tetracarbomethoxy-1, 5-dinitro-3-azapentan (IIIa) zeigte den Schmp. 69～71°C.

$C_{12}H_{17}O_{12}N_3$ (395.3)
Ber. C 36.46 H 4.34 N 10.63
Gef. C 36.29 H 4.29 N 10.39

Molekulargewicht (nach Rast): 416.

1, 1, 5, 5-Tetracarbäthoxy-1, 5-dinitro-3-azapentan (IIIb).—*a) Aus Hydroxymethyl-nitromalonsäure-diäthylester (IIb).*—Aus 23.5 g (0.1 Mol) Hydroxymethyl-nitromalonsäure-diäthylester (IIb) und 15.2 g (0.2 Mol) Ammoniumacetat in 30 ccm Wasser. Ausbeute 21 g (93% d. Theorie). Schmp. 40～42°C.

$C_{16}H_{25}O_{12}N_3$ (451.4)
Ber. C 42.57 H 5.58 N 9.31
Gef. C 42.57 H 5.50 N 9.30

Molekulargewicht (nach Rast): 427; 470.

b) Aus Nitromalonsäure-diäthylester (Ib).—20.5 g (0.1 Mol) Nitromalonsäure-diäthylester(Ib) wurden in eine Lösung von 13.8 g (0.2 Mol) Ammoniumacetat in 130 ccm warmen Wasser unter Schüttelung gelöst

und mit 10 g (3.7 g Formaldehyd, 0.12 Mol) 37% Formalin versetzt. Dabei schied sich ein schweres Öl unter Wärmeentwicklung ab. Man schüttelte die Reaktionsmischung 30 Min auf 60°C und ließ sie über Nacht im Eisschrank stehen. Gelegentliche Schüttelung oder Reibung mit dem Glasstab förderte die Kristallisation. Die cremefarbigen Kristalle wurden kalt abgesaugt, mit eiskaltem 50 proz. Alkohol nachgewaschen und getrocknet. 21.0～22.5 g (94～100% d. Theorie). Schmp. 30～35°C. Nach Umkristallisierung aus Alkohol- oder Essigsäure-Wasser erhielt man weiße, grobe Kristalle vom Schmp. 42～43°C.

$C_{16}H_{25}O_{12}N_3$ (451.4)

Ber. C 42.57 H 5.58 N 9.31
Gef. C 42.76 H 5.63 N 9.32

Banden im IR-Spektrum bei: 3384 cm^{-1} (>NH); 1755 cm^{-1} (>C=O) 1570 cm^{-1} ($-NO_2$).

Beim Mischschmelzen von den aus Ib und den aus IIb dargestellten Kristallen wurde keine Schmelzpunkterniedrigung beobachtet.

Bestimmung optimaler Bedingung für Alkylierung des Indols mit Azapentan (III).—Da sich bei dieser Alkylierungsreaktion Ammoniakgas entwickelte, wurde seine Menge durch Rücktitrierung mit Natronlauge bestimmt, nachdem es sich in Schwefelsäure absorbieren ließ. Der unten geschilderte Versuch stellt ein typisches Beispiel für solche Bedingungsbestimmung dar.

Zu 4 ccm trocknem Xylol, welches sich im langen 20 ccm-Kolben mit einem Stickstoff-Einleitungsröhrchen und einem Kühler befindet, wurden 395 mg (0.001 Mol) 1, 1, 5, 5-Tetracarbomethoxy - 1, 5 - dinitro-3-azapentans (IIIa) und 468 mg (0.004 Mol) Indol gegeben. Der Kolben wurde im Ölbade von 140°C gehalten; während des Erhitzens wurde durch das in die Lösung eintauchendes Glasröhrchen ein lebhafter Strom des mit Calciumchlorid getrockneten Stockstoffs geleitet, welcher zusammen mit dem abgespalteten Ammoniakgas zu verd. Schwefelsäure mit bekannter Normalität geführt wurde. Nach 6 stdg. Kochen wurde die Reaktion abgebrochen. Aliquote der Schwefelsäure-Lösung wurden aufgenommen und mit N/50 NaOH rücktitriert. Molzahl des abgespalteten Ammoniaks während der Reaktion war 0.000840. Also 84% der Theorie. Über andere Versuchsergebnisse siehe Tabelle I und Abbild. 2.

α-Nitro-α-carbomethoxy-β-(3-indolyl)propionsäure-methylester (IVa). — 3.95 g (0.01 Mol) 1, 1, 5, 5 - Tetracarbomethoxy - 1, 5-dinitro-3-azapentan (IIIa) und 5.85 g (0.015 Mol) Indol wurden in 20 ccm trocknem Xylol gelöst und unter kräftigem Rühren 8 Stdn lang auf 130°C erhitzt. Während des Erhitzens wurde ein lebhafter Strom des Stickstoffs geleitet. Schon bei einer Temperatur von 110°C begann eine Entwicklung des Ammoniaks und war auf dem Siedepunkt von Xylol sehr lebhaft. Nach beendeter Reaktion verdampfte man Xylol unter vermindertem Druck und unterwarf dann den Rückstand einer kontinuierlichen Extraktion mit Petroläther. Nach 36 stdg. Extraktion wurde das hinterbliebene rote Öl in 80 ccm Äther aufgenommen und die ätherische Lösung wurde zweimal mit je 10 ccm 10 proz. Salzsäure, zweimal mit 15 ccm Wasser, dann zweimal mit je 10 ccm 5 proz. Na_2CO_3 und schließlich dreimal mit je 15 ccm Wasser ausgeschüttelt und über Natriumsulfat getrocknet. Das nach dem Abdampfen des Äthers erhaltene Öl wurde auf 100°C unter 1 mmHg gehalten. α-Nitro-α-carbomethoxy-β-(3-indolyl)propionsäure-methylester (IVa) war ein viskoses rotes Öl, das weder kristallisierbar noch unzersetzt destillierbar war. Ausb. 4.2 g.

$C_{14}H_{14}O_6N_2$ (306.3) Ber. N 9.15 Gef. N 9.64.

α-Nitro-α-carbäthoxy-β-(3-indolyl)propionsäure-äthylester (IVb).—Nach der oben bei der Darstellung von IVa beschriebenen Methode. Zähflüssiges, rotes Öl.

α-Nitro-β-(3-indolyl)propionsäure-methylester (Va). — Der Ester (Va) kann nach dem bekannten Verfahren[7] aus IVa gewonnen werden. Wir konnten auch aus IIIa den Ester (Va) direkt darstellen, ohne daß man IVa isolierte. Denn bei unsrer Synthese wurde ein Überschuß Indol verwendet und dessen Entfernung nahm zur Gewinnung von IVa, wie bereits erwähnt, viel Zeit in Anspruch.

Eine Lösung von 11 g (0.0279 Mol) rohem 1, 1, 5, 5-Tetracarbomethoxy - 1, 5-dinitro-3-azapentan (IIIa) und 13 g (0.111 Mol) Indol in 50 ccm trocknem Xylol wurden in einen 200 ccm-Vierhalskolben gesetzt, welcher mit Rührer, Einleitungsrohr und Rückflußkühler versehen war. Die Lösung wurde unter kräftigem Rühren und lebhaftem Strom des Stickstoffs 5 Stdn lang auf 130～140°C erhitzt. Nach Erkalten fügte man zum Reaktionsgemisch 50 ccm Äther hinzu, schüttelte die Lösung mit 5 proz. HCl, H_2O, 5 proz. Na_2CO_3 und H_2O aus und trocknete diese über Natriumsulfat. Die getrocknete Lösung wurde unter Feuchtigkeitsausschluß und Rühren mit einer Lösung von 1.3 g Natrium in 40 ccm absol. Alkohol im Verlauf von 40

min. tropfenweise versetzt. Nach 5 stdg. Weiterrühren ließ man die Reaktionsmischung im Eisschrank stehen, sodann ließ man 100 ccm eiskaltes Wasser unter kräftigem Rühren hinzufließen, wodurch das Natriumsalz von *α-aci*-Nitro-β-(3-indolyl)propionsäure-methylester in die wässrige Phase überging, während das an der Reaktion nicht beteiligte Indol im organischen Lösungsmittel blieb. Man trennte die beiden Schichten voneinander, extrahierte die organische Schicht dreimal mit je 30 ccm eiskaltem Wasser, und vereinigte die Auszüge mit der wässrigen Schicht. Die wässrige Lösung wurde dann mit wenig Chloroform ausgezogen, mit 100 ccm Äther überschichtet und mit 10 ccm 10 proz. HCl unter kräftiger Schüttelung angesäuert, wobei der freie Ester (Va) in Äther überging. Nach dreimaliger Extraktion der wässrigen Lösung mit 30 ccm Äther wurde die vereinigte ätherische Lösung zweimal mit je 30 ccm Wasser gewaschen und auf Natriumsulfat getrocknet. Nach der Abdestillation des Äthers erhielt man 11.2 g α-Nitro-β-(3-indolyl)-propionsäuremethylester(Va) als ein zähflüssiges rotes Öl. Ein Teil des rohen Produktes wurde *i. Vak.* destilliert und das Destillat erstarrte kristallinisch beim Stehenlassen. $Sdp_{0.04\ mm}$. 160～165°C. Schmp. 44～46°C.

Das Kaliumsalz zersetzte sich unter Aufschäumung bei 218～219°C.

$C_{12}H_{11}O_4N_2K$(286.3)

Ber. C 50.34 H 3.87 N 9.78
Gef. C 49.27 H 4.11 N 9.69

Banden im IR-Spektrum bei: 3400 cm^{-1} (>NH); 3043 cm^{-1} (=CH—); 1756 cm^{-1} (Ester C=O); 1550 cm^{-1} (—NO_2).

α-Nitro-β-(3-indolyl)propionsäure-äthylester (Vb). — Nach der beim entsprechenden Methylester (Vb) angegebenen oder der früher durch Weisblat[7] angegebenen Vorschrift wurde Vb dargestellt, das aber bei uns keinesfalls zur Kristallisation gebracht werden konnte.

Tryptophan (VI) und Tryptophan-äthylester. — 11.2 g (0.0452 Mol) α-Nitro-β-(3-indolyl)-propionsäure-methylester (Va) in 50 ccm Methanol wurden in Gegenwart von 2 g Nickel-Aluminium-Legierungen dargestellten Raney-Nickel-Katalysatoren in einem Stahlhochdruckautoklav unter mechanischer Schüttelung bei 80～90°C und 100 Atm Wasserstoffdruck hydriert. Innerhalb von 2 Stdn nahm die Lösung die berechnete Menge Wasserstoff auf. Nach Einengen der vom Katalysator abfiltrierten Lösung blieb ein rotes Öl, welches mit 30 ccm 10 proz. Natronlauge auf dem Wasserbade 2 Stdn auf 80～90°C erwärmt wurde. Danach gab man der Lösung 20 ccm Alkohol, entfärbte mit Kohle und stellte sie heiß mit Essigsäure auf pH 5.9 ein. Nach 3 tägigem Stehenlassen im Eisschrank wurden weiße Blättchen von DL-Tryptophan (VI) abgesaugt. Die Ausbeute betrug. 7.1 g (77% d. Theorie). Es zersetzte sich bei 263～265°C.

$C_{11}H_{12}O_2N_2$(204.2)

Ber. C 64.69 H 5.92 N 13.72
Gef. C 64.55 H 6.20 N 13.84

Beim Arbeiten mit α-Nitro-β-(3-indolyl)-propionsäure-äthylester (Vb) erhielt man Tryptophan in fast gleicher Ausbeute.

$C_{11}H_{12}O_2N_2$(204.2)

Ber. C 64.69 H 5.92 N 13.72
Gef. C 64.59 H 6.27 N 13.72

Aus rohem Reduktionsprodukt wurde Tryptophan-äthylester-hydrochlorid isoliert. Schmp. 233°C (Zers.) (aus Alkohol-Äther).

$C_{13}H_{17}O_2N_2Cl$(268.7)

Ber. C 58.10 H 6.38 N 10.43
Gef. C 57.76 H 6.14 N 10.42

Zusammenfassung

1. Es wird eine neue Synthese des Tryptophans aus Nitromalonester in einer Gesamtausbeute von rund 50-Prozent beschrieben.

2. Die Schlüsselreaktion, die auf diese Synthese angewandt ist, ist eine neue Alkylierung des Indols mit 1, 1, 5, 5-Tetracarbäthoxy-1, 5-dinitro-3-azapentan, einem bis-substituierten Amin, welches leicht erhältlich ist durch Mannich-Reaktion von Nitromalonester, Ammoniak und Formaldehyd. Die optimale Bedingung für die Alkylierungsreaktion wurde auch untersucht.

Meinem verehrten Lehrer, Herrn Prof. Dr. S. Akabori bin ich für die Förderung dieser Arbeit zu großem Dank verpflichtet. Ebenso danke ich Herren Dr. S. Sakurai und Dr. Y. Izumi für freundliche Unterstüzung.

Institut für Eiweißforschung
der Universität Osaka
Tosabori, Nishi-ku, Osaka

*Total Synthesis of Isorenieratene**, **

By Masaru YAMAGUCHI

(Received April 3, 1959)

It has been shown by degradative oxidation that isorenieratene, one of the C_{40}-carotenoid hydrocarbons discovered in a sea-sponge, *Reniera japonica*[1], has a remarkable constitution I[2], in which substituted benzene rings are present as terminal groups in place of ionone rings. As the natural carotenoids have so far been aliphatic or alicyclic compounds, the above finding is very significant, and, therefore, it is of importance to make a further confirmation of this exceptional structure of isorenieratene by a synthetic study.

Recently, several routes involving many interesting intermediates have been developed for the total syntheses of carotenoids[3], some of these routes giving considerably good yields. For the present study, however, a method established by Karrer et al.[4] has been applied for the reason of the simplicity of the method, though the overall yields attained by them are not so satisfactory.

The starting material, 2,3,6-trimethylbenzaldehyde (II), was condensed with acetone to give 2,3,6-trimethylbenzalacetone (III), which corresponds to β-ionone, a starting material in the β-carotene syntheses. The ketone (III) was converted into an acetylenic alcohol (IV), which by condensation with 4-octene-2,7-dione gave a C_{40}-diynetetraol (V). Partial hydrogenation of V followed by dehydration gave

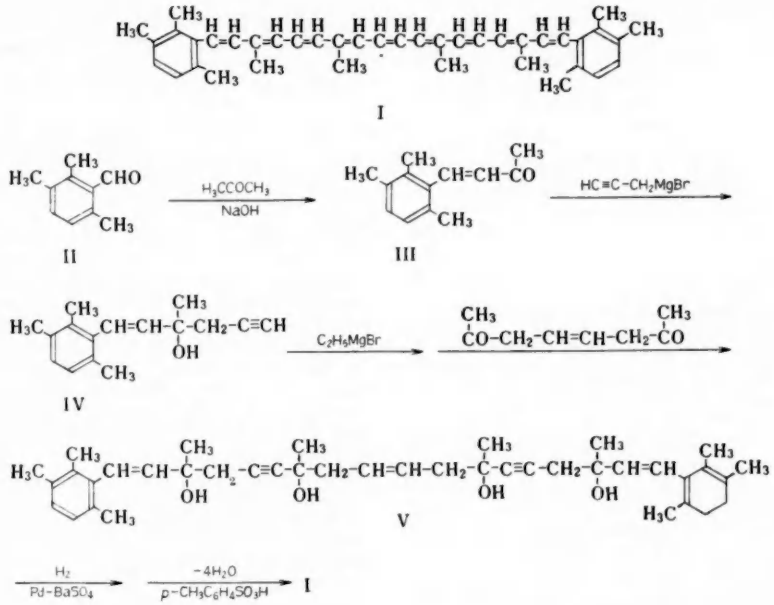

* "Pigments of Marine Animals", VIII. VII of this series: T. Mukai, *Memoirs of the Faculty of Science, Kyushu University, Series C., Chemistry*, **3**, No. 2, 29 (1958).

** Read before the 12th Annual Meeting of the Chemical Society of Japan, Kyoto, April, 1959.

1) T. Tsumaki, M. Yamaguchi and T. Tsumaki, *J. Chem. Soc. Japan, Pure Chem. Sec.* (*Nippon Kagaku Zasshi*), **75**, 297 (1954).

2) M. Yamaguchi, This Bulletin, **31**, 51 (1958).

3) For example: H. H. Inhoffen and H. Siemer, *Fortschr. Chem. org. Naturstoffe*, **9**, 1 (1952); O. Isler et al., *Helv. Chim. Acta*, **39**, 249, 274, 449, 454, 463, 2041 (1956); **40**, 456, 1242, 1256 (1957); B. C. L. Weedon et al., *J. Chem. Soc.*, **1953**, 3286, 3294, 3299.

4) P. Karrer and C. H. Eugster, *Helv. Chim. Acta*, **33**, 1172 (1950); C. H. Eugster, C. Garbers and P. Karrer, ibid., **35**, 1179 (1952).

isorenieratene (I) in a small yield.

Isorenieratene thus obtained forms purplish-red fine needles, m. p. 199~200°C, and is indistinguishable in the appearance from the specimen isolated from the sea-sponge. Furthermore, a mixed melting point, a mixed chromatography, and UV- and IR-spectra established perfect identity. (IR-spectra : Fig. 1).

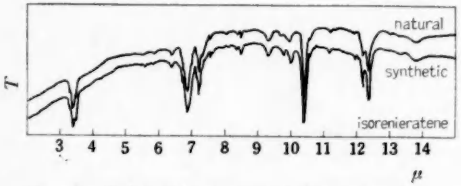

Fig. 1. Infrared spectra of isorenieratene (nujol mull).

Experimental

Solutions were evaporated under diminished pressure unless otherwise mentioned. Anhydrous sodium sulfate was employed for drying solutions.

4-(2, 3, 6-Trimethylphenyl)-3-buten-2-one (III).—A 10% aqueous sodium hydroxide solution (3.1 cc.) was added dropwise during five minutes to a stirred mixture of 2, 3, 6-trimethylbenzaldehyde (14 g.), acetone (16 g.) and water (10 cc.) at room temperature. After stirring for eight hours, the upper layer was separated, combined with the extract (benzene, 20 cc.) of the lower aqueous layer, washed successively with water, 3% hydrochloric acid and water, dried and evaporated. Distillation of the residue gave at first trimethylbenzaldehyde (2.5 g.) and then 4-(2, 3, 6-trimethylphenyl)-3-buten-2-one (11 g.) as an almost colorless oil, b.p. 127~132°C/6 mmHg.

Anal. Found: C, 82.98; H, 8.67. Calcd. for $C_{13}H_{16}O$: C, 82.93; H, 8.57%.

The semicarbazone, colorless needles, m.p. 223~225°C.

Anal. Found: C, 68.37; H, 7.83. Calcd. for $C_{14}H_{19}ON_3$: C, 68.54; H, 7.81%.

The 2, 4-dinitrophenylhydrazone, red plates, m.p. 178~180°C.

Anal. Found: C, 61.79; H, 5.37. Calcd. for $C_{19}H_{20}O_4N_4$: C, 61.95; H, 5.47%.

The residue of the distillation solidified on cooling, which on recrystallization from benzene-ethanol gave 1, 5-bis(2, 3, 6-trimethylphenyl)-1, 4-pentadien-3-one (1.9 g.) in pale yellow plates, m.p. 153~154°C.

Anal. Found: C, 86.67; H, 8.15. Calcd. for $C_{23}H_{26}O$: C, 86.74; H, 8.23%.

The 2, 4-dinitrophenylhydrazone, red needles from acetic acid, m.p. 166~168°C.

Anal. Found: C, 70.11; H, 5.95. Cacld. for $C_{29}H_{30}O_4N_4$: 69.86; H, 6.07%.

1-(2, 3, 6-Trimethylphenyl)-3-methyl-1-hexen-5-yn-3-ol (IV).—A Grignard solution was prepared by dropwise addition (1.5 hr.) of propargyl bromide (5.9 g.) in dry ether (20 cc.) to magnesium (1.5 g.) covered with dry ether (60 cc.) under vigorous stirring. Magnesium was previously activated with a 1% aqueous solution of mercuric chloride. The excess of magnesium was removed by filtration and the solution was added during a half hour to a well stirred solution of the above C_{13}-ketone (III) (9 g.) in dry ether (20 cc.). The mixture was refluxed under stirring for additional one hour, and then decomposed with ice and 5% aqueous sulfuric acid. The ethereal layer was washed with water, dried and evaporated. The oily residue was dissolved in absolute ethanol (80 cc.), a solution of Girard reagent P (6 g.) in acetic acid (6.3 g.) was added, and the mixture was refluxed for an hour. The cooled solution was poured into ice water (300 cc.) containing sodium hydrogen carbonate (7.95 g.) and extracted with ether (3×50 cc.). The ethereal solution was washed, dried and evaporated. Distillation of the residue gave 1-(2, 3, 6-trimethylphenyl)-3-methyl-1-hexen-5-yn-3-ol (4.3 g.) as a faint colored viscus oil, b.p. 110~115°C/0.04 mmHg.

Anal. Found: C, 83.92; H, 9.05. Calcd. for $C_{16}H_{20}O$: C, 84.16; H, 8.83%.

C_{40}-diyntetraol (V).—A solution (ca. 30 cc.) of ethylmagnesium bromide prepared from ethyl bromide (3.9 g.) was filtered, and added dropwise during one and a half hour to a well stirred mixture of above acetylenic alcohol (4.1 g.), cuprous chloride (50 mg.) and dry ether (16 cc.). The mixture was refluxed for an additional one hour. A solution of 4-octene-2, 7-dione[5] (840 mg.) in dry ether (18 cc.) was then added dropwise during thirty minutes under efficient stirring. After refluxing for one hour, the mixture was allowed to stand overnight, and decomposed with 1 N sulfuric acid under ice-cooling. Ether (30 cc.) was added, and the ethereal layer was washed with dilute sulfuric acid, an aqueous solution of sodium hydrogen carbonate and water, dried and evaporated. The yellow brown oily residue was adsorbed on alumina (95 g., standardized according to Brockmann), from a benzene solution (15 cc.). The column was washed successively with benzene (115 cc., the elute gave an oily residue, 1.7 g.), with ether (100 cc., it gave 1.4 g. of residue), and with ether-methanol (10:1, 180 cc.). The last fraction contained C_{40}-tetraol, which is obtained by evaporation of the solvent as a yellowish colored glasslike mass (1.8 g.).

Anal. Found: C, 79.39; H, 8.82. Calcd. for $C_{40}H_{52}O_4$: C, 80.50; H, 8.78%.

It showed somewhat low C-value, and was employed for the next step without further purification.

Isorenieratene (I).—A solution of tetraol (300 mg.) in ethyl acetate (10 cc.) was agitated with active charcoal (100 mg.) for 10 min., filtered, and shaken with palladium barium sulfate catalyst (1%, 20 mg.) in an atmosphere of hydrogen. Occasional additions of the catalyst (ca. 5 mg.) were necessary until 2 mol. (23.6 cc., 13°C/760 mmHg) of hydrogen was adsorbed (2.5

5) P. Karrer and C. H. Eugster, ibid. ,32, 1934 (1949).

hr.). The catalyst was removed and the solution was evaporated to give a glassy residue. A boiling solution of toluene-*p*-sulfonic acid (40 mg., dehydrated by melting in vacuo) in toluene (5 cc.) was added at a time to a boiling solution of the above residue in toluene (10 cc.) and the mixture was boiled for ca. eighty seconds, the water which formed being removed by azeotropic distillation. The greenish brown solution was cooled and poured into a mixture of a saturated aqueous solution of sodium hydrogen carbonate and petroleum ether (50 cc.). On shaking, the color changed into deep red. The petroleum ether solution was then washed once with water and thrice with 90% methanol, dried and evaporated. The reddish brown residue was dissolved in petroleum ether and chromatographed on alumina (2×20 cm.). The chromatogram was developed with petroleum ether, giving (i) a diffuse faint yellow band (least strongly adsorbed); (ii) an orange zone which is somewhat heterogeneous due to the presence of *cis* isomer; (iii) a small orange brown zone; (iv) a small brown zone. The orange zone (ii) was eluted with benzene-methanol (10:1). The residue of the elute was treated with a mixture of petroleum ether and ethanol (1 : 1, 3 cc.), and left to stand overnight in an ice chamber to giv a red precipitate (4.5 mg.). From the mother liquor was obtained an additional quantity of the pigment (1 mg.) after isomerization with iodine. In this way, 900 mg. in total of the tetraol was worked up giving 14 mg. of the pigment. Several recrystallizations from benzene-methanol gave the analytically pure pigment (9 mg.), in purplish red fine needles, m.p. 199~200°C. The mixed melting point with isorenieratene (m.p. 199~200°C) which was isolated from the sea-sponge, *Reniera japonica*, was 199~200°C. A mixed chromatography of the synthetic and the natural pigments showed no separation. They gave the same UV-curves with maxima at 492 ($\varepsilon=12.3\times10^4$) and 463 m$\mu$ ($\varepsilon=10.4\times10^4$) (in benzene, spectrophotoelectric method). IR-curves: Fig. 1.

Anal. Found: C, 90.58; H, 9.24. Calcd. for $C_{40}H_{48}$: C, 90.85; H, 9.15%.

The author wishes to express his thanks to Professor Tokuichi Tsumaki for his exceedingly kind direction throughout this work. The author also thanks Mr. Ryoichi Shimada for UV-spectra measurement and Mr.Michio Shido for micro-analysis. The cost of this work has been partially covered by the Scientific Research Grant of the Ministry of Education.

Department of Chemistry
Faculty of Science
Kyushu University
Hakozaki, Fukuoka

*Magnetochemical Investigation on Thermal Decomposition of Silver Oxide**

By Shōtaro TOBISAWA

(Received April 20, 1959)

The thermal decomposition of silver oxide in oxygen under atmospheric pressure, was investigated by Lewis[1], and was found to follow the equation $dx/dt = kx(1-x)$, where x is the fraction of silver produced. His result was confirmed by Hood and Murphy[2]. On the other hand, it was found by Garner and Reeves[3] that the decomposition in vacuo did not hold Lewis' equation but gave the equation $\sqrt[3]{p} = kt - C$ for the initial part of the decomposition, where p is the pressure of oxygen evolved with the progress of decomposition.

The rates of thermal decompositions of the type A (solid)→B (solid) + C (gas) have been interpreted in terms of the formation and growth of nuclei by many investigators[4]. It may, therefore, be considered that the formation and growth of nuclei depend on the origins of silver oxide and also on the experimental conditions under which the decompositions are carried out.

All the previous work on the kinetics of the decomposition of silver oxide had been carried out by measuring the pressures of the oxygen gas evolved. Although this pressure-method is the most common for kinetic measurements of solid decomposition, it is undesirable for an accurate

* Presented before the 11th Annual Meeting of the Chemical Society of Japan, Tokyo, April, 1958.

1) G. N. Lewis, *Z. physik. Chem.*, **52**, 310 (1905); *J. Am. Chem. Soc.*, **28**, 139 (1906).

2) G. C. Hood and G. W. Murphy, *J. Chem. Educ.*, **26**, 169 (1949).

3) W. E. Garner and L. W. Reeves, *Trans. Faraday Soc.*, **50**, 254 (1954).

4) W. E. Garner, "Chemistry of the Solid State", Butterworths Scientific Publications, London (1955), p. 213.

measurement of the reaction rate on account of the existence of a considerable space from a reaction chamber to a piece of equipment for pressure measurement. The present author has constructed a recording magnetic balance of Hirone's type[5] with many improvements. This balance has been used continuously with very high sensitivity for many hours and as a thermal balance without magnetic field. By using it as the magnetic balance, the kinetics of the decomposition of silver oxide can be investigated by the measurement of change in magnetic susceptibility, due to the oxygen gas evolved. By using it as the thermal balance, the kinetics can be studied by the measurement of the loss in weight with the progress of decomposition. In the case of magnetic balance, silver oxide was charged into a small bulb and was sealed after being evacuated. The pressure of oxygen in contact with the undecomposed silver oxide became higher as the reaction proceeded. However, in the case of thermal balance, the sample was packed in an open bulb and the decomposition was carried out under costant reduced pressure.

The purpose of the present work is to show the results of kinetic measurements obtained under the above two experimental conditions, together with the measurements of the magnetic susceptibility of silver oxide and of metallic silver produced by the complete decomposition of silver oxide.

Experimental

Materials.—In the present work, four samples were used. Samples A and B were guaranteed reagents of the Kanto Chemical Co. Ltd., and of Kahlbaum, respectively. Silver carbonate contained in the above samples could easily be converted into silver oxide by heating under vacuum according to the equation, $Ag_2CO_3 = Ag_2O + CO_2$. Samples C and D were obtained by heating the samples A and B at 250°C for an hour under the vacuum of 10^{-5} mmHg, respectively. This treatment was carried out before each measurement.

Apparatus.—The magnetic balance was operated by the Faraday method, because this method is convenient to measure the change in magnetic susceptibility of the reaction system at high temperatures. As indicated in Fig. 1a, a small bulb of fused quartz was suspended in the position giving the maximum value of $H \cdot \partial H/\partial x$, which was determined from Fig. 2. Here H is the field strength and $\partial H/\partial x$ is its gradient along

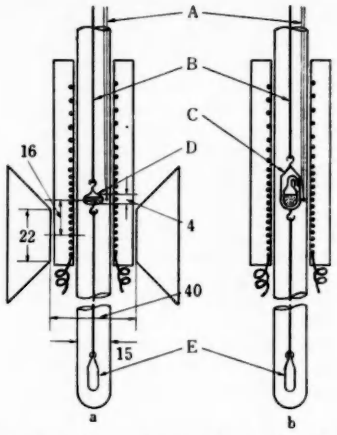

Fig. 1. Positions of sample bulbs in the magnetic balance a and the thermal balance b, showing in mm. unit.
A: $Pt-Pt \cdot Rh$ (13%) thermocouple (0.3 mm. in diameter)
B: Fused quartz rod (1.2 mm. in diameter)
C: Fused quartz basket
D: Fused quartz bulb (ca. 0.10 cc. in volume)
E: Weight of copper

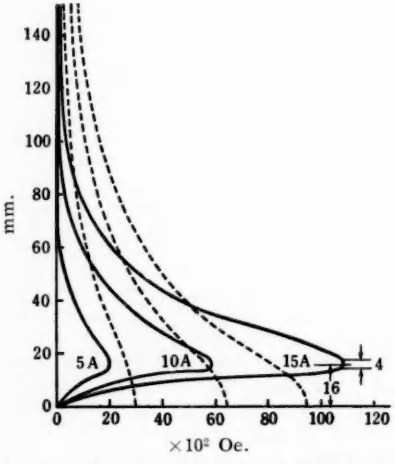

Fig. 2. Diagram of H (---) and $H \cdot \partial H/\partial x$ (—). The origin is the middle point between two centers of pole pieces.

the vertical line passing through the center of the gap between the pole pieces. The bulb 4 mm. high could be held within the error of about one per cent of the maximum value of $H \cdot \partial H/\partial x$.

The recorder used here could plot three values, the magnetic forces acting on a bulb containing a sample, the temperatures of a sample, and the currents supplied to an electromagnet, on a chart at regular intervals of 15 sec., respectively. The

5) T. Hirone, S. Maeda and N. Tuya, *Rev. Sci. Instr.*, **25**, 516 (1954); *Sci. Rep. Res. Inst. Tohoku Univ.*, **A6**, 67 (1954).

magnetic force could be indicated by the current which was proportional to the force, and was calibrated by the magnetic susceptibility of the empty bulb of fused quartz in each measurement. The susceptibility of the fused quartz was -0.46×10^{-6} units per gram[6], and it scarcely depended on temperature at all. The full scale of the recording chart was 10 milliamp. The apparatus was modulated to make it possible to indicate changes of 0.1 milliamp. corresponding to -0.58×10^{-6} e. m. u. in magnetic susceptibility, on a recording chart. The temperature scale of the recorder was calibrated by using the freezing points of four Kahlbaum reagents: tin, zinc, antimonium and silver. Each measurement was carried out in the constant magnetic field of 8250 Oersteds.

When the balance was used as a thermal balance, the recorder could give the losses in weight and the corresponding temperatures of the sample. One millimeter on the recording chart corresponded to 0.015 mg. A sample was packed in the bulb shown in Fig. 1b and was thermally decomposed under the constant pressure of 50 mmHg.

Results

Decomposition Temperature.—The decomposition temperature of silver oxide was determined by the above two methods by raising the temperature at constant rate, 200°C per hour. The results obtained by means of the thermal balance, are shown in Figs. 3 (for the samples A and B) and 4 (for the samples C and D). The first losses in weight for the samples A and B occur at 148°C and the second ones at 372°C. The first losses in weight for the

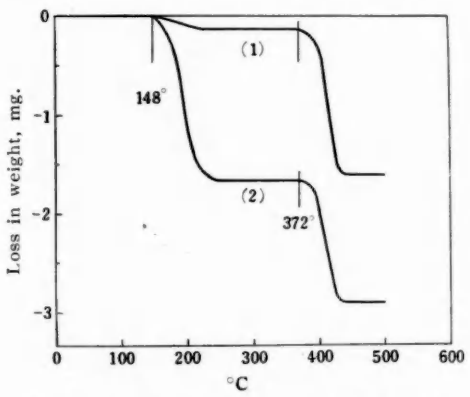

Fig. 3. Loss in weight-temperature curves. (1) Sample A (wt. 20.0 mg.); (2) Sample B (wt. 20.0 mg.).

6) S. S. Bhatnagar and K. N. Mathur, "Physical Principles and Applications of Magnetochemistry", Macmillan & Co., Ltd., London (1935), p. 354.

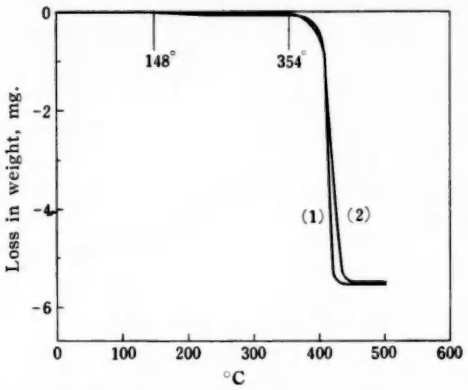

Fig. 4. Loss in weight-temperature curves. (1) Sample C (wt. 80.0 mg.); (2) Sample D (wt. 80.0 mg.).

samples C and D are negligibly small and the second ones occur at 354°C.

The curves of magnetic susceptibility against temperature for the reaction system are given in Fig. 5. The sample used in each measurement was about 50 mg. and was sealed in a bulb after being evacuated for several hours under a vacuum of 10^{-5} mmHg. The curves for the samples A and B deflect obviously toward the paramagnetic sides owing to the paramagnetism of oxygen gas evolved at the decomposition at 372°C. The curve of the sample C shown in a broken line in Fig. 5, indicates that the silver oxide decomposes at 354°C. All the samples treated with heating under evacuation, decomposed at the same temperature. It is apparent from the magnetic measurements that the first losses at 148°C are not due to oxygen gas.

Moisture had no responsibility for the loss in weight at 148°C, because each sample was freed from moisture by evacuation. A preliminary qualitative analysis of carbon dioxide with barium hydroxide solution, showed that the silver oxide was partly converted into silver carbonate. The first loss in weight at 148°C in Fig. 3 is, therefore, due to the thermal decomposition of silver carbonate contained in the sample. The negligibly small amount of loss in weight in Fig. 4 can be ascribed to the decomposition of silver carbonate which had been formed by combining the silver oxide with carbon dioxide in air, within two hours or so before the beginning of the measurement. From the above experimental results, it

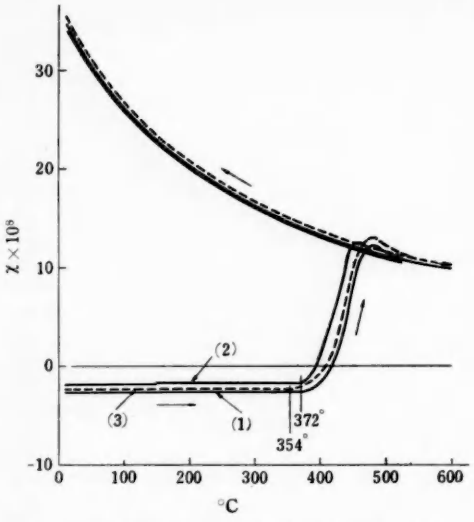

Fig. 5. Magnetic susceptibility-temperature curves.
(1) Sample A (wt. 50.0 mg.); (2) Sample B (wt. 50.0 mg.); (3) Sample C (wt. 49.3 mg.).

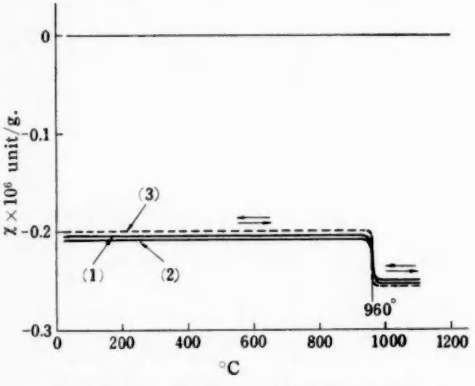

Fig. 6. Magnetic susceptibility-temperature curves.
(1) Metallic silver obtained from sample A;
(2) Metallic silver obtained from sample B;
(3) Kahlbaum silver metal.

is found that the decomposition temperature of silver oxide is apparently affected by silver carbonate contained in the oxide.

Magnetic Susceptibilities of Metallic Silver and Silver Oxide.—In order to know whether paramagnetic or ferromagnetic impurity was present in the samples A and B, the magnetic susceptibilities of metallic silver obtained by the complete decomposition, were measured. In addition, the susceptibility of Kahlbaum silver was measured. The curves obtained are shown in Fig. 6. The magnetic susceptibilities of metallic silver produced by the decomposition of the samples A and B were -0.21×10^{-6} units per gram and that of Kahlbaum silver was -0.20×10^{-6} units per gram at room temperature. The curves in Fig. 6 show that the magnetic susceptibility of metallic silver is independent of temperature below 1100°C, except for a slight increase at the melting point. These facts indicate that no magnetic impurities are involved in either sample, and that the metallic silver is normally diamagnetic and takes no supercooling. The curve obtained by Honda[7] shows that the magnetic susceptibility of metallic silver increases with increasing temperature. On the other hand, Selwood[8] mentioned that the magnetic susceptibility of metallic silver was almost independent of temperature.

The magnetic susceptibility of silver oxide from which carbon dioxide was removed, was -0.48×10^{-6} units per gram at room temperature. It was less than the value of -0.58×10^{-6} units per gram[9], reported previously.

Kinetic Measurements.—(1) Photo. 1 is an example of the chart obtained by means of the thermal balance, showing the losses in weight and the corresponding temperatures. In each measurement a required constant temperature could be obtained within a few minutes. Curves of the loss in weight (x) against time (t) at 380, 390, 400 and 410°C for 80 mg. of the sample D are shown in Fig. 7. It was ascertained that the rate of decomposition held neither

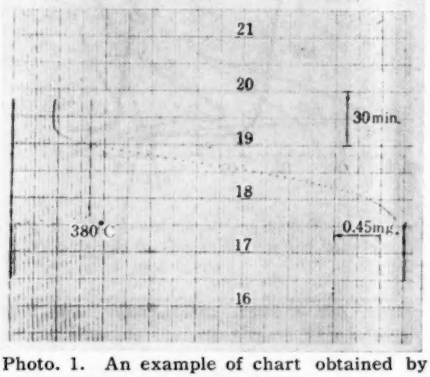

Photo. 1. An example of chart obtained by means of the thermal balance.

7) K. Honda, *Ann. Physik*, **32**, 1027 (1910).
8) P. W. Selwood, "Magnetochemistry", 2nd Ed., Interscience Publishers, New York (1956), p. 362.
9) See reference 8, p. 214.

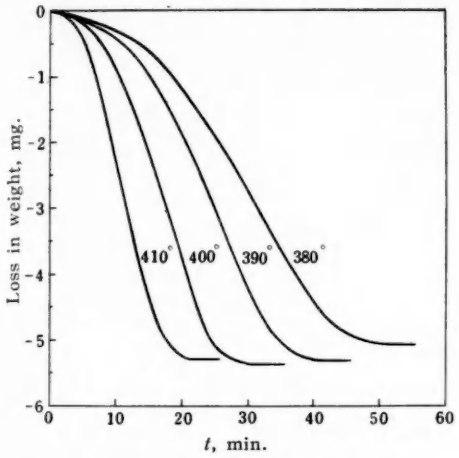

Fig. 7. Loss in weight-time curves for sample D.

Lewis' equation nor that of Prout-Tompkins[10]. The validity of the equation, $\sqrt[3]{x} = kt - C$, presented by Garner et al. for the initial part of the decomposition, was examined by plotting $\sqrt[3]{x}$ against t in Fig. 8. The values of k were obtained from the figure. The activation energy of 29.4 kcal. per mole was estimated from the slope of line which was obtained by plotting $\log k$ against $1/T$. The activation energies reported for this decomposition are as follows: 31.8[1] 35~36[11], 10.5[12] and 45.6~46.2 kcal. per mole[2].

(2) Examining in detail the plots in Fig. 8, it is seen that these plots show the curves with several inflection points. The plots of dx/dt against t are shown in Fig. 9. The time was calculated by setting zero time at the point where the half of

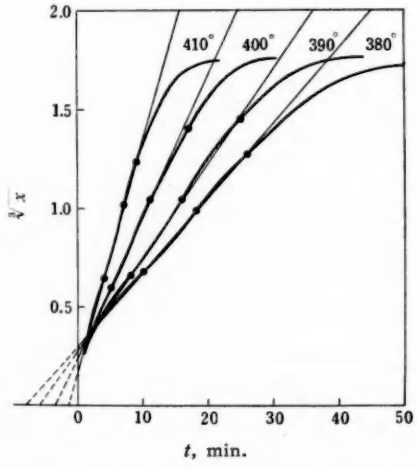

Fig. 8. Curves obtained according to Garner's equation.
●: Inflection point.

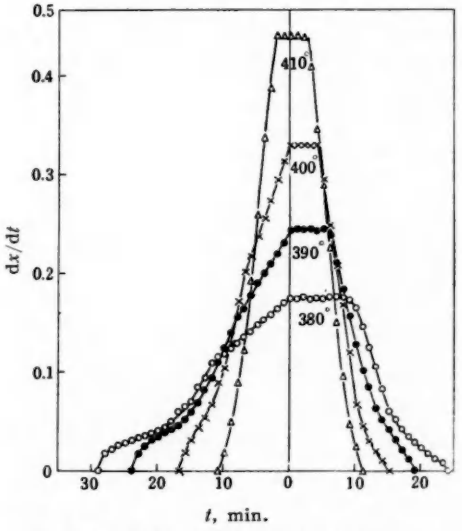

Fig. 9. Plots of dx/dt against time for sample D.

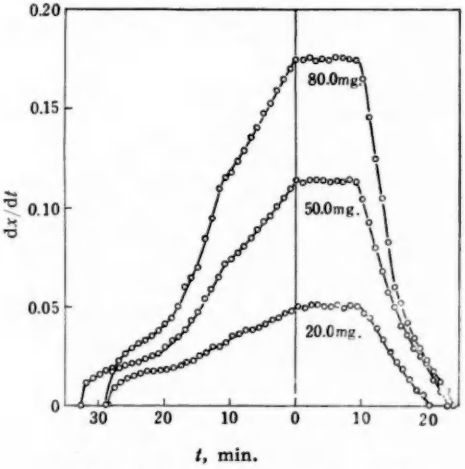

Fig. 10. Plots of dx/dt against time for sample D at 380°C.

10) E. G. Prout and F. C. Tompkins, *Trans. Faraday Soc.*, **40**, 488 (1944).
11) A. F. Benton and L. C. Drake, *J. Am. Chem. Soc.*, **28**, 139 (1906).
12) M. M. Pavlyuchenko and E. Gurevich, *Zhur. Obshchei Khim.*, **21**, 467 (1951); *Chem. Abstr.*, **45**, 5006 (1951).

TABLE I. VALUES FOR α AND β

Stage	380°C		390°C		400°C		410°C	
	α	β	α	β	α	β	α	β
1	1.72×10^{-2}	0.39	1.74×10^{-2}	0.52	1.75×10^{-2}	0.83	1.79×10^{-2}	1.44
2	0.09×10^{-2}	1.65	0.16×10^{-2}	1.65	0.42×10^{-2}	1.65	1.32×10^{-2}	1.65
3	0.81×10^{-2}	0.91	0.79×10^{-2}	1.09	2.29×10^{-2}	0.95	3.76×10^{-2}	1.13
4	1.77×10^{-1}	0	2.45×10^{-1}	0	3.30×10^{-1}	0	4.42×10^{-1}	0
5	1.44×10^{12}	− 7.50	3.69×10^{11}	− 7.50	1.61×10^{7}	− 5.00	6.63×10^{4}	− 3.64
6	1.35×10^{23}	−14.14	2.95×10^{28}	−18.14	1.15×10^{20}	−14.14	1.95×10^{16}	−12.00

silver oxide was decomposed. All the curves in Fig. 9 indicate that the rate of decomposition varies discontinuously, and that the period constant rate is recognized in the curve. The plots of dx/dt against t obtained for 20, 50 and 80 mg. of the sample D at the same temperature, 380°C, are given in Fig. 10. The figure shows that the period of constant rate is not affected by the difference in weight of sample. By plotting $\log dx/dt$ against $\log t$ in Fig. 11, the breaking points become very distinctive. The curve for the whole course of the decomposition can be divided into several linear parts. Each linear part can be represented by the equation $\log dx/dt = \log\alpha + \beta\log t$ or $dx/dt = \alpha t^{\beta}$. The estimated values for α and β from Fig. 11 are listed in Table I. The value of α depends on temperature except in the case of the first stage, and β also varies with temperature except in the cases of the certain stages.

As indicated in Fig. 12, the curves of

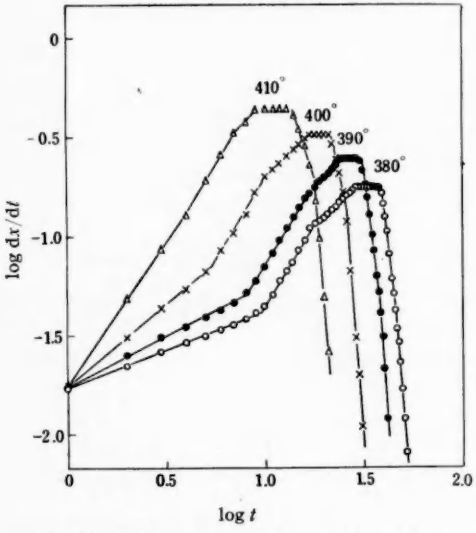

Fig. 11. Plots of $\log dx/dt$ against $\log t$ for sample D.

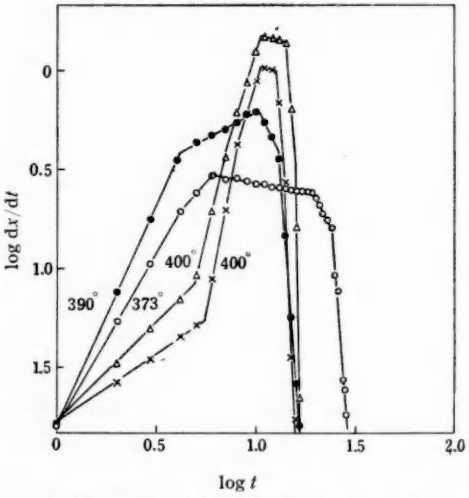

Fig. 12. Plots of $\log dx/dt$ against $\log t$ for sample C (wt. 80.0 mg.).
—△—: wt. 150.0 mg.

$\log dx/dt$ against $\log t$ for the sample C can also be divided into several linear parts for the whole course of the decomposition, as found in the case of sample D.

(3) In the magnetic measurements, the balance was modulated to make it possible to indicate only the change of paramagnetic nature with very high sensitivity. Thus, the small values of diamagnetic susceptibilities of silver oxide and of metallic silver produced by decomposition could be neglected. To determine the weight of oxygen gas evolved in the bulb, the value of paramagnetic susceptibility obtained under a constant temperature was compared with the theoretical value calculated from Van Vleck's equation[13]. In each experiment, the estimated weight of oxygen gas evolved in the bulb at the end of the experiment, was in good agreement with the difference between an initial

13) J. H. Van Vleck, "The Theory of Electric and Magnetic Susceptibilities", Oxford University Press, London (1932), p. 266.

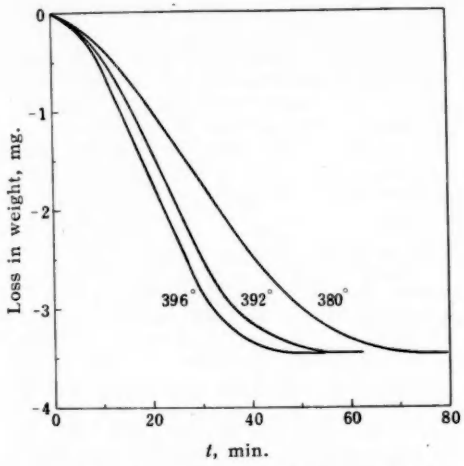

Fig. 13. Loss in weight-time curves for sample D.

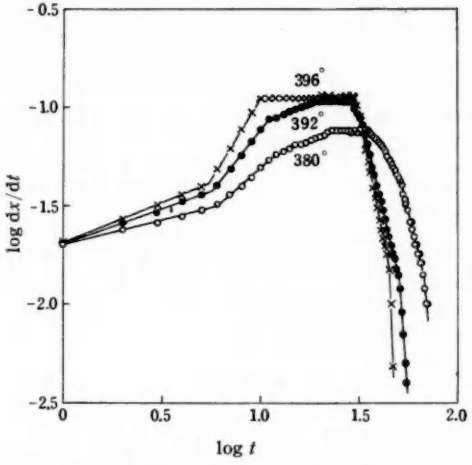

Fig. 15. Plots of $\log dx/dt$ against $\log t$ for sample D.

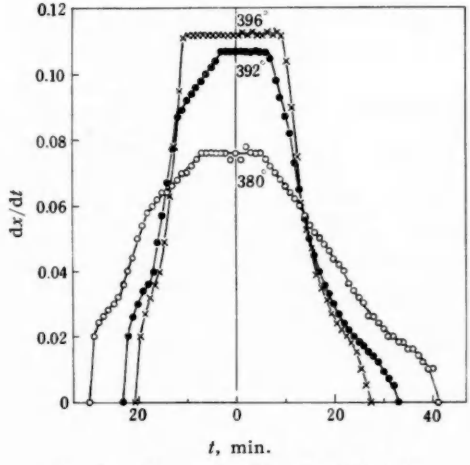

Fig. 14. Plots of dx/dt against time for sample D.

weight of bulb containing a sample and the one containing the residue obtained by removing the oxygen gas evolved in the bulb. In every measurement, the sample used was about 50 mg., and the temperature of the sample was controlled similarly as in the case of the thermal balance. The curves of x against t for the sample D at 380, 392 and 396°C, and the curves of dx/dt against t are shown in Figs. 13 and 14, respectively. The rate of decomposition is represented by the curves with the period of constant rate, as found in the case of the thermal balance. From the plots of $\log dx/dt$ against $\log t$ in Fig. 15, it is apparent that the curves can be divided into the several linear parts. The equation $dx/dt = \alpha' t^{\beta'}$ can, therefore, be applied to the result obtained under the condition in which the sample is decomposed in contact with the evolved gas. The estimated values for α' and β' are given in Table II. The value of α' depends on temperature except for the first stage, β' also varies with temperature except for certain stages. These features are similar to those found in the

TABLE II. VALUES FOR α' AND β'

Stage	380°C		392°C		396°C	
	α'	β'	α'	β'	α'	β'
1	2.00×10^{-2}	0.26	2.03×10^{-2}	0.35	2.04×10^{-2}	0.42
2	0.65×10^{-2}	0.88	0.42×10^{-2}	1.26	0.29×10^{-2}	1.61
3	2.04×10^{-2}	0.42	3.80×10^{-2}	0.34	0.29×10^{-2}	1.61
4	0.76×10^{-1}	0	1.07×10^{-1}	0	1.12×10^{-1}	0
5	4.10	−1.12	7.95×10	−1.95	3.93×10^{7}	−5.09
6	9.04×10	−1.95	3.76×10^{6}	−4.35	3.93×10^{7}	−5.09
7	4.34×10^{6}	−4.10	3.76×10^{6}	−4.35	3.93×10^{7}	−5.09
8	5.01×10^{18}	−10.70	1.10×10^{22}	−13.40	3.38×10^{39}	−24.40

experimental results obtained by the thermal balance.

It was noteworthy that several breaking points appear on the curve in each constant temperature, in spite of the entirely different origins and experimental conditions. This fact shows that fresh potential sites at which nuclei can be formed, are created at intervals as the reaction proceeds. It may be considered that the formation of fresh potential sites is due to a strain which is induced by the reaction product at a surrounding undecomposed portion when the reaction product grows to a certain magnitude.

Summary

(1) It was found, by means of the thermal and magnetic balance, that the decomposition temperatures of silver oxide and of silver oxide containing silver carbonate are 354 and 372°C, respectively.

(2) The magnetic susceptibilities of metallic silver obtained by the decomposition and of silver oxide are -0.21×10^{-6} and -0.48×10^{-6} units per gram at room temperature, respectively. Metallic silver is normally diamagnetic from room temperature to 1100°C.

(3) Under the present experimental conditions, the rate of decomposition is represented by the equation $dx/dt=a_i t^{b_i}$ for the whole course of the decomposition, where i is the subscript for each stage, and generally both a_i and b_i depend on the temperature. It is considered that nuclei are created at intervals as the reaction proceeds.

The author wishes to express his sincere gratitude to Professor Y. Nomura for his suggestions regarding this work and for his helpful advice during the course of the construction of the apparatus.

Department of Chemistry
Defense Academy
Yokosuka

The Kinetic Study of Surface-chemical Reactions at Extremely Low Pressures. IV. The Thermal Reaction between Water Vapor and a Tungsten Filament. Part IV

By Takuya HAMAMURA

(Received April 21, 1959)

Tungsten compound formed by the reaction of water vapor with tungsten at high temperatures has been studied by some investigators. Smithells[1] has studied the reaction by using a gas-filled electric bulb and reported that tungsten was removed from the hotter part of the filament as WO_2 and deposited as W on the colder part. Alterthum[2] assumed the formation of WO_2 in their estimation of equilibrium constants of the system W–H_2O at high temperatures, and Dushman[3] showed thermodynamically that water vapor could oxidize W to WO_2 or W_2O_5. In the previous experiments[4-6] concerning the heating of a tungsten filament in water vapor at low pressures, however, it was found that a blue deposit was formed on the wall of the reaction vessel as the reaction proceeded.

Since WO_2 is brown, this deposit seemed to correspond to another compound. This difference may come from the fact that other authors' results are those at the equilibrium state and not applicable to the present case. It is the aim of the present work to identify the blue deposit and to explain the process of its formation.

1) C. J. Smithells, "Tungsten", Chapman & Hall, Ltd., London (1952), p. 141.
2) H. Alterthum and F. Koref, *Z. Elektrochem.* **31**, 508 (1925).
3) S. Dushman, "Vacuum Technique", John Wiley & Sons, Inc., New York (1949), p. 822.
4) N. Sasaki and T. Hamamura, This Bulletin, **29**, 365 (1956).
5) T. Hamamura, ibid., **32**, 845 (1959).
6) T. Hamamura, ibid., **32**, 848 (1959).

Experimental

The tungsten compound formed by the reaction vaporizes from the filament at high temperatures to produce the deposit on the wall of the vessel. The composition of deposit was determined by means of an electron diffraction method and an indirect method mentioned below.

Electron Diffraction Method. — A film of formval attached on a sheet mesh was placed in the reaction vessel to deposit the product on it; and after the reaction ended, it was taken out of the vessel and a diffraction pattern was taken with a micro-diffraction apparatus.

Indirect Method. — Composition of the deposit was determined from the weight loss of the filament and the amount of hydrogen produced. Since no layer of the product was formed on the filament above 1200°K and the evaporation of tungsten was negligible below 2400°K, the weight loss of filament gave the weight of tungsten converted to the product. On the other hand, if one molecule of hydrogen was assumed to be formed from one molecule of water vapor, the quantity in moles of hydrogen was equal to twice that of oxygen combined with tungsten. Therefore, the mean apparent composition was determined from the weight loss of filament and the amount of hydrogen produced.

Apparatus. — The experimental apparatus was the same as that described in the previous papers, except that the filaments were made removable from the lead wires for weighing, i. e., they were clamped at both ends by nickel strips welded to the leads. The filaments used were taken from the same spool as that used in the previous experiments and pretreated in a similar manner. Six filaments, 0.114 mm. in diameter and 75 mm. long each, were mounted perpendicular to the axis of the reaction vessel at a distance of 5 cm. from each other. One of them was used for a standard to compensate all the weight changes that were not caused by the reaction itself; for example, the change caused by the oxidation and adsorption during the weighing process and the evaporation during the degassing process and so on. The filament was degassed in a similar manner as the others, but not heated in water vapor. The other five filaments were used for the determination of the composition. A glass balloon of 10.278 l. was used to introduce hydrogen into it and the pressure was measured with a McLeod manometer.

Procedure.—Prior to the mounting, each filament was weighed with a micro-balance and mounted in the vessel in a manner such as that mentioned above. The procedures of evacuating the apparatus, degassing the filaments and introducing water vapor into the vessel were similar to those of the previous experiments, except that the filaments were degassed at 2200°K for 6 hr. When the flow of water vapor became stationary, one of the filaments was heated at a definite temperature and the hydrogen liberated was carried by the diffusion pump into the balloon. After a certain interval of time, the filament was cooled and the pressure of the balloon was measured to obtain the amount of hydrogen. Thus, five filaments were heated one by one under different filament temperatures and pressures of water vapor. After five filaments had been heated, all the filaments were heated again in high vacuum at 2000°K for twenty minutes. Then the filaments were taken out of the vessel, removed from the leads and weighed again with a micro-balance. The net weight loss was obtained as a difference of weight loss of the respective filament and the weight change of the standard filament.

The experiments were made at temperatures from 1480 to 1950°K and initial pressures of water vapor from 63×10^{-5} to 200×10^{-5} mmHg. The hydrogen pressure in the vessel was controlled whenever it was necessary. The temperature of the vessel remained at room temperature throughout the experiments.

The hydrogen in the balloon was compressed by a diffusion pump into a sampling bulb of one liter up to about 0.1 mmHg and analyzed with a Consolidated Electrodynamics Corporation mass-spectrometer model 21-401.

Results and Discussion

Electron Diffraction Method. — All the diffraction patterns obtained consisted of diffused lines, presumably because the deposits were too fine crystalline or amorphous. Therefore, this method was not used for identification of the products.

Indirect Method. — Results obtained are given in Table IV*, representing the composition in form of WO_x. It is evident from this table that the compositions are about $WO_{2.80}$ independent of filament temperatures, pressures of water vapor and hydrogen pressures. The colors of all the deposits were blue by transmitted light.

From the color and composition the deposits seem to be composed of some of the following oxides[7,8] or hydroxides[9-11] of tungsten, e. g., β-($WO_{2.9}$) and γ-($WO_{2.72}$) for oxide and $H_{0.1}WO_3$, $H_{0.33}WO_3$ and $H_{0.5}$-WO_3 for hydroxide. These are blue or violet, respectively, and have compositions close to those of the blue deposits, (hydroxide has the apparent composition of $WO_{2.95}$, $WO_{2.83}$ and $WO_{2.75}$ respectively, if determined by means of the indirect

* Tables, figures and equations in the present paper are numbered after those of the previous papers.

7) O. Glemser and H. Sauer, *Z. anorg. u. allgem. Chem.*, **252**, 144 (1943).

8) A. J. Hegedüs, T. Millner, J. Neugebauer and U. Sasvari, ibid., **281**, 64 (1955).

9) O. Glemser and C. Neuman, ibid., **265**, 288 (1951).

10) O. Glemser, U. Hauschild and G. Lutz, ibid., **269**, 93 (1952).

11) F. Ebert and H. Flasch, ibid., **226**, 65 (1935).

TABLE IV

Temp. of filament K°	Initial press. of H_2O mmHg$\times 10^5$	Press. of H_2 in vessel mmHg$\times 10^5$	Net weight loss of filament mol.$\times 10^6$	Amount of H_2 produced mol.$\times 10^5$	Composition	Gas. product mass No. %
1480	176	2	3.96	1.11	$WO_{2.81}$	
1580	63	2	4.04	1.12	$WO_{2.78}$	
1580	179	5	4.22	1.19	$WO_{2.82}$	
1700	63	6	4.59	1.28	$WO_{2.79}$	
1700	200	16	4.86	1.35	$WO_{2.77}$	28 0.4% 32 —
1730	103	8	3.89	1.09	$WO_{2.80}$	
1730	103	9	5.17	1.46	$WO_{2.83}$	
1730	103	127	5.56	1.55	$WO_{2.79}$	
1800	103	11	5.07	1.43	$WO_{2.82}$	
1900	103	16.5	7.00	1.97	$WO_{2.82}$	
1950	103	24	3.88	1.09	$WO_{2.81}$	
1950	103	24	7.94	2.20	$WO_{2.78}$	

method). It is known that these oxides are formed by reduction of WO_3 with hydrogen and the hydroxides by reduction of WO_3 with atomic hydrogen.

The following two processes may be considered for the production of the blue deposit:

1) the product vaporizes from the filament as a blue compound to make a blue deposit on the wall.

2) the product vaporizes from the filament as trioxide and its colorless deposit is secondarily reduced on the wall to form a blue deposit.

The process, by which the deposit was, produced was studied by vaporizing γ-oxide from the filament in high vacuum. When a tungsten filament was heated at 700°C in about 0.01 mmHg pressure of oxygen, a dark violet layer of γ-oxide[12] was formed on the filament. After forming a certain thickness of the layer, excess oxygen was evacuated and the filament was heated above 1500°K. Then the oxide layer vaporized from the filament and made a deposit on the wall of the vessel. The experiments were carried out at various thicknesses of deposit up to about 1000 Å and vaporizing temperatures up to about 2200°K. It was found that the deposits produced were always colorless regardless of the thickness of the deposit and the vaporizing temperature and the blue deposit was not formed at all. The thickness was estimated from the amount of oxygen combined with the filament to make γ-oxide. It was found experimentally that deposit of about 100 Å thick was detectable as a blue film when it was formed by the reaction of water vapor with tungsten. Blackburn[13] has found that WO_2 decomposed completely to W and WO_3 above 1300°K and made WO_3 deposit on the wall. γ-Oxide and probably β-oxide, too, would behave similarly. Hydroxides are not likely to vaporize from the filament as they are. $H_{0.5}WO_3$ is known[9] to decompose into $WO_{2.9}$, hydrogen and water vapor above 60°C. Other hydroxides seem to behave in a similar manner, although their thermal stability is not known. As a result, it is probable that the blue deposit was formed not primarily by the deposition of blue compounds, but secondarily by the reduction of a colorless deposit of WO_3 with hydrogen on the wall.

As for the reduction, the following facts are known in the present stage of research. It is evident that the reduction was not carried out with hydrogen in gas phase, because the composition of the deposit and the reaction rate[6] were independent of the hydrogen pressure in the vessel. Accordingly, the reduction should be carried out with hydrogen liberated by the reaction of water vapor with tungsten. The hydrogen would contain the molecules excited in the electronic or the vibrational energy and even the atoms, if generated. These will be discussed in a subsequent paper.

The independence of the composition $WO_{2.80}$ of deposit upon the filament temperatures and others mentioned above may be due to the fact that the reduction rate becomes smaller at the lower oxidation state. The reduction rate was studied by means of a static method by heating

12) H. Hashimoto, K. Tanaka and E. Yoda, *J. Electron-Microscopy*, **6**, 8 (1958).

13) P. E. Blackburn, M. Hoch and H. L. Johnston, *J. Phys. Chem.*, **62**, 769 (1958).

a tungsten filament in hydrogen within a reaction vessel whose wall had been covered with WO_3 deposit formed by heating the filament in a definite amount of oxygen. The hydrogen pressure was measured as a function of the heating time of the filament and the extent of reduction was determined from the pressure decrease of hydrogen. Two examples are shown in Fig. 10, where the filament

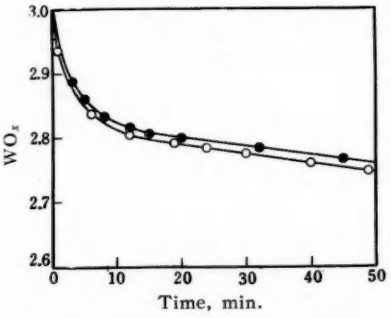

Fig. 10. Reduction of WO_3 with atomic hydrogen.
● 100 Å, 100×10^{-4} mmHg
○ 50 Å, 50×10^{-4} mmHg

temperature was 1740°K and the thickness of WO_3 was about 50 and 100 Å, respectively, and the initial pressure of hydrogen was 50×10^{-4} and 100×10^{-4} mmHg each. It is evident from the figure that the reduction proceeds swiftly down to about $WO_{2.80}$ but the rate slows down appreciably at the lower oxidation state. It is obvious in these experiments that the reduction is carried out mainly with atomic hydrogen formed from the molecules by the dissociation in contact with the filament, and not with hydrogen molecules which rebound from the filament, because the mean temperature of rebounding molecules is about 280°C (for the filament temperature of 1740°K) which is too low to reduce WO_3, since the accomodation coefficient of hydrogen on tungsten surface is 0.19[14].

Result of analysis of hydrogen is shown in Table IV. Only a small amount of gas of mass number 28, presumably carbon monoxide formed from carbon in the filament and water vapor, is contained. The fact that oxygen was not detected in hydrogen suggests that WO_3 was formed by a direct reaction of water vapor with tungsten and not by the reactions through the thermal decomposition of water vapor

$$2H_2O \rightarrow 2H_2 + O_2$$
$$W + 3/2O_2 \rightarrow WO_3$$

If oxygen was liberated, a part of it would leave the vessel without reacting with the filament and be introduced into the balloon, and a part would react with the filament to form WO_3 deposit. The ratio of the former oxygen to the latter can be evaluated by the kinetic theory of gases as follows; the quantity in moles of oxygen which leaves the vessel per second is given similar to Eq. 12 by

$$A'\bar{B}''P'' \qquad (13)$$

where $A'\bar{B}''$ is a constant determined experimentally and P'' the partial pressure of oxygen in the vessel. While the quantity which reacts with the filament per second is given similar to Eq. 2 by

$$k''SB''P'' \qquad (14)$$

where k'' is the reaction probability of oxygen with tungsten. From these formulae, the ratio is calculated as a function of filament temperature as shown in Table V, where values of k'' are determined experimentally by using a filament taken from the same spool. It is evident that if WO_3 was formed by a reaction of gaseous oxygen with tungsten at 1700°K, oxygen had to be detected by the mass spectrometer which was able to detect 0.1% oxygen in hydrogen.

TABLE V

Temp. of filament °K,	1600	1700	1800	1900
Ratio	1.7	1.1	0.64	0.51

Summary

1) Reaction product vaporizes from the filament as tungsten trioxide and its colorless deposit is reduced with hydrogen liberated by the reaction. Consequently, the blue deposit having the mean apparent composition of $WO_{2.80}$ can be obtained.

2) The WO_3 deposit is reduced readily with atomic hydrogen down to $WO_{2.80}$, but the reduction rate becomes appreciably slower at the lower oxidation state.

3) Oxygen is not contained in hydrogen. This suggests that WO_3 is not formed by a reaction of tungsten with gaseous oxygen liberated by thermal decomposition of water vapor, but is formed directly by a reaction of tungsten with water vapor.

The author wishes to express sincere thanks to Professor N. Sasaki of Kyoto

14) I. Langmuir, *J. Am. Chem. Soc.*, **38**, 1145 (1916).

University and Professor K. Kodera of Kyoto Technical University for their kind discussions and encouragement, to Messrs. R. Ueda and T. Makita of Kyoto University for electron diffraction and mass spectrometer, respectively, and to Mr. T. Naiki of Kyoto Technical University for electron diffraction.

Department of Chemistry
Faculty of Industrial Art
Kyoto Technical University
Sakyo-ku, Kyoto

Crystallinity Studies of Polychlorotrifluoroethylene by the Infrared Method. II. Kinetics of the Crystallization

By Hiroshi MATSUO

(Received April 30, 1959)

The isothermal rate of spherulitic growth of polychlorotrifluoroethylene (PCTFE) was studied by Price[1] by direct microscopic observation. He observed, however, that there was an ordering process, detectable by X-rays, which developed much more rapidly than did the spherulites. Allen[2] also suggested that there would be no necessary simple connection between the rate of growth of a spherulite and the rate of change of density. On the other hand, Morgan[3] and Flory[4] demonstrated that spherulitic growth was a true measure of the crystallization rate in the cases of polyethylene terephthalate and polydecamethylene sebacate, respectively.

In the preceding paper[5] it was shown that the infrared method was available for reliable estimates of crystallinity in PCTFE, completely independent of other methods. Furthermore, this method is responsive to crystallinity changes taking place rapidly. The investigation reported in the present paper was undertaken with the objective of measuring the isothermal rate of crystallization and to understand the crystallization kinetics of PCTFE by employing this technique. These results were discussed, comparing them with those obtained by other methods.

Experimental

The crystalline band at 440 cm^{-1} of the infrared spectrum was used to follow the production of crystalline material as the crystallization proceeded.

To determine the isothermal rate of crystallization, a procedure was used similar to that used by Reding and Brown[6] to measure the rate of crystallization of polyethylene. Two ovens, one directly over the other, were mounted on a Perkin-Elmer Model 112 infrared spectrometer with potassium bromide optics. The ovens were separately controlled; the upper oven was heated to 230°C of melting temperature and the lower one was heated to any desired growth temperature between 190 and 170°C by circulating a rapid stream of air through an insulated duct from the heaters. A calibrated thermocouple inserted in the lower oven very close to the sample led to a recorder-controller. The controller served to keep the growth temperature within the accuracy of ±0.5°C.

A thin film (0.03~0.06 mm. thick) of commercial PCTFE (NST 270) was clamped in a thin metal holder and placed in the upper oven. After five minutes at 230°C the sample holder was dropped into the lower oven so that it was in the path of the infrared radiation. The melt sample was estimated to reach the desired growth temperature in less than ten seconds. Since the spectrometer was responsive to changes taking place in three seconds or more, this technique proved adequate to follow the crystallization at high rates.

Results

The crystallized fraction of the sample was calculated from the experimental curves. Measurements of the rate of crystallization were carried out at temperatures between 174 and 190°C. Fig. 1 is

1) F. P. Price, *J. Am. Chem. Soc.*, **74**, 311 (1952).
2) P. W. Allen, *Trans. Faraday Soc.*, **48**, 1178 (1952).
3) L. B. Morgan, *Phil. Trans.* (*London*), **A247**, 23 (1954).
4) P. J. Flory and A. D. McIntyre, *J. Polymer Sci.*, **18**, 592 (1955).
5) H. Matsuo, ibid., **25**, 234 (1957); This Bulletin, **30**, 593 (1957).
6) F. P. Reding and A. Brown, *J. Appl. Phys.*, **25**, 848 (1954).

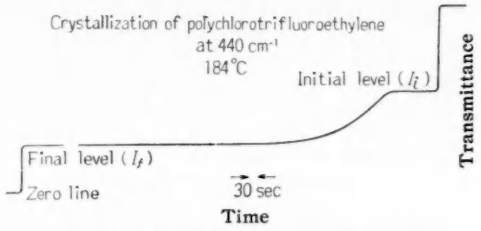

Fig. 1. Typical experimental record.

a typical experimental record obtained in this manner at 184°C. The optical density at time t is defined as

$$D_t \log = (I_i/I_t)$$

Similarly, obtical densities at final and initial states of the crystallization process are obtained by

$$D_f = \log(I_i/I_f), \quad \text{and} \quad D_i = 0$$

The continuously determined data for one curve at each growth temperature were plotted to form Fig. 2. The sigmoid-shaped curves seem to indicate that the crystallization process consists of an induction period, an intermediate period of accelerating rate of crystallization, and a final period to approach an equilibrium state. The degree of crystallinity of the sample, which completed the crystallization process, was measured by the infrared method[5] at room temperature. It is shown in Fig. 3.

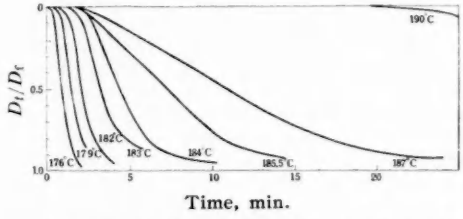

Fig. 2. Ratio of optical density at time t to that at completion of the process, plotted against t at various growth temperatures.

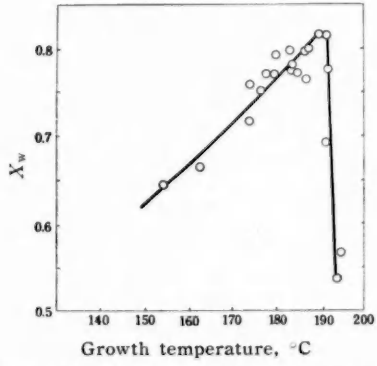

Fig. 3. Degree of crystallinity at completion of crystallization vs. growth temperature.

Discussion

In general, it is found[7] that

$$\ln(V_f - V_t)/(V_f - V_i) = (-1/X_w)kt^n \quad (1)$$

where V_t, V_f and V_i denote the specific volumes at time t, final and initial states of the crystallization process, respectively. X_w is the degree of crystallinity at the completion of the process, and k is the crystallization rate constant. Since the proportionality between the optical density of 440 cm^{-1} and the specific volume for the crystallization process of the polymer is known[5], Eq. 1 becomes

$$\ln(D_f - D_t)/D_f = (-1/X_w)kt^n \quad (2)$$

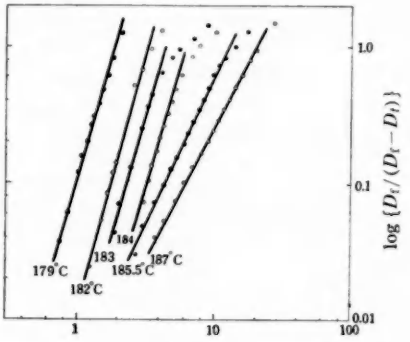

Fig. 4. Plot of log log $[D_f/D_f - D_t)$ vs. log t.

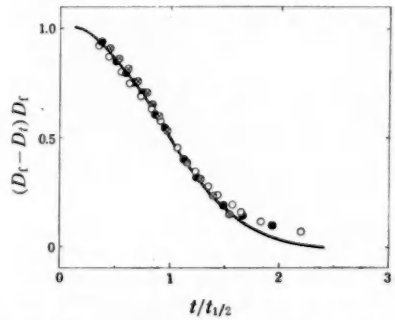

Fig. 5a. Superposition of isotherms at 188°C (⊗); 187°C (○); 185.5°C (●) to Eq. 2 for $n=2.2$.

7) L. Mandelkern, ibid., **26**, 443 (1955); *Chem. Revs.*, **56**, 903 (1956).

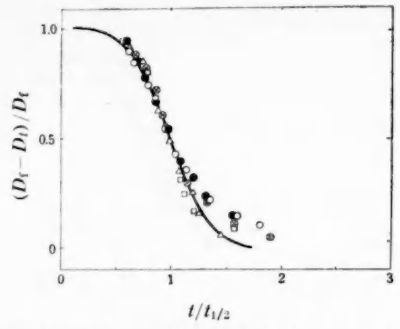

Fig. 5b. Superposition of isotherms at 184°C (●); 183°C (○); 182°C (⊗); 179°C (△); 178°C (□) to Eq. 2 for $n=3.4$.

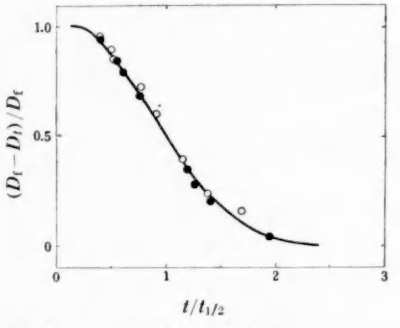

Fig. 5c. Superposition of isotherms at 176°C (●); 174°C (○) to Eq. 2 for $n=2.2$.

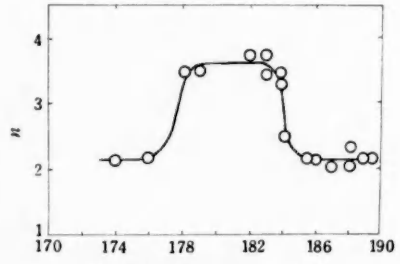

Fig. 6. Values of n at various growth temperatures.

By plotting ln $\ln(D_f-D_t)/D_f$ against ln t, the value of n can be obtained from the slope of the resultant straight line in Fig. 4. In Fig. 5 typical isotherms are plotted according to Eq. 2, where the half time $t_{1/2}$ indicates that the time at $D_t=1/2\,D_f$. The solid lines represent the theoretical isotherms. Good agreement can be obtained for the early stages of the process, but as the crystallization proceeds, the calculated amount of crystallinity is systematically greater than the observed.

The experimental values of n at various growth temperatures are plotted in Fig. 6. The value of n in Avrami's analysis[8] is dependent upon the type of crystallites in nucleation and growth as Table I shows.

TABLE I

Type of growth	Type of nucleation	n
spherical	homogeneous	4
disk	homogeneous	3
spherical	heterogeneous	3
disk	heterogeneous	2

It is, therefore, conceivable that at the growth temperature between 190 and 185°C the nucleation process will be promoted by any heterogeneities which are present in the melt. A fixed number of stable nuclei are present and subsequent transformation is a consequence only of the disk-type lineal growth of these centers. At the growth temperature between 184 and 178°C the nucleation process will be mainly governed by homogeneous nucleation. Price[1] observed by the microscopic method that at temperatures between 190 and 175°C the spherulites are heterogeneously nucleated, and at 170°C and below they are both heterogeneously and homogeneously nucleated. The difference in the results obtained by Price and the present method will be mainly due to the differences in molecular weight, thickness, form of the sample, and in the melting temperature and time, just as has been pointed out in the case of polyethylene terephthalate[3]. In this experiment samples could not be preserved physically as films at higher melting temperatures for a long time prior to the initiation of the crystallization process. Therefore, it will be difficult to say whether the variation of the exponent n with growth temperature is an inherent property of the polymer or not. Very recently, Hoffman[9] indicated that crystallization of the polymer is a results of one-dimensional growth of primary nuclei that are born at later and later dates, and that no obvious relation exists between the growth of primary nuclei and that of spherulites. Furthermore, he pointed out that the polymer has to be heated to the vicinity of 305°C prior to crystallization so as to destroy virtually all of the embryos in the crevices of the heterogeneities.

8) M. Avrami, *J. Chem. Phys.*, **7**, 1103 (1939); **8**, 212 (1940); **9**, 177 (1941).

Next, the temperature coefficient of the crystallization rate was examined. In the vicinity of $T_m(\Delta T=25-30°C)$ the growth rate of crystallites shows a great negative temperature coefficient, in contradiction to the concept of growth controlled by diffusion. The fact leads to the concept of growth governed by secondary nucleation at the spherulite surface[4]. Accurate measurement of the rate of crystallization in the lower growth temperature range was prevented by the rapid onset of crystallization as the material was cooled from the melt through the temperature region of the maximum rate of crystallization, however short the time spent there. It will be, however, expected by Fig. 7 that the maximum rate of crystallization of the polymer locates at a lower temperature near 170°C[9].

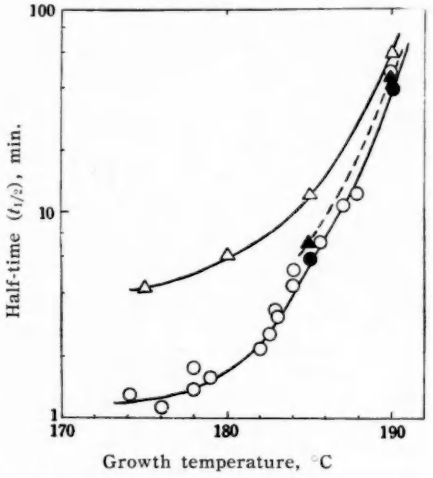

Fig. 7. Half-time vs. growth temperature.
(○) obtained by the infrared method (NST 270);
(●) obtained by the density method (NST 270);
(▲ and △) obtained by the microscopic method (NST 240 and 300).

Considering the formation of disk nuclei of fixed thickness which possess only lateral surface energy, the free energy, ΔF_d, can be expressed as

$$\Delta F = 2\pi rl\sigma - \pi r^2 l\Delta f_0 \qquad (3)$$

where σ is the interfacial free energy per unit area for the cylindrical surface, and Δf_0 is the bulk free energy of fusion per unit volume. Maximizing Eq. 3 with respect to r and equating Δf_0 to $(\Delta T/T_m)\Delta h_u$, where Δh_u is the heat of fusion per unit volume of repeating unit, there is obtained

$$\Delta F^* = (\pi l\sigma^2/\Delta h_u)(T_m/\Delta T) \qquad (4)$$

The rate of nucleation in condensed systems may be expressed by

$$A = A_0 \exp(-E/kT - \Delta F^*/kT) \qquad (5)$$

Furthermore, assuming the growth to be mainly diffusion controlled, then

$$G = G_0 \exp(-E/kT) \qquad (6)$$

Therefore, the rate constant may be expressed[10]

$$k = k_0 \exp\{-3E/kT - (\pi l\sigma^2/H_u)T_m/\Delta T \cdot kT\} \qquad (7)$$

Over the small temperature range of the present experiments the pre-exponential factor may be considered to remain constant, then

$$\log k = A - B(T_m/\Delta T \cdot T) \qquad (8)$$

The plot of $\log k$ against $T_m/T \cdot T$ is shown in Fig. 8. Here the melting point of the polymer is taken as 215°C and the values of k in the microscopic method[1] are calculated by

$$k = \frac{4}{3}NS^3$$

where N is the number density and S is the growth rate of spherulites. In this

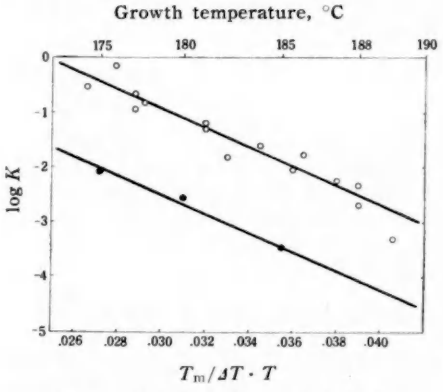

Fig. 8. Plot of $\log k$ vs. $T_m/\Delta T \cdot T$.
(○) obtained by the infrared method;
(●) obtained by the microscopic method.

9) J. D. Hoffman of the National Bureau of Standards, private communications.

10) M. Takayanagi and T. Yamashita, *J. Polymer Sci.*, **22**, 552 (1956).

figure the results obtained by both the microscopic and the infrared methods can be approximated by straight lines which indicate the same negative temperature coefficient.

Finally, the effect of melting temperature on the rate of crystallization of the polymer was examined by the present method. After samples had been maintained at different melting temperatures (273~210°C) for five minutes, the half-times of crystallization at 188, 187 and 183°C were measured. They are shown in Fig. 9. The increase in the rate of

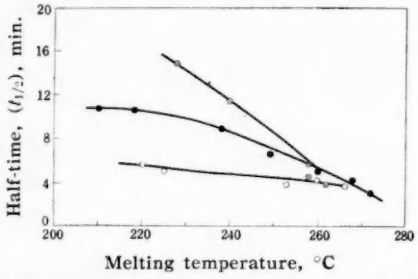

Fig. 9. Half-times as a function of melting temperature for crystallizations at 188°C (⊗), 187°C (●), and 183°C (○).

crystallization with an increase of the melting temperature was indicated contrary to the cases of Nylon 66[2] and polyethylene terephthalate[3]. The fact had been explained by Price[1] as due to degradation of the polymer at a higher melting temperature. Recently, thin films of the polymer of NST 300 and 290 were supplied. The average molecular weight of the polymers were estimated to be approximately 81,000 and 78,000, respectively. Using these samples the half-time of crystallization at 183°C and the degree of crystallinity at the completion of the crystallization process were measured. The half-times were 4.6 and 7.4 min., respectively; the degree of crystallinity at the completion of the crystallization process were 74 and 64%, respectively. It will be expected that both the rate of crystallization and the degree of crystallinity at the completion of the crystallization process increase as the molecular weight of the polymer decreases.

Summary

The isothermal rate of crystallization in polychlorotrifluoroethylene was measured at temperatures ranging from 172 to 190°C below the melting point by following the change of observed absorbance of crystalline band at 440 cm^{-1}. The isothermal rate of crystallization and apparent induction time are dependent on temperature. The data on the kinetics of the crystallization are compared with the result of Avrami's analysis. At temperatures between 190 and 185°C the nucleation process will be promoted by heterogeneities which exist in the melt. Between 184 and 178°C it will be mainly governed by homogeneous nucleation.

Electrical Communication Laboratory
Nippon Telegraph and Telephone
Public Corporation
Musashino-shi, Tokyo

Ultraviolet Absorption Spectra of Substituted Phenylureas

By Yojiro Tsuzuki, Shinichi Motoki and Kazuko Migita

(Received April 30, 1959)

Dulcin(*p*-ethoxypenylurea) has been a well known substance as one of the strongest sweetening agents, whereas the ortho isomer is tasteless and the *m*-ethoxyphenylurea rather bitter.

In an earlier work on the sweetness of organic compounds one of the authors has pointed out that the sweetness of aromatic compounds is closely related to the resonance structures, and has shown that the greater the sweetness of the compound, the greater is the resonance energy[1]; thus, the resonance energy in dulcin isomers decreases in the order of $p>o>m$.

Since the ethoxy group, being associated with the carbamide group, would contribute to the resonance stabilization of the molecule in different ways to cause electronic effects according to the relative position of the two groups, the mode of the resonance in these compounds could be analyzed, provided the electronic nature of the carbamide group is elucidated. The purpose of this paper is to obtain whatever information is possible on these problems.

As is well known the ultraviolet absorption spectrum of benzene exhibits the characteristic peaks at 203.5 mμ (K-band, $\varepsilon=7400$) and 240~260 mμ (B-band, $\varepsilon=250$). When a substituent is introduced into the nucleus, both of the absorption bands are displaced towards the region of longer wavelengths owing to the resonance attributed to the conjugation of the substituent with the nucleus. In disubstituted benzenes the following semiquantitative relations have been established by Doub and Vandenbelt[2,3] between the absorption displacement and the electronic properties of the two groups, thus:

1. In the absorption spectrum of the disubstituted benzenes, one substituent of which is electron-attracting and the other electron-releasing.

a) The absorption shift of the 203.5 mμ band of benzene is, in the case of *p*-compounds ($\Delta\lambda$), considerably greater than the sum of those of the corresponding monosubstituted compounds ($\Delta\lambda_1+\Delta\lambda_2$), namely,

$$\Delta\lambda \gg \Delta\lambda_1+\Delta\lambda_2$$

Example:

	p-$H_2N\cdot C_6H_4\cdot NO_2$		$C_6H_5NO_2$		$C_6H_5NH_2$
λ_{max} (mμ)	381		268.5		230
$\Delta\lambda$ (mμ)	177.5	$\gg$	65	+	26.5
	‖		‖		‖
	$\Delta\lambda$		$\Delta\lambda_1$		$\Delta\lambda_2$

b) As to the orientation effect, the following order of red-shift is observed:

$$\lambda_{max}\ p>o>m$$

Example:

$H_2N\cdot C_6H_4\cdot NO_2$	p	o	m
K-band	381	282.5	280
B-band	—*	412	358

2. In the spectra of disubstituted benzenes the groups of which are both electron-attracting or both electron-releasing.

a) In the case of *p*-compounds:

$$\Delta\lambda<\Delta\lambda_1+\Delta\lambda_2$$

Example:

	p-$NO_2\cdot C_6H_4\cdot CO_2H$		$C_6H_5NO_2$		$C_6H_5\cdot CO_2H$
$\Delta\lambda$ (mμ)	55	<	65	+	26.5

b) In the case of nuclear isomers:

$$\lambda_{max}\ p>m>o$$

Example:

$H_2N\cdot C_6H_4\cdot NH_2$	p		m		o
K-band	245	>	240	>	233
B-band	320	>	289	$\geqq$	289

3. In the spectra of disubstituted benzenes, one substituent of which is a halogen atom or a methyl radical.

a) In the case of *p*-compounds:

$$\Delta\lambda \geqq \Delta\lambda_1+\Delta\lambda_2$$

This relation always holds, regardless of whether the electronic property of the other substituent be electron-attracting or electron-releasing.

b) In the case of three isomers:

$$\lambda_{max}\ p>m>o$$

1) Y. Tsuzuki, S. Kato and H. Okazaki, *Science [Japan] (Kagaku)*, **24**, 523 (1954).
2) L. Doub and J. M. Vandenbelt, *J. Am. Chem. Soc.*, **69**, 2714 (1947).
3) L. Doub and J. M. Vandenbelt, ibid., **71**, 2414 (1949).

* The absorption corresponding to the B-band often disappeared with *p*-compounds.

Few exceptions have been, however, found in this case.

On the basis of these empirical rules, one might determine, by means of spectroscopy, the stabilization due to resonance in disubstituted benzenes and the electronic effect of the substituent.

In the present investigation several substituted phenylureas containing various substituents of typical electronic nature such as NO_2, EtO, CH_3, Br were prepared and the spectra of these compounds were measured for the purpose of determining the electronic effect of the carbamide group and comparing with each other the magnitudes of the resonance of the nuclear isomers of dulcin.

Results and Discussion

The experimental results are shown in Table I.

TABLE I. ULTRAVIOLET ABSORPTION SPECTRA OF SUBSTITUTED PHENYLUREAS ($R \cdot C_6H_4 \cdot NHCONH_2$)

Substituent R	K-band λ_{max}	K-band ε_{max}	B-band λ_{max}	B-band ε_{max}
o-NO_2	275	4350	365	3260
m-NO_2	270	5130	338	1660
p-NO_2	322	13200	—	—
o-EtO	241	15400	281	3830
m-EtO	240.5	13500	280	2550
p-EtO	242	18200	290	1980
o-CH_3	236	10400	270	660
m-CH_3	240	17600	277	770
p-CH_3	240	18400	281	1090
p-Br	247	25300	276	1370

Table II is given to see how the above stated relations are applicable to the present results. It is seen from this table that the absorption maxima of the three isomers $EtO \cdot C_6H_4 \cdot NHCONH_2$ appear in the order of $p>o>m$ for both K- and B-bands. The results may be interpreted as indicating the resonance energy decreasing in the order $p>o>m$, which shows that the carbamide group is electron-attracting. The conclusion is well in accordance with the tentative theory of the relation between the sweetness and the resonance. On the other hand, the slight resemblance of the spectra of nitrophenylureas to those of nitroaniline rather leads us to a somewhat opposite conclusion that the carbamide group is slightly electron-releasing.

TABLE II. ANALYSIS OF ABSORPTION DATA

a) *p*-Substituted phenylureas

p-$R \cdot C_6H_4 \cdot NHCONH_2$

Substituent R	Relation				
	$\Delta\lambda$	>	$\Delta\lambda_1$**	+	$\Delta\lambda_2$
NO_2	118.5	>	33.5	+	65
	$\Delta\lambda$	<	$\Delta\lambda_1$	+	$\Delta\lambda_2$
EtO	38.5	<	33.5	+	16
	$\Delta\lambda$	=	$\Delta\lambda_1$	+	$\Delta\lambda_2$
CH_3	36.5	=	33.5	+	3
	$\Delta\lambda$	>	$\Delta\lambda_1$	+	$\Delta\lambda_2$
Br	43.5	>	33.5	+	6.5

b) Nuclear isomers of substituted phenylureas

Substituent R	Relation	
	K-band	B-band
NO_2	$p>o>m$	$o>m$
EtO	$p>o>m$	$p>o>m$
CH_3	$p=m>o$	$p>m>o$

It follows therefore that this group is to be regarded as electronically amphoteric, behaving in an electron-attracting or releasing manner, depending on the other group.

Since such a peculiar organic group has never been known in the chemical literature, further investigation is now being made to ascertain the new interpretation of these structural problems, the results of which will be published in the near future.

Experimental

Preparation of Samples. — Commercial dulcin was used after purification by repeated recrystallization from water.

o-Nitrophenylurea was synthesized according to the direction of Arndt[4] with slight modification.

$$o\text{-}NO_2C_6H_4NH_2HCl \xrightarrow[NaOH]{Pb(SCN)_2} (o\text{-}NO_2C_6H_4NHCSNH_2)$$

$$\xrightarrow[-H_2S]{} o\text{-}NO_2C_6H_4NHCN \xrightarrow[HCl]{H_2O} o\text{-}NO_2C_6H_4NHCONH_2$$

The other substituted phenylureas were prepared from potassium cyanate and the corresponding nuclear substituted anilines by the methods given in "Organic Syntheses"[5].

o-Nitrophenylurea, m. p. 183~184°C, the *m*-isomer, m. p. 189°C, the para, m. p. 235°C.

o-Ethoxyphenylurea, m. p. 134°C, the *m*-isomer, m. p. 112°C, the para, m. p. 175°C.

o-Methylphenylurea, m. p. 195°C, the *m*-compound, m. p. 145°C, the para, m. p. 183°C.

p-Bromophenylurea m. p. 220°C.

** Phenylurea has two absorption peaks at 237 mμ (ε=17700) and 266~275 mμ (ε=1100) corresponding to K-band and B-band, respectively. W. A. Schroeder et al., *Anal. Chem.*, **23**, 1740 (1951).

4) F. Arndt, *Ber.*, **46**, 3528 (1913).

5) F. Kurzer, "Organic Syntheses", Vol. 31, John Wiley & Sons, Inc., New York (1951), p. 8.

Absorption Spectra.—The absorption spectra were measured in the region of 200~350 mμ by means of a Beckman Model DU Quartz spectrophotometer with the above samples dissolved in absolute ethanol to the concentration of ca. 1/10,000 mol./l.

Summary

Ultraviolet absorption spectra of several nuclear substituted phenylureas have been measured with the attempt to study the electronic effect of the carbamide group, and the resonance stabilization in three dulcin isomers.

Department of Chemistry
Tokyo College of Science
Kagurazaka, Shinjuku-ku
Tokyo

Analysis of Non-Newtonian Flow by Falling-Sphere Method

By Sadao HIROTA and Masao TAKADA

(Received May 12, 1959)

Thixotropic solution must be handled without any strong agitation in order to obtain so-called "virgin-state viscosity". Neither the capillary nor the rotating cylinder viscometer is suitable for this purpose, while the falling-sphere method is applicable, because (a) the agitation of the sample in this measunement is far less compared with that in other methods, and (b) the sphere always falls contacting with a new, so-called "virgin-state" solution.

In order to devise the falling-sphere method for this purpose it is necessary to obtain general flow curves by this method because the fluidity of these solutions normally shows shear dependence as well as time dependence.

Shear stress S_R at the equator of a sphere was given[1] by

$$S_R = R\Delta\rho g/3 \qquad (1)$$

where R is the radius of the sphere and $\Delta\rho$ is the density difference between sphere and fluid. Eq. 1 was later proved to be applicable also to non-Newtonian flow. And a necessary shear stress could be obtained by selecting a sphere of suitable radius.

For Newtonian flow, the shear rate at the equator of the sphere $(du/dr)_R$ followed immediately from Stokes' equation.

$$(du/dr)_R = 3U_0/2R \qquad (2)$$

Sheppard[2], however, pointed out that Eq. 2 fails to express the true shear rate in a non-Newtonian nitrocellulose solution. Phipps[3] claimed the necessity of non-Newtonian correction for Eq. 2. Many attempts[4-9] have been made to utilize the falling-sphere method for non-Newtonian systems without success establishing the corrected equation for Eq. 2 so far. The aim of this paper is to find it and to examine its applicability.

In the previous study[10] we obtained empirically

$$(du/dr)_R = (3U_0/2R) \times [1 + 2.4(d\log U_0/d\log R - 2)] \qquad (3)$$

adopting the capillary viscometer method as the standard for which a standardized treatment of data had been proposed by Krieger and Maron[11]. In the present study, a similar result has been obtained theoretically.

Theoretical

In Newtonian Flow.—Consider a steady flow around a sphere of radius R falling

1) H. Lamb, "Hydrodynamics", 3rd Ed., Cambridge Univ. Press, London (1906), p. 553.
2) S. E. Sheppard, *J. Ind. Eng. Chem.*, **9**, 523 (1917).
3) H. E. Phipps, *Colloid Symposium Monograph*, **5**, 259, (1928).
4) A. G. Pasynskii and A. I. Ravinovich, *Zhur. Fiz. Khim.*, **5**, 521 (1934); *Chem. Abstr.*, **29**, 7753 (1935).
5) A. De Waele, *J. Rheology*, **2**, 141 (1936).
6) A. K. Skrjabin, *Lief.*, **17**, 7 (1936); cited from Kulakoff's paper.
7) N. N. Kulakoff, *Kolloid-Z.*, **80**, 204 (1937).
8) J. C. Williams and E. I. Fulmer, *J. Appl. Phys.*, **9**, 760 (1938).
9) J. Schurz, *Naturwissenschaften*, **42**, 339 (1955).
10) M. Takada and S. Hirota, *J. Chem. Soc. Japan, Pure Chem. Sec.* (*Nippon Kagaku Zasshi*), **80**, 956 (1956).
11) I. M. Krieger and S. H. Maron, *J. Appl. Phys.*, **25**, 72 (1954).

slowly at the velocity U_0 in a Newtonian fluid. The rate of flow U at the distance r from the center is given[12] by

$$U = -R^3 \Delta\rho g(3+R^2/r^2)\phi/18r \quad (4)$$

Where ϕ = fluidity = 1/viscosity

Differentiating Eq. 4 by r, we obtain the shear rate.

$$du/dr = R^3 \Delta\rho g(1+R^2/r^2)\phi/6r^2 \quad (5)$$

Shear stress S is then

$$S = (du/dr)/\phi = R^3 \Delta\rho g(1+R^2/r^2)/6r^2 \quad (6)$$

At $r=R$, Eq. 6 becomes Eq. 1. Eq. 1 has also been obtained directly from the calculation based on the balance between shear force and gravity without being confined to the Newtonian flow[9]. And Eq. 1 is also applicable to the non-Newtonian flow.

In Non-Newtonian Flow. — Non-Newtonian fluidity $P(S)$ is a function of S. Since the latter is a function of R and r, $P(S)$ may be regarded as a function of R and r.

$$(du/dr)/S \equiv P(S) = F(R, r) \quad (7)$$

If we assume that only the shear rate is responsible for the non-Newtonian anomaly, and that Eq. 6 is still applicable* to the non-Newtonian flow, we may introduce Eq. 6 into Eq. 7.

$$du/dr = R^3 \Delta\rho g(1+R^2/r^2)\cdot F(R, r)/6r^2 \quad (8)$$

Though the form of $F(R, r)$ or du/dr is unknown, the following functional equation holds.

$$U_0 = \int_R^\infty (du/dr)dr = \int_R^\infty R^3 \Delta\rho g(1+R^2/r^2) \times F(R, r)/6r^2 \cdot dr \quad (9)$$

Since non-Newtonian fluidity increases with increasing S in many cases, it increases with increasing R and decreases with increasing r. Therefore, if we assume

$$P(S) \equiv F(R, r) = f(R)\cdot g(r) \quad (10)$$

$f(R)$ is an increasing function of R and $g(r)$ is a decreasing function of r.

Defining apparent fluidity, F_a, analogous to Stokes' equation, as

$$F_a = 9U_0/2R^2 \Delta\rho g \quad (11)$$

and substituting Eqs. 10 and 11 into Eq. 9, we obtain

$$4F_a/3R^3 \cdot f(R) = (1/R^2)\cdot \int_R^\infty g(r)/r^4 \cdot dr + \int_R^\infty g(r)/r^4 \cdot dr \quad (12)$$

which may be differentiated by R to become

$$2F_a/3R\cdot f(R)\cdot [(d\log F_a/d\log R) - (d\log f(R)/d\log R) - 3] = -g(R)/R - \int_R^\infty g(r)/r^2 \cdot dr \quad (13)$$

At $r=R$, since $F(R, R) \propto F_a$**

$$d\log F(R, R)/d\log R = d\log F_a/d\log R = H \quad (14)$$

From Eq. 10

$$\log F(R, R) = \log f(R) + \log g(R) \quad (15)$$

$$H = (d\log f(R)/d\log R) + G \quad (16)$$

where

$$G = d\log g(R)/d\log R \quad (17)$$

Introducing Eq. 16 into Eq. 13 and differentiating it again by R

$$F(R, R) = 2F_a[(G-1)(G-3) + dG/d\log R]/3(2-G) \quad (18)$$

From Eq. 10

$$(\partial \log P(S)/\partial \log r)_R = (d\log P(S)/d\log S)\cdot(\partial \log S/\partial \log r)_R = d\log g(r)/d\log r \quad (19)$$

where, from Eq. 6

$$\partial \log S/\partial \log r = [2r^2/(r^2+R^2)] - 4 = -3 \quad (\text{at } r=R) \quad (20)$$

and from Eq. 1, $d\log S_R = d\log R$, then

$$d\log P(S)/d\log S = d\log F(R, R)/d\log R = H \quad (21)$$

$$d\log g(r)/d\log r = d\log g(R)/d\log R = G \quad (22)$$

Substituting Eqs. 20—22 into Eq. 19,

$$\left.\begin{aligned} G &= -3H \\ dG &= -3dH \end{aligned}\right\} \quad (23)$$

Thus, Eq. 18 becomes

$$F(R, R) = F_a(1+4H+3H^2 - dH/d\log R) \times [1-(3H/2)+(3H/2)^2 \cdots\cdots] \quad (24)$$

There is an empirical fact that, for many non-Newtonian fluids, the slope of a plot of $\log F_a$ vs. $\log R$ is constant over a wide range of shear stress and is usually small as compared with unity. For example, $H=0.143$ in 1% NaCMC aq. (MW. $=8\times10^4$, Deg.Eth. $=0.654$) as in Fig. 1.

12) Derived from, for example, B. Fujimoto, "Ōyō Ryutairikigaku (Applied Fluid Dynamics)", Maruzen Co., Ltd., Tokyo (1941), p. 340.

* Discussion on the applicability will be given in another paper.

** This proportionality follows from Krieger-Maron's relation, $P(S)=F_a[1+A(S)]$, where $A(S)$ has been known to be constant over a wide range of S[11].

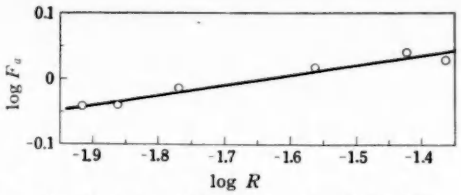

Fig. 1. Plot of $\log F_a$ vs. $\log R$ for 1% NaCMC. aq. (MW.=8×10^4, Deg. Eth.=0.654) by falling sphere method at 25°C.

Thus,

$$\left.\begin{aligned} &\mathrm{d}\log F_a/\mathrm{d}\log R = H = \text{const.} < 1 \\ &\mathrm{d}H/\mathrm{d}\log R = 0,\ H^3 \fallingdotseq 0,\ H^4 \fallingdotseq 0, \cdots \end{aligned}\right\} \quad (25)$$

Substituting Eq. 25 into Eq. 24, we have

$$F(R,R) \fallingdotseq F_a[1+2.5(\mathrm{d}\log F_a/\mathrm{d}\log S_R) - (3/4)(\mathrm{d}\log F_a/\mathrm{d}\log S_R)^2] \quad (26)$$

or

$$(\mathrm{d}u/\mathrm{d}r)_R \fallingdotseq (3U_0/2R) \times [1+2.5(\mathrm{d}\log U_0/\mathrm{d}\log R-2) - (3/4)(\mathrm{d}\log U_0/\mathrm{d}\log R-2)^2] \quad (27)$$

which agrees very well with the empirical equation (Eq. 3).

Now, using Eqs. 1 and 27, we can obtain the exact flow curve, and hence the true viscosity by the falling-sphere method.

Experimental

For the measurement a glass tube about 20 cm. long and of 2.0 cm. in inside diameter was used, fixed in a thermostat regulated to 25±0.1°C. Glass spheres were made in the manner reported previously[10]. The fall of the sphere (density 2.50) was measured by a stop-watch over a definite distance in the sample. From these data, S_R and $(\mathrm{d}u/\mathrm{d}r)_R$ were calculated by means of Eqs. 1 and 27. Table I gives some examples of data and calculations. Values of $\mathrm{d}\log F_a/\mathrm{d}\log R$ in Table I were obtained from the slope in Fig. 1. The resulting flow curve is shown in Fig. 2.

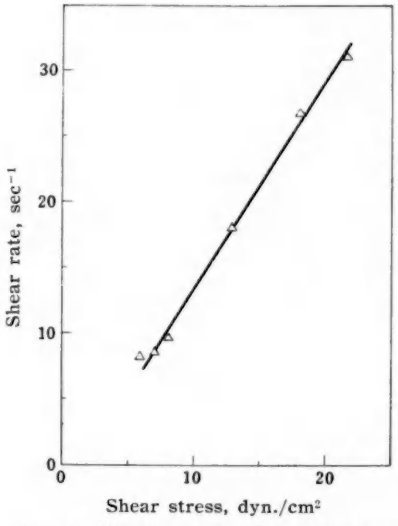

Fig. 2. Flow curve for 1% NaCMC. aq. (MW. 8×10^4, Deg. Eth. 0.654) by falling sphere method at 25°C.

TABLE I. FALLING-SPHERE METHOD. DATA AND SAMPLE CALCULATIONS FOR 1% NaCMC. aq. (MW.=8×10^4, Deg. E.=0.654) AT 25°C

$R\times10^2$	cm.	4.35	3.78	2.74	1.70	1.37	1.21
S_R Eq. 1	dyn./cm^2	21.35	18.5	13.4	8.36	6.72	5.95
U_0	cm./sec.	0.666	0.515	0.250	0.0913	0.0558	0.0435
F_a	l./pois.	1.071	1.10	1.04	0.963	0.908	0.904
$\log F_a$		0.030	0.041	0.017	−0.016	−0.042	−0.044
$\log R$		−1.363	−1.423	−1.563	−1.769	−1.863	−1.917
$\mathrm{d}\log F_a/\mathrm{d}\log R$		0.143	0.143	0.143	0.143	0.143	0.143
$(\mathrm{d}u/\mathrm{d}r)_R$ Eq. 27	1/sec.	31.2	27.8	18.6	10.9	8.26	7.30

TABLE II. SAMPLES USED FOR THE EXPERIMENT (Fig. 3)

No.	Solution	Mol. wt.	Deg. eth.	Concn., %
I	Methylcellulose aq.		0.654	1.0
II	NaCMC. aq.	8×10^4	0.654	1.0
III	NaCMC. aq.	8×10^4	0.301	1.0
IV	NaCMC. aq.	$(10\sim12)\times10^4$	0.649	1.0
V	NaCMC. aq.	8×10^4	0.654	1.2
VI	Nitrocellulose in butylacetate			12.0

Results

From Fig. 3 it is seen that the flow curves from the proposed falling-sphere method coincide very well with those from Krieger and Maron's capillary method. The difference between the empirical equation (Eq. 3) and the theoretical one (Eq. 27) is also negligibly small. These results seem to indicate the validity of our formula.

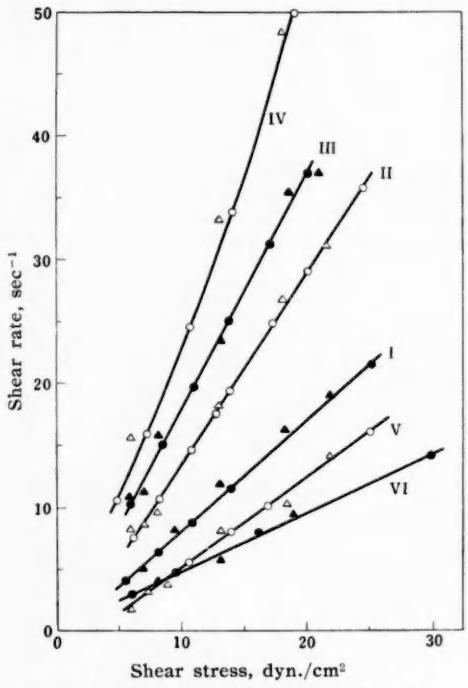

Fig. 3. Flow curves for samples in Table II at 25°C.
Falling sphere method·····▲△
Capillary method ·····●○

Summary

A procedure to obtain a general flow curve by falling-sphere method is presented. The shear stress S_R and shear rate $(du/dr)_R$ at the equator of the sphere are given as

$$S_R = R\Delta\rho g/3$$

$$(du/dr)_R = (3U_0/2R) \times [1+2.5(d\log U_0/d\log R-2) - (3/4)(d\log U_0/d\log R-2)^2]$$

where $\Delta\rho$ is the density difference between sphere and fluid, R the radius and U_0 the falling velocity of the sphere.

The authors wish to express their hearty thanks to Dr. Tsurutaro Nakagawa and Dr. Hirotaro Kambe of the University of Tokyo for their valuable suggestion and discussion and also to Dr. Junzo Shinoda and Dr. Kazuo Miyatake of Daiichi Pharmaceutical Company, Limited for their kind encouragement and permission to publish this paper.

Yanagishima Plant
Daiichi Pharmaceutical Co., Ltd.
Sumida-ku, Tokyo

The Preparation and Properties of N-Salicylideneglycinato-aquo-copper(II), Sodium N-Salicylideneglycylglycinato-cuprate(II) and Related Compounds

By Akitsugu NAKAHARA

(Received May 13, 1959)

It was demonstrated by Eichhorn and Marchand[1] that the coordination of copper(II) ion with the Schiff base produced from salicylaldehyde and glycine results in a stabilization of the >C=N-double bond under conditions that would promote its rupture in the absence of the metal. However, the formation of the copper(II) chelate of salicylideneglycine was observed only in a solution on the basis of a spectroscopic investigation; and the composition of the complex was deduced from an extension of the method of continuous variation to a three component system, copper : salicylaldehyde : glycine. In the present work the same compound, *N*-salicylideneglycinato-aquo-copper(II), **A**, was isolated in the crystalline state and investigated as to its properties. Sodium *N*-salicylideneglycylglycinato-cuprate(II), **B**, was also prepared and investigated as to its structure.

Experimental

Preparation of Copper(II) Chelates.—*N-Salicylideneglycinato-aquo-copper(II).*—To a solution of 6 g. of glycine in 100 ml. water was added 10 g. of salicylaldehyde. The resulting mixture was stirred and heated at about 60°C.

Upon the addition of 16 g. of crystalline cupric acetate, a dark-green solution was formed. A yellowish-green crystalline solid of *N*-salicylideneglycinato-aquo-copper(II) was then gradually deposited within half an hour. The reaction mixture was allowed to cool and filtered by suction. The additional crude product was also obtained by evaporating the filtrate. The yield, in total, was almost quantitative. Recrystallization from a large amount of water gave acicular crystals which decomposed at 240°C.

Anal. Found: C, 32.46; H, 5.39; N, 4.21; H_2O, 26.9. Calcd. for tetrahydrate of **A**: C, 32.60; H, 5.14; N, 4.23; H_2O, 27.2%.

In the above procedure cupric sulfate in place of acetate was observed to give the same result. Furthermore, the same compound was prepared also by reactions between: (1) bis-glycinato-copper(II) and bis-salicylaldehyde-copper(II) in 1:1 molar ratio; (2) bis-glycinato-copper(II) and salicylaldehyde in 1:2 molar ratio; (3) glycine and bis-salicylaldehyde-copper(II) in 2:1 molar ratio.

However, the yield of reaction 2) or 3) was only half of that of 1), since the copper was not sufficient to give the same amount of the product.

The compound is soluble in water, methanol and ethanol, though the solubility is comparatively small, especially in the latter two solvents.

Sodium N-salicylideneglycylglycinato-cuprate(II).—To a solution of 5.3 g. of glycylglycine and 3.2 g. of sodium hydroxide in 100 ml. water was added 8 g. of crystalline cupric acetate. After heating the resulting mixture on a water bath, a deep-blue solution characteristic of copper(II) chelates of peptides was gradually formed. Upon the addition of 5 g. of salicylaldehyde the color of the solution changed to violet. The solution was stirred and heated for thirty more minutes, and was then filtered. The filtrate was concentrated to a small volume and allowed to stand, whereupon beautiful violet needles were obtained. These were recrystallized from their concentrated aqueous solution by adding alcohol or acetone.

Anal. Found: C, 30.69; H, 5.02; N, 6.32; H_2O, 25.8. Calcd. for hexahydrate of **B**: C, 30.81; H, 4.91; N, 6.54; H_2O, 25.2%.

A complete dehydration of the compound was performed by heating the crystals in vacuo at 56°C.

Anal. Found: C, 41.00; H, 3.04; N, 8.89. Calcd. for **B**: C, 41.2; H, 2.81; N, 8.75%.

As described above, an aqueous solution of the compound is violet, but reversibly changes to green in an acid solution.

Potassium salt of the same copper(II) chelate was also obtained in the same way by employing potassium hydroxide instead of sodium hydroxide.

In order to identify the potassium salt, a precipitation of potassium hexanitro-cobaltate(III) was ascertained.

Copper(II) chelate of N-salicylideneglycineethylester.—This compound, **F**, was prepared according to the direction of Pfeiffer et al.[2] by treating the copper(II) complex of salicylaldehyde with hydrochloride of glycineethylester in the presence of sodium acetate in alcohol. It was also confirmed that a reaction in an aqueous suspension between bis-salicylaldehyde-copper(II) and hydrochloride

1) G. L. Eichhorn and N. D. Marchand, *J. Am. Chem. Soc.*, **78**, 2688 (1956).

2) P. Pfeiffer, W. Offermann and H. Werner, *J. prakt. Chem.*, **159**, 313 (1942).

of glycineethylester in the presence of sodium hydroxide is more convenient than the previously reported one[2]. After recrystallization from pyridine or ethanol olive-green crystals were obtained, which decomposed at 200°C, showing a good agreement with the previous datum[2].

Glycylglycinato-aquo-copper(II)[3]. — Freshly precipitated cupric hydroxide was treated in an aqueous suspension with a slight excess of glycylglycine. The resulting deep-blue solution was filtered and concentrated to a small volume, and was then filtered again. The filtrate was allowed to stand for several days over sodium hydroxide, whereupon deep-blue prisms were obtained. These were recrystallized from their concentrated aqueous solution by adding alcohol.

Anal. Found: C, 20.99; H, 4.53; N, 12.09; H_2O, 14.73. Calcd. for monohydrate of **C**: C, 20.85; H, 4.35; N, 12.18; H_2O, 15.65%.

Measurements. — The visible and ultraviolet absorption spectra were determined with a Beckman DU Spectrophotometer at room temperature. The concentration of the solutions varied from 10^{-2} to 10^{-5} F/l.

The infrared spectra were obtained by a Hilger H 800 Infrared Spectrophotometer using a sodium chloride prism. The potassium bromide disk method was employed.

Discussion

The result of analyses and other small tests described in the preceding section afford good reasons to assign structures **A** and **B** for the copper(II) chelate of *N*-salicylideneglycine and that of *N*-salicylideneglycylglycine, respectively. Structure **A** is exactly the same as that postulated by Eichhorn and Marchand[1] on the basis of a spectroscopic investigation. Though they reported also on the formation of 1:2:2copper:salicylaldehyde:glycine complex at pH 5, no such compound was isolated in the present investigation even under conditions that would favor its formation. For example, in the case of the reaction between bis-glycinatocopper(II) and salicylaldehyde or between glycine and bis-salicylaldehyde-copper(II) a 1:2:2 ratio of copper, salicylaldehyde and glycine was employed in a neutral solution, but the reaction product was only the 1:1:1 complex, **A**. The disagreement might be understood by taking the low solubility of **A** into consideration, since there might be an equilibrium between 1:1:1- and 1:2:2-complex in the system.

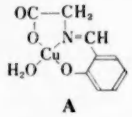

A

Inspection of the chemical quations of the reactions used in this work reveals that the formation of **A** is accompanied by a liberation of acid:

$$CuSO_4 + C_6H_4\langle^{OH}_{CHO} + NH_2CH_2COOH \rightarrow \mathbf{A} + H_2SO_4$$

$$Cu(CH_3COO)_2 + C_6H_4\langle^{OH}_{CHO} + NH_2CH_2COOH \rightarrow \mathbf{A} + 2CH_3COOH$$

In fact, it was ascertained that the solution was considerably strong acid when the reaction was over. Thus, the present work supports the previous conclusion[1] that the cordination of copper(II) with salicylideneglycine stabilizes >C=N- double bond to such an extent that the Schiff base complex is capable of existence even in acid media, where the uncomplexed Schiff base is dissociated.

It may further be speculated that the tremendous effect of this kind, of metal, may play an important role also in the case of the non-enzymatic transamination reaction of pyridoxal[4-6].

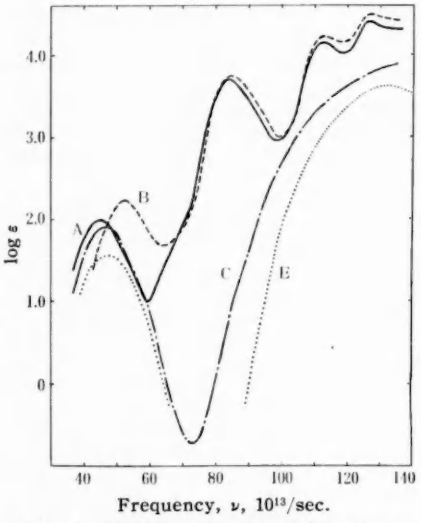

Fig. 1. Visible and ultraviolet absorption spectra of: **A**, *N*-salicylideneglycinato-aquo-copper(II); **B**, sodium *N*-salicylideneglycylglycinato-cuprate(II); **C**, glycylglycinato-aquo-copper(II); **E**, bis-glycinato-copper(II), in aqueous solutions.

3) A. R. Manyak, C. B. Murphy and A. E. Martell, *Arch. Biochem. Biophys.*, **59**, 373 (1955).
4) F. Schlenk and A. Fischer, *Arch. Biochem.*, **12**, 69 (1947).
5) D. E. Metzler, M. Ikawa and E. E. Snell, *J. Am. Chem. Soc.*, **76**, 648 (1954).
6) J. B. Longenecker and E. E. Snell, *Proc. Natl. Acad. Sci.*, **42**, 221 (1956).

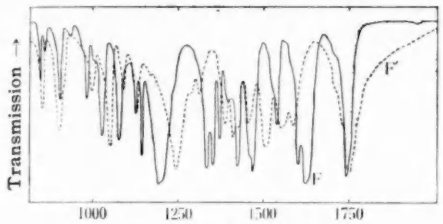

Fig. 2. Infrared absorption spectra of: **F**, copper(II) chelate of *N*-salicylideneglycineethylester; **F'**, hydrochloride of glycineethylester.

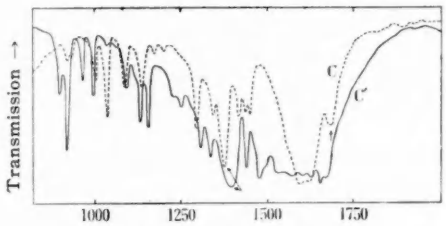

Fig. 3. Infrared absorption spectra of: **C**, glycylglycinato-aquo-copper; **C'**, glycylglycine.

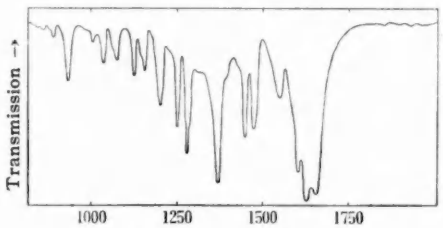

Fig. 4. Infrared absorption spectrum of *N*-salicylideneglycinato-aquo-copper(II), **A**.

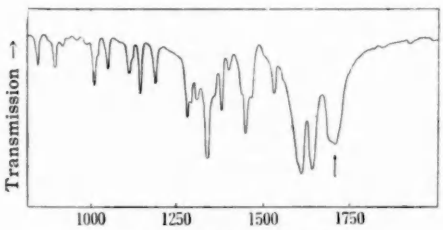

Fig. 5. Infrared absorption spectrum of sodium *N*-salicylideneglycylglycinato-cuprate(II), **B**.

Contrary to the case of *N*-salicylideneglycine which is coordinated to copper(II) ion as a terdentate chelate ligand even at a low pH value, *N*-salicylideneglycylglycine behaves as a quadridentate ligand in neutral or basic media and perhaps as a bidentate in acid media.

Formula **B** corresponds to the structure of the copper(II) chelate in neutral or basic media, while **D** would correspond to that in acid media.

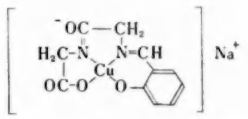

B

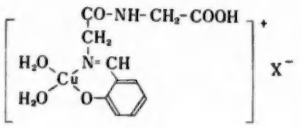

D

Though there is no decisive reason for the latter the fact that it is green in acid media seems to favor the formula, **D**, in which the peptide nitrogen and carboxylate oxygen are detached from the copper.

As to the process of the formation of **A** the first step may be the coordination of copper(II) with glycinate ion, since a deep-blue solution characteristic of copper(II) chelates of amino acids was first observed before any other marked change occurred, regardless of the methods of preparation employed in this investigation. A chelate ligand in coordination very often increases its reactivity on account of the effect of the metal[7]. Therefore, it may be considered that the glycinate ligand in coordination gains greater activity and becomes easier to form the Schiff base with salicylaldehyde. In contrast with this type of reactions, Sato et al.[8] already reported that bis-glycinato-copper(II) reacts with acetaldehyde in a basic solution to give threonine in a very good yield. The difference between the above two reactions may be attributed to the effect of the –OH group in the molecule of salicylaldehyde.

Visible and Ultraviolet Absorption Spectra.—

7) A. E. Martell and M. Calvin, "Chemistry of the Metal Chelate Compounds", New York Prentice-Hall, Inc., New York (1952) p. 336.

8) M. Sato, K. Okawa and S. Akabori, This Bulletin, **30**, 937 (1957).

TABLE I. ABSORPTION MAXIMA OF COPPER(II) COMPLEXES IN THE VISIBLE REGION

Compounds	Solvent	ν_{max} 10^{13} sec^{-1}	log ε_{max}	Type of complexes with respect to the kind of donor atoms
$CuSO_4 \cdot 5H_2O$*	water	36.5	1.09	40
$(NH_4)_4[CuO_6Mo_6O_{18}H_6] \cdot 5H_2O$*,a)	〃	37.1	1.06	40
[Cusalgly(H_2O)]·$4H_2O$, **A**	〃	45.3	1.98	1 N 30
$CuSO_4$·en·$3H_2O$*	1/4 F en·$2HClO_4$ solution	45.3	1.51	
[Cugly$_2$]·H_2O, **E**	water	48.0	1.54	
[Cuala$_2$]·H_2O	〃	48.8	1.54	
[Cu($C_5H_{10}O_2N)_2$]·$2H_2O$*b)	1/100 F ligand solution	49.5	2.04	2 N 20
[Cuglygly(H_2O)]·H_2O, **C**	water	46.5	1.89	
Na[Cusalglygly]·$6H_2O$, **B**	〃	52.2	2.20	
[Cu($NH_3)_4$]$SO_4 \cdot H_2O$*	$(NH_4)_2SO_4 + NH_3$ solution	49.2	1.76	4 N
[Cuen$_2$]$SO_4 \cdot 2H_2O$*	water	54.0	1.85	4 N

* Reported by H. Ito[9].

a) Ammonium hexa-molybdato-cuprate(II).

b) Di-α-methylamino-isobutyrato-copper(II).

Absorption curves of **A** and **B**, and of the copper(II) chelate of glycine, **E**, and glycylglycine, **C**, are shown in Fig. 1. The curves of **C** and **E** consist of two each

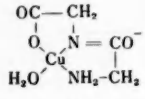

C

of typical absorption bands, whereas both **A** and **B** contain some additional absorption bands in the ultraviolet region. These additional bands apparently belong to the specific absorption bands, being due to the salicylaldimino group of the ligand in coordination. On the other hand, the small absorption bands on each curve in the visible region are the characteristic band of copper(II) complexes. Their numerical data together with those of some other copper(II) complexes are tabulated in Table I. Inspection of Table I reveals that the absorption maximum of **B** is hypsochromically shifted to a considerable degree compared with those of the same type of complexes with respect to the kind of donor atoms. In fact, the color of **B** rather resembles that of bis-ethylenediamine-copper(II) complex, in which all the four donor atoms are nitrogens. From this point of view, it may be supposed[9] that *N*-salicylideneglycylglycinato-cuprate-(II), **B**, belongs to a typical dsp^2-type complex.

Infrared Absorption Spectra. — Infrared absorption curves of **A**, **B**, **C**, and of the copper(II) chelate of *N*-salicylideneglycine-ester, **F**, are shown in Figs. 2—5.

From a comparison of the spectrum of **A** with that of **F**, in which two carboxylate groups of the ligand are protected from coordination by being bound to ethyl groups, it may be concluded that the carboxylate group of **A** is apparently coordinates to copper(II). This is owing to the fact that there is no very strong absorption band in the region of 1700~1740 cm^{-1} on the curve of **A**, contrary to the case of **F**.

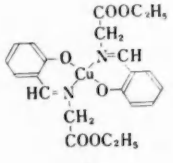

E

The carbonyl peak of the carboxylate groups is usually shifted toward lower frequencies upon coordination[10,11]. In the present case, however, the carbonyl peak which is expected to shift toward lower frequencies can not be assigned, since there are some very strong absorptions of salicylaldimino group of the ligand in the expected region.

In the case of the curve, **C**, the carbonyl peak of the coordinated carboxyl group

9) H. Ito, *J. Chem. Soc. Japan, Pure Chem. Sec.* (*Nippon Kagaku Zasshi*), **78**, 1395 (1956).

10) D. H. Busch and J. C. Bailar, Jr., *J. Am. Chem. Soc.*, **75**, 4574 (1953).

11) S. Kirschner, ibid., **78**, 2372 (1956).

is observed at about 1600 cm^{-1}. Not only the anti-symmetric C–O stretching band, but also the shifting of the symmetric stretching band from 1400 to 1370 cm^{-1} affords an additional evidence for the structure with a coordinated carboxyl group[12].

Of interest is a weak absorption at 1680 cm^{-1}, which is supposed to be concerned with the carbonyl group of the peptide link. The concerned band in the free peptide molecule normally appears at about 1655 cm^{-1} [13].

However, the coordination of copper(II) with the nitrogen atom of peptide may shift the band to some extent. Richard and Thompson[14] have pointed out, for example, that electrophilic substituents on the nitrogen atom can give rise to an increase in the frequency up to 1680 cm^{-1}.

The same kind of shifting of the peptide carbonyl band is more effectively presented in **B**. In this case, however, the absorption band is much stronger than that of **C**; and the degree of shifting is even greater. This fact may indicate that the linkage between copper(II) and peptide nitrogen is stronger in **B** than in **C**, and is consistent with the conclusion that **B** might be a typical dsp^2-type complex.

12) K. Nakamoto, J. Fujita, S. Tanaka and M. Kobayashi, ibid., **79**, 4904 (1957).
13) L. J. Bellamy, "The Infra-red Spectra of Complex Molecules", John Wiley & Sons, Inc., New York (1954), p. 192.
14) R. E. Richards and H. W. Thompson, *J. Chem. Soc.*, **1947**, 1248.

Summary

The two new compounds, *N*-salicylideneglycinato-aquo-copper(II) and sodium *N*-salicylideneglycylglycinato-cuprate(II) were prepared and investigated as to their structure.

Their infrared, visible and ultraviolet absorption spectra together with those of some related compounds were measured and discussed.

The author wishes to express his sincere thanks to Professor R. Tsuchida for his encouragement throughout the course of this work, and to Dr. S. Yamada and Mr. Y. Yamamoto for their valuable discussion.

Inorganic Chemistry Laboratory
South College, Osaka University
Abeno-ku, Osaka

Polymerization of Methyl Methacrylate Initiated by Phenylazo p-Tolyl Sulfone

By Ryoichi UEHARA

(Received May 15, 1959)

Phenylazo *p*-tolyl sulfone was first prepared by Koenigs[1] through the reaction of benzenediazonium chloride with sodium *p*-toluenesulfinate:

$$C_6H_5N_2Cl + CH_3C_6H_4SO_2Na = C_6H_5N_2SO_2C_6H_4CH_3 + NaCl$$

Copolymerization of butadiene and styrene (GR–S rubber) by the use of various arylazo aryl sulfones as initiators have been carried out by Brown[2]. It has been reported by Theobold[3] that solution-polymerization of acrylonitrile in ethanol takes place very smoothly at 40°C by means of phenylazo *p*-tolyl sulfone and a very small amount of cupric chloride. The present author has examined the effect of phenylazo *p*-tolyl sulfone upon the polymerization of methyl methacrylate. Phenylazo *p*-tolyl sulfone was an efficient initiator of the polymerization, but it was not suitable for use in manufacture of polymethyl methacrylate, because the polymer formed was dark orange in color. On the other hand, it appears of interest that dimethylaniline acted as an accelerator for this polymerization. In the present paper, results of experiments about the

1) P. Koenigs, *Ber.*, **10**, 1531 (1877).
2) R. S. Brown, U. S. Pat., 2,527,393 (1950); *Chem. Abstr.*, **45**, 383 (1951).
3) C. W. Theobold, U. S. Pat., 2,584,306 (1952); *Chem. Abstr.*, **46**, 3798 (1952).

relation between the initial rate of polymerization and the concentrations of phenylazo *p*-tolyl sulfone, dimethylaniline and methyl methacrylate are given, and the nature of the initiating reaction is discussed from the standpoint of the reaction kinetics.

The dependence of the initial rate of polymerization (R) upon the concentration of phenylazo *p*-tolyl sulfone ([AZS]) in the solution-polymerization in benzene (concentration of methyl methacrylate, 30%) were studied at 41, 51 and 60°C. As are shown in Fig. 1, the square root dependence of the rate upon the concentration was observed at each temperature. When the logarithms of the initial rates (phenylazo *p*-tolyl sulfone 1.1×10^{-2} mol./l.) were plotted against the reciprocals of the temperatures, a straight line was obtained (Fig. 2). The overall activation energy of the polymerization calculated from the slope of the straight line in Fig. 2 was found to be 12.2 kcal./mol.

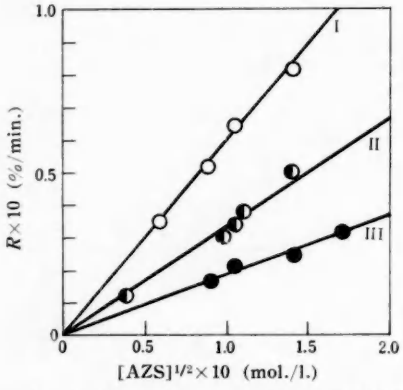

Fig. 1. Dependences of R upon $[AZS]^{1/2}$ at 60 (I), 51 (II) and 41°C (III) ([MMA]=30% in benzene).

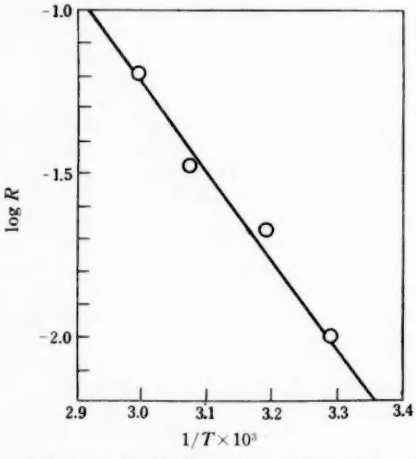

Fig. 2. Relationship between $\log R$ and $1/T$ ([AZS]=1.1×10^{-2} mol./l. and [MMA]=30% in benzene).

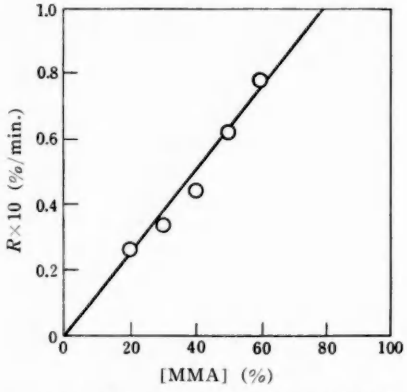

Fig. 3. Correlation of R with [MMA] at 51°C ([AZS]=1.1×10^{-2} mol./l.).

Fig. 3 shows a relationship between the initial rate and the concentration of methyl methacrylate ([MMA]) in benzene (at 51°C and phenlazo *p*-tolyl sulfone 1.1×10^{-2} mol./l.). The rate was linearly proportional to the concentration of methyl methacrylate.

Relationships shown in Figs. 1 and 3 are represented by Eq. 1:

$$R=k_0[AZS]^{1/2}[MMA] \qquad (1)$$

where k_0 is a constant. This equation is quite similar to that which is usually known to hold in the polymerization of vinyl monomers initiated by benzoyl peroxide or α,α'-azo-bis-isobutyronitrile[4]. Eq. 1, therefore, suggests a unimolecular first order decomposition of phenylazo *p*-tolyl sulfone as the initiating reaction of the polymerization.

The polymerization of methyl methacrylate initiated by phenylazo *p*-tolyl sulfone is accelerated by addition of dimethylaniline. When the concentration of phenylazo *p*-tolyl sulfone was kept constant and various amounts of dimethylaniline were added, the initial rate of polymerization was linearly dependent upon the square root of the concentration of dimethylaniline ([DMA]). Fig. 4 shows

4) P. J. Flory, "Principles of Polymer Chemistry", Cornell University Press, Ithaca, N. Y. (1953), p. 116.

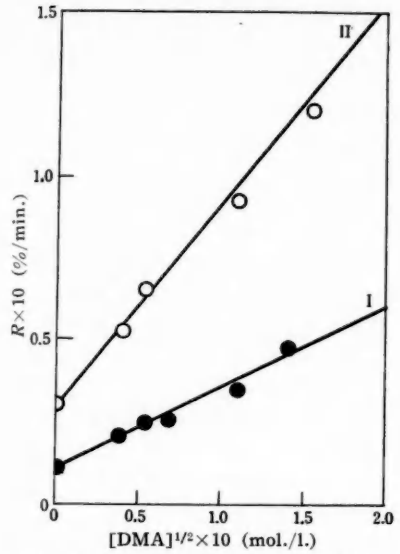

Fig. 4. Correlations of R with $[DMA]^{1/2}$ at 51°C ($[MMA]=30\%$, $[AZS]=0.15\times10^{-2}$ for line I and 0.96×10^{-2} mol./l. for line II).

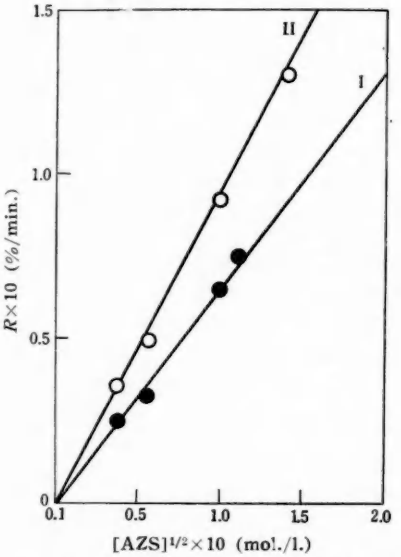

Fig. 5. Correlations of R with $[AZS]^{1/2}$ at 51°C ($[MMA]=30\%$, $[DMA]=0.29\times10^{-2}$ for line I and 1.2×10^{-2} mol./l. for line II).

examples of this relationship (concentration of methyl methacrylate 30%; concentration of phenylazo *p*-tolyl sulfone 0.15×10^{-2} and 0.95×10^{-2} mol./l. at 51°C). In the case when the concentration of dimethylaniline was held constant and that of phenylazo *p*-tolyl sulfone was varied, the initial rate of polymerization was proportional to the square root of the concentration of phenylazo *p*-tolyl sulfone. Examples of this correlation are shown in Fig. 5 (methyl methacrylate 30%, and dimethyl- aniline 0.29×10^{-2} and 1.2×10^{-2} mol./l. at 51°C). It is evident from Figs. 1 and 4 that the polymerization takes place at measurable rates at 51°C by means of phenylazo *p*-tolyl sulfone alone. Therefore, in the case where the concentration of methyl methacrylate is kept constant, the correlations shown in Figs. 4 and 5 can be represented by the following equation:

$$R=k[AZS]^{1/2}+k'[AZS]^{1/2}[DMA]^{1/2} \quad (2)$$

where k and k' are constants.

Eq. 2 suggests that the polymerization of methyl methacrylate by means of phenylazo *p*-tolyl sulfone and dimethylaniline is initiated by two reactions, i.e., a unimolecular first order decomposition of phenylazo *p*-tolyl sulfone and a bimolecular reaction between phenylazo *p*-tolyl sulfone and dimethylaniline, k and k' being the rate constants respectively. From Eq. 2, the following equation is derived:

$$R=k[AZS]^{1/2}(1+k'/k[DMA]^{1/2}) \quad (3)$$

k'/k, the ratio of the rate constants of the two initiating reactions of the polymerization, can be calculated from the slops of the straight lines in Fig. 4. It was found to be 2.00 from line I and 2.18 from line II (at 51°C and methyl methacrylate 30% in benzene).

Imoto and others[5] have reported a rate-concentration equation similar to Eq. 2 or 3 for the polymerization of methyl methacrylate initiated with benzoyl peroxide and dimethylaniline, and suggested a similar mechanism to that mentioned above.

Experimental

Materials.—Purification of methyl methacrylate, dimethylaniline and benzene have been mentioned in a previous paper by the present author[6]. Phenylazo *p*-tolyl sulfone was obtained by addition of sodium *p*-toluenesulfinate (21 g.) into an aqueous solution of benzenediazonium chloride which was prepared from aniline (10 g.), 30%

5) M. Imoto et al., *J. Chem. Soc. Japan, Ind. Chem. Sec.* (*Kogyo Kagaku Zasshi*), **58**, 451 (1955).
6) R. Uehara, This Bulletin, **31**, 685 (1958).

aqueous HCl (40 cc.) and $NaNO_2$ (8 g.). The crude product was recrystallized three times from pure methanol, giving pure phenylazo *p*-tolyl sulfone (17.5 g.), m. p. 87.5°C with decomposition (83.5°C by Brown[2]). This compound was not quite stable at room temperature under sunlight. In a colorless, transparent glass vessel, it changed into a resinous meterial during several weeks in summer.

Polymerization. — Polymerization was carried out in sealed test tubes which were 15 mm. in diameter and 10 cm. in height and made of brown-colored glass so as to reduce the effects of sunlight upon the polymerization. Phenylazo *p*-tolyl sulfone was dissolved in benzene. Methyl methacrylate was cooled in an ice-salt bath. Measured amounts of the benzene-solution and methyl methacrylate were placed in a test tube and mixed. The test tube was immersed in a dry ice-methanol bath and flushed with nitrogen and sealed. The extent of the polymerization was estimated from the weight of polymethyl methacrylate, and the rate of polymerization was expressed in unit of per cent per minute. Details of the procedures of the polymerization and the determination of the initial rate of polymerization have been reported previously[6].

Summary

The effects of phenylazo *p*-tolyl sulfone upon the polymerization of methyl methacrylate were examined. In the solution-polymerization in benzene, the initial rate of polymerization was linearly dependent respectively upon the square root of the concentration of phenylazo *p*-tolyl sulfone and upon the concentration of methyl methacrylate. A unimolecular first order decomposition of phenylazo *p*-tolyl sulfone is suggeted as the initiating reaction of the polymerization. Dimethylaniline acted as an accelerator for this polymerization. In this case, the initial rate of polymerization was linearly proportional to the square root of each of the concentrations of phenylazo *p*-tolyl sulfone and dimethylaniline. A bimolecular reaction between phenylazo *p*-tolyl sulfone and dimethylaniline has been proposed for the acceleration of the polymerization.

The author wishes to express his hearty thanks to Professor Osamu Simamura of the University of Tokyo for his interests in this work and Mr. Tsurahide Cho, the President of Tama Kagaku Kogyo Co. for permission to publish this work.

Tama Kagaku Kogyo Co.
2-28 *Minamirokugo*
Ota-ku, Tokyo

---

*Synthesis of 3,6-Dimethyl-2,3-dihydro-1H-cyclopent[a]anthracene. A Possible Dehydrogenation Product of Anthranoid Rearrangement Product of Steroids**

By Masao NAKAZAKI and Sachihiko ISOE

(Received February 11, 1959)

A number of works have been accumulated on the dienone-phenol rearrangement of the steroid A ring, and there can be found scrupulous studies on the structures of the products of this rearrangement[1], the relation between the products and the reaction conditions[2], and the effects of the structures on the rearrangement course[3]. Stimulated by these studies on steroids, various model compounds were synthesized and the same pattern of reaction was demonstrated[4].

* A preliminary note appeared in *Chem. & Ind.*, **1958**, 43.

1) H. Minlon, *Naturwissenschaften*, **36**, 765 (1938); R. B. Woodward, H. H. Inhoffen, H. O. Larson and K. H. Menzel, *Chem. Ber.*, **86**, 594 (1955); and Inhoffen's preceeding papers, **1940—1953**.

2) A. S. Dreiding and Ann Voltman, *J. Am. Chem. Soc.*, **68**, 1715 (1946); A. S. Dreiding, W. J. Pummer and A. J. Tomosewski, ibid., **75**, 3159 (1953).

3) A. L. Wilds and C. Djerassi., ibid., **68**, 1715 (1946); and numerous studies by Djerassi, ibid., **70**, 1911, 3962 (1948); **72**, 4540 (1950); **73**, 990, 1523 (1951); **76**, 1741 (1954); and *J. Org. Chem.*, **15**, 896 (1950).

4) R. B. Woodward and T. Singh, *J. Am. Chem. Soc.*, **72**, 494 (1950); R. T. Arnold, ibid., **71**, 1781 (1949); **69**, 2322 (1947); **72**, 3153 (1950); F. M. Marbell and E. Magoon, ibid., **77**, 2542 (1955); **76**, 5118 (1954).

But, as to the dienone-phenol rearrangement of the steroid B ring[5], thorough study is still lacking and the structures of the rearrangement products have remained obscure. Tsuda's group[6] was the first to carry out the structural study of a dienone-phenol rearrangement product of the steroid B ring. Namely, 7-keto-5,8(9)-cholestadien-3β-yl acetate (I)[6,7], prepared by chromic acid oxidation of 5,8(9)-cholestadien-3β-yl acetate in acetic acid, was treated with concentrated sulfuric acid in acetic anhydride to give phenol acetate(IIa). After hydrolysis of IIa with ethanolic potassium hydroxide to a phenol IIb, m. p. 261~265°C, they submitted this phenol to selenium dehydrogenation to obtain, among other products, a hydrocarbon (oil) $C_{19}H_{18}$ in the form of picrate, m. p. 133.5~134°C. The ultraviolet absorption which showed an anthracene type pattern, was attributed by them to the structure IV, and consequently structure IIb was assumed for the phenol, m. p. 261~265°C.

This type of rearrangement is not the only one which can convert the perhydrophenanthrene skeleton of steroids into the perhydroanthracene skeleton, but a smooth "anthrasteroid" rearrangement studied by Mosettig and coworkers[8] can be counted as another type of conversion leading to the anthracene skeleton. Tsuda and coworker[9] also carried out a modification of "anthrasteroid" rearrangement of $\Delta^{5,8}$-cholestadien-3β-ol to the product III, in the presence of mercuric acetate and toluenesulfonic acid in ethanol under the influence of strong irradiation[10]. Dehydrogenation of product III with selenium afforded the same hydrocarbon $C_{19}H_{18}$, which they obtained from II previously. Since 3,6-dimethyl-2,3-dihydro-1-*H*-cyclopent[*a*]anthracene (IV) is a dehydrogenation product to be expected from the "anthranoid rearrangement" product and corresponds to Diels' hydrocarbon usually obtained by the dehydrogenation of steroids, the synthesis of this compound IV is considered to be important[11]. In this paper we report the synthesis of compound IV.

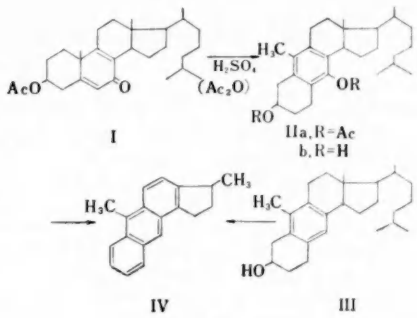

Fig. 1

Whereas the synthetic routes to the phenanthrene type dehydrogenation products of steroids have been well explored[12], there have been few to prepare the anthracene type like IV. Compound VII appears to be the most promising starting material which could be transformed into IX by Johnson's modification of Stobbe condensation[13](Fig. 2). 1-Methyl-2-naphthoic acid (VIa), prepared either

5) D. H. R. Barton and B. R. Thomas, *J. Chem. Soc.*, **1953**, 1842, converted 7-ketolanosta-5,8-dien-3β-yl acetate into "isomeric phenol" by boiling with acetic acid and zinc dust. P. Bladon, *J. Chem. Soc.*, **1955**, 2176, obtained a phenol from 3β-acetoxylumista-5,8 (9), 20-trien-7-one (λ_{max} 246 mμ, ε 11,800) by the action of acetic acid and zinc dust, and discussed the structure. They also pointed out another possible route of dienone-phenol rearrangement by methyl migration.

6) K. Tsuda, K. Arima and R. Hayatsu, *J. Am. Chem. Soc.*, **76**, 2933 (1954). Compound I shows ultraviolet absorption at λ_{max} 238 mμ (log ε 4.475), $[\alpha]_D^{22}$−67.3°. m. p. 151~152°C. Semicarbazone: m. p. 210~212°C (decomp.). The same compound prepared by Inhoffen by another route has m. p. 169~170°C $[\alpha]_D^{20}$−9°, λ_{max} 248 mμ, ε 12,800 (methanol). H. H. Inhoffen and W. Menzel, *Chem. Ber.*, **87**, 146 (1954).

7) Other steroids possessing 5,8(9)-dien-7-one structure show maxima of ultraviolet absorption as follows: 3β-hydroxy-5,8(9), 20-ergostatrien-7-one, λ_{max} 247 mμ (ε 21,000) (D. C. Burke, J. H. Turnbull and W. Wilson, *J. Chem. Soc.*, **1953**, 3237); 3β-acetoxy-5,8(9), 20-ergostatrien-7-one, λ_{max} 245 mμ (ε 11,800) (J. Elks, R. M. Evans, A. G. Long and G. H. Thomas, ibid., **1954**, 451); λ_{max} 246 mμ (ε 12,800) (J. Elks, R. M. Evans, J. F. Oughton and G. H. Thomas, ibid., **1954**, 463).

8) E. Mosettig and I. Scheer, *J. Org. Chem.*, **17**, 764 (1952); W. R. Nes and E. Mosettig, *J. Am. Chem. Soc.*, **75**, 2787 (1953); **76**, 3182, 3186 (1954); W. R. Nes, ibid., **78**, 193 (1956); I. Scheer, W. R. Nes and P. B. Smeltzer, ibid., **77**, 3300 (1955); W. R. Nes, R. B. Kostic and E. Mosettig, ibid., **78**, 36 (1956). We would like to propose the general term "anthranoid rearrangement" for all rearrangements of steroids to the compounds possessing an anthracene skeleton, and to restrict the term "anthrasteroid rearrangement" to the type of Mosettig's reaction.

9) K. Tsuda and R. Hayatsu, *J. Am. Chem. Soc.*, **77**, 3089 (1955).

10) Being a photochemical reaction accompanied by simultaneous dehydrogenation, the mechanism appears complicated. But the product is in sharp contrast to the product of Mosettig's rearrangement in maintaining the 3-hydroxyl group unattacked.

11) After we completed the synthesis of IV, A. W. Burgstahler, *J. Am. Chem. Soc.*, **79**, 6047 (1957), published a paper in which he described an elegant proof of the structure of anthracholestatetraene proposed by Mosettig et al.

12) L. F. Fieser and M. Fieser, "Natural Products Related to Phenanthrene", 3rd Ed., Reinhold Pub. Corp., New York (1949), p. 148–154.

13) W. S. Johnson and G. H. Daub, "Organic Reactions", Vol. **6**, John Wiley & Sons, Inc., New York (1951), p. 1.

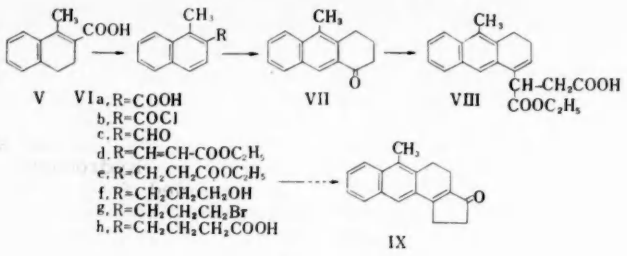

Fig. 2.

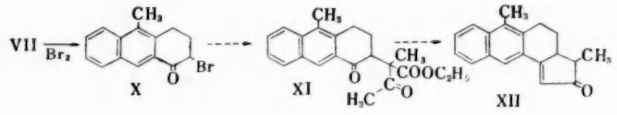

Fig. 3.

by dehydrogenation[14] of V by means of bromine or by the Grignard synthesis from α-(chloromethyl)naphthalene, was converted into the aldehyde VIc via the aicd chloride VIb by means of the Rosenmund reduction with Pd-$BaSO_4$. By the Claisen condensation with ethyl acetate, VIc gave the unsaturated ester VId, which in turn was catalytically hydrogenated to VIe. The alcohol VIf, obtained by lithium aluminum hydride reduction of VIe, was treated with phosphorus tribromide to afford the bromide VIg, which gave the acid VIh by the usual nitrile synthesis and hydrolysis.

The Stobbe condensation of the ketone VII, easily accessible from the acid VIh by Wilds' method[15], led to the formation of VIII, but the ring closure to IX by Johnson's method[16] using zinc chloride was unsuccessful, probably owing to the vulnerability of the α-position of the naphthalene nucleus to the cationoid attack which would direct the ring closure in an undesired direction. Although the plan to build up the D ring by Johnson's method failed, various synthetic routes which can be carried out in a basic medium so as to avoid the complicated side reaction encountered above, were tried with the ketone VII to secure the D ring.

Condensation of the bromoketone X, provided by the bromination of the ketone VII in ether, with potassium ethyl methylacetoacetate[17] in *tert*-butanol failed to give XI, which was expected to afford XII by ring closure.

Another route tried was an indirect one (Fig. 4). The alcohol XVII which would be prepared following the scheme whereby Johnson achieved his brilliant equilenine synthesis[18], might give IV on dehydrogenation accompanied by the simultaneous migration of the angular methyl group to the position originally occupied by the hydroxyl group.

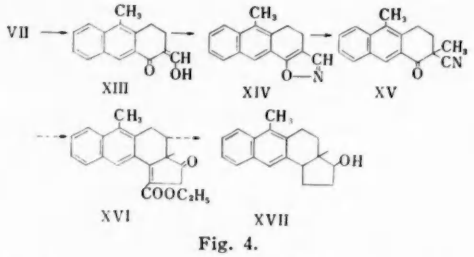

Fig. 4.

The process leading to XV was carried out smoothly, but again the Stobbe condensation of the α-cyanomethylketone to afford XVI was fruitless, probably owing to the ready opening of the ketone XV with the base. The sequence of the steps which finally led to IV is shown in Fig. 5.

14) When dehydrogenation was carried out in acetic acid, the bromination product i was the main product, which could be converted into the lactone ii by hydrolysis with methanolic potassium hydroxide followed by acidification.

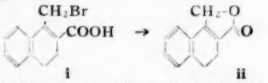

15) A. L. Wilds, *J. Am. Chem. Soc.*, **64**, 1424 (1942).
16) W. S. Johnson and J. W. Peterson, ibid., **67**, 1367 (1945).
17) Wilds succeeded in the same type of condensation using ethyl acetoacetate, *J. Am. Chem. Soc.*, **64**, 1421 (1949).
18) W. S. Johnson et al., ibid., **69**, 2942 (1947).

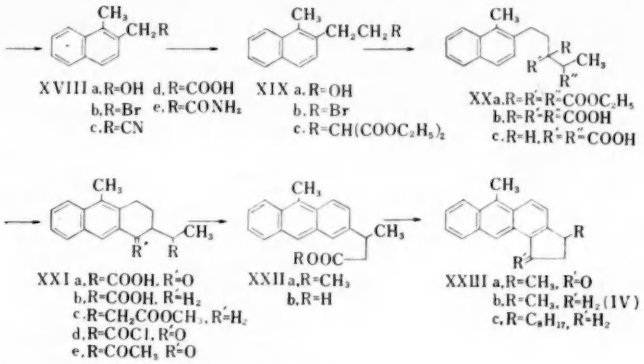

Fig. 5.

1-Methyl-2-naphthoic acid (VIa) was reduced with lithium aluminum hydride to give the alcohol XVIIIa, and its side chain was extended to the homologous alcohol XIXa by the usual sequence of reactions (bromide XVIIIb→cyanide XVIIIc →acid XVIIId→alcohol XIXa). The alcohol XIXa was treated with phosphorus tribromide in benzene to yield the bromide XIXb, which gave the condensation product XIXc with ethyl sodiomalonate.

Condensation of XIXc with ethyl α-bromopropionate in the presence of potassium *tert*-butoxide led to the triester XXa. The tricarboxylic acid XXb obtained by the hydrolysis of XXa with methanolic potassium hydroxide was decomposed to the dicarboxylic acid XXc, which was cyclized to the ketocarboxylic acid XXIa by PCl_5-$SnCl_4$ method of Wilds[15,19], whereas the ring closure using polyphosphoric acid[20] resulted only in the recovery of the starting material.

After the carbonyl group of XXIa was removed by the Clemensen-Martin reduction, the resulting acid XXIb[21] was transformed into the methyl ester of the homologous acid XXIc by the Arndt-Eistert method. Heating with 30% Pd-C at 290~300°C, followed by hydrolysis, converted the ester XXIc into the anthracene derivative XXIIb, m. p. 160~160.5°C, which showed an ultraviolet absorption spectrum characteristic of an anthracene type (see *Experimental*).

The appearance of new bands in the infrared absorption spectrum (11.90 and 12.30 μ) which can be attributed to the 1,2,4-trisubstituted benzene structure[22], together with the characteristic absorption in ultraviolet region, leaves no doubt about the anthracene structure of the compound. The ring closure[23] of the acid XXIIb by PCl_5-$SnCl_4$ method accomplished the ketone XXIIIa, which exhibited infrared absorption band at 5.93 μ (indanone)[24] and 12.2 μ (two adjacent hydrogens on aromatic hydrocarbon). The ultraviolet absorption spectrum which is very close to α-acetylanthracene (see Table I) also confirms the structure of the ketone.

The final stage to IV was the Clemensen-Martin reduction of the ketone XXIIIa. The oily product was purified by chromatography on alumina column to provide colorless crystals, m. p. 78~79.5°C after recrystallization from methanol. The picrate melted at 128~128.5°C (the picrate of Tsuda's hydrocarbon, m. p. 133~134°C), and the 2,4,6-trinitrobenzolate at 142~142.5°C. The ultraviolet absorption spectrum of the hydrocarbon XXIIIb (IV) could in almost every detail be overlapped on the spectrum of Mosettig's hydrocarbon XXIIIc (dehydroanthracholesterol), whereas Tsuda's hydrocarbon showed an anomalous absorption in the long wavelength, presumably owing to impurity[25].

19) To get the methyl ketone XXIe, which would give a five membered D ring was tried in vain. Cf. A. L. Wilds et al., *J. Am. Chem. Soc.*, **69**, 3079 (1947); **66**, 1688 (1944).

20) D. D. Gardner and W. J. Horton, ibid., **74**, 4976 (1953).

21) Two racemates of compound XXIb can be expected, but no attempt was made to separate them.

22) H. Dannenberg, U. Shiedt and W. Sheidle, *Z. Naturforsh.* **B8**, 269 (1953).

23) The reactivity to cationoid attack is much greater at α-position on anthracene than at β-position. Cf. L. F. Fieser and H. Heymann, *J. Am. Chem. Soc.*, **63**, 2333 (1941) and W. S. Johnson, "Organic Reactions", Vol. 2, John Wiley & Sons, Inc., New York (1946). p. 114.

24) H. Dannenberg and D. D. Dannenberg, *Ann.*, **585**, 1 (1954), reported the absorption at 5.92 μ in the similar system.

25) The selenium dehydrognation of IIb may lead, although it is highly unlikely, to another structure than IV, but in the case of dehydrogenation of III to IV, there is no reason to expect serious change of the skeleton.

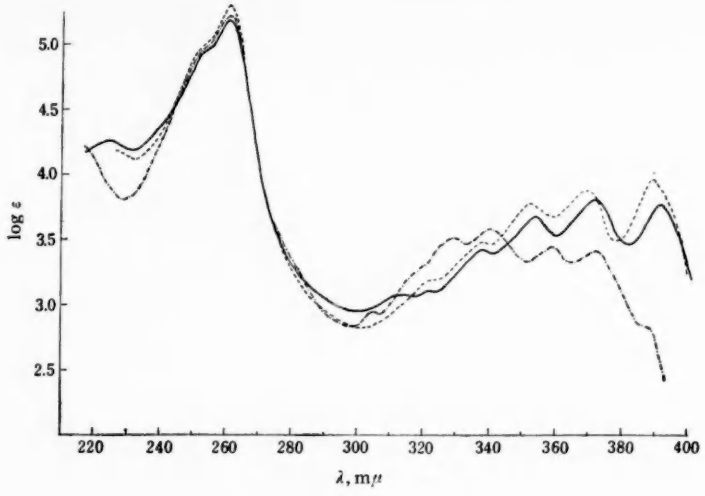

Fig. 6.

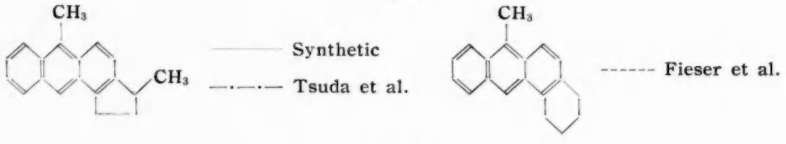

TABLE I.

XXIIIa[1]		α-Acetyl anthracene[2]		IV (synthetic)[3]		IV (Tsuda)[4]		XXIIIc (Mosettig)[5]		1,2,3,4-Tetrahydro-10-methylbeazanthrene[6]	
λ_{max}	log ε	λ_{max}	log ε	λ_{max}	ε	λ_{max}	ε	λ_{max}	ε	λ_{max}	log ε
245	4.72	241	4.76	226	18,040			227	16,550		
263	4.73	254	4.84	238	21,530			234	17,550		
332	3.22	330	3.24	255	93,750						
346	3.49	346	3.53	261	145,200	262	123,600	262	165,000	261	5.3
363	3.66	366	3.71	308	1,270	303	790				
395	3.77	385	3.73	323	1,317	328	3,170				
				338	2,650	341	4,150	338	2,750	336	3.5
				354	4,765	358	4,000	354	5,000	351	3.8
				372	6,690	372	2,980	372	7,420	368	3.9
				393	6,260	388	710	391	7,520	388	4.0

1) In ethanol.
2) In ethanol: R. N. Jones, *J. Am. Chem. Soc.*, **67**, 2127 (1945). β-Acetylanthracene: see R. N. Jones, *Chem. Revs.*, **41**, 353 (1947).
3) In ethanol.
4) In solvent unspecified: K. Tsuda, K. Arima and R. Hayatsu, *J. Am. Chem. Soc.*, **76**, 2933 (1954); K. Tsuda and R. Hayatsu, ibid., **77**, 3089 (1955).
5) In isooctane: W. R. Nes, R. B. Kostic and E. Mosettig, ibid., **78**, 436 (1956).
6) In ethanol: L. F. Fieser and E. B. Hershberg, ibid., **60**, 940, (1938).

Experimental**

Ethyl α-Aceto-γ-phenylbutyrate.—To a stirred and cooled solution of sodium ethoxide prepared from 450 cc. of absolute ethanol and 23 g. of sodium, 143 g. of ethyl acetoacetate was added in an atmosphere of nitrogen, and the reaction mixture was warmed to 60~70°C. After the addition of 197 g. of phenethyl bromide (b. p. 96~98°C/11 mmHg) over a period of 2 hr., the mixture was heated at 70~75°C for 5 hr., 80~85°C

** All ultraviolet spectra were measured with a Beckmann spectrophotometer DK 2, and infrared spectra with a Perkin Elmer Model 12 C. The anlyses were performed in the Microanalytical Laboratory of the Institute of Polytechnics, Osaka City University, Osaka.

for an additional 5 hr., and refluxed for 6 hr. on a water bath. After the solvent was removed, the residue was poured into water, made sligitly acidic with hydrochloric acid, and extracted with ether. The organic layer was washed with water and dried over anhydrous sodium sulfate, and the ether was removed.

The ester distilled at 124~127°C/1 mmHg, and weighed 163 g. (Yield, 69.5%).

1-Methyl-3, 4-dihydro-2-naphthoic Acid.—Ninety grams of ethyl α-aceto-γ-phenylbutyrate was added dropwise to 375 cc. of concentrated sulfuric acid chilled at −4°C with stirring more than 40 min., and the mixture was kept at this temperature for 2 hr. After the reaction mixture was poured on crushed ice, the crystals were collected and washed thoroughly with water. After being dried, they weighed 64.5 g. (yield, 84.2%), and were used in dehydrogenation without further purification. A small portion was recrystallized from petroleum ether, m. p. 127~130°C. (literature[26]: m. p. 129~130°C).

1-Methyl-2-naphthoic Acid (VIa).—*Dehydrogenation of V.*—To a solution of 58 g. of V in 300 cc. of carbon tetrachloride, 54 g. of bromine was added at 65~70°C over a period of 2 hr. with stirring. After additional heating (70~75°C) for 2 hr. with stirring, the mixture was cooled to deposite crystals.

The crude crystalline product (55.6 g.) was dissolved in a solution of 40 g. of sodium hydroxide in 750 cc. of water and the solution was heated on a water bath for 2 hr., and treated with Norit. The alkaline solution was freed from Norit, and made acidic with 1 N hydrochloric acid to afford 34.5 g. of crude VIa (yield, 44.1%), which was recrystallized, m. p. 177.5~178°C (literature[26]: 177~178°C).

Grignard synthesis from α-(chloromethyl)naphthalene.—To a suspension of 35 g. of magnesium in 360 cc. of absolute ether, was added 85 g. of α-(chloromethyl)naphthalene in 200 cc. of ether with stirring for more than 5 hr., and the mixture was refluxed for 1 hr.

The Grignard solution was filtered through glass wool to remove excessive magnesium, and added to a chilled solution of 215 g. of ethyl chlorocarbonate in 160 cc. of ether taking more than 40 min. After being kept at room temperature for 30 min., the mixture was decomposed with dilute sulfuric acid and ice, and the organic layer was washed in turn with water and dilute sodium carbonate solution. Romoval of the solvent gave a liquid, which boiled at 140~143°C/2~3 mmHg and weighed 46.6 g. Hydrolysis of the ester with 20 g. of potassium hydroxide, 25 cc. of water and 50 cc. of methanol gave 28.6 g. of VIa, m. p. 160~170°C. Recrystallization from benzene raised the m. p. to 175~176°C.

1-Bromomethyl-3, 4-dihydro-2-naphthoic Acid (i).—To a solution of 15 g. of V (m. p. 127~130°C) in 60 cc. of glacial acetic acid, a mixture of 13.8 g. of bromine and 20 cc. of acetic acid was added with stirring for more than 1.5 hr. The color of bromine disappeared rather rapidly. The solution was warmed at 55°C for 30 min., and a small amount of sodium sulfite was added to discharge the bromine color.

Crystals, precipitated by the addition of water, were collected and washed with water to give 20 g. of the bromide i, which was recrystallized from benzene to give prismatic crystals, m. p. 177°C (decomp.).

Anal. Found: C, 54.44; H, 4.23; Br, 29.96. Calcd. for $C_{12}H_{11}O_2Br$: C, 53.50; H, 4.15; Br, 29.93%.

The Lactone (ii).—Five grams of i was dissolved in a solution of 5 g. of potassium hydroxide in 1 cc. of water and 30 cc. of methanol, and the solution was refluxed on a water bath for 40 min. After the addition of 30 cc. of water, the alkaline solution was made acidic to precipitate an oil, which was decanted from superfluous liquid. The viscous oil could be crystallized by trituration with a cold dilute sodium hydroxide solution.

Recrystallization from petroleum ether gave the lactone ii melting at 112~113°C.

Anal. Found C, 77.48; H, 5.68. Calcd. for $C_{12}H_{10}O_2$: C, 77.42; H, 5.38%.

1-Methyl-2-naphthoyl Chloride (VIb).—A mixture of 35.0 g. of VIa and 44.5 g. of thionyl chloride was refluxed on a water bath for 2 hr. The excess of thionyl chloride was removed to give an oil, which distilled at 136~138°C/2 mmHg, m. p. 79~80.5°C and weighed 36.5 g. The anilide was recrystallized from ethanol m. p. 212~214°C.

Anal. Found: C, 82.75; H, 6.04; N, 5.55. Calcd. for $C_{18}H_{15}ON$: C, 82.73; H, 5.79; N, 5.36%.

1-Methyl-2-naphthaldehyde (VIc).—A stream of hydrogen was introduced into a stirred mixture of 36.5 g. of VIb and 3.4 g. of 5% Pd/$BaSO_4$[27] in 330 cc. of xylene at 110°C. When the evolution of hydrogen chloride ceased (in about 2 hr.), the reaction mixture was cooled and freed from the catalyst. Removal of the solvent in vacuo followed by distillation gave 15.4 g. of an oil (yield, 50.6%), which solidified gradually on standing. The semicarbazone was recrystallized from dilute acetic acid, m. p. 227~231°C (decomp.).

Anal. Found: C, 69.16; H, 5.61. Calcd. for $C_{13}H_{13}ON_3$: C, 68.70; H, 5.77%.

Ethyl β-(1-Methyl-2-naphthyl)acrylate (VId).—A mixture of 42 cc. of ethyl acetate and 0.3 cc. of absolute ethanol was added all at once to the cooled powdered sodium[28] provided by vigorous stirring of 2.7 g. of molten sodium under refluxing xylene followed by decantation from the xylene. After stirring for 10 min. at −5°C, a solution of 15.2 g. of the aldehyde VIc in 30 cc. of ethyl acetate was added over a period of 1.5 hr. and the mixture was stirred for 1.5 hr. at −6°C. The dark red reaction mixture was decomposed by adding 9 cc. of acetic acid and then 200 g. of ice, and the aqueous layer was extracted with ethyl acetate twice. The combined extract was washed

26) K. V. Auwers and K. Möller, *J. prakt. Chem.*, **109**, 124 (1925).

27) R. Mozingo "Organic Syntheses", Vol. 26, John Wiley & Sons, Inc., New York (1946), p. 77.

28) C. S. Marvel and W. B. King, ibid., Col. Vol. 1, (1948), p. 252.

with water, 5% sodium bicarbonate solution and water. After drying, the solvent was removed to afford a pale yellow liquid, which was distilled to give 10.1 g. of a colorless liquid, b. p. 167～173°C/2 mmHg, (yield, 47%), which solidified on standing and recrystallized from petroleum ether, m. p. 62～63°C.

Anal. Found: C, 80.25; H, 6.97. Calcd. for $C_{16}H_{16}O_2$: C, 79.97; H, 6.71%.

Ethyl β-(1-Methyl-2-naphthyl)propionate (VIe).—Catalytic hydrogenation of 15.3 g. of the unsaturated ester VId with 0.4 g. of 10% Pd/C in 180 cc. of ethanol gave an oil which boiled at 161～162°C/2 mmHg and weighed 11.4 g. (yield, 75%).

Anal. Found: C, 79.59; H, 7.71. Calcd. for $C_{15}H_{18}O_2$: C, 79.31; H, 7.49%.

3-(1-Methyl-2-naphthyl)-1-propanol (VIf).—To a slurry of 0.95 g. of lithium aluminum hydride in 40 cc. of ether, a solution of 5.4 g. of the ester VIe in 20 cc. of ether was added with stirring. After refluxing for 1 hr., the excess of the reducing reagent was decomposed by adding 4 cc. of ethyl acetate and then 25 cc. of water and 15 cc. of concentrated hydrochloric acid. The organic layer was washed with water, 5% sodium bicarbonate solution and water again. After drying over anhydrous magnesium sulfate, the solvent was removed to give an oil, which was purified by distillation in vacuo, b. p. 173～174°C/3 mmHg. 4.1 g. (yield, 91.9%). The phenylurethane was recrystallized from benzene-petroleum ether, m. p. 113～114°C.

Anal. Found; C, 78.96; H, 7.03. Calcd. for $C_{21}H_{21}O_2N$: C, 78.97; H, 6.63%.

1-Bromo-3-(1-methyl-2-naphthyl)-propane (VIg).—A solution of 5.0 g. of the alcohol VIf in 19 cc. of benzene was added dropwise to a stirred mixture of 5.0 g. of phosphorus tribromide and 125 cc. of benzene. After heating at 70～75°C for 4 hr., the mixture was poured into ice water and saturated with sodium chloride. The benzene layer was separated, and the aqueous layer was extracted with ether. The combined benzene solution and ether were washed with water and dried over anhydrous magnesium sulfate. The residue freed from the solvent was distilled at 135～136°C/0.002 mmHg, to give the bromide VIg weighing 5.2 g. (yield, 80.4%).

3-(1-Methyl-2-naphthyl)-1-propanecarboxylic Acid (VIh).—A mixture of 5.2 g. of the bromide VIg, 89 cc. of ethanol, 5.0 g. of potassium cyanide and 20 cc. of water was refluxed for 26 hr. After removal of the ethanol, the mixture was poured onto ice, acidified with 20 cc. of concentrated hydrochloric aicd, and extracted with ether.

After removal of the ether the residual oil was hydrolyzed by boiling with 59 cc. of acetic acid and 33 cc. of concentrated hydrochloric acid for 7 hr., while 1.2 cc. of concentrated hydrochloric acid was added every hour. The crystals deposited on cooling melted at 123～125°C and weighed 4.3 g. (yield, 94.6%). Recrystallization from benzene-petroleum ether raised the melting point to 126～127°C.

Anal. Found: C, 79.62; H, 7.05. Calcd. for $C_{15}H_{16}O_2$: C, 78.92; H, 7.06%.

1-Oxo-10-methyl-1, 2, 3, 4-tetrahydroanthracene (VII).—To a solution of 5.1 g. of the carboxylic acid VIh in 44 cc. of dry benzene, 9.2 g. of phosphorus pentachloride was added. After stirring at room temperature for 1 hr., the mixture was heated for 10 min. at 45～50°C, and then a solution of 28.6 g. of stannic chloride in 22 cc. of benzene was added to the chilled solution. The orange-red solution was stirred for 50 min. with cooling in an ice bath, and was decomposed with 200 cc. of water. Addition of 22 cc. of concentrated hydrochloric acid was followed by extraction with ether, and the organic layer was washed with water, 1 N sodium hydroxide solution and water. After drying over anhydrous magnesium sulfate, the solvent was removed to give a solid weighing 4.3 g. (yield, 91.7 g.), which was recrystallized from methanol, m. p. 99.5～100.5°C, 4.0 g. An infrared absorption spectrum indicated a peak at 5.97 μ.

Anal. Found: C, 85.95; H, 7.62. Calcd. for $C_{15}H_{14}O$: C, 85.68; H, 6.71%.

The Stobbe Condensation of VII.—In a stream of nitrogen, 1.2 g. of potassium was dissolved in 22 cc. of *tert*-butanol. To the solution was added a mixture of 5.4 g. of the ketone VII, 7.2 g. of diethyl succinate and 7.5 g. of *tert*-butanol and the mixture was heated at 110°C for 50 min. To the cooled solution, 8.5 cc. of concentrated hydrochloric acid and 50 cc. of water was added, the separated brown oil was extracted with ether. After being washed with water, the ether layer was extracted with three portions of 160 cc. of 1 N ammonia water to separate the half ester VIII. The turbid solution was cleared with Norit, and was acidified with 4 N hydrochloric acid to precipitate an oil, which was extracted with ether. The ether extract was washed with water and dried over anhydrous magnesium sulfate. To the brown residue (5.3 g.) was added 50 cc. of acetic acid and then a solution of 25 cc. of acetic acid and 1.5 g. of zinc chloride. The solution was heated on a free flame for 5 hr. The reaction mixture turned blue-black in color, and was filled with a voluminous amorphous solid, from which no traceable material was isolated.

1-Oxo-2-bromo-10-methyl-1, 2, 3, 4-tetrahydroanthracene (X).—To a chilled suspension of 2.6 g. of the ketone VII in 20 cc. of ether, a solution of 2.0 g. of bromine in 10 cc. of ether was added over a period of 10 min. with stirring. After stirring at room temperature for 2 hr., precipitated crystals were collected and recrystallized from methanol-acetone (3 : 1), m. p. 136～137°C. Yield, 2.7 g.

Anal. Found: C, 62.46; H, 4.71. Calcd. for $C_{15}H_{13}OBr$: C, 62.28; H, 4.50%.

The Condensation of the Bromoketone X with Ethyl Methylacetoacetate.—To a cold solution of potassium *tert*-butoxide prepared from 0.33 g. of potassium and 11 cc. of *tert*-butanol, 1.35 g. of ethyl methylacetoacetate was added and the mixture was stirred for 5 hr. at room temperature in an atmosphere of nitrogen. After a solution

of 2.4 g. of the bromoketone X in 28 cc. of dry benzene was added taking more than 10 min., the reaction mixture was stirred at room temperature for 5 min., and refluxed for 1.5 hr. The solution was acidified with 10 cc. of 1 N hydrochloric acid and ice, and the organic layer was in turn washed with water and 2% sodium hydroxide solution. Removal of the solvent gave a brown oil (3.4 g.) from which no traceable material was isolated by chromatographic adsorption on alumina.

1-Oxo-2-oxymethylene-10-methyl-1, 2, 3, 4-tetrahydroanthracene (XIII).—To pulverized sodium methoxide prepared from 0.82 g. of sodium and 20 cc. of methanol, a solution of 2.64 g. of ethyl formate in 30 cc. of benzene was added with stirring and cooling in a gentle stream of nitrogen. A mixture of 3.7 g. of the ketone VII and 40 cc. of benzene was added dropwise with stirring for more than 17 min. The color of the solution changed from yellow-green to green-yellow. After heating at 8~20°C for 6 hr., ice water was added to precipitate the sodium salt of the oxymethylene ketone XIII, which was separated and washed with water. A reddish brown oil, separated on addition of hydrochloric acid to the aqueous solution of the sodium salt, was extracted with ether and the extract was washed with water and dried. Removal of the solvent gave 3.9 g. of a viscous oil, which showed a violet color reaction with ferric chloride and was used directly to prepare the isoxazole XIV.

The Isoxazole XIV.—To a solution of 3.90 g. of the crude oxymethylene ketone XIII in 144 cc. of acetic acid, was added 1.67 g. hydroxylamine hydrochloride and the mixture was heated at 75~80°C for 7 hr. After the solvent (about 120 cc.) was removed by evaporation in vacuo, 100 cc. of water was added to the mixture to precipitate an oil, which solidified upon standing. The crude isoxazole (3.65 g.) was recrystallized from diluted methanol to give needles melting at 111~112°C.

Anal. Found: C, 81.61; H, 5.67; N, 6.46. Calcd. for $C_{16}H_{13}ON$: C, 81.68; H, 5.57; N, 5.94%.

The Cyanoketone XV.—To a solution of potassium *tert*-butoxide provided from 1.68 g. of potassium and 47 cc. of *tert*-butanol, was added 3.15 g. of the isoxazole XIV, and the mixture was heated for 10 min. at 70°C. To the orange-red solution, 13.5 cc. of methyl iodide was added taking more than 7 min. at 70~73°C. After heating at 75°C for 25 min. the solvent was removed and water was added to precipitate crystals. They were collected and washed with water, m. p. 141~142°C. Yield, 3.25 g. The melting point was raised by recrystallization from ethanol to 142~143°C.

Anal. Found: C, 82.21; H, 6.16; N, 5.93. Calcd. for $C_{17}H_{15}ON$: C, 81.90; H, 6.06; N, 5.62%.

The Stobbe Condensation of the Cyanoketone XV.—To a solution of potassium *tert*-butoxide prepared from 0.75 g. of potassium and 30.5 cc. of *tert*-butanol, was added 6.8 cc. of diethyl succinate taking more than 5 min. with stirring and cooling, and then 2.15 g. of the cyanoketone XV. The mixture was stirred for 2 hr. at room temperature, heated at 50°C for 1 hr., and then stirred for 5 hr. at room temperature. After being kept overnight, 20 cc. of 2 N hydrochloric acid solution was added with cooling, when carbon dioxide was evolved. After removal of the solvent in vacuo at 40°C, the aqueous layer was extracted with ether, from which the acidic material was transferred into 5% potassium hydroxide solution. Upon evaporation of the ether, the organic layer gave a small amount of a solid melting at 220~221°C after recrystallization from benzene.

Anal. Found: C, 81.22; H, 6.90%.

This was not investigated further because of the small amount available. The alkaline solution which contained the acidic material was acidified with hydrochloric acid to afford a very viscous oil, which was not studied further.

1-Methyl-2-hydroxymethyl-naphthalene (XVIIIa).—To a slurry of 5.75 g. of lithium aluminum hydride in 120 cc. of ether, a solution of 16 g. of 1-methyl-2-naphthoic acid in 340 cc. of ether was added taking more than 30 min., and the mixture was refluxed for 1 hr. on a water bath. After the excess of the reducing reagent was destroyed with ethyl acetate, the white voluminous precipitate was dissolved in dilute hydrochloric acid, and extracted with ether. The ether extract was washed with water, sodium bicarbonate solution and water. Removal of the solvent gave 14.0 g. of crystals melting at 124~126°C, which were recrystallized from benzene, m. p. 126~126.5°C.

. *Anal.* Found: C, 83.88; H, 7.26. Calcd. for $C_{12}H_{12}O$: C, 83,69; H, 7.02%.

1-Methyl-2-bromomethyl-naphthalene (XVIIIb).—To a solution of 25.3 g. of the alcohol XVIIIa in 90 cc. of acetic acid, 63 g. of acetic acid saturated with hydrobromic acid was added for more than 15 min. After the solution was heated at 50~52°C for 20 min., the precipitate was collected (35.1 g.). Recrystallization from acetic acid afforded crystals melting at 68~69°C, 41.3 g. (yield, 90.6%).

For analysis this was further recrystallized from ligroin to give crystals melting at 69~70°C.

Anal. Found: C, 61.37; H, 4.97. Calcd. for $C_{12}H_{11}Br$: C, 61.28; H, 4.68%.

1-Methyl-2-cyanomethyl-naphthalene (XVIIIc).—A mixture of 10 g. of the bromide XVIIIb, 100cc. of ethanol, 5.0 g. of potassium cyanide and 20 cc. of water was refluxed for 5.5 hr. After the ethanol was removed, 300 cc. of water was added to the solution to precipitate a solid which showed m. p. at 75.5~76.5°C after recrystallization from ligroin, and weighed 7.2 g. (yield, 93.5%).

Anal. Found: C, 85.97; H, 6.24; N, 7.98. Calcd. for $C_{13}H_{11}N$: C, 86.16; H, 6.12; N, 7.73%.

(1-Methyl-2-naphthyl)-acetic Acid (XVIIId) and its Amide (XVIIIe).—A mixture of 6.8 g. of the cyanide XVIIIc, 10 cc. of acetic acid, 10 cc. of concentrated hydrochloric acid and 10 cc. of water was refluxed for 30 min. After cooling, crystals (m. p. 146~158°C) were collected and washed with 5% sodium hydroxide solution to remove the acid XVIIId. The amide could be further hydrolyzed with concentrated hydrochloric acid and acetic acid to give the acid

XVIIId.

Anal. Found: C, 78.36; H, 6.60; N, 7.05. Calcd. for $C_{13}H_{13}ON$: C, 78.36; H, 6.58; N, 7.03%.

The alkaline extract was acidified to precipitate the acid XVIIId which was recrystallized from benzene to afford prisms, m. p. 165~166°C, weighed 5.7 g.

Anal. Found: C, 78.00; H, 6.03. Calcd. for $C_{13}H_{12}O_2$: C, 77.98; H, 6.04%.

When an attempt was made to hydrolyze the crude cyanide XVIIIc directly, the overall yield of the acid was 83%.

2-(1-Methyl-2-naphthyl)-ethanol (XIXa).—To a slurry of 5.03 g. of lithium aluminum hydride in 120 cc. of ether, was added a solution of 14 g. of the acid XVIIId in 300 cc. of ether with stirring for more than 30 min., and the mixture was refluxed for 3 hr. The excess of the reducing reagent was destroyed with 20 cc. of ethyl acetate, and the mixture was decomposed with dilute hydrochloric acid.

The organic layer was separated and the aqueous layer was extracted with ether. After drying, removal of the ether gave an oil, which was distilled to give a liquid boiling at 140~143°C/1 mmHg and weighing 11.7 g. (yield, 90.0%). For analysis a small sample was recrystallized from ligroin, m. p. 54~55°C.

Anal. Found: C, 83.95; H, 7.63. Calcd. for $C_{13}H_{14}O$: C, 83.83; H, 7.58%.

1-Bromo-2-(1-methyl-2-naphthyl)-ethane (XIXb).—To a solution of 17.5 g. of the alcohol XIXa in 60 cc. of benzene, 19 g. of phosphorus tribromide in 24 cc. of benzene was added taking more than 25 min., and the mixture was stirred for 3 hr. at 60~70°C. The reaction mixture was poured onto crushed ice, and the bromide was taken into ether. After the ether layer was washed with saturated sodium chloride solution and water, it was dried over anhydrous sodium sulfate. Removal of the solvent gave a liquid, which was distilled to afford the bromide XIXb, boiling at 124~126°C/0.006 mmHg and weighing 14.4 g. (yield, 61.5%).

Anal. Found: C, 63.10; H, 5.50. Calcd. for $C_{13}H_{13}Br$: C, 62.60; H, 5.23%.

Diethyl 1-(1-Methyl-2-naphthyl)-3, 3-propanedicarboxylate (XIXc).—Under 40 cc. of xylene, 2.52 g. of sodium was pulverized, and the xylene was decanted off and replaced by 18 cc. of benzene. To this mixture, 16.2 cc. of absolute ethanol was added for more than 5 min., and heated for 5 min. After 25.2 cc. of diethyl malonate was added over a period of 10 min., the solution was heated for 10 min. on a water bath, and a solution of 14.3 g. of the bromide XIXb in 118 cc. of benzene was added taking more than 20 min. Then the mixture was heated at 60~63°C for 8 hr. at 70°C for 2 hr., and refluxed for an additional 4 hr. The solution was poured onto ice, acidified with diluted hydrochloric acid, and extracted with ether. The ether extract was washed with water and dried. The residue, obtained by evaporation of the solvent, was distilled to give an oil, b. p. 160~165°C/0.005 mmHg. Yield, 18.1 g. (96.3%).

Anal. Found: C, 72.00; H, 7.41. Calcd. for $C_{20}H_{24}O$: C, 73.14; H, 7.37%.

Triethyl 5-(1-Methyl-2-naphthyl)-2, 3, 3-pentanetricarboxylate (XXa).—To a solution of potassium *tert*-butoxide in *tert*-butanol, provided from 1.1 g. of potassium and 26 cc. of *tert*-butanol in an atmospher of nitrogen, 8.0 g. of the diethyl ester XIXc was added, the mixture was stirred for 3 min. at room temperature, and 5.4 g. of ethyl α-bromopropionate was added for more than 10 min. The solution was stirred for an additional 30 min. After the *tert*-butanol was removed, the residue was poured into ice water and extracted with ether. After washing with water and drying, the solvent was removed to leave an oil, which was distilled at 195~200°C/0.006~0.008 mmHg. Yield, 9.5 g. (91.5%).

Anal. Found: C, 70.08; H, 7.59. Calcd. for $C_{25}H_{32}O_6$: C, 70.07; H, 7.53%.

5-(1-Methyl-2-naphthyl)-2, 3-pentanedicarboxylic Acid (XXc).—A solution of 11.7 g. of the ester XXa in 40 cc. of methanol was added to a solution of 26.5 g. of potassium hydroxide in 93 cc. of methanol and the mixture was refluxed for 1 hr., to precipitate the potassium salt. Water (34 cc.) was added and the mixture was refluxed for 2 hr. After the addition of 30 cc. of water, the methanol was removed and 50 cc. of water was added to the solution. Unsaponified material was removed with ether, and the aqueous layer was acidified with 6 N hydrochloric acid. The tricarboxylic acid was extracted with ether. The ether was removed to give a semisolid which was decarboxylated by heating at 180~185°C. The acid was taken into 10% sodium hydorxide solution, precipitated with 6 N hydrochloric acid, and then extracted with ether. Removal of the ether gave 8.5 g. of tan-yellow semisolid, which was cyclized to XXa without further purification.

α-2-(10-Methyl-1-oxo-1, 2, 3, 4-tetrahydroanthryl)-propionic Acid (XXIa).—To a solution of 3.8 g. of the dicarboxylic acid XXc in 30 cc. of benzene, 9.7 g. of phosphorus pentachloride was added with stirring, and the mixture was heated at 20°C for 1 hr., and at 45°C for 5 min. To the cold stirred solution, a solution of 37.0 g. of stannic chloride in 15 cc. of benzene was added taking more than 5 min., and the mixture was stirred for 1 hr. at room temperature. The mixture was poured onto a mixture of 200 g. of ice and 30 cc. of concentrated hydrochloric acid, and extracted with ether. The ether extract was washed with water and shaken with 10% sodium hydroxide solution to extract the acid XXIa. The ketoacid (1.15 g., m.p. 179.5~181.5°C) was obtained by acidification followed by extraction with ether, and recrystallized from benzene to give needles melting at 181~182°C.

Anal. Found: C, 76.58; H, 6.59. Calcd. for $C_{18}H_{18}O_3$: C, 76.57; H, 6.45%.

The infrared spectrum indicated peaks at 6.00 and 5.90 μ.

α-2-(10-Methyl-1, 2, 3, 4-tetrahydroanthryl)-propionic Acid (XXIb).—A mixture of 1.0 g. of the ketoacid XXIa, 5 g. of zinc amalgam, 6 cc. of acetic acid and 6 cc. of concentrated hydrochloric acid was covered with a layer of 4 cc. of toluene

and the whole was refluxed for 24 hr., while 1 cc. of concentrated hydrochloric acid was added to the solution every four hours (5 cc. in total). The solution, freed from excessive zinc, was diluted with water and extrated with ether. After the ether layer was washed with water and dried over anhydrous sodium sulfate, the solvent was removed to give crystals melting at 133~154°C and weighing 0.48 g. From mother liquor the second crop (0.28 g.) was obtained, m. p. 133~138°C. The combined material was recrystallized from dilute methanol to give a mixture of stereoisomers of the acid XXIb. The infrared spectrum showed peaks at 5.85 μ and lacked the carbonyl band at 6.00 μ of the ketocarboxylic acid XXIa.

Anal. Found: C, 80.87; H, 7.66. Calcd. for $C_{18}H_{20}O_2$: C, 80.56; H, 7.51%.

Methyl β-2-(10-Methyl-1, 2, 3, 4-tetrahydroanthryl)-butyrate (XXIc).—To a solution of 1.58 g. of the carboxylic acid XXIb in 19 cc. of benzene, 5 cc. of thionyl chloride was added and the mixture was heated on a water bath for 1 hr. After removal of the thionyl chloride and benzene in vacuo, 10 cc. of benzene was added and the solvent was evaporated so as to remove the excess of the thionyl chloride completely, and the residue was dissolved in 20 cc. of cold benzene. This solution of the acid chloride was added to a dried etheral solution of diazomethane provided from 6.3 g. of nitrosomethylurea. The reaction mixture was allowed to stand in an ice bath for 50 min., and at room temperature for 3 hr., while vigorous effervescence was observed. After the solvent was evaporated below 25°C, the residue was dissolved in 20 cc. of methanol and the solution was added to a slurry of 0.4 g. of silver oxide in 40 cc. of methanol and the mixture was refluxed for 2 hr.[29] The solution was filtered, and 0.2 g of silver oxide was added. After refluxing for 30 min., again 0.2 g. of silver oxide was added and the mixture was refluxed for an additional 30 min. After filtering off the silver and silver oxide, the solvent was removed to give a viscous liquid weighing 1.38 g., which was directly dehydrogenated to the ester XXIIa.

β-(10-Methyl-2-anthryl)-butyric Acid (XXIIb).—A mixture of 1.35 g. of the methyl ester XXIc and 0.2 g. of 30% Pd/C[30] was heated in an atmosphere of nitrogen at 250~280°C for 12 min. at 290~300°C for 1 hr. and at 310°C for 30 min. The reaction mixture was taken into boiling benzene, and freed from the catalyst. Removal of the solvent afforded a viscous orange oil possessing violet-green fluorescence. Beside the carbonyl band at 5.75 μ, the infrared spectrum showed peaks at 12.3 and 11.9 μ which are characteristic of the 1, 2, 4-trisubstituted benzene nucleus. The methyl ester was directly hydrolyzed. The mixture of 1.11 g. of the ester, 3 cc. of 40% potassium hydroxide solution, 5 cc. of water and 5 cc. of methanol was refluxed for 2 hr. in an atmosphere of nitrogen. After cooling, water was added and the solution was washed with ether to remove unsaponified material. The aqueous layer was acidified with hydrochloric acid, and extracted with ether. The ether extract was washed with water and dried. Removal of the solvent left an oil, which could be brought to crystallization by trituration with a small amount of benzene. The crystals collected weighed 0.60 g. and melted at 148~153°C. These were recrystallized from benzene to yield 0.5 g. of the acid XXIIb, m. p. 154~157°C. From mother liquor, the second crop (0.28 g., m. p. 157~158°C) was obtained by sublimation at 0.5 mmHg. The combined crystals were recrystallized from benzene, m. p. 160~160.5°C. The infrared spectrum showed peaks at 5.90 μ (carboxyl group) and 12.3 μ (1, 2, 4-trisubstituted benzen nucleus). The ultraviolet spectrum in ethanol indicated the following maxima: λ_{max} mμ (log ε): 258 (5.20), 332 (3.41), 347 (3.66), 365 (3.80), 385 (3.75).

Anal. Found: C, 82.07; H, 6.74. Calcd. for $C_{19}H_{19}O_2$: C, 81.98; H, 6.52%.

1-Oxo-3,6-dimethyl-2, 3-dihydro-1*H*-cyclopent[*a*]-anthracene (XXIIIa).—To a solution of 0.68 g. of the carboxylic acid XXIIb in 20 cc. of benzene, 0.9 g. of phosphorus pentachloride was added and the mixture was stirred for 30 min. at 0°C and 1 hr. at room temperature. To the well chilled and stirred solution, a solution of 0.6 g. of stannic chloride in 2 cc. of benzene was added and the mixture was stirred for 30 min. at 0°C and 1 hr. at room temperature. The reaction mixture was decomposed with a cold solution of 7 cc. of concentrated hydrochloric acid in 30 cc. of water, and extracted with ether. The ether extract was washed with 6 N hydrochloric acid, water, 5% sodium carbonate solution, and water. After drying, the solvent was removed to yield a residue which gave 0.41 g. of crystals, m. p. 135~141.5°C, upon trituration with methanol. For analysis they were recrystallized from methanol to afford needles, m. p. 142~143.5°C. The infrared spectrum indicated peaks at 5.93 μ, and the ultravioled spectrum is shown in Table I.

Anal. Found: C, 87.47; H, 6.23. Calcd. for $C_{19}H_{16}O$: C, 87.66; H, 6.17%.

3,6-Dimethyl-2,3-dihydro-1*H*-cyclopent[*a*]-anthracene (IV).—A mixture of 0.32 g. of the ketone XXIIIa, 5 g. of zinc amalgam, 5 cc. of concentrated hydrochloric acid, 5 cc. of acetic acid and 5 cc. of toluene was refluxed for 22 hr., while 7.5 cc. in total of concentrated hydrochloric acid was added from time to time. After the solution was cooled, the toluene layer was separated and the aqueous layer was extracted with ether. The combined toluene solution and ether were washed with water and dried over anhydrous sodium sulfate. Removal of the solvent yielded 0.265 g. of an orange oil with blue green fluorescence, which was dissolved in 40 cc. of benzene and chromatographed on 15 g. of alumina. Elution with 40 cc. of benzene gave 216 mg. of a pale yellow liquid. This was dissolved in 15 cc. of petroleum ether, and chromatographed again on

29) W. E. Bachmann and W. S. Struve, "Organic Reactions", Vol. 3, John Wiley & Sons, Inc., New York (1943), p. 38.

30) N. D. Zelinsky and M. B. Turowa Pollak, *Ber.*, 58, 1298 (1925); H. St. Pfau and Pl. A. Plattner, *Helv. Chim. Acta.*, **23**, 78, (1940).

10 g. of alumina. Elution with 60 cc. of petroleum ether gave first 64 mg. of an almost colorless liquid, which was followed by 134 mg. of a pale yellow liquid eluted with 20 cc. of petroleum ether-benzene (1 : 1) and 30 cc. of benzene. The yellow oil solidified on standing to give crystals, m. p. 64~68°C, which were recrystallized twice from methanol, m. p. 78~79.5°C. The ultraviolet spectrum is given in Fig. 6 and Table I. The molecular weight determination by Rast's method gave the value 236 ($C_{19}H_{18}$: 246.33).

Anal. Found: C, 92.06; H, 7.86. Calcd. for $C_{19}H_{18}$: C, 92.63; H, 7.37%.

The picrate was recrystallized from ethanol to give reddish brown needles, m. p. 128~128.5°C.

Anal. Found: C, 63.25; H, 4.66; N, 9.13. Calcd. for $C_{25}H_{21}O_7N_3$: C, 63.15; H, 4.45; N, 8.84%.

The 2, 4, 6-trinitrobenzolate was recrystallized from ethanol to afford scarlet needles, m. p. 142~142.5°C.

Anal. Found: C, 65.48; H, 4.65; N, 9.12. Calcd. for $C_{25}H_{21}O_6N_3$: C, 65.35; H, 4.61; N, 9.15%.

The authors are indebted to Dr. Takeo Sakan and Dr. Masazumi Nakagawa for many helpful suggestions. The authors wish also to thank Mr. Eiichi Togashi, Shiono Koryo Kaisha, for a generous gift of phenethyl alcohol.

Department of Chemistry
Institute of Polytechnics
Osaka City University
Kita-ku, Osaka

Spectrophotometric Study of the Iodine-Complexes of cis- and trans-Stilbene

By Shigeru YAMASHITA

(Received March 25, 1959)

Results of the experiments[1], carried out recently in this laboratory, on the iodine-catalyzed *cis-trans* isomerization of stilbene in *n*-hexane led to the suggestion that the molecular complex formed between iodine and stilbene may play an important role in the photochemical as well as in the thermal isomerization at low temperatures around room temperature. It seemed then desirable to investigate the equilibria in the formation of iodine-complexes of both *cis*- and *trans*-stilbene quantitatively, since only limited information was available about these equilibria and related thermodynamic quantities. The present paper reports a spectrophotometric study of these complexes. The equilibrium constants, the heats and the entropy changes for the formation of iodine-complexes of *cis*-stilbene in *n*-hexane and of *trans*-stilbene in *n*-hexane and in carbon tetrachloride have been determined.

Experimental

Materials.—*Iodine.*—The commercial reagent of special grade was used without any further purification.

cis-Stilbene.—The preparation described in "Organic Syntheses"[2] was followed. After several repetitions of vacuum distillation, the product (b. p. 114~119°C/3.5~4.0 mmHg) was stored in the dark under reduced pressure. The absorption curve was in good agreement with that previously reported[3].

trans-Stilbene.—The commercial reagent (m. p. 119~120°C) was used without any further purification. The absorption curve was again in good agreement with that previously reported[3].

n-Hexane.—The commercial reagent of chemically pure grade was treated with fuming sulfuric acid, concentrated sulfuric acid and an aqueous solution of potassium permanganate, successively. After drying over anhydrous calcium chloride, the product was fractionally distilled.

Carbon tetrachloride.—The commercial reagent was successively treated with potassium hydroxide and anhydrous calcium chloride and then fractionally distilled.

Methods.—The absorption spectra were measured with an EPB-U type Hitachi-spectrophotometer. A quartz cell with a glass stopper (10.0 mm. light path) was used for the measurement in all wavelength regions.

The temperature of the absorption cell was kept constant in a water-circulating thermostat equipped with windows, as described by Bell[4].

1) To be published in a later paper.

2) R. E. Buckles and N. G. Wheeler, "Organic Syntheses", Vol. 33, John Wiley & Sons, New York (1953), p. 88.

3) G. P. Mueller and D. Pickens, *J. Am. Chem. Soc.*, **72**, 3526 (1950); M. Orchin et al., *J. Chem. Educ.*, **34**, 493 (1957).

4) P. H. Bell, *Science*, **105**, 15 (1947).

All the operations were carried out in a dark place in order to avoid the occurrence of iodine-catalyzed *cis-trans* photoisomerization of stilbene.

Results and Discussion

Visible Absorption Bands of Iodine-Stilbene Complexes.—Iodine has an absorption maximum at 520 mμ in *n*-hexane, its absorbance over the range from 430 to 270 mμ being very weak. *cis*-Stilbene shows no absorbance in the range longer than 350 mμ in the same solvent. As *cis*-stilbene is added in increasing amounts to a dilute solution of iodine in *n*-hexane, the absorption peak at 520 mμ characteristic of the free iodine diminishes and is replaced by a new peak at 420 mμ as shown in Fig. 1. This new peak at 420 mμ may, therefore, be interpreted as a blue shift of iodine such as is frequently observed for iodine-complexes[5]. The charge-transfer band of the complex which may also be expected to appear in a still shorter wavelength region has not been studied in this work on account of difficulties due to the overlapping intense absorption of *cis*-stilbene.

Preliminary experiments in which the ratio of concentration of iodine to that of *cis*-stilbene was varied, keeping the sum of these constant, showed that the optical density at the absorption maximum was greatest in the equimolar mixture,

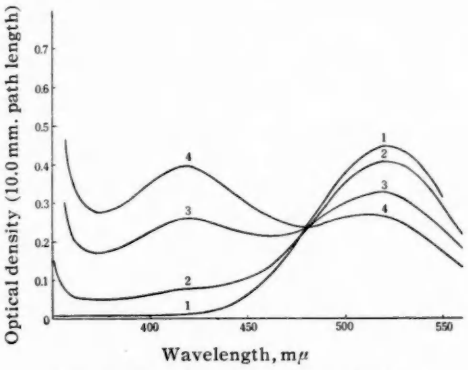

Fig. 1. Variation of the absorption band of iodine with increasing concentration of *cis*-stilbene: solvent, *n*-hexane; temperature, 24°C; concentration of I_2, 5.0×10^{-4} M; concentrations of *cis*-stilbene, 0, 2.0×10^{-2}, 1.0×10^{-1}, and 1.9×10^{-1} M for curves 1—4, respectively.

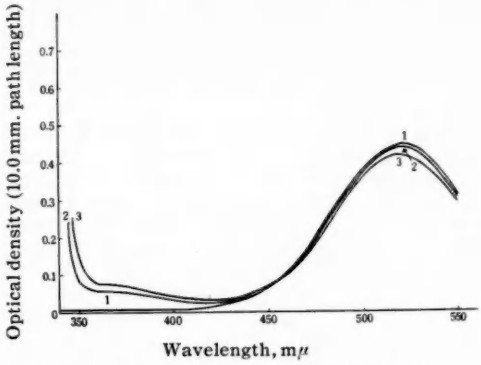

Fig. 2. Variation of the absorption band of iodine with increasing concentration of *trans*-stilbene: solvent, *n*-hexane; temperature, 24°C; concentration of I_2, 50×10^{-4} M; concentrations of *trans*-stilbene, 0, 5.0×10^{-2}, 9.5×10^{-2} M for curves 1—3, respectively.

indicating that the composition of the complex formed is 1:1. Isosbestic points such as those seen in Fig. 1 and less clearly in Fig. 2 have frequently been observed for 1:1 complexes.

Results obtained with *trans*-stilbene in the same solvent were, on the whole, similar to those with *cis*-stilbene. Here, however, the equilibrium constant for the complex formation has a lower value than for *cis*-stilbene as shown below. Consequently, the new maximum at 365 mμ which may again be taken as a blue shift of iodine is, as seen in Fig. 2, less sharp than that for *cis*-stilbene.

Andrews and Keefer[6a] reported an absorption maximum at 373 mμ, and a molar extinction coefficient of 7140 at this wavelength for the iodine-complex of *trans*-stilbene in carbon tetrachloride. In order to compare them with these results[6], measurements in carbon tetrachloride have been traced for the iodine-complex of *trans*-stilbene. The results obtained, together with those in *n*-hexane, are given in Table I where molar extinction coefficients determined as described below are included. As for the *trans*-stilbene complex in carbon tetrachloride, the values of λ_{max} obtained by the present author and by Andrews and Keefer agree with each other, but those of ε_{max} differ considerably from each other. Though the reason for the discrepancy in ε_{max} is not

5) H. A. Benesi and J. H. Hildebrand, *J. Am. Chem. Soc.*, **71**, 2703 (1949); C. Reid and R. S. Mulliken, ibid., **76**, 3869 (1954); S. Nagakura, ibid., **80**, 520 (1958); P. A. D. de Maine, *J. Chem. Phys.*, **26**, 1192 (1957).

6) (a) L. J. Andrews and R. M. Keefer, *J. Am. Chem. Soc.*, **74**, 4500 (1952); see also (b) R. Bhattacharya and S. Basu, *Trans. Faraday Soc.*, **54**, 1286 (1958).

clear yet*, Table I shows that all the values of ε_{max} found in this work for the iodine-stilbene complexes are nearly equal to each other and are of the same order of magnitude as those for free iodine. This is consistent with the interpretation that the observed absorption maxima are caused by the blue shifts of iodine since ε_{max} of the blue shift does not differ much from that of free iodine for many iodine-complexes, while far greater values, around 10000, have been reported for charge-transfer bands[5,7].

Equilibrium Constants.—Equilibrium constants for the iodine-stilbene complexes were determined, as usual, by a series of experiments in which the concentration of the donor component was varied, keeping that of iodine constant. As the latter concentration was relatively low in this work, the following equation[8,9] was applied to the optical densities obtained at respective absorption maxima.

$$1/(\varepsilon_A-\varepsilon_F) = 1/(\varepsilon_C-\varepsilon_F)(1/K_C)(1/C_D) + 1/(\varepsilon_C-\varepsilon_F) \quad (1)$$

n this equation ε_F and ε_C are, respectively, the molar extinction coefficients for free iodine and the complex in the mixture, and $\varepsilon_A = d/[(I_2)l]$, where d is the measured optical density of the solution containing the complex, (I_2) is the total concentration of iodine (free and complexed) and l is the path length of the absorption cell (1 cm.); C_D is actually the concentration of donor left free in the mixture but can be equated to its total concentration when an amount much greater than that of iodine is employed, as was the case in the present work; K_C is the equilibrium constant for the formation of the 1:1 complex.

Figs. 3 and 4 show that the linear relation required by Eq. 1 between $1/(\varepsilon_A-\varepsilon_F)$ and $1/C_D$ holds for *cis*- as well as for *trans*-stilbene in *n*-hexane, indicating that the compositions of these complexes are equally 1:1, as already inferred for

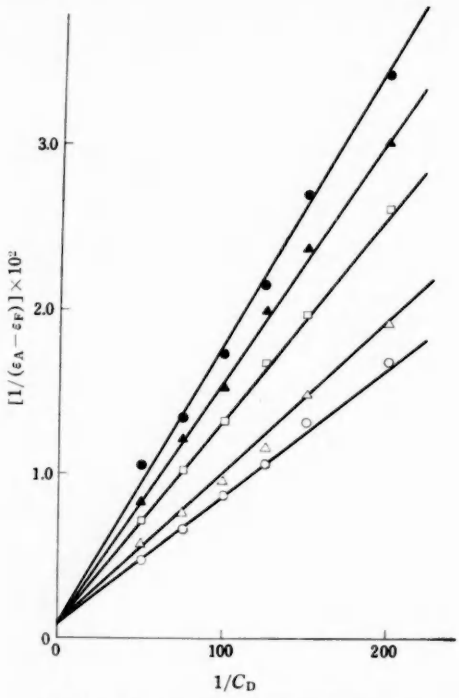

Fig. 3. $1/(\varepsilon_A-\varepsilon_F)$—$1/C_D$ diagram for the *cis*-stilbene—iodine system in *n*-hexane.
—●— 30°C, —▲— 25°C, —□— 20°C, —△— 15°C, —○— 10°C.

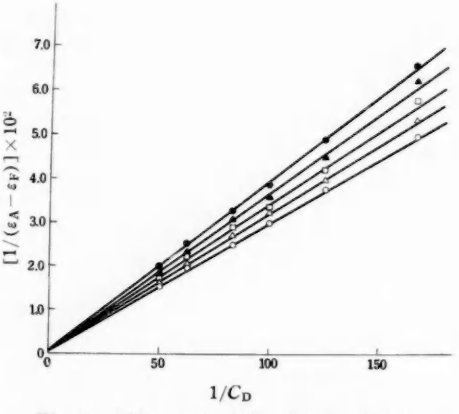

Fig. 4. $1/(\varepsilon_A-\varepsilon_F)$—$1/C_D$ diagram for the *trans*-stilbene–iodine system in *n*-hexane.
—●— 30°C, —▲— 25°C, —□— 20°C, —△— 15°C, —○— 10°C.

cis-stilbene. Silmilar results were obtained with *trans*-stilbene in carbon tetrachloride. Values of ε_C calculated from intercepts of these straight lines have already been

* Andrews and Keefer determined ε_{max} from the intercept of a Benesi-Hildebrand plot at 25°C using the optical densities corrected for free iodine. Their extrapolation at a single temperature is liable to produce a considerable error; however, it is not clear whether this is the sole reason for the large discrepancy in question. In the present work, as seen in Figs. 3 and 4, extrapolations at five different tempertures gave a constant intercept, making the value of ε_{max} thus determined much more reliable.

7) L. E. Orgel, *Quart. Revs.*, **8**, 422 (1954).
8) L. J. Andrews and R. M. Keefer, *J. Am. Chem. Soc.*, **77**, 4202 (1955).
9) J. A. A. Ketelaar et al., *Rec. trav. chim.*, **71**, 1104 (1952).

TABLE I. ABSORPTION MAXIMA AND MOLAR EXTINCTION COEFFICIENTS FOR IODINE AND IODINE-STILBENE COMPLEXES

Absorbing species	Solvent	λ_{max} mμ	ε_{max}
I_2	*n*-Hexane	520	8.40×10^2
I_2	Carbon tetrachloride	520	1.20×10^3
I_2—*cis*-Stilbene	*n*-Hexane	420	1.32×10^3
I_2—*trans*-Stilbene	*n*-Hexane	365	1.38×10^3
I_2—*trans*-Stilbene	Carbon tetrachloride	374	1.48×10^3

TABLE II. EQUILIBRIUM CONSTANTS FOR IODINE-STILBENE COMPLEXES

Complex	Solvent	K_C				
		10°C	15°C	20°C	25°C	30°C
I_2—*cis*-Stilbene	*n*-Hexane	9.74	8.35	6.13	5.10	4.42
I_2—*trans*-Stilbene	*n*-Hexane	2.42	2.22	2.10	1.97	1.82
I_2—*trans*-Stilbene	Carbon tetrachloride	—	1.68	1.53	1.45	1.36

TABLE III. THERMODYNAMIC CONSTANTS FOR COMPLEX FORMATION AT 25°C

Complex	Solvent	$-\Delta H$ kcal./mol.	$-\Delta F$ kcal./mol.	$-\Delta S$ e. u./mol.
I_2—*cis*-Stilbene	*n*-Hexane	7.54	0.965	22.1
I_2—*trans*-Stilbene	*n*-Hexane	2.54	0.402	7.18
I_2—*trans*-Stilbene	Carbon tetrachloride	2.40	0.220	7.32

given in Table I as ε_{max}'s and those of K_C obtained from the slopes are listed in Table II.

Heats and Entropy Changes.—Fig. 5 shows plots of log K_C against the reciprocal temperature for the three systems investigated. The heats of the complex formation obtained from these plots are given in Table III, together with free energy and entropy changes calculated at 25°C. As seen in the table, the change of solvent from *n*-hexane to carbon tetrachloride produces only slight changes, as would usually be expected, while there exist significant differences between the values for *cis*- and *trans*-stilbene. Apparently, *cis*-stilbene forms a more stable and rigid complex with iodine than *trans*-stilbene. A plausible explanation for such a difference may be given as follows. Since the molecule of stilbene is planar in the *trans*-form and also nearly planar in the *cis*-form[10], iodine will attach to either form of stilbene on either side of its molecular plane to form a molecular complex.

trans-Stilbene has, however, two phenyl groups projected almost in the opposite direction, while *cis*-stilbene has a bent and therefore much more compact structure. Hence the complex of *cis*-stilbene may have a more rigid structure than that of *trans*-stilbene, and, at the same time, the former complex may be more stable owing primarily to a greater van der Waals attraction.

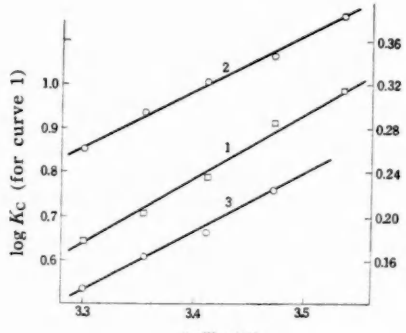

Fig. 5. Plots of log K_C vs. $1/T$:
1, I_2+*cis*-stilbene in *n*-hexane;
2, I_2+*trans*-stilbene in *n*-hexane;
3, I_2+*trans*-stilbene in carbon tetrachloride.

The author is particularly indebted to Professor O. Toyama of the College of Engineering and to Dr. T. Hayakawa for their discussions and encouragement during this investigation. The author wishes also to thank Mr. Y. Hayashibara for his assistance. A part of the expense of this study has been defrayed by the Scientific Research Grant from the Ministry of Education.

Department of Chemistry
College of General Education
The University of Osaka Prefecture
Mozu-higashino-cho, Sakai

10) G. N. Lewis, T. T Magel and D. Lipkin, *J. Am. Chem. Soc.*, **62**, 2973 (1940).

The Crystal Structure of Bis(glutaronitrilo)copper(I) Nitrate

By Yukio KINOSHITA, Ikuo MATSUBARA and Yoshihiko SAITO*

(Received April 2, 1959)

In a previous paper[1] the authors have reported the crystal structure of bis-(succinonitrilo)copper(I) nitrate. As a continuation of our crystallographic study of a series of complexes prepared from nitriles of aliphatic dibasic acids and univalent copper, the present paper reports the determination of the crystal structure of bis(glutaronitrilo)copper(I) nitrate, $[Cu(NC\text{-}CH_2\text{-}CH_2\text{-}CH_2\text{-}CN)_2]NO_3$. This work was undertaken to elucidate the mechanism of cuprous ion dyeing of polyacrylonitrile fibers[2], and the structure of bis(glutaronitrilo)copper(I) nitrate may be particularly interesting in this complex series, because, as Rath et al.[3] have suggested, it is considered to be most suitable as the model substance of the polyacrylonitrile fibers dyed with cuprous ion technique.

Experimental

Bis(glutaronitrilo)copper(I) nitrate was prepared according to the directions of Rath et al.[3] similar to those described in the previous paper[1].

Anal. Found: C, 38.15; H, 4.08; N, 22.12; Cu, 20.27. Calcd. for $C_{10}H_{12}N_5O_3Cu$: C, 38.28; H, 3.86; N, 22.32; Cu, 20.25%.

Minute prismatic crystals were chosen for X-ray study in order to minimize the effects of absorption.

Rotation and Weissenberg photographs, taken with Cu $K\alpha$ radiation (λ=1.542 Å), showed the crystals to be tetragonal with $a=8.25\pm0.01$ Å, and $c=9.71\pm0.01$ Å.

The observed extinction, $(h\,h\,l)$ with $l=2n+1$ and $(h\,0\,0)$ with $h=2n+1$, is characteristic of the space group $P4_12_1c-D_{4d}^4$.

The observed density of the crystals, measured by flotation, is 1.587 g./cc., while the density calculated on the basis of two formula units in each unit cell is 1.577 g./cc.

Complete intensity data for the $(h\,k\,0)$ and $(0\,k\,l)$ zones were obtained from Weissenberg photographs in conjunction with the multiple film technique. The $(h\,k\,0)$ data comprise 41 different reflections out of a total of 48 that are accessible, and the $(0\,k\,l)$ data represent 95 forms out of all 106 forms available.

All intensities were estimated visually. After being corrected for the Lorentz and polarization factors, the intensities were reduced to relative F_o values which were later converted into absolute values by comparison with calculated ones.

Determination of Atomic Positions

In the space group $P\bar{4}2_1c$ there are two independent sets of twofold positions: 000; $\frac{1}{2}\frac{1}{2}\frac{1}{2}$ and $00\frac{1}{2}$; $\frac{1}{2}\frac{1}{2}0$. Since there are two formula units of $[Cu(NC\text{-}CH_2\text{-}CH_2\text{-}CH_2\text{-}CN)_2]NO_3$ in each unit cell, the copper atoms and the nitrogen atoms of nitrate ions must occupy these positions; the copper atom may be placed arbitrarily at the origin and the nitrogen atoms at $00\frac{1}{2}$. The point symmetry of these twofold positions is $\bar{4}$. This is in accordance with the expected tetrahedral coordination of a univalent copper atom. The nitrate ions thus centered at $00\frac{1}{2}$ are also required to have the same symmetry. However, trigonal nitrate ions could have the apparent symmetry $\bar{4}$ only if disorder exists in the crystal. The central carbon atom of each glutaronitrile molecule must occupy one of the two sets of fourfold positions and all other atoms probably lie on general positions. Consequently a glutaronitrile molecule must have a twofold axis of symmetry. Patterson projections upon (001) and (100) were calculated. These served to confirm the arrangement of heavy atoms. Both Patterson projections could be readily solved on the basis of the knowledge of interatomic distances and bond angles obtained for crystals of bis(succinonitrilo)copper(I) nitrate[1], and the orientation of the glutaronitrile molecule in the crystal could be successfully deduced. In this way, all the coordinates of atoms except those of oxygen atoms were approximately fixed. It is almost evident that the phase angles of the structure factors for a complete set can be determined on the

* Institute of Polytechnics, Osaka City University, Kita-ku, Osaka.

1) Y. Kinoshita, I. Matsubara and Y. Saito, This Bulletin, **32**, 741 (1959).

2) R. H. Blaker, S. M. Katz, J. F. Laucius, W. R. Remington and H. E. Schroeder, *Discussions Faraday Soc.*, No. **16**, 210 (1954).

3) H. Rath, H. Rehm, H. Rummler and E. Specht, *Melliand Textilber.*, **38**, 431, 538 (1957).

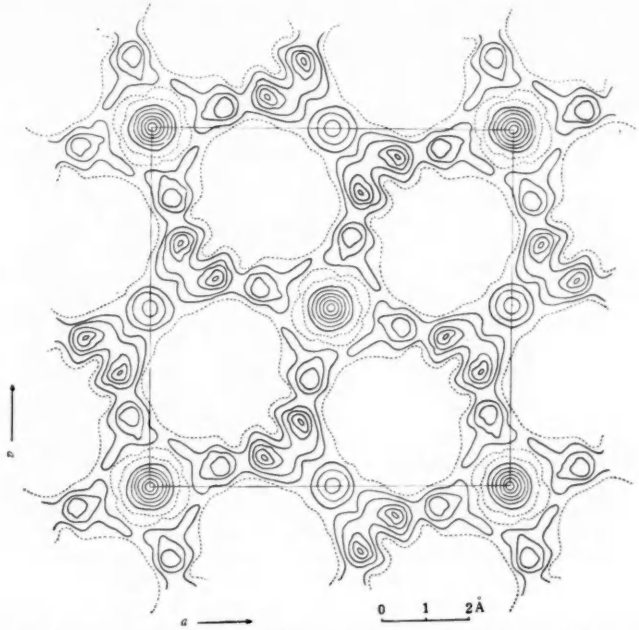

Fig. 1. Final Fourier projection of electron density upon (001). Contours are drawn at intervals of 8e Å^{-2} for copper and those for other atoms are at intervals of 2e Å^{-2}, the lowest being 2e Å^{-2}.

basis of these parameters. Fourier projections of electron density, $\rho(xy)$ and $\rho(yz)$ were then evaluated, the phase angles of which were calculated from the above mentioned parameter values. The projections so obtained showed the heavy copper atoms as well as ligand molecules clearly resolved, together with rather faint outlines of oxygen atoms in the nitrate ions. From the distribution of peaks around the nitrogen atoms, statistical orientations of nitrate ions were deduced. Calculation of structure amplitudes including the contribution of oxygen atoms improved the agreement

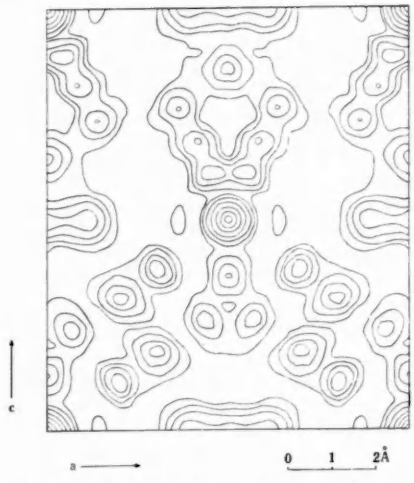

Fig. 2. Final Fourier projection of electron density upon (100). Contours are drawn at intervals of 6e Å^{-2} for copper and those for other atoms are at intervals of 2e Å^{-2}, the lowest being 2e Å^{-2}.

TABLE I. FINAL ATOMIC COORDINATES

Atom	Number of positions and Wyckoff notation	x/a	y/b	z/c
Cu	2 *a*	0.000	0.000	0.000
N_1	8 *e*	0.192	0.053	0.113
C_1	8 *e*	0.297	0.088	0.183
C_2	8 *e*	0.447	0.138	0.267
C_3	4 *d*	0.500	0.000	0.362
N_2*	2 *b*	0.000	0.000	0.500
O**	8 *e*	0.150	0.000	0.500
	8 *e*	0.130	0.075	0.500
	8 *e*	0.075	0.130	0.500

* Nitrogen atom of nitrate ion.

** Six oxygen atoms are statistically distributed on these three sets of eightfold positions with weights 1/4.

TABLE II. COMPARISON OF OBSERVED AND CALCULATED STRUCTURE FACTORS

Index	$\|F_o\|/4$	$F_c/4$	Index	$\|F_o\|/4$	$\|F_c\|/4$	$\alpha°$	Index	$\|F_o\|/4$	$\|F_c\|/4$	$\alpha°$
200	22.4	+24.3	011	8.1	9.1	0	006	11.6	11.9	0
400	8.0	+ 9.9	021	5.9	6.4	90	016	< 0.3	0.2	270
600	6.8	+ 7.9	031	9.7	10.5	0	026	7.8	8.3	0
800	2.6	+ 2.6	041	4.1	5.0	270	036	2.0	1.5	270
1000	3.1	+ 2.7	051	8.3	7.6	0	046	4.9	5.8	0
			061	1.2	1.4	270	056	2.3	2.5	90
110	10.6	+12.9	071	2.1	1.9	0	066	4.0	4.0	0
210	12.0	+10.4	081	1.8	1.8	90	076	< 0.3	0.1	270
310	8.2	+ 8.7	091	1.4	1.3	0	086	3.2	3.3	0
410	6.2	+ 6.3	0101	0.8	0.7	270	096	1.1	1.3	90
510	6.9	+ 7.5								
610	1.4	+ 2.1	002	11.8	11.1	0	017	3.8	2.5	0
710	4.7	+ 4.4	012	0.6	1.1	90	027	< 0.3	0.2	90
810	0.6	− 0.1	022	13.4	14.6	0	037	3.2	3.4	0
910	2.5	+ 2.1	032	1.1	0.8	90	047	0.5	0.3	270
1010	< 0.3	− 0.3	042	9.6	10.2	0	057	4.2	4.1	0
			052	3.6	3.8	270	067	0.6	0.6	270
220	7.1	− 7.1	062	6.6	7.1	0	077	3.1	2.2	0
320	< 0.2	− 0.2	072	2.1	2.6	270	087	0.3	0.5	270
420	10.6	+ 9.7	082	4.3	4.5	0				
520	1.2	+ 0.6	092	0.4	0.8	270	008	9.6	10.7	0
620	11.6	+11.4	0102	1.4	2.2	0	018	< 0.3	0.5	90
720	< 0.4	− 0.7					028	6.9	7.5	0
820	5.3	+ 5.6	013	3.6	3.4	180	038	2.0	2.0	270
920	1.7	+ 0.9	023	7.4	7.1	90	048	4.3	4.1	0
1020	3.3	+ 2.9	033	6.7	6.6	0	058	1.1	0.2	270
			043	3.3	3.2	90	068	4.1	4.1	0
330	4.9	+ 4.6	053	8.2	8.4	0	078	0.3	0.4	270
430	1.9	− 1.4	063	2.2	1.9	270	088	1.6	2.1	0
530	6.2	+ 6.1	073	3.9	4.1	0				
630	0.7	− 0.6	083	1.4	1.3	270	019	3.7	3.0	0
730	2.6	+ 2.9	093	2.3	2.6	0	029	0.9	1.3	270
830	< 0.3	+ 0.5	0103	0.6	0.9	270	039	3.4	3.4	0
930	2.6	+ 2.1					049	0.6	0.1	90
1030	0.8	+ 0.8	004	13.7	14.0	0	059	3.6	4.0	0
			014	0.3	0.2	90	069	< 0.2	0.7	90
440	8.3	+ 7.6	024	11.0	11.9	0	079	< 0.2	0.1	180
540	0.7	+ 0.8	034	2.4	3.5	90				
640	6.7	+ 7.1	044	2.0	2.9	0	0010	5.0	5.6	0
740	2.6	− 2.0	054	1.1	0.5	90	0110	1.5	1.9	270
840	4.6	+ 4.7	064	3.0	4.4	0	0210	2.2	2.8	0
940	< 0.3	− 0.1	074	1.7	1.8	90	0310	1.5	1.0	90
			084	4.4	4.4	0	0410	2.1	2.0	0
550	6.3	+ 6.6	094	0.3	0.6	270	0510	0.6	0.6	270
650	2.4	− 2.4	0104	< 0.2	0.6	0	0610	1.1	1.5	0
750	1.8	+ 2.2								
850	< 0.3	− 0.0	015	1.8	1.2	0	0111	1.5	1.2	0
950	0.9	+ 0.9	025	4.1	4.6	270	0211	1.6	1.2	90
			035	9.5	10.0	0	0311	2.1	2.1	0
660	2.9	+ 3.6	045	< 0.3	0.9	270	0411	< 0.2	0.3	90
760	0.6	+ 0.9	055	1.8	2.1	0	0511	< 0.1	0.6	0
860	2.6	+ 2.5	065	2.5	1.9	90				
			075	2.7	2.8	0	0012	1.7	2.6	0
770	2.8	+ 2.0	085	0.4	0.2	90	0112	1.9	1.9	90
870	< 0.2	+ 0.4	095	1.7	1.8	0	0212	2.0	1.9	0
							0312	< 0.1	0.4	90

between calculated and observed intensities. The best agreement is found if the nitrate ions lie perpendicularly to the *c*-axis, taking four different azimuthal orientations in such a way that the direction of one N–O bond coincides with one of the *a*-axis. Thus the apparent symmetry of the nitrate ions becomes $\bar{4}$, in accordance with the requirement of the space group. Although structure factors were also calculated under the assumption of free rotation of nitrate ions, the result gave a slightly greater *R*-value.

By the usual method of successive approximation the final projections were obtained. The final Fourier projections upon (001) and (100) are shown in Figs. 1 and 2, respectively. The final atomic coordinates are listed in Table I. Observed and calculated structure factors as well as phase angles are listed in Table II. The agreement on the whole is quite good and values of $R=\sum||F_o|-|F_c||/\sum|F_o|$ are 0.106 and 0.117 for $(h\,k\,0)$ and $(0\,k\,l)$, respectively. In the calculation of the structure factors, the atomic scattering curves calculated by Berghuis et al.[4] were employed. A temperature correction, $\exp-B(\sin\theta/\lambda)^2$, was applied with $B=3.0$ Å^2.

Interatomic distances and bond angles calculated on the basis of the atomic parameters listed in Table I are given in Table III.

TABLE III. INTERATOMIC DISTANCES AND BOND ANGLES

$Cu-N_1$	1.98 Å	$\angle CuN_1C_1$	176°
C_1-N_1	1.14	$\angle N_1C_1C_2$	176
C_1-C_2	1.54	$\angle C_1C_2C_3$	110
C_2-C_3	1.53	$\angle C_2C_3C_{2'}$	106
N_2-O	1.24		

Calculation of the structure factors as well as that of the electron density was carried out with a Remington Rand UNIVAC 120 electronic computer quite effectively.

Description of the Structure

The projections of the structure of bis(glutaronitrilo)copper(I) nitrate upon (001) and (100) are shown in Figs. 3 and 4, respectively. It consists of infinite two-dimensional networks of the complex ion $[Cu(NC-CH_2-CH_2-CH_2-CN)_2]^{n}_{n}{}^{+}$ and nitrate ions. A copper atom is tetrahedrally surrounded by four nitrogen atoms at a distance of 1.98 Å. Each glutaronitrile molecule is coordinated to two different copper atoms with nitrogen atoms at both ends. As a consequence, all the copper atoms in a plane perpendicular to the *c*-axis are linked together with ligand molecules, forming a two-dimensional network of complex ions. A glutaronitrile molecule possesses a twofold axis of symmetry and takes a *gauche-gauche* configuration with respect to the C_2–C_3 and C_3–$C_{2'}$ bonds. The angles of internal rotation were found to be 115° with the *trans* position taken as the origin. The carbon-carbon distances and bond angles agree well with those usually found in other organic crystals. The carbon-nitrogen bond distance is 1.14 Å and the Cu–N–C–C group is close to linear, which is similar to the case of bis(succinonitrilo)copper(I) nitrate. These facts indicate that the bond character of the carbon-nitrogen bond may be expressed as C≡N. Because of the rigidity of the triple bond and the tetrahedral coordination of copper atoms, the network of the complex ion is puckered. Nevertheless, the mode of packing of each layer is considered to be satisfactory with reasonable van der Waals distances between successive sheets. At the center of each mesh of the network of the complex ion a nitrate ion is located perpendicularly to the *c*-axis. The trigonal nitrate ion seems to have statistical azimuthal orientations and its apparent symmetry becomes $\bar{4}$. Just above and below the nitrate ion lie two copper atoms of adjacent layers at a distance of 4.86 Å, which should be compared with the corresponding distance of 4.77 Å found for the crystals of bis(succinonitrilo)copper(I) nitrate. That is to say, there is a cavity in the packed layers of the two-dimensional complex ions and a nitrate ion is at the center of the cavity. The interatomic distances between oxygen atoms of nitrate ions and the carbon atoms of the nearest methylene groups in the complex ion are longer than 3.14 Å. This is to be compared with the distance of 3.12 Å found between the carbon atom of a methylene group and the oxygen atom of a water molecule in the crystals of $[Co\,en_3]Cl_3\cdot 3H_2O$[5].

Further discussions of the structure will be made after the crystal structure of bis(adiponitrilo)copper(I) nitrate[6] has been determined.

4) J. Berghuis et al., *Acta Cryst.*, **8**, 478 (1955).

5) K. Nakatsu, Y. Saito and H. Kuroya, This Bulletin, **29**, 428 (1956).

6) Y. Kinoshita, I. Matsubara, T. Higuchi and Y. Saito, ibid., **32**, 1221 (1959).

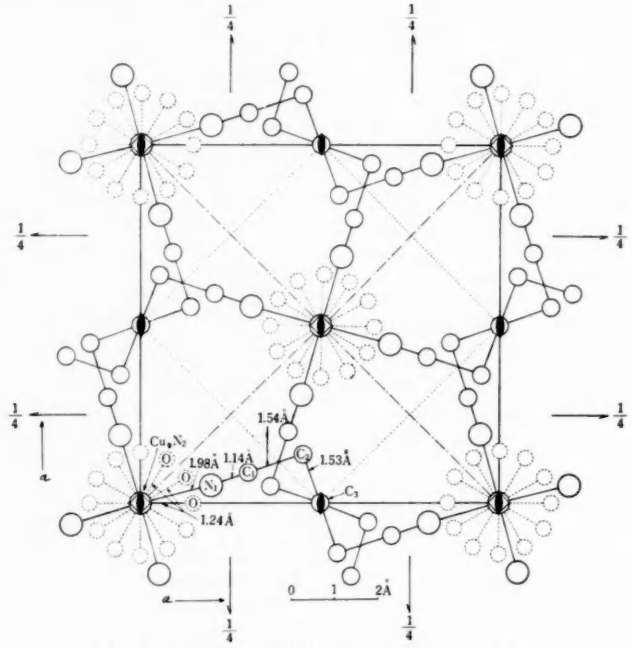

Fig. 3. Projection of the structure upon (001).

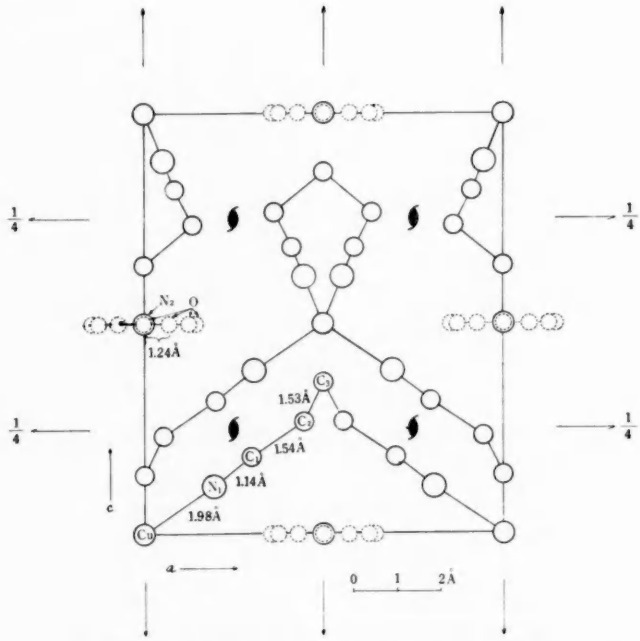

Fig. 4. Projection of the structure upon (100).

Summary

The crystal structure of bis(glutaronitrilo)copper(I) nitrate has been determined by the two-dimensional Fourier method. It is tetragonal $P\bar{4}2_1c$ with two formula units in a cell of dimensions: $a=8.25\pm0.01$ Å and $c=9.71\pm0.01$ Å.

The crystal consists of infinite two-dimensional networks of complex ion $[Cu(NC-CH_2-CH_2-CH_2-CN)_2]_n^{n+}$ and nitrate ions. A copper atom is tetrahedrally surrounded by four nitrogen atoms at a distance of 1.98 Å. Each glutaronitrile molecule is coordinated to two different copper atoms with nitrogen atoms at both ends and takes a *gauche-gauche* configuration with respect to the two C–C bonds. The nitrate ions lie perpendicularly to the *c*-axis. The trigonal nitrate ions seem to have statistical azimuthal orientations in the crystal and the apparent symmetry of the nitrate ion is $\bar{4}$.

All the atoms in the group Cu–N–C–C lie approximately on a straight line. This fact and the observed carbon-nitrogen distance of 1.14 Å suggest that the bond character in the carbon-nitrogen group may essentially be expressed as C≡N.

The authors wish to express their hearty thanks to Dr. K. Hoshino and Dr. K. Kato of the Central Research Laboratories of Toyo Rayon Co., Ltd. for their kind encouragement in the course of this study. They also wish to thank Mr. K. Yoshida of Toyo Rayon Co., Ltd. for carrying out the mechanical computations.

Central Research Laboratories
Toyo Rayon Co., Ltd.
Otsu, Shiga

The Crystal Structure of Bis(adiponitrilo)copper(I) Nitrate

By Yukio KINOSHITA, Ikuo MATSUBARA, Taiichi HIGUCHI* and Yoshihiko SAITO*

(Received April 27, 1959)

We have previously reported on the crystal structures of some complexes prepared from nitriles of aliphatic dibasic acids and univalent copper[1,2], which may be of interest in relation to the mechanism of cuprous ion dyeing of polyacrylonitrile fibers. In the course of our study on crystal structures of this series of complexes, the crystal structure of bis(adiponitrilo)copper(I) nitrate, $[Cu(NC-CH_2-CH_2-CH_2-CH_2-CN)_2]NO_3$, has been determined by means of two-dimensional Fourier methods.

The crystal structure will be discussed together with those of homologues reported in the previous papers, and some remarks will be made on the mechanism of dyeing polyacrylonitrile fibers.

Experimental

Bis(adiponitrilo)copper(I) nitrate was prepared according to the method of Rath et al.[3] by dissolving silver nitrate into adiponitrile at 60°C and adding an excess of copper powder. After some black spongy silver was deposited, the mixture was filtered. On cooling, the clear filtrate deposited yellowish crystals.

Anal. Found: C, 42.05; H, 4.70; N, 20.54; Cu, 18.52. Calcd. for $C_{12}H_{16}N_5O_3Cu$: C, 42.16; H, 4.72; N, 20.49; Cu, 18.59%.

The crystals are orthorhombic and the unit cell dimensions, as determined from rotation and Weissenberg photographs taken with Cu $K\alpha$ radiation ($\lambda=1.542$ Å), are $a=9.41\pm0.02$ Å, $b=13.73\pm0.02$ Å and $c=5.85\pm0.01$ Å. Systematic extinctions occur only for $(h\,k\,0)$ with $h+k$ odd, $(0\,k\,l)$ with $k+l$ odd and $(h\,0\,l)$ for $h+l$ odd. The space group is therefore $Pnnn-D_{2h}^{2}$.

Assuming two formula units in the unit cell, the calculated density is 1.502 g./cc., in good agreement with the measured density 1.516 g./cc.

The intensities of the spectra recorded on multiple-film zero-layer Weissenberg photographs were estimated visually and corrected for Lorentz and polarization factors. In view of the small size of the crystals no corrections were made

* Institute of Polytechnics, Osaka City University, Kita-ku, Osaka.

1) Y. Kinoshita, I. Matsubara and Y. Saito, This Bulletin, **32**, 741 (1959).

2) Y. Kinoshita, I. Matsubara and Y. Saito, ibid., **32**, 1216 (1959).

3) H. Rath, H. Rehm, H. Rummler and E. Specht, *Melliand Textilber.*, **38**, 431, 538 (1957).

for the absorption effect. The resulting F^2's were correlated so that all observed data were on the same relative intensity scale. They were later converted into an absolute scale by comparison with calculated values.

Determination of Atomic Positions

Since the general point position in the space group *Pnnn* is eightfold, and since there are only two formula units of $[Cu(NC-CH_2-CH_2-CH_2-CH_2-CN)_2]NO_3$ in the unit cell, it follows that the copper atom must occupy one of the four sets of special positions; 0, 0, 0; 1/2, 1/2, 1/2, etc. All these positions are the intersecting points of three twofold axes which are parallel to the three principal axes respectively. Should the copper atoms occupy a set of these positions, the $(h\,k\,l)$ intensities should conform approximately to the extinction condition of body centered lattice. Equi-inclination Weissenberg photographs revealed that this condition was actually fulfilled. The positions of the copper atoms are, therefore, arbitrarily chosen as 0, 0, 0; 1/2, 1/2, 1/2.

Similarly the nitrogen atoms of nitrate ions must lie on a set of these special positions. The point symmetry of these twofold positions is 222. This is not in accordance with the trigonal symmetry of the nitrate ion. The nitrate ion could have apparent symmetry 222 only if disorder exists in the crystal.

The Patterson projections onto (001), (010) and (100) are very similar to the corresponding Fourier projections, since copper atoms at the origin and the center of the unit cell make all signs of zero-layer reflections positive and moreover the plane group symmetry of the Patterson projections are similar to that of Fourier projections. Therefore, preliminary Fourier projections were computed with all signs positive. Because the *c*-axis is as short as 5.85 Å, the extended chain form of methylene groups in the adiponitrile molecule, which apparently connects the copper atom at the origin with that at the center of the unit cell, is clearly shown on $P(uv)$ and $\rho(xy)$. Further, it has been found from $(0\,k\,l)$ data that the atoms in adiponitrile molecules are concentrated in (031) planes, because the orders of reflection from (031) are exceptionally intense and the intensity decreases through four orders according to a normal decline. Consideration of the above facts with the aid of the Patterson projection upon (100) has led to the conclusion that an adiponitrile molecule is coordinated with the nitrogen atoms of both ends to two copper atoms at 0, 0, 0 and at 1/2, 1/2, 3/2, taking a planar zigzag configuration. Thus the approximate coordinates of all the atoms in the ligand molecule could be fixed. However, from the Patterson projections and the preliminary Fourier maps of electron density only, locations of the atoms in the nitrate ions could not be fixed unequivocally. As a consequence, the approximate parameters of these atoms were determined by trial calculations of structure amplitudes. The best agreement between observed and calculated structure amplitudes was obtained when the nitrate ion was placed perpendicularly to the *a*-axis, taking four different azimuthal orientations as shown in Table I. Thus, the apparent symmetry of the nitrate ion becomes 222 in accordance with the requirement of the space group. Determination of the more precise atomic parameters was achieved by successive

TABLE I. FINAL ATOMIC COORDINATES

Atom	Number of positions and Wyckoff notation		x/a	y/b	z/c
Cu	2	*a*	0.000	0.000	0.000
N_1	8	*m*	0.129	0.076	0.200
C_1	8	*m*	0.194	0.110	0.341
C_2	8	*m*	0.292	0.164	0.509
C_3	8	*m*	0.201	0.223	0.667
N_2	2	*b*	0.000	0.500	0.500
O_1	4	*j* (1/4)*	0.000	0.410	0.500
O_2	4	*l* (1/4)*	0.000	0.500	0.288
O_3	8	*m* (1/4)*	0.000	0.455	0.317
O_4	8	*m* (1/4)*	0.000	0.422	0.394

* Oxygen atoms are statistically distributed with weights shown in parentheses.

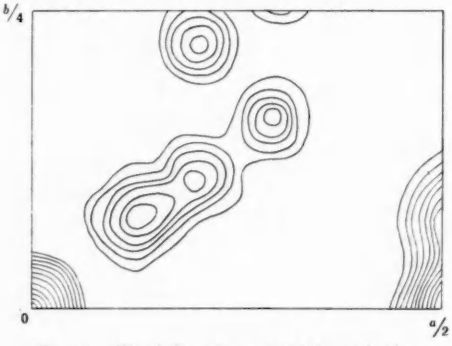

Fig. 1. Final Fourier projection of electron density upon (001). Contours are drawn at intervals of 4e Å^{-2} for copper and those for other atoms are at intervals of 1e Å^{-2}, the lowest being 2e Å^{-2}.

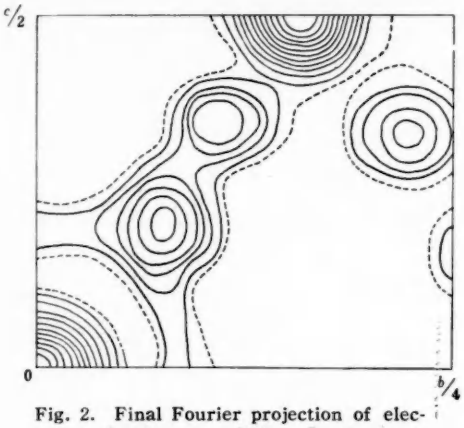

Fig. 2. Final Fourier projection of electron density upon (100). Contours are drawn at intervals of 5e Å^{-2} for copper and those for other atoms are at intervals of 1e Å^{-2}, the lowest being 2e Å^{-2} (broken).

Fourier syntheses. The final Fourier projections upon (001) and (100) are shown in Figs. 1 and 2, respectively.

The atomic parameters of the asymmetric unit are recorded in Table I and the calculated interatomic distances and bond angles are shown in Table II. The comparison of observed and calculated structure amplitudes is given in Table III, the reliability factors $R=\sum||F_o|-|F_c||/\sum|F_o|$ being 0.107, 0.116 and 0.112 for $(h\,k\,0)$, $(h\,0\,l)$ and $(0\,k\,l)$, respectively, with a weighted mean value of 0.110.

TABLE II. INTERATOMIC DISTANCES AND BOND ANGLES

$Cu-N_1$	1.98 Å	$\angle CuN_1C_1$	169°
C_1-N_1	1.13	$\angle N_1C_1C_2$	172
C_1-C_2	1.54	$\angle C_1C_2C_3$	108
C_2-C_3	1.50	$\angle C_2C_3C_{3'}$	108
$C_3-C_{3'}$	1.53		
N_2-O	1.24		

A mean isotropic temperature factor with $B=3.0$ Å^2 was found to be satisfactory for the three principal zones. Calculation of electron density as well as that of structure factors were carried out on a Remington Rand UNIVAC 120 electronic computer quite effectively.

Description of the Structure

The projections of the structure of bis(adiponitrilo)copper(I) nitrate upon (001) and (100) are shown in Figs. 3 and 4, respectively.

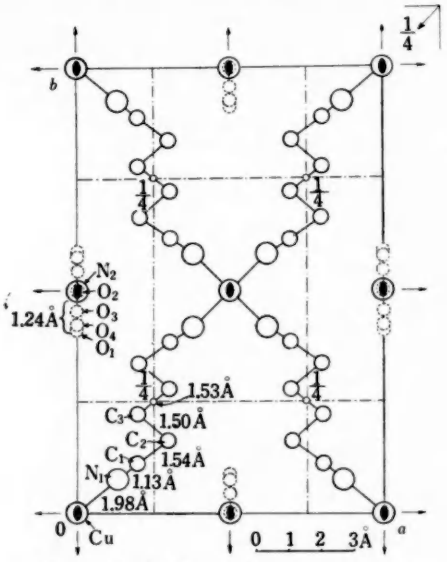

Fig. 3. Projection of the structure upon (001).

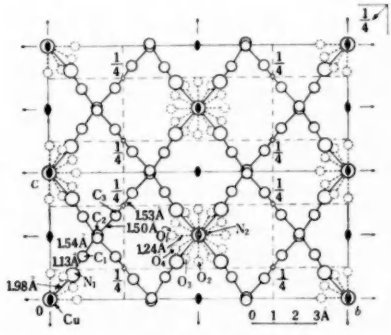

Fig. 4. Projection of the structure upon (100).

It is evident from the figures that the structure consists of infinite three-dimensional networks of the complex ion $[Cu(NC-CH_2-CH_2-CH_2-CH_2-CN)_2]_n^{n+}$ and nitrate ions. A copper atom is surrounded tetrahedrally by four nitrogen atoms at a distance of 1.98 Å, which is in good agreement with the corresponding values observed for the related compounds reported previously[1,2]. Each adiponitrile molecule is coordinated to two different copper atoms, resulting in a complicated three-dimensional network of the complex ion. A copper atom at the origin is linked to four copper atoms belonging to different unit cells at 1/2, 1/2, 3/2; −1/2, −1/2, 3/2; 1/2,

TABLE III. COMPARISON OF OBSERVED AND CALCULATED STRUCTURE FACTORS

Index	F_o	F_c	Index	F_o	F_c	Index	F_o	F_c
200	6	7	280	22	23	705	12	9
400	72	70	480	40	35	802	14	12
600	70	64	680	22	16	804	18	16
800	26	28	880	7	3	901	14	12
1000	32	33	1080	10	11	903	17	14
1200	< 2	−1	190	41	33	905	< 2	8
020	64	69	390	< 5	−1	1002	11	12
040	22	24	590	43	47	1004	7	6
060	5	4	790	9	−6	1101	< 3	0
080	26	23	990	10	12	1103	< 2	12
0100	31	28	2100	29	25	011	54	60
0120	30	28	4100	23	20	031	102	117
0140	19	20	6100	16	14	051	28	26
0160	4	4	8100	11	9	071	18	29
002	24	23	1110	20	16	091	25	24
004	34	32	3110	14	16	0111	30	27
006	34	35	5110	< 5	1	0131	12	16
110	34	39	7110	14	17	0151	16	21
310	34	−35	9110	< 3	4	0171	< 4	4
510	< 4	3	2120	22	20	022	28	31
710	18	16	4120	13	13	042	30	31
910	13	7	6120	13	13	062	71	74
1110	< 4	2	8120	10	14	082	32	33
220	113	124	1130	14	14	0102	13	15
420	40	37	3130	9	8	0122	21	24
620	37	37	5130	< 5	0	0142	8	7
820	34	40	7130	11	12	0162	< 5	7
1020	7	9	2140	16	17	013	28	23
1220	10	15	4140	7	7	033	32	30
130	29	25	6140	7	9	053	34	32
330	19	21	1150	10	10	073	19	23
530	18	17	3150	6	6	093	51	55
730	14	13	5150	< 4	4	0113	10	8
930	12	13	2160	13	16	0133	< 7	4
1130	< 4	0	4160	< 3	5	0153	4	7
240	78	72	101	26	21	024	38	30
440	55	47	103	40	41	044	24	23
640	30	26	105	26	19	064	37	37
840	20	21	107	5	4	084	12	11
1040	8	9	202	49	44	0104	8	8
150	19	18	204	39	41	0124	17	20
350	66	61	206	< 4	0	0144	8	9
550	28	27	301	10	12	015	28	25
750	15	16	303	6	8	035	38	34
950	11	9	305	6	−2	055	12	9
1150	< 3	10	307	11	6	075	10	8
260	38	35	402	56	60	095	10	11
460	50	50	404	24	21	0115	11	13
660	15	13	406	18	15	0135	< 3	7
860	10	9	501	11	9	026	8	8
1060	10	9	503	66	64	046	8	9
170	13	14	505	7	6	066	9	9
370	68	64	602	23	20	086	11	10
570	16	19	604	18	14	0106	7	8
770	22	20	606	13	13	017	< 5	0
970	< 5	2	701	14	13	037	13	13
1170	< 2	10	703	17	12	057	10	9

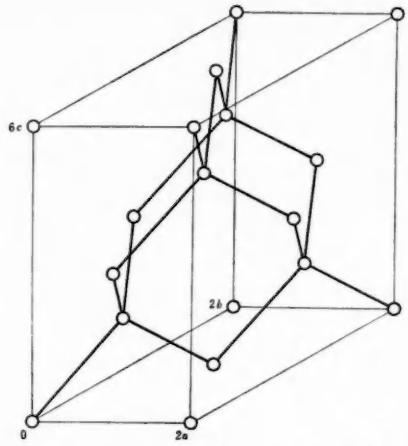

Fig. 5. Schematic diagram of a single 4-connected network in the crystal of bis(adiponitrilo)copper(I) nitrate.

$-1/2, -3/2; -1/2, 1/2, -3/2$. In this way the copper atoms and the ligand molecules form a three-dimensional 4-connected network[4], in which all the copper atoms are arranged on a distorted diamond lattice and are linked by the ligand molecules with each other. Fig. 5 schematically illustrates the constitution of the network. The figure shows a single 4-connected network. For simplicity, adiponitrile molecules are drawn as straight lines connecting two copper atoms. The structure of bis(adiponitrilo)copper(I) nitrate consists of a superposition of six sets of this 4-connected network displaced through c with respect to each other.

Each adiponitrile molecule has a center of symmetry between the two central carbon atoms. All the carbon atoms of the adiponitrile molecule are less than 0.06 Å from the plane (031) and constitute a planar zigzag chain configuration, while the nitrogen atoms of nitrile groups are 0.10 Å distant from that plane. All the carbon-carbon bond lengths and bond angles in the methylene groups are close to normal values. The carbon-nitrogen bond distance is 1.13 Å and the Cu–N–C–C group is close to linear as in the cases of the related compounds reported previously[1,2]. These facts indicate that the bond character of the carbon-nitrogen bond may be expressed as C≡N.

The nitrate ions lie perpendicularly to the a-axis. The trigonal nitrate ion seems to have statistical azimuthal orientations in the crystal and its apparent symmetry becomes 222. The interatomic distances between the oxygen atoms of the nitrate ions and the carbon atoms of the nearest methylene groups in the complex ion are longer than 3.19 Å. This is to be compared with the corresponding value of 3.14 Å found in the crystals of bis(glutaronitrilo)-copper(I) nitrate[2].

4) For the definition of the term, see A. F. Wells, *Acta Cryst.*, **7**, 545 (1954).

Remarks on the Mechanism of Cuprous Ion Dyeing of Polyacrylonitrile Fibers

As pointed out in the previous paper[1], cuprous ion is readily absorbed by polyacrylonitrile fibers which then acquire an almost unlimited affinity for anionic dyes, which ordinarily can not be applied to this class of fibers. Blaker et al.[5] and Rath et al.[3] have suggested that the high affinity of cuprous ion for polyacrylonitrile is due to the inherent capability of nitrile groups in the fibers to absorb cuprous ion through formation of complexes, which may act as positive sites for fixation of dye anions. It has been established by the present investigations that, in the complexes prepared from univalent copper and nitriles of aliphatic dibasic acids, four nitrogen atoms of nitrile groups enter into combination with a cuprous ion, forming a stable tetrahedral complex. This fact strongly indicates that there may exist a strong interaction of the same kind between cuprous ions and nitrile groups of polyacrylonitrile molecules in the dyeing of fibers with cuprous ion technique. However, by analogy with the structures of these complexes it is very unlikely that stable chelate rings of the type,

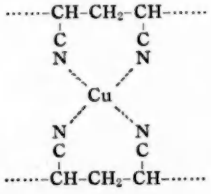

are formed between cuprous ions and polyacrylonitrile molecules. In fact, it can easily be understood that such a chelate ring with reasonable bond distances and bond angles can never be obtained, owing to the rigidity of the Cu–N–C–C

5) R. H. Blaker, S. M. Katz, J. F. Laucius, W. R. Remington and H. E. Schroeder, *Discussions Faraday Soc.*, No. **16**, 210 (1954).

group. Therefore, Blaker and Rath's suggestion is only valid in the sense that the nitrile groups of polyacrylonitrile molecules are involved in the formation of complexes similar to those of simple nitriles as described in this and the preceding papers.

In the structures of these complexes, nitrate ions are located in cavities which are formed in the polymeric chain or network of complex ions owing to the rigidity of the Cu–NC–CH_2– group and the tetrahedral nature of the Cu–N bonds. This fact may suggest that in the polyacrylonitrile-Cu(I) complex the dye anions are trapped in cavities analogous to those mentioned above and are fixed by electrostatic interactions with the positive cuprous ions.

Summary

The crystal structure of bis(adiponitrilo)-copper(I) nitrate has been determined by the two-dimensional Fourier method. It is orthorhombic *Pnnn* with two formula units in a cell of dimensions: $a=9.41\pm0.02$ Å, $b=13.73\pm0.02$ Å and $c=5.85\pm0.01$ Å.

The crystal consists of infinite three-dimensional networks of complex ion $[Cu(NC-CH_2-CH_2-CH_2-CH_2-CN)_2]_n^{n+}$ and nitrate ions. A copper atom is tetrahedrally surrounded by four nitrogen atoms at a distance of 1.98 Å. Each adiponitrile molecule is coordinated to two different copper atoms with nitrogen atoms of both ends, forming a planar zigzag configuration of methylene groups. Thus the copper atoms and the ligand molecules form a complicated three-dimensional 4-connected network. The nitrate ions lie perpendicularly to the *a*-axis. The trigonal nitrate ion seems to have statistical azimuthal orientations in the crystal and its apparent symmetry becomes 222.

All the atoms in the group Cu–N–C–C lie approximately on a straight line. This fact and the observed carbon-nitrogen distance of 1.13 Å suggest that the bond character in the carbon-nitrogen group may essentially be expressed as C≡N.

On the basis of the structures of this and the other related complexes, some remarks have been made on the mechanism of cuprous ion dyeing of polyacrylonitrile fibers.

The authors wish to express their hearty thanks to Dr. K. Hoshino and Dr. K. Kato of the Central Research Laboratories of Toyo Rayon Co., Ltd. for their kind encouragement in the course of this study. They also wish to thank Mr. K. Yoshida of Toyo Rayon Co., Ltd. for carrying out the mechanical computations.

Central Research Laboratories
Toyo Rayon Co., Ltd.
Otsu, Shiga

π-Electronic Structures of o-Quinones

By Akira KUBOYAMA

(Received April 17, 1959)

Previously[1], we studied the π-electronic structures of *p*-quinones (*p*-benzoquinone, α-naphthoquinone and anthraquinone) by the aid of the simple LCAO MO method and succeeded in explaining the following problems concerning the near UV absorption bands of the *p*-quinones: 1) a similarity among the $\pi-\pi$ transition bands of these *p*-quinones, 2) a relative magnitude of the $n-\pi$ transition energy of *p*-benzoquinone, α-naphthoquinone, and anthraquinone, 3) the effect of the electron-donating group on the $\pi-\pi$ transition bands of α-naphthoquinone and anthraquinone. In the present paper, similar theoretical studies have been extended to absorption spectra of *o*-quinones such as *o*-benzoquinone, β-naphthoquinone, and phenanthrenequinone. The calculations on β-naphthoquinone and phenanthrenequinone by the MO method have never been carried out. The obtained results are now reported.

1) A. Kuboyama, This Bulletin, **31**, 752 (1958).

Method of Calculation

The method employed in the present calculation is exactly the same as that used in the case of *p*-quinones. The coulomb (α_i) and exchange (β_{ij}) integrals were determined on the basis of the same principles as described in the previous paper. They are as follows:

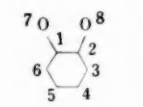

$\alpha_7=\alpha+1.3\beta$, $\alpha_1=\alpha+0.2\beta$
$\alpha_3=\alpha_4=\alpha$
$\beta_{17}=\beta_{34}=\beta$, $\beta_{12}=0.8\beta$
$\beta_{23}=\beta_{45}=0.9\beta$

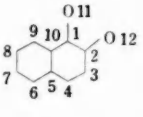

$\alpha_{11}=\alpha_{12}=\alpha+1.3\beta$
$\alpha_1=\alpha_2=\alpha+0.2\beta$
$\alpha_3=\alpha_4=\cdots\cdots=\alpha_9=\alpha_{10}=\alpha$
$\beta_{1-11}=\beta_{2-12}=\beta_{34}=\beta_{56}=\beta_{67}$
$=\cdots\cdots=\beta_{9-10}=\beta_{5-10}=\beta$
$\beta_{12}=0.8\beta$,
$\beta_{23}=\beta_{45}=\beta_{1-10}=0.9\beta$

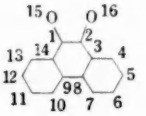

$\alpha_{15}=\alpha+1.3\beta$, $\alpha_1=\alpha+0.2\beta$
$\alpha_3=\alpha_4=\alpha_5=\alpha_6=\alpha_7=\alpha_8=\alpha$
$\beta_{1-15}=\beta_{34}=\beta_{45}=\beta_{56}=\beta_{67}$
$=\beta_{78}=\beta_{38}=\beta$
$\beta_{12}=0.8\beta$, $\beta_{23}=\beta_{89}=0.9\beta$

Among these values, those concerning the quinone nuclei were set equal to the values evaluated for *o*-benzoquinone by the self-consistent method[2].

Results

The obtained molecular diagrams are given below.

In the above diagram, the unpaired electron densities are the ones in the lowest unfilled orbitals[3]. In the molecular diagram for *o*-benzoquinone the values in brackets are the ones previously calculated by the self-consistent method. The agreement between these two molecular diagrams for *o*-benzoquinone is substantially good. Further, the energy levels of *o*-benzoquinone calculated by the two methods mentioned above are in good agreement with each other. The energy levels evaluated with these quinones are given in Fig. 1. Furthermore, the dependence* of the energy levels upon the coulomb integral of the oxygen atom was

Charge densities

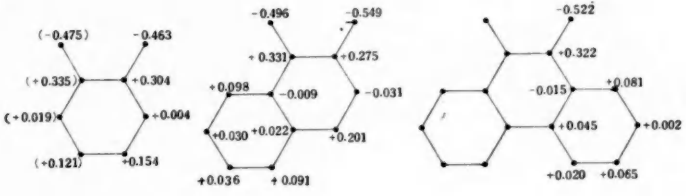

Bond orders

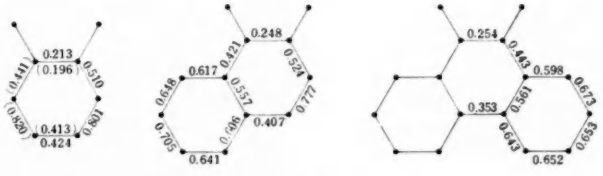

Free valences and unpaired electron densities

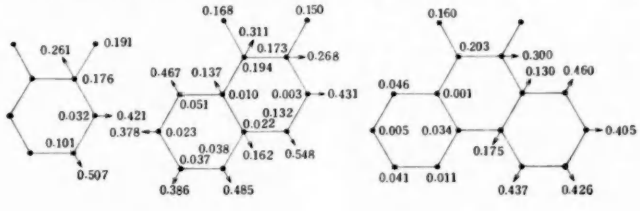

2) S. Nagakura and A. Kuboyama, *J. Chem. Soc. Japan, Pure Chem. Sec.* (*Nippon Kagaku Zasshi*), **74**, 499 (1953); S. Nagakura and A. Kuboyama, *J. Am. Chem. Soc.*, **76**, 1003 (1954).

3) H. M. McConnell, *J. Chem. Phys.*, **24**, 632 (1956).

* The similar figure for *p*-benzoquinone was given by L. E. Orgel, *Trans. Faraday Soc.*, **52**, 1172 (1956).

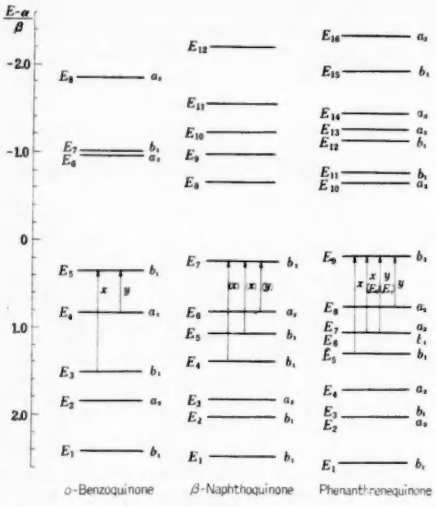

Fig. 1.

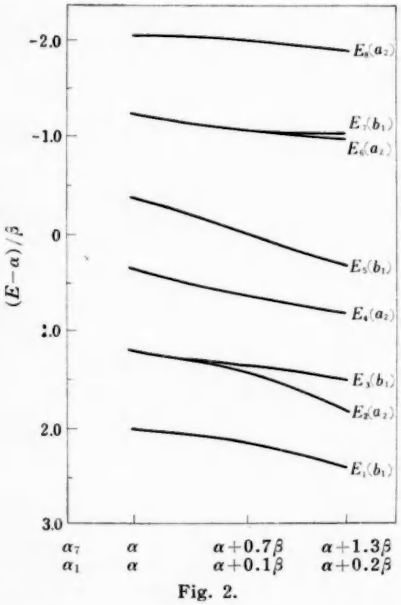

Fig. 2.

studied with *o*-benzoquinone. The result is shown in Fig. 2. The energy levels are classified according to the symmetry properties of the corresponding orbitals in the symmetry groups of these *o*-quinones (C_{2v}), taking the molecular symmetry axis as the *x*-axis and the molecular plane as the *xy* plane. For β-naphthoquinone which has no molecular symmetry axis, the symmetry properties of the orbitals are considered in relation to the quinone nucleus. The letters *x* and *y* attached to the arrow showing the transition between the energy levels denote the directions of the polarization in the allowed transitions. In phenanthrenequinone, the E_2 and E_6 orbital energies are a little lower than the E_3 and E_7 orbital energies, respectively.

Discussion

Molecular Diagrams. — The molecular diagrams of the three *o*-quinones are also similar in many points as well as those of the *p*-quinones. As for charge distributions, the negative charges of oxygen atoms slightly increase in the order of *o*-benzoquinone < β-naphthoquinone < phenanthrenequinone. In β-naphthoquinone, the carbonyl group (C_1–O_{11}) is relatively electronically more negative than the one (C_2–O_{12}). Positions 3 and 4 of β-naphthoquinone are relatively electronically more negative and positive, respectively, than the corresponding positions of *o*-benzoquinone. The result that position 3 of β-naphthoquinone is electronically somewhat negative explains the remarkable fact[4] that at this position the nitro group substitution reaction occurs. The calculated dipole moments of *o*-benzoquinone, β-naphthoquinone, and phenanthrenequinone are ca. 8.1, 11.0, and 9.9 D, relatively. If the contribution of the inductive effect between two large dipoles belonging to adjacent carbonyl bonds (ca. 1.5 D)** is in every case subtracted from these values, the final values are 6.6, 9.5 and 8.4 D, respectively, which are considerably greater than the experimental values (5.1[2], 5.6[2] and 5.6 D[5], respectively). These differences between the calculated and the experimental values are commonly observed in the simple MO calculations. As for bond orders, in β-naphthoquinone the value for the C_2–C_3 bond is greater than the one for the C_{10}–C_1 bond and the value for the C_3–C_4 bond is nearly equal to the corresponding one of *o*-benzoquinone. The diagrams also show that the six-membered carbon rings attached to the quinone nuclei of β-naphthoquinone and

4) L. F. Fieser and M. Fieser, "Organic Chemistry", 2nd Ed. (1950), translated into Japanese, Maruzen Co., Ltd., Tokyo (1957), p. 748.

** The contribution of the inductive effect was calculated by the same method as that described in the following reference; H. M. Smallwood and K. F. Herzfeld, *J. Am. Chem. Soc.*, **52**, 1919 (1930).

5) C. C. Caldwell and R. J. W. LeFèvre, *J. Chem. Soc.*, **1939**, 1614.

phenanthrenequinone are correctly approximated by the benzene nucleus. Free valence values for position 4 of *o*-benzoquinone and β-naphthoquinone are great, particularly in the case of the latter. The unpaired electron densities in the lowest unfilled orbitals are thought to be roughly equal to the unpaired electron densities in the corresponding semiquinone ions[3]. In the three *o*-quinones, the parts greater than seventy per cent of the total unpaired electron densities exist at the carbonyl groups. Previously, McConnell[3] reported that between the splitting constant, a_i, in the hfs in the electron paramagnetic resonance absorption of semiquinone ions and the unpaired electron density, ρ_i (i denotes the position of a carbon atom to which a proton bonds), the following relationship can be formulated.

$$a_i = 34\,\rho_i \qquad (1)$$

Recently M. Adams[6] reported the measured values of the splitting constants of various semiquinone ions. In *o*-benzoquinone, the values calculated following formula 1 (3.44 and 1.07 gauss) are in good agreement with the measured values (3.65 and 0.95 gauss). In β-naphthoquinone, the unpaired electron density of position 4 is considerably great and the value calculated by formula 1 is 4.48 gauss. As in β-naphthoquinone the measured values are 1.3 and 0.24 gauss, a doublet with a large splitting constant is probably overlooked. In accordance with the experimental result that in phenanthrenequinone 5 quintets resulting from the two sets of four equivalent protons were found, the calculated results show that the unpaired electron densities at positions 4, 6, 11, 13 and positions 5, 7, 10, 12 are mutually nearly equal in each group, respectively.

The Energy Levels. — From the energy levels given above, the following two points are noticeable, as in the *p*-quinones. First, the differences between the high filled and the lowest vacant orbitals are similar in these *o*-quinones. In the region 300 ~ 400 mμ, *o*-benzoquinone has one $\pi-\pi$ transition band, and β-naphthoquinone and phenanthrenequinone have two $\pi-\pi$ transition bands and all these bands are relatively weak***. Further, these three *o*-quinones have one $\pi-\pi$ transition band near 250 mμ***. Those of β-naphthoquinone and phenanthrenequinone are strong, and the one of *o*-benzoquinone is relatively weak. In the above energy levels all the transitions are allowed. Now, it is thought that the longest wavelength $\pi-\pi$ bands are assigned as $E_4 \rightarrow E_5$ (*o*-benzoquinone), $E_6 \rightarrow E_7$ (β-naphthoquinone) and $E_8 \rightarrow E_9$ (phenanthrenequinone), and the second long wavelength $\pi-\pi$ transition bands as $E_5 \rightarrow E_7$ (β-naphthoquinone) and E_6, $E_7 \rightarrow E_9$ (phenanthrenequinone), and the bands near 250 mμ as $E_3 \rightarrow E_5$ (*o*-benzoquinone), $E_4 \rightarrow E_7$ (β-naphthoquinone), and $E_5 \rightarrow E_9$ (phenanthrenequinone), respectively. Though there remains a π unfavorable point that the band near 250 mμ of *o*-benzoquinone alone is relatively weak, the above assignments are thought to be reasonable, considering the similarity of the energy levels among the three *o*-quinones. Second, the energy levels are as a whole a little elevated as the size of the *o*-quinone molecule becomes larger. Now, the lone-pair orbital energies of the oxygen atoms in the three *o*-quinones are thought to be nearly equal. Thus, as was previously reported[1], this result explains the fact that the $n-\pi$ transition energy becomes greater as the size of the *o*-quinone molecule becomes larger. The average value of the highest filled and the lowest vacant orbital energies of each *o*-quinone as a measure of the elevation of the energy levels is $\alpha+0.628\beta$, $\alpha+0.514\beta$ and $\alpha+0.469\beta$ for *o*-benzoquinone, β-naphthoquinone and phenanthrenequinone, respectively.

The Effect of the Electron-Donating Substituent on the $\pi-\pi$ Transition Bands. — As was previously reported[7,1], the greater the C_{mi}^2 value is, and the smaller the C_{ni}^2 value, the greater the extent of the red-shift of the band corresponding to the transition ($m \rightarrow n$) is, and the C_{mi}^2 value has a much greater effect than the C_{ni}^2 value, where C_{mi} and C_{ni} are the coefficients of the i-th atomic orbital in the LCAO MO, m and n, respectively. Now, let us examine this rule for *o*-benzoquinone and β-naphthoquinone. In Figs. 3[8] and 4[9], the absorption spectra of some methyl group substituted *o*-benzoquinones and methoxyl group substituted β-naphthoquinones are given, respectively. All the π-orbitals of the three *o*-quinones are intrinsically non-degenerate and we can reasonably assume that the quasi-π-orbital energy of the methyl group and the lone-pair orbital

6) M. Adams, *J. Chem. Phys.*, **28**, 774 (1958).

*** In view of the intensity and the solvent effect[2], these bands are thought to be due to $\pi-\pi$ transition.

7) A. Kuboyama, *J. Chem. Soc. Japan, Pure Chem. Sec.* (*Nippon Kagaku Zasshi*), **77**, 1062 (1956).

8) H. J. Teuber and G. Steiger, *Ber.*, **88**, 802 (1955).

9) H. J. Teuber and N. Götz, ibid., **87**, 1236 (1954).

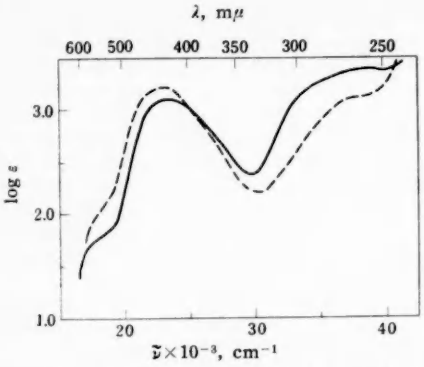

Fig. 3[9]. —— 3,4,5-Trimethyl-*o*-benzoquinone
---- 3,4,6-Trimethyl-*o*-benzoquinone
Solvent, chloroform.

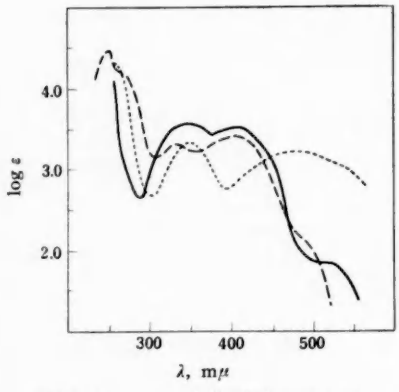

Fig. 4[9]. —— β-Naphthoquinone
------ 3-Methoxy- 〃
---- 4-Methoxy- 〃
Solvent, chloroform.

TABLE I. THE SQUARE VALUES OF THE COEFFICIENTS IN *o*-BENZOQUINONE
(The numbers in the first row denote the positions of the substitutions)

	3	4
$E_3(b_1)$	0.103	0.290
$E_4(a_2)$	0.296	0.101
$E_5(b_1)$	0.032	0.101

TABLE II. THE SQUARE VALUES OF THE COEFFICIENTS IN β-NAPHTHOQUINONE

	3	4
$E_4(b_1)$	0.113	0.231
$E_5(b_1)$	0.001	0.002
$E_6(a_2)$	0.290	0.074
$E_7(b_1)$	0.003	0.132

energy of the oxygen atom in the methoxyl group as a substituent are lower than the E_3 (*o*-benzoquinone) and the E_4 (β-naphthoquinone) orbital energies, respectively. Thus, the above method can be applied to these cases. In Fig. 3, the longer and the shorter wavelength $\pi-\pi$ transition bands of *o*-benzoquinone largely shift toward longer wavelengths for 3- and 4-substitutions, respectively. The data in Table I clearly fit these facts. In Fig. 4, the band near 400 mμ and the band near 250 mμ of β-naphthoquinone largely shift toward longer wavelengths for 3- and 4-substitutions, respectively. The data in Table II clearly explain these facts. In addition, the absorption spectra of some hydroxyl group substituted at the benzene nucleus attached to the quinone nucleus of β-naphthoquinones are also generally explained by the calculated results. Thus, in general, the effect of the electron-donating substituent on the $\pi-\pi$ transition bands in the near UV region of *o*-benzoquinone and β-naphthoquinone can be clearly explained by the above method as well as in the case of the *p*-quinones.

The good agreements between the results calculated by the simple MO method and the experimental results, concerning the near UV absorption spectra in the *o*- and the *p*-quinones, are thought to be due to the quinoid field****, characteristic of quinone compounds, which differs from the round fields, characteristic of the aromatics, presented by J. R. Platt[10].

Summary

Electronic structures of *o*-benzoquinone, β-naphthoquinone and phenanthrenequinone were studied with the simple MO method, using the same integral values as those adopted in the self-consistent MO calculation for *o*-benzoquinone. As for charge distributions, the negative charges of oxygen atoms slightly increase in the order of *o*-benzoquinone, β-naphthoquinone, and phenanthrenequinone. The calculated dipole moments (6.6, 9.5 and 8.4 D for *o*-benzoquinone, β-naphthoquinone and phenanthrenequinone, respectively) seem a little greater than the experimental values. As for bond orders, reasonable results were obtained. The calculated results predict the existence of a doublet with a large splitting constant (ca. 4.5 gauss) in the hfs of the electron paramagnetic resonance absorption of β-naphtho-semiquinone ion. Three problems

**** The similar discussion was given in J. W. Sidman's work: *J. Am. Chem. Soc.*, **78**, 4567 (1956).

10) J. R. Platt, *J. Chem. Phys.*, **18**, 1168 (1950).

concerning the near UV absorption bands [1) the similarity among the $\pi-\pi$ transition bands of the three *o*-quinones, 2) the relative magnitude of the $n-\pi$ transition energy of *o*-benzoquinone, β-naphthoquinone, and phenanthrenequinone, 3) the effect of the electron-donating group on the $\pi-\pi$ transition bands of *o*-benzoquinone and β-naphthoquinone] can be clearly explained by the calculated results, as in the cases of the *p*-quinones.

The author wishes to express his sincere thanks to Professor S. Nagakura of the Institute for Solid State Physics, the University of Tokyo, for his kind guidance. The author's thanks are also due to Mr. H. Kônosu for his kind cooperation in this research.

Government Chemical Industrial Research Institute, Tokyo
Shibuya-ku, Tokyo

*Behavior of Surface Active Molecules at an Interface. II. Statistical Thermodynamics of Monolayers of Rod-Like Molecules**

By Masayuki NAKAGAKI

(Received May 20, 1959)

A monolayer is often considered to be a two-dimensional system. However, this standpoint is not acceptable in detailed discussions, because a monolayer has a certain thickness and has a thermodynamic freedom in the direction perpendicular to the monolayer as well as in the two directions along the interface. An effort to consider the monolayer as a three-dimensional existence has been made in the preceding paper of this series[1] by considering the possibility that the end groups of the molecules in a monolayer are not necessarily on one plane, in order to explain the shape of the pressure-area curves of condensed monolayers.

Another example that definitely requires the three-dimensional consideration comes out from rather expanded monolayers in which molecules are supposed to be inclined to the normal of the interface so that the collision diameter of the molecules in the monolayer depends on the degree of the inclination of the molecules. This will be discussed in the present paper.

As for the equation of the state of the monolayer insoluble in the substrate, it has already been pointed out by Akamatsu and the present author[2] that the two dimensional analogue of the van der Waals equation can be used. Then, the equation applicable, at least empirically, is:

$$(F+a/A^2)(A-A_0)=kT \qquad (1)$$

where F is the surface pressure, A is the area per one molecule, k is the Boltzmann constant, T is the absolute temperature and a and A_0 are constants. A_0 corresponding to the constant b in the van der Waals equation is given by

$$A_0=(\pi/2)d^2 \qquad (2)$$

if the molecules are spherical and the diameter is d. However, fatty acid molecules and substances of much interest in surface chemistry is not spherical but is rod-like. If all the rod-like molecules are vertical to the interface and thickness of each molecule is d in diameter, it is then obvious that Eq. 2 can be used. Generally the rod-like molecules are, however, inclined to the interface or lying flat on the interface, so that Eq. 2 can not be used. For the molecules inclined to the interface, theoretical equations to be used instead of Eq. 2 will be derived, and the equations will be applied to experimental data already known in literature.

Theoretical Calculation of the Constant A_0

Principle of the Calculation. — For three-dimensional solutions, Zimm[3] calculated the van der Waals constant b for rod-like

* Presented before the 11th Symposium on Colloid Chemistry, the Chemical Society of Japan, Sendai, Sept. 5, 1958.

1) M. Nakagaki, This Bulletin, **29**, 64 (1956).

2) H. Akamatsu and M. Nakagaki, ibid., **23**, 232 (1950).

3) B. Zimm, *J. Chem. Phys.*, **14**, 164 (1946).

molecules by using the method of McMillan and Mayer[4]. This method is to obtain the second virial coefficient from the value of the phase integral over the entire range of the overlapping of two molecules. By analogy with the three-dimensional osmotic pressure equation in the above mentioned papers, the second virial coefficient A_2 in the expression of the surface pressure F as a power series of surface concentration c:

$$F = RT\{(1/M)c + A_2c^2 + \cdots\} \quad (3)$$

is given by the equation,

$$A_2 = -(N_0/2SM^2)\int g_2\{2\}\,\mathrm{d}\{2\} \quad (4)$$

where N_0 is the Avogadro number, M is the molecular weight of the surface active substance, S is the area of the interface. The integral will be explained later on. Since the surface concentration c is related to the area per one molecule A by the equation:

$$c = M/N_0A \quad (5)$$

Eq. 3 is rewritten as

$$FA/kT = 1 + (A_2M^2/N_0)(1/A) + \cdots \quad (6)$$

On the other hand, Eq. 1 expanded in a power series of $(1/A)$ is

$$FA/kT = 1 + (A_0 - a/kT)(1/A) + \cdots \quad (7)$$

where the term A_0 comes from the repulsion due to the overlapping of two molecules and the term (a/kT) comes from the intermolecular attraction.

On comparing Eqs. 6 and 7, two methods will be suggested for further calculations. The one, which is theoretically accurate but difficult to put in practice, is to calculate the integral in Eq. 4 by taking both the overlapping and the attraction into account, and to assign the value of (A_2M^2/N_0) thus obtained to $(A_0 - a/kT)$. The other method, which is theoretically rather arbitrary but easy to put in practice, is to calculate the integral in Eq. 4 by taking only the overlapping into account and neglecting the intermolecular attraction, and to assign the value of (A_2M^2/N_0) thus obtained to A_0. The latter method is adopted in the present paper because the term A_0 is of main interest and because the calculation of the integral is very complicated if the first method is used. Therefore,

$$A_0 = -(1/2S)\int g_2\{2\}\,\mathrm{d}\{2\} \quad (8)$$

4) McMillan and Mayer, *J. Chem. Phys.*, **13**, 376 (1954).

The g-function of two molecules g_2 is calculated from distribution functions F_n by the equation

$$g_2(1,2) = F_2(1,2) - F_1(1)F_1(2) \quad (9)$$

where the suffix of both g- and F-functions designates the number of molecules in the system considered, and $\{n\}$ means the assembly of all the coordinates of n molecules, while (i) means the coordinates of the i-th molecule. The distribution function $F_2(1,2)$ must be zero in the region where the two molecules overlap. On the other hand, in the region where the molecules do not overlap, the function must be a constant, since the intermolecular attraction is to be neglected in the present method of the calculation. The value of the constant is determined by a normalization equation,

$$(1/S^n)\int F_n\{n\}\,\mathrm{d}\{n\} = 1 \quad (10)$$

This equation can be rewritten as

$$F_n\{n\} = S^n/\int \mathrm{d}\{n\} \quad (11)$$

if $F_n\{n\}$ is a constant.

The Case in which All Molecules are Vertical to the Interface ($\theta = 0°$).—Since all the rod-like molecules are assumed to be vertical to the interface, the overlapping of two circles of diameter d in one plane is to be considered. Therefore, the result must be identical with the case of spherical molecules given by Eq. 2. The calculation will be described in some detail for this simplest case in order to explain the process followed repeatedly in the later part of this paper.

As shown in Fig. 1a, the location of the axis of rod 1 is given by the coordinates X and Y, and that of rod 2 relative to rod 1 is given by the coordinates r and φ. Then,

$$\mathrm{d}\{2\} = \mathrm{d}X\mathrm{d}Y r\mathrm{d}r\mathrm{d}\varphi \quad (12)$$

By using Eq. 11,

$$F_2(1,2) = \begin{cases} 1 \text{ when rods 1 and 2 do not overlap} \\ 0 \text{ when rods 1 and 2 overlap} \end{cases} \quad (13)$$

$$F_1(1) = F_1(2) = 1$$

Now, rods 1 and 2 overlap when $0 < r < d$, so that by Eq. 9,

$$\begin{aligned} g_2(1,2) &= -1 \quad \text{when } 0 < r < d \\ g_2(1,2) &= 0 \quad \text{in all other ranges of coordinates} \end{aligned} \quad (14)$$

Therefore,

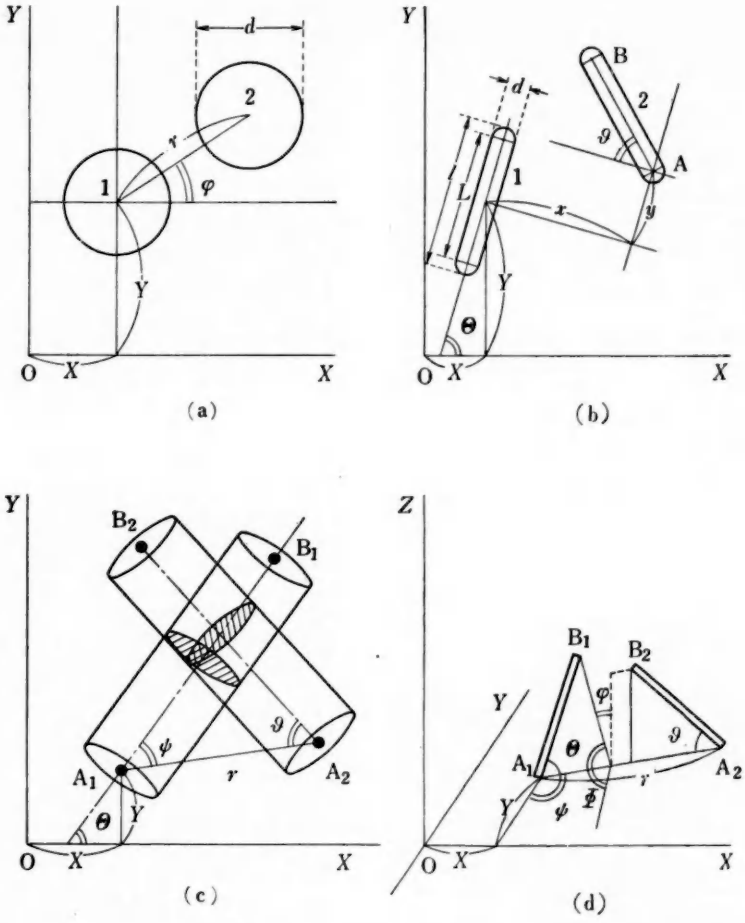

Fig. 1. Coordinate systems used in the cases of (a) $\theta=0°$; (b) $\theta=90°$; (c) $\theta=\theta_0$; and (d) θ is indefinite.

$$\int g_2\{2\}\,\mathrm{d}\{2\} = -\int_S \mathrm{d}X\mathrm{d}Y\int_0^{2\pi}\mathrm{d}\varphi\int_0^d r\mathrm{d}r$$
$$= -\pi S d^2 \qquad (15)$$

By combining this with Eq. 8, an equation exactly identical with Eq. 2 is obtained.

The Case in which All Molecules are Lying Flat upon the Interface ($\theta=90°$).—In order to avoid the complication arising from the overlapping of the edges of the rods, and to make the results of the present calculation comparable to the preceding results, the molecules are assumed to have round edges. To describe this shape of the molecule, it is assumed that a rod is composed of a circular cylinder of length L and diameter d and two hemispheres of diameter d at both ends of the circular cylinder, the center of the hemispheres being A and B, as shown in Fig. 1b.

When all rods are lying flat on the interface, the position and the orientation of a rod are designated by using three coordinates. For the three coordinates of rod 1, Cartesian coordinates X and Y of the center of gravity and the angle Θ between the X-axis and the axis of the rod may be used. For rod 2, the Cartesian coordinates x and y of the center of a hemisphere A (the origin of which is the center of gravity of rod 1 and the direction of the coordinate axes is perpendicular and

parallel to the direction of the axis of rod 1), and the angle ϑ between the axis of rod 2 and the coordinate axis $(-x)$ may be used as shown in Fig. 1b.

Then, $d\{2\}$ is $dXdYd\Theta dxdyd\vartheta$, $F_2\{2\}$ is $(1/4\pi^2)$ when two rods do not overlap with each other and is zero when they overlap, and $F_1\{1\}$ is $(1/2\pi)$. Therefore, the value of $g_2(1,2)$ is equal to $(-1/4\pi^2)$ when the rods overlap and is equal to zero when they do not. Therefore, the value of the integral calculated over the entire range of the coordinates corresponding to the overlapping of the rods is

$$\int g_2\{2\}d\{2\} = -(2S/\pi)(L^2+2\pi dL+\pi^2d^2/2) \tag{16}$$

This agrees with Eq. 15 if $L=0$. If the total length of the rod (that is $L+d$) is designated by l, and the value of A_0 is calculated from Eq. 8 by the aid of Eq. 16, then,

$$A_0=(1/\pi)l^2+2(1-1/\pi)dl+(\pi/2-2+1/\pi)d^2 \tag{17}$$

This agrees with Eq. 2 if $d=l$. Now, if the rods are very thin, $(d \ll l)$,

$$A_0 = (1/\pi)l^2 \tag{18}$$

The Case in which All Molecules are Inclined by the Same Angle($\theta=\theta_0$). — When all rods are inclined to the normal of the surface by the same angle θ_0, the position and the orientation of a rod may be specified by three coordinates. Fig. 1c shows the projection of rod 1 (A_1B_1) and of rod 2 (A_2B_2) onto the plane XY parallel to the interface. The three coordinates of rod 1 may be X and Y to give the location of the lower end A_1 of the axis and angle Θ to give the direction of the rod. The three coordinates of rod 2 may be r and ψ to give the location of A_2 and ϑ to give the direction. Then, $d\{2\}$ is $dXdYd\Theta rdrd\psi d\vartheta$, and $g_2\{2\}$ is $(-1/4\pi^2)$ when two rods overlap and is zero when they do not.

The calculation of the range of overlapping is rather complicated in this case and needs some approximation. If the rods are sufficiently thin, rods 1 and 2 overlap with each other when $\vartheta=\psi$, and the height of the intersection h from the surface is $r/2\cos\psi\tan\theta_0$. Now, considering the rods of some thickness, the cross section of the rods will be an ellipse when the cross section is parallel to the interface. The range of the angle ϑ to give the overlapping of the ellipses at the hight of h will give the condition of the overlapping of the rods. It is not easy, however, to estimate this range of ϑ, because the mutual orientation of the ellipses depends on the value of r and ψ. To avoid this mathematical complication, the ellipses will be replaced in this approximate calculation with circles of the same area. Then, the diameter of the equivalent circles d_0 will be $(d/\sqrt{\cos\theta_0})$ where d is the diameter of the rods. If the rods are sufficiently thin and long, that is, $2\sin\theta_0 > d_0/l$, the rods overlap approximately when

$$\psi-(2d_0/r)\cos\psi<\vartheta<\psi+(2d_0/r)\cos\psi \tag{19}$$

The final results thus obtained and applicable when $d/2l<\theta_0<\pi/2-d/l$ are

$$A_0=(\pi-4/\pi)d^2/2\cos\theta_0 + (\sin\theta_0/\sqrt{\cos\theta_0})dl \tag{20}$$

If $d \ll l$,

$$A_0=(\sin\theta_0/\sqrt{\cos\theta_0})dl \tag{21}$$

The Case in which Molecules can be Inclined at Any Angle with Equal Probability ($0<\theta<\pi/2$). — In this case, the position and the orientation of two rods 1 and 2 are defined by eight coordinates, X, Y, r, ψ, Θ, ϑ, Φ and φ. As is shown in a perspective, Fig. 1d, X and Y give the position of A_1. r gives the distance between A_1 and A_2. ψ gives the direction of A_1A_2. Θ gives the angle $B_1A_1A_2$. ϑ gives the angle $B_2A_2A_1$. Φ gives the angle between the plane $B_1A_1A_2$ and the plane XY. φ gives the angle between the plane $B_1A_1A_2$ and $B_2A_2A_1$. Here A_1 and A_2 are the lower end of rods 1 and 2, respectively, and B_1 and B_2 are the upper ends of rods 1 and 2. If the rods are sufficiently thin and $d \ll l$, the two rods overlap in the following three cases:

(1) $0<\Theta<\pi/2$, $0<\vartheta<\pi/2$, $0<r<l(\cos\Theta+\cos\vartheta)$ and $-(d/r)(1/\tan\Theta+1/\tan\vartheta) < \varphi < (d/r)(1/\tan\Theta+1/\tan\vartheta)$;

(2) $\pi/2<\Theta<\pi$, $0<\vartheta<\pi-\Theta$, $0<r<l(\cos\vartheta+\sin\vartheta/\tan\Theta)$ and $-(d/r)(1/\tan\Theta+1/\tan\vartheta) < \varphi < (d/r)(1/\tan\Theta+1/\tan\vartheta)$;

(3) $\pi/2<\vartheta<\pi$, $0<\Theta<\pi-\vartheta$, $0<r<l(\cos\Theta+\sin\Theta/\tan\vartheta)$ and $-(d/r)(1/\tan\Theta+1/\tan\vartheta) < \varphi < (d/r)(1/\tan\Theta+1/\tan\vartheta)$.

Then, by using the value of a definite integral, $\int_0^1(\tan^{-1}x/x)dx=0.9160$, the following equation can be obtained under the

assumption that $d \ll l$.

$$A_0 = 1.7014\, dl \qquad (22)$$

Eq. 22 corresponds to Eq. 21 with $\theta_0 = 71.8°$. This value of θ_0 is considered to be the statistically averaged value of θ for freely orienting molecules.

Applications for Gaseous Films of Fatty Acids

The theoretical equations derived above are to be applied to gaseous films and not to condensed films because multiple collisions, important in condensed films, are not taken into account in the derivations of these theoretical equations.

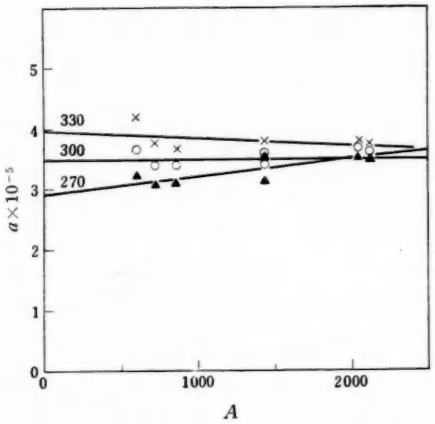

Fig. 2. The dependence of a on A for tridecylic acid, the parameter being A_0.

Therefore, the equations are applied to gaseous films of fatty acid using the experimental data given by Adam and Jessop[5]. In order to obtain the values of the constants a and A_0 of the van der Waals type equation, Eq. 1 was rewritten in the following form:

$$a = [kT/(A - A_0) - F]\, A^2 \qquad (23)$$

and the value of a for systematically varied values of A_0 are calculated by using experimental values of A and F given by Adam and Jessop. The value of a thus calculated for tridecylic acid are shown in Fig. 2. It is seen that the value of a is independent of A if the value of A_0 is assumed to be 300 Å^2. The values of a and A_0 thus obtained for tridecylic acid and myristic acid are shown in Table I.

TABLE I. CONSTANTS OF GASEOUS FILMS

	A_0	$a\times10^{-5}$	M	a/M^2	
Myristic acid	320	4.02	228	7.74	7.71
Tridecylic acid	300	3.52	214	7.68	

The data used for these calculations are shown in Fig. 3 with ○ for myristic acid and with △ for tridecylic acid. Curves in the figure shows the values calculated by Eq. 1, using the values of constants given in Table I. These curves explain well the experimental plots. Horizontal lines in the figure show where a two-dimensional phase change occurs. It is obvious that Eq. 1 does not hold over the pressure of the phase change.

As for the constant a, it is often said

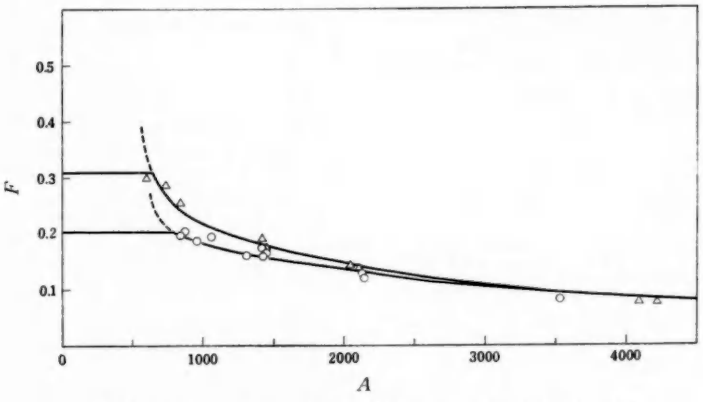

Fig. 3. Gaseous films of myristic acid and tridecylic acid.
○: Myristic acid △: Tridecylic acid

5) N. K. Adam and G. Jessop, *Proc. Roy. Soc.* (*London*), **A110**, 423 (1926).

that its value is proportional to the square of the molecular weight. This is valid in this case since the value of a/M^2 in Table I gives the relation,

$$a = 7.71 \times M^2 \qquad (24)$$

In order to compare the values of A_0 given in Table I with the theoretical equations derived above, the molecules are assumed to be rods of 5.0 Å in diameter and of $(6.0+1.3m)$Å in length, where m is the number of carbon atoms in the hydrocarbon chain of the molecule. The values thus assumed are cited in Table II.

TABLE II. THE CONSTANT A_0 FOR GASEOUS FILMS

	d Å	l Å	A_0 $\theta=0°$ Å²	A_0 $\theta=71.8°$ Å²	A_0 $\theta=90°$ Å²
Myristic acid	5.0	22.9	39.3	270	320
Tridecylic acid	5.0	21.6	39.3	258	294
Lauric acid	5.0	20.3	39.3	247	267

These values seem reasonable on the basis of various surface chemical studies and are compatible with the values already used by the present author[6]. Using these values of d and l, values of A_0 are calculated for vertical orientation, $\theta=0°$, by Eq. 2; for free orientation by Eq. 20 with $\theta_0=71.8°$; and for horizontal orientation, $\theta=90°$, by Eq. 17. The values thus calculated are shown in Table II. Comparing these with those in Table I, it may be concluded that the molecules of myristic acid and tridecylic acid are lying flat upon the interface.

In the case of lauric acid, the F–A curve obtained experimentally by Adam and Jessop is different from those of myristic and tridecylic acid, because lauric acid does not show any definite phase transition at the range of some hundred Å², as shown with ○ in Fig. 4. If it is assumed that the molecules of lauric acid are rods of $d=5.0$ Å and $l=20.3$ Å, and lying flat on the interface, A_0 should be 267 Å² as shown in Table II. On the other hand, a should be 3.08×10^5 for lauric acid according to Eq. 24. By using these values with Eq. 1, the solid curve in Fig. 4 is obtained. The curve can explain the experimental data to some extent in the region of larger A values, but the experimental data for smaller A values neither coincide with the van der Waals equation shown by the solid curve nor show any phase transition. The data will be explained by the assumption that the molecules at first lying flat on the interface gradually stand up according to the compression of the monolayer.

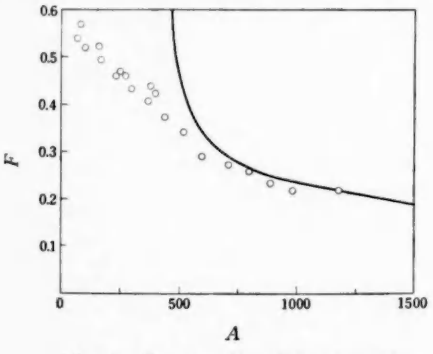

Fig. 4. Gaseous film of lauric acid.

Assuming that the molecules of lauric acid are rods of the above described dimensions, the value of A_0 is calculated as a function of the angle θ, that is the angle between the normal of the interface and the axis of the molecule. The curve in Fig. 5 is thus obtained by using Eqs. 2, 17 and 20. The point f in the figure shows the value of A_0 for the case in which the molecules can take any value of θ with equal likelihood.

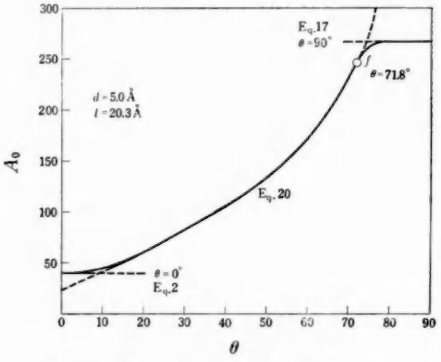

Fig. 5. The relationship between A_0 and θ for lauric acid.

By using, on the other hand, Eq. 1 together with the value of $a=3.08\times10^5$, the value of A_0 can be calculated as a function of the area A from the experimental data shown in Fig. 4. From this value of A_0, the value of θ can be obtained on the basis of Fig. 5. The relation between θ and A thus obtained are shown in Fig. 6. The horizontal line in the

6) M. Nakagaki, *J. Chem. Soc. Japan, Pure Chem. Sec.* (*Nippon Kagaku Zasshi*), **72**, 113 (1951).

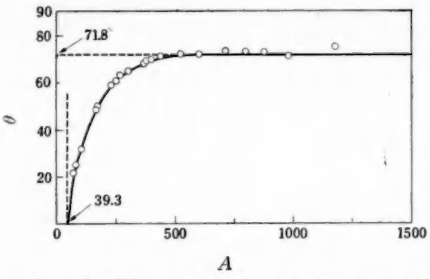

Fig. 6. The orientation of lauric acid molecules as a function of A.

figure shows the case of free orientation, in which the statistically averaged value of θ is 71.8°, and the vertical line shows the case in which all molecules are vertical to the interface. Molecules of lauric acid are in free orientation when the area A is very large, but the molecules interfere with each other and θ becomes smaller when A is les than about 500 Å^2. At last, all the molecules are vertical when A is 39.3 Å^2.

Summary

On the basis of the two-dimensional analogy of the method of McMillan and Mayer, the van der Waals constant A_0 for monolayers of rigid rod-like molecules is calculated theoretically for the cases in which all molecules are (1) vertical to the interface; (2) lying flat upon the interface; (3) inclined by a constant angle θ_0; and (4) orienting freely.

The theoretical equations thus obtained are used to discuss the orientation of molecules in gaseous films of myristic acid, tridecylic acid and lauric acid. As the results, it is concluded that the molecules of myristic acid and tridecylic acid are lying flat upon the interface in the gaseous film until the phase transition to a condensed film occurs. On the other hand, molecules of lauric acid are freely orienting when the area per one molecule is large, and the orientation becomes the more vertical, the more the monolayer is compresssed. The molecular orientations during this compression process were described quantitatively.

Faculty of the Science of Living
Osaka City University
Nishi-ku, Osaka

Dielectric Constants of Binary Mixtures; 1,2-Dichloroethane and Nonpolar Solvents

By Ryoichi FUJISHIRO and Ko KIMURA

(Received May 25, 1959)

The molecular structure of 1,2-dichloroethane has been studied in detail by many authors[1]. This molecule has steric isomers arising from the internal rotation and the equilibrium between these isomers in solutions is determined by the intramolecular interaction in the dichloroethane molecule and by the intermolecular interaction with solvent molecules. For example, the greater part of the dichloroethane molecules exists as the *gauche* form in the liquid state, whereas the dilution by adding nonpolar solvents causes decrease of the fraction of the *gauche* form. This is particular interest and worth being examined from various standpoints, that is, the dielectric and the thermodynamic behaviors of mixtures.

The thermodynamic behavior of such mixtures has already been discussed from the measurements of heats of mixing[2], and the excessive enthalpy was explained to some extent by considering the equilibrium between the steric isomers. The dielectric behavior of mixtures of dichloroethane with nonpolar solvents, however, has not been studied in detail except in the low concentration range of dichloroethane.

In this report the dielectric properties of mixtures of dichloroethane with nonpolar solvents such as carbon tetrachloride,

1) S. Mizushima, "Structure of Molecules and Internal Rotation", Academic Press, New York (1954).

2) K. Amaya and R. Fujishiro, This Bulletin, 31, 90 (1958).

cyclohexane, benzene and carbon disulfide, will be examined experimentally over all the concentrations and discussed on the basis of the Onsager theory and the theory extended by Fujishiro[3] and Scholte[4].

Outlines of the Theory

According to Onsager, we select the spheroidal cavity of the molecular dimension and put a point dipole in the center of this cavity. The surroundings of the spheroidal cavity are replaced by the continuum of the macroscopic dielectric constant. When the long and the short axes of the spheroid are $2a$ and $2b$, respectively, and the dipole is located along the long axis, the local field $\vec{f}$[5] is given by

$$\vec{f}=\vec{G}+\vec{R}=\varepsilon/[\varepsilon+(1-\varepsilon)A]\vec{E}+g\vec{m} \qquad (1)$$

where $\vec{G}$, $\vec{R}$ and $\vec{E}$ express the cavity, the reaction and the external fields, respectively, and $\vec{m}$ is the electric dipole moment in dielectrics in the presence of an external field. A is the constant determined by the geometric shape of the cavity and has the following expression[5],

$$A=\frac{ab^2}{2}\int_0^\infty \frac{\mathrm{d}\xi}{(\xi+a^2)^{3/2}(\xi+b^2)}$$

g is called the factor of the reaction field and is given by

$$g=\frac{3}{ab^2}\cdot\frac{A(1-A)\cdot(\varepsilon-1)}{\varepsilon+(1-\varepsilon)A}$$

When we assume the optical polarizability of dichloroethane to be isotropic, $\vec{m}$ is generally related to both $\vec{\mu}$ and $\vec{f}$ by the formula,

$$\vec{m}=\vec{\mu}_v+\alpha\vec{f} \qquad (2)$$

μ_v and α being the electric dipole moment and the optical polarizability of the *gauche* form of dichloroethane, respectively. From Eqs. 1 and 2, we obtain

$$\vec{f}=\frac{g}{1-\alpha g}\vec{\mu}_v+\frac{\varepsilon}{\varepsilon+(1-\varepsilon)A}\cdot\frac{\vec{E}}{1-\alpha g} \qquad (3)$$

Then the average dipole moment $\bar{m}$ is written as follows:

$$\bar{m}=<\vec{m}\cdot\vec{e}>$$
$$=\int_\Omega(\vec{m}\cdot\vec{e})e^{-U/kT}\mathrm{d}\Omega\Big/\int_\Omega e^{-U/kT}\cdot\mathrm{d}\Omega$$
$$=\frac{\varepsilon}{\varepsilon+(1-\varepsilon)A}\left\{\frac{\alpha}{1-\alpha g}+\frac{1}{(1-\alpha g)^2}\cdot\frac{\mu_v^2}{3kT}\right\}E \qquad (4)$$

The symbols $\vec{e}$ and U are a unit vector in the direction of the external field and the potential energy of the system in the presence of the external field, respectively. Then the dielectric constant of a mixture containing N_1 molecules of 1-compound, N_2 molecules of 2-compound and so on per cc., is given by the following formula,

$$\varepsilon-1=4\pi\textstyle\sum_z\cdot N_z\bar{m}_z/E \qquad (5)$$

If we take the mixture containing N_g molecules of the *gauche* form of dichloroethane, N_t molecules of the *trans* form ($N_d=N_g+N_t$) and N_s molecules of a non-polar solvent per cc., we obtain from Eqs. 4 and 5

$$\varepsilon-1=4\pi\left[N_g\cdot\frac{\varepsilon}{\varepsilon+(1-\varepsilon)A}\left\{\frac{1}{(1-\alpha g)^2}\cdot\frac{\mu_v^2}{3kT}\right\}+N_d\cdot\frac{\varepsilon}{\varepsilon+(1-\varepsilon)A}\cdot\frac{\alpha}{1-\alpha g}+N_s\frac{\varepsilon}{2\varepsilon+n_s^2}a_s^3(n_s^2-1)\right] \qquad (6)$$

In the derivation of this equation, we used the following assumption and relation:

(i) A or α for the *trans* form is equal to that for the *gauche* from, though this assumption is not strictly correct.

(ii) Assuming that a solvent molecule is spherical, A for the solvent molecule may be substituted by the value 1/3 for the spherical cavity, and the polarizability of the solvent molecule is replaced by the Lorentz-Lorenz relation,

$$\frac{n_s^2-1}{n_s^2+2}=\frac{\alpha}{a^3}$$

n and a being the refractive index and the radius of the spherical solvent molecule, respectively. Strictly speaking, as there is the contribution of atomic polarization to α, it is expressed by the Clausius-Mossotti relation instead by that of Lorentz-Lorenz. However, the atomic polarization is generally equal to only a few per cent of the electronic polarization. Hence we have conventionally used the latter relation.

Now, as the dielectric constant of the

3) R. Fujishiro, *J. Chem. Soc. Japan, Pure Chem. Sec.* (*Nippon Kagaku Zasshi*), **65**, 352 (1949).
4) T. G. Scholte, *Physica*, **15**, 437 (1949).
5) H. Fröhlich, "Theory of Dielectrics", Oxford University Press, London (1949).
6) C. G. Bötter, "Theory of Electric Polarisation", Elsevier Publishing Co., Houston (1952).

mixture itself is concerned not only with N_d, but also with N_g in the mixture as already shown in Eq. 6, we need to know the ratio N_g/N_d in the equilibrium state of the mixture. Factors determining the equilibrium are the intramolecular energy difference ΔE between the *gauche* and the *trans* forms of dichloroethane, the free energy ΔG for the electrostatic stabilization of the polar *gauche* form in the dielectrics, and the intermolecular dispersion energy between dichloroethane and solvent molecules. As is well known, ΔG is given by

$$\Delta G = \frac{1}{2} \cdot \frac{g}{1-\alpha g} \mu_v^2 \tag{7}$$

So far as the dispersion energy is concerned, it is natural to consider that the interaction of the *gauche* form of dichloroethane with a solvent molecule is approximately equal to that of the *trans* form. Thus, one interaction parameter w instead of two may be introduced as follows:

$$w = w_{ds} - \frac{1}{2}(w_{dd} + w_{ss})$$

where w_{ij} is the ordinary dispersion energy between i and j molecules and d or s expresses dichloroethane or a solvent. Then the configurational partition function[7] may be written as

$$Z = 2^{N_g} \phi_d^{N_d} \phi_s^{N_s} \frac{(N_d+N_s)!}{N_t!\, N_g!\, N_s!} \exp\left(\frac{-Xw}{kT}\right) \times \exp\left\{\frac{-N_g(\Delta E - \Delta G)}{kT}\right\} \tag{8}$$

where ϕ_d and ϕ_s represent the internal partition functions of dichloroethane and a solvent molecule respectively, and X is the number of dichloroethane solvent pairs. As the chemical potential of the *gauche* form of dichloroethane is equal to that of the *trans* form in the equilibrium state, we write

$$\frac{\partial \ln Z}{\partial N_g} = \frac{\partial \ln Z}{\partial N_t} \tag{9}$$

Hence the ratio of N_g/N_t is easily derived by using Eqs. 8 and 9 as follows:

$$N_g/N_t = 2 \exp\left\{\left(-\Delta E + \Delta G + N_g \cdot \frac{\partial \Delta G}{\partial N_g}\right) \Big/ kT\right\} \tag{10}$$

The value ε and at the same time the ratio N_g/N_t are determined at any composition and temperature by the method of "trials and errors" from Eqs. 6, 7 and 10.

7) The detailed description was given in a previous paper. See reference 2.

Experimental

In order to compare the theoretical results with the experimental ones, we measured the dielectric constants of the mixture of dichloroethane and nonpolar solvents such as carbon tetrachloride, cyclohexane, benzene and carbon disulfide. The apparatus[8] for the measurement of the dielectric constant was already described and the capacity of a dielectric cell used in this experiment was about 5 pf. All materials were purified according to the standard method[9].

Comparison of the Theoretical Results with the Observed Values

Fig. 1 shows the theoretical curves of the dielectric constants plotted against the mole fraction of dichloroethane for the dichloroethane-carbon tetrachloride mixture at 25 and 60°C. In this calculation the following values are used;

$\mu = 2.55$ D, $\alpha = 0.838 \times 10^{-23}$ cc.
E[10] $= 1.27$ kcal./mol.

	n_s^2	v_d (molecular volume of dichloroethane)	v_s (molecular volume of carbon tetrachloride)
25°C	2.124	1.325×10^{-22}	1.612×10^{-22}
60°C	2.072	1.375×10^{-22} cc.	1.676×10^{-22} cc.

All the calculations were carried out on the assumption that there is no volume change on mixing, i.e., $N_d v_d + N_s v_s = 1$. This

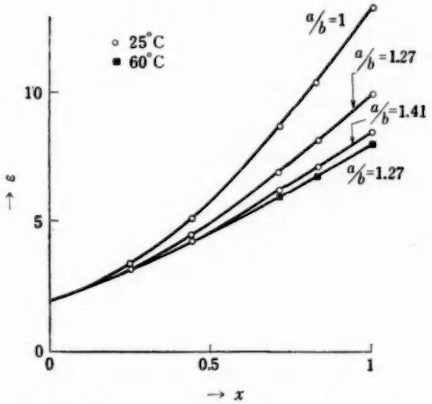

Fig. 1. The calculated dielectric constants of the mixture; dichloroethane-carbon tetrachloride.

8) I. Nakagawa, *J. Chem. Soc. Japan, Pure Chem. Sec.* (*Nippon Kagaku Zasshi*), **79**, 1353 (1958); K. Kimura and R. Fujishiro, This Bulletin, **32**, 433 (1959).
9) A. Weissberger et al., "Organic Solvents", Interscience Publishers, Inc., New York (1955).
10) A. Wada, *J. Chem. Phys.*, **22**, 198 (1954).

assumption was confirmed to be reasonable by the measurements of densities of the mixture.

The ratio a/b of the *gauche* form of dichloroethane is to be estimated by the use of the atomic distances and van der Waals radii of component atoms of the dichloroethane molecule. But the dichloroethane molecule is not strictly spheroidal. Only the long axis along which the dipole

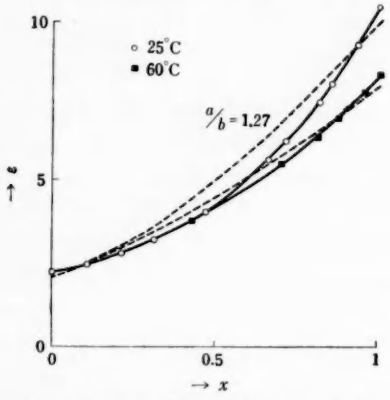

Fig. 2. Comparison of the calculated dielectric constants of the mixture, dichloroethane - carbon tetrachloride, with the observed dielectric constants. ------ Calculated, —— Observed

is located is determined uniquely, whereas the selection of the short axis is arbitrary. The ratio a/b, therefore, can take any value from 1.27 in the case of the maximum short axis to 1.57 of minimum short axis. Values of a/b used in the actual calculation are 1.27 and 1.41, the latter of which is the geometric mean of 1.27 and 1.57. For the sake of comparison the theoretical results in the case of $a/b=1$ are also shown in Fig. 1. From this figure, we may infer that the modification of the shape of the cavity leads to considerable variation of the calculated values of the dielectric constants. This means that the reaction field is overestimated in the Onsager model, i.e., $a/b=1$ and underestimated in the case of $a/b=1.41$. Fig. 2 shows the experimental results corresponding to those of Fig. 1. As seen from these figures, the most satisfactory agreement with experiments is obtained when we adopt as a/b a value 1.27 which corresponds to the allowed maximum of the short axis. This result is of particular interest from the viewpoint of the selection of the short axis. Moreover, the experimental curves representing the dielectric constants of the mixture against the mole fraction x of dichloroethane are more concave than the theoretical curves. The curvatures of the experimental curves themselves are different for different solvents as is seen later, and for different temperatures.

When we compare the theoretical values with the observed ones at 25 and 60°C, we find a better agreement with the experimental results at 60°C than at 25°C as is

TABLE I. THE OBSERVED DIELECTRIC CONSTANTS OF THE MIXTURE; DICHLOROETHANE-CARBON TETRACHLORIDE AT 25° AND 60°C

25°C x	ε	60°C x	ε
0	2.227	0	2.165
0.098	2.501	0.248	2.879
0.207	2.889	0.450	3.774
0.333	3.478	0.679	5.282
0.475	4.347	0.766	5.998
0.667	5.875	0.851	6.823
0.722	6.428	0.940	7.776
0.841	7.778	1	8.492
0.928	8.948		
1	10.022		

shown in Fig. 2 and Table I. This result is the same as that deduced from the equation for the dielectric constants of polar liquids proposed by Yasumi-Komooka[11]. Their conclusion was that a better agreement with the experimental data is obtained near the boiling point than near the melting point.

On the other hand, when we examine the calculated ratio N_g/N_d, we find that it decreases more gradually in the spheroidal model than in the spherical, as is shown in Fig. 3. The calculated ratio N_g/N_d in $x=1$ at 25°C is about 0.75 which

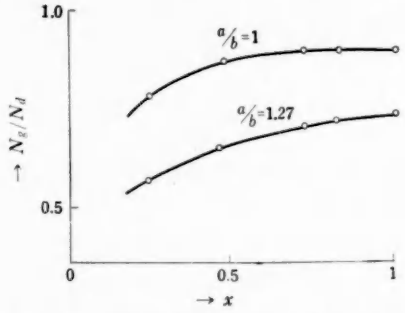

Fig. 3. The calculated ratio N_g/N_d in the mixture, dichloroethane-carbon tetrachloride at 25°C.

11) M. Yasumi and H. Komooka, This Bulletin, **29**, 407 (1956).

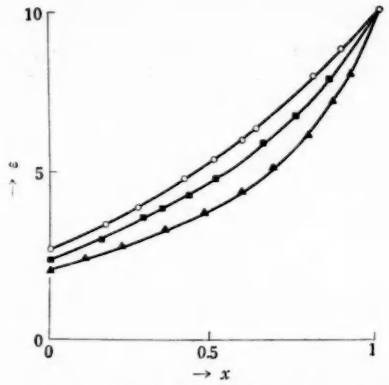

Fig. 4. The experimental results of mixtures, dichloroethane-cyclohexane —○—, dichloroethane-benzene —■— and dichloroethane-carbon disulfide —▲—.

TABLE II. THE OBSERVED DIELECTRIC CONSTANTS OF THE MIXTURES AT 25°C

Dichloroethane-cyclohexane		Dichloroethane-benzene		Dichloroethane-carbon disulfide	
x	ε	x	ε	x	ε
0	2.018	0	2.273	0	2.601
0.101	2.216	0.117	2.803	0.152	3.298
0.232	2.655	0.226	3.345	0.241	3.774
0.350	3.163	0.326	3.897	0.407	4.865
0.475	3.863	0.419	4.468	0.607	6.413
0.548	4.379	0.510	5.084	0.629	6.594
0.649	5.239	0.613	5.863	0.779	7.892
0.743	6.213	0.721	6.801	0.876	8.839
0.826	7.249	0.815	7.779	1	10.073
0.888	8.163	1	10.070		
1	10.073				

is somewhat larger than the value 2/3 measured by the spectroscopic method, but the apparent dipole moment calculated from N_g/N_d when $x \to 0$ agrees fairly well with that estimated experimentally by the use of Debye's equation for dilute solutions.

Finally, the experimental results on mixtures of dichloroethane with other nonpolar solvents at 25°C are summarized in Fig. 4 and Table II. By comparing the experimental curves representing the dielectric constants of mixtures against x with one another, it will be found that the curvatures of the curves are different for different mixtures, and diminish in the following order; cyclohexane and carbon tetrachloride > benzene > carbon disulfide. The excess enthalpy[2] of each mixture decreases in the same order, that is, cyclohexane > carbon tetrachloride > benzene, although the heats of mixing for the carbon disulfide solution have not been measured as yet. Now, the actual calculation of the dielectric constants was carried out only for the mixture dichloroethane-carbon tetrachloride. However, the concentration dependence of the dielectric constants in other mixtures may be inferred to some extent from the calculated results for the mixture dichloroethane-carbon tetrachloride. The case in which the best agreement of the theoretical results with experiments is obtained is the carbon disulfide solution, and next to it, the satisfactory agreement of the theoretical values with the experimental ones is found in the case of benzene solution. The reason why the better agreement even in this simple model is obtained in the case of the carbon disulfide and the benzene solutions is not clear, but some specific interaction may be responsible for this coincidence, considering that the thermodynamic and the spectroscopic[12] measurements suggest the anomalous behavior in the benzene solution. This interesting point may be elucidated partly by examining in detail the temperature dependence of the dielectric constants of the mixtures.

Summary

The dielectric constant for the mixture dichloroethane-carbon tetrachloride was calculated by making use of a model proposed by Onsager, Fujishiro and Scholte. The calculated values agree rather well with the experimental. The higher the temperature is, the better is the agreement. The dielectric constants of other mixtures such as dichloroethane-cyclohexane, dichloroethane-benzene and dichloroethane-carbon disulfide were also measured only at 25°C and compared with one another. The coincidence of the theoretical values with the experimental was obtained in the following order; carbon disulfide, benzene, carbon tetrachloride and cyclohexane.

The cost of this research has been partly defrayed by a grant from the Ministry of Education.

Department of Chemistry
Faculty of Science
Osaka City University
Kita-ku, Osaka

12) A. Wada and Y. Morino, *J. Chem. Phys.*, **22**, 1276 (1954).

Estimation of the Energy of Hydrogen Bonds Formed in Crystals. I. Sublimation Pressures of Some Organic Molecular Crystals and the Additivity of Lattice Energy

By Ariyuki AIHARA

(Received May 25, 1959)

A considerable number of investigations have been done on the problem of hydrogen bonds from both experimental and theoretical points of view, especially since the introduction of the infrared technique in this field of study. Thus, it may safely be said that there is little left to be studied on these topics, so far as they are concerned with hydrogen bondings in solutions of, e. g., phenols, amides and amines in appropriate solvents. One of the questions, however, which is not completely solved as yet, is how to estimate the strength of hydrogen bonds when they are formed in the crystalline state. In this connection, the author has been engaged in the measurement of sublimation pressures of a number of amides and amines with the hope of getting knowledge concerning the relation between the energy of hydrogen bonds in crystals and the heat of sublimation[1].

The principle of estimating the energy of hydrogen bonds in crystals, which has hitherto been adopted by several investigators[1-3], is first to measure the heat of sublimation of a substance in question and then to subtract from it the amount of contribution to the lattice energy due to dispersive and dipolar interaction between molecules in the lattice. Here, the interaction energy due to dispersive force can be calculated theoretically by the Slater-Kirkwood formula[4] if the crystal structure is fully analyzed by X-ray diffraction or by any other methods, while the dipolar interaction can be estimated by the usual procedure or by assuming point charge models.

In case the crystal structure is too complicated to permit theoretical calculation of lattice energy or if it is not analyzed yet, a conventional method has been used in which one assumes the heat of sublimation of a substance, isoelectronic with that in question, as equivalent to the portion of lattice energy due to dispersive and dipolar interaction between molecules in the crystal of a substance forming a hydrogen bond, thereby estimating the energy of the hydrogen bond according to the method already mentioned. A trouble is that an appropriate isoelectronic molecule is not always available to follow the above procedure.

To overcome this difficulty the author has tried first to establish the approximate method of estimating the lattice energy of molecular crystals empirically, assuming its additivity, and then to make use of this method to estimate the energy of hydrogen bonds in crystals of phenols, amides and amines. In this paper, the additivity rule for lattice energy of organic molecular crystals will be examined together with experimental results of sublimation pressure measurement for a number of molecular crystals.

Experimental

Sublimation pressures were measured with a viscosity gauge of the type first designed by Haber[5], Langmuir[6] and later modified by Sasaki[7]. It consists of a Λ shaped fine quartz fiber mounted on a piece of a quartz rod and set in a measuring cell. The diameter of the fiber is 0.1 mm. and the length of the isosceles side of the triangle formed is nearly 10 cm. To facilitate the setting of vibration of the fiber from outside of the cell by a small magnet, a piece of iron wire is attached to the top of the fiber. Samples are fractionally sublimed or distilled under high vacuum and are introduced directly into the cell without allowing them to

1) A. Aihara, *J. Chem. Soc. Japan, Pure Chem. Sec.* (*Nippon Kagaku Zasshi*), **73**, 855 (1952); ibid., **74**, 437, 631, 634 (1953); ibid., **76**, 492, 495, 497 (1955).
2) L. Pauling, "The Nature of the Chemical Bnod", Cornell Univ. Press, Ithaca, N. Y. (1945), p. 304—306.
3) S. Seki et al., This Bulletin, **29**, 127 (1956); ibid., **32**, 137 (1959).
4) J. C. Slater and J. G. Kirkwood, *Phys. Rev.*, **37**, 682 (1931).
5) F. Haber and F. Kerschbaum, *Z. Elektrochem.*, **20**, 296 (1914).
6) I. Langmuir, *J. Am. Chem. Soc.*, **35**, 107 (1913).
7) N. Sasaki, "Handbook Experimental Chemistry (Kagaku Jikken Gaku)", Vol. I—3, Kawade Shobo Co., Ltd., Tokyo (1950), p. 321.

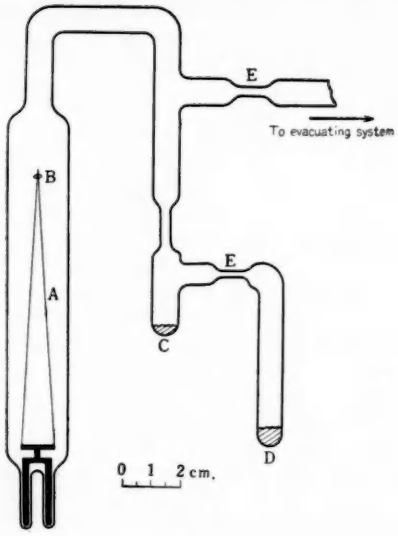

Fig. 1. Viscosity gauge.
A, quartz fiber; B, iron ring
C, sample (purified); D, sample (crude);
E, to be sealed off after evacuation.

make contact with air. The device is shown in Fig. 1[1].

Like most of other vapor pressure measuring gauges, the viscosity gauge must be calibrated with an absolute manometer, such as the McLeod or Knudsen gauge. Here, the calibration was made by subjecting the gauge to saturated vapor of carefully purified benzophenone at several temperatures at which the vapor pressure of benzophenone was already known[8]. According to Haber and Kerschbaum[5], the relation between the pressure in the gauge, P, and the damping time rebuired for the amplitude of the vibration of the fiber to decrease to its half value, t, can be expressed as follows; $P\sqrt{M}=b/t-a$. Here a and b are constants of the gauge and M is the molecular weight of the vapor in it. Thus by observing the damping time, t, at several temperatures and putting the corresponding values of vapor pressures into the above equation, the values of a and b can be determined by the method of least squares. An example of the above procedure is shown in Table I. The values of vapor pressure in the last column of the table were calculated by an equation obtained by Nitta and Seki[8]: $\log P= 12.434-4654.3/T$. The constants, a and b, thus obtained are the average values at 30°C, and correction must be made as they vary with $\sqrt{T}$ when measurements are made at different temperatures.

Most of the materials used are commercial products of high grade and are purified several times by fractional sublimation or distillation

8) I. Nitta and S. Seki, *J. Chem. Soc. Japan, Pure Chem. Sec.* (*Nippon Kagaku Zasshi*), **71**, 378 (1950).

Table I. Relation between the damping time and the vapor pressure of benzophenone at several temperatures

T°C	t sec.	P(mmHg)$\times 10^4$
20.3	351	3.78
23.0	261	5.26
25.4	197	7.03
28.1	144	9.91
30.5	110	12.8
33.2	81.7	17.7
36.0	59.1	25.2
38.8	44.1	32.9

$a=5.66\times10^{-4}$, $b=2.00$

under high vacuum. Their melting points are shown in the following tables together with sublimation pressure obtained.

Results

The observed sublimation pressures of biphenyl, diphenylmethane, dibenzyl, triphenylmethane, benzil, benzoylacetone, naphthalene, 2,3-dimethylnaphthalene, 2,6-dimethylnaphthalene, 2-acetylnaphthalene,

Table II. Sublimation pressure of biphenyl

T°K	P(mmHg)$\times 10^3$	T°K	P(mmHg)$\times 10^3$
279.3	0.972	290.6	3.51
281.7	1.28	292.7	4.61
282.8	1.49	295.9	6.16
285.8	2.11	297.5	7.04
288.1	2.59	299.1	8.43
289.7	3.23		

$\log P(\text{mmHg})=11.168-3959.4/T$: m. p. 69.5°C

Table III. Sublimation pressure of diphenylmethane

T°K	P(mmHg)$\times 10^3$	T°K	P(mmHg)$\times 10^3$
277.9	1.26	288.4	4.52
279.3	1.48	290.8	5.70
280.9	1.79	292.3	6.44
282.6	2.22	294.4	7.75
284.1	2.71	296.0	9.16
286.4	3.57	297.9	10.26

$\log P(\text{mmHg})=12.594-4307.8/T$: m. p. 26.8°C

Table IV. Sublimation pressure of dibenzyl

T°K	P(mmHg)$\times 10^4$	T°K	P(mmHg)$\times 10^4$
286.6	7.77	295.0	23.6
288.6	10.1	298.5	31.8
290.7	12.7	299.6	36.3
293.1	16.8	301.4	44.0
294.3	19.8	307.4	83.7

$\log P(\text{mmHg})=12.194-4386.0/T$: m. p. 53.2°C

acenaphthene, and *p*-acetylanisole are shown in Tables II—XIII, respectively. Vapor pressure equations for these substances, obtained by the method of least squares, are also shown together with their melting points.

TABLE V. SUBLIMATION PRESSURE OF TRIPHENYLMETHANE

T°K	P(mmHg)$\times 10^4$	T°K	P(mmHg)$\times 10^4$
325.6	4.04	336.2	13.2
327.3	4.93	336.6	13.7
329.0	5.75	340.0	19.4
330.0	6.61	344.3	30.2
333.0	8.99	349.3	48.7

$\log P(\text{mmHg}) = 12.661 - 5227.9/T$: m. p. 94.0°C

TABLE VI. SUBLIMATION PRESSURE OF BENZIL

T°K	P(mmHg)$\times 10^4$	T°K	P(mmHg)$\times 10^4$
318.7	3.83	328.1	10.9
321.1	5.07	329.7	12.8
322.4	5.89	333.1	18.2
324.1	6.92	336.1	25.7
325.2	7.83	340.1	41.1

$\log P(\text{mmHg}) = 12.708 - 5140.8/T$: m. p. 95.5°C

TABLE VII. SUBLIMATION PRESSURE OF BENZOYLACETONE

T°K	P(mmHg)$\times 10^4$	T°K	P(mmHg)$\times 10^4$
278.6	4.12	288.8	14.9
280.4	5.28	290.5	18.6
282.8	7.06	294.4	28.4
284.6	8.88	296.6	36.2
286.7	11.3	299.5	51.0

$\log P(\text{mmHg}) = 12.317 - 4374.6/T$: m. p. 58.3°C

TABLE VIII. SUBLIMATION PRESSURE OF NAPHTHALENE

T°K	P(mmHg)$\times 10^3$	T°K	P(mmHg)$\times 10^3$
275.9	6.63	281.1	11.6
277.8	8.32	283.2	14.1
279.5	9.47		

$\log P(\text{mmHg}) = 10.376 - 3462.6/T$: m. p. 81.7°C

TABLE IX. SUBLIMATION PRESSURE OF 2,3-DIMETHYLNAPHTHALENE

T°K	P(mmHg)$\times 10^4$	T°K	P(mmHg)$\times 10^4$
278.5	3.32	287.4	9.91
280.4	4.27	290.0	13.5
282.6	5.59	291.6	15.9
283.0	5.80	293.8	20.5
283.7	6.31	295.4	24.3
284.9	7.44	297.3	29.7
285.6	7.89	301.3	45.9
286.3	8.55		

$\log P(\text{mmHg}) = 11.510 - 4172.6/T$: m. p. 105.3°C

TABLE X. SUBLIMATION PRESSURE OF 2,6-DIMETHYLNAPHTHALENE

T°K	P(mmHg)$\times 10^4$	T°K	P(mmHg)$\times 10^4$
279.0	2.72	289.3	10.2
280.5	3.32	290.5	11.7
282.1	4.13	293.7	16.9
283.8	5.17	296.7	24.2
285.6	6.55	299.7	33.8
286.8	7.44	303.8	52.2

$\log P(\text{mmHg}) = 12.165 - 4386.4/T$: m. p. 106.2°C

TABLE XI. SUBLIMATION PRESSURE OF 2-ACETYLNAPHTHALENE

T°K	P(mmHg)$\times 10^4$	T°K	P(mmHg)$\times 10^4$
295.1	3.95	305.5	13.3
297.2	5.16	309.5	21.3
299.3	6.59	315.8	41.4
302.5	9.49		

$\log P(\text{mmHg}) = 12.153 - 4589.9/T$: m. p. 55.8°C

TABLE XII. SUBLIMATION PRESSURE OF ACENAPHTHENE

T°K	P(mmHg)$\times 10^3$	T°K	P(mmHg)$\times 10^3$
291.1	1.03	298.3	2.40
292.2	1.20	301.0	3.22
292.9	1.29	304.4	4.64
293.8	1.44	307.3	6.20
295.8	1.79	310.6	8.54
297.3	2.09		

$\log P(\text{mmHg}) = 11.758 - 4290.5/T$: m. p. 95.0°C

TABLE XIII. SUBLIMATION PRESSURE OF *p*-ACETYLANISOLE

T°K	P(mmHg)$\times 10^4$	T°K	P(mmHg)$\times 10^4$
275.8	4.53	287.4	18.1
277.7	5.72	289.1	21.9
280.3	7.78	293.1	33.9
282.0	9.76	296.4	48.3
284.4	12.8	298.8	61.6
285.1	13.8	300.4	72.4

$\log P(\text{mmHg}) = 11.367 - 4056.1/T$: m. p. 38.4°C

Some of the results of the measurements of sublimation pressure of biphenyl, published previously by several investigators[9-11], are compared in Fig. 2 with the author's. As can be seen in the figure, the author's result is in good agreement with that of Seki and Suzuki, while the others show considerable deviations from the author's, Bradley's data being too high and Bright's too low. The fact that the results obtained by different methods, i. e., a method using viscosity gauge by the

9) N. F. H. Bright, *J. Chem. Soc.*, **1951**, 624.
10) S. Seki and K. Suzuki, This Bulletin. **26**, 209 (1953).
11) R. S. Bradley, *J. Chem. Soc.*, **1953**, 1690.

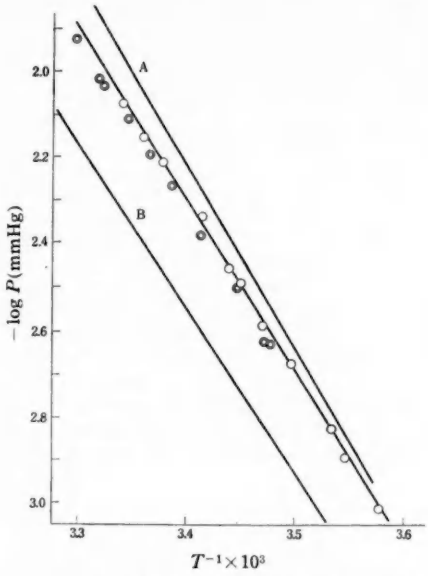

Fig. 2. Sublimation pressure of biphenyl.
○, Aihara; ◎, Seki & Suzuki;
A, Bradley; B, Bright.

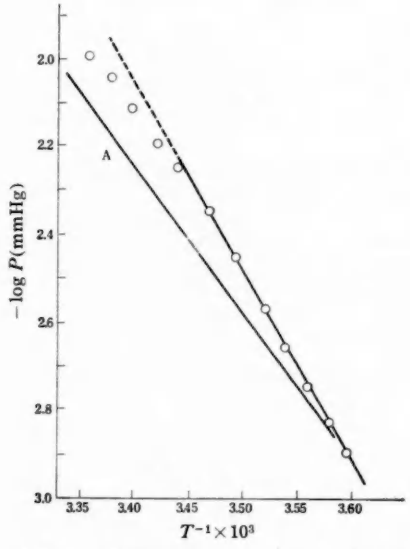

Fig. 3. Sublimation pressure of diphenylmethane.
○, Aihara; A, Bright.

author and an effusion method by Seki and Suzuki, give a good agreement, clearly shows the reliability of these data.

The sublimation pressure of diphenylmethane measured by Bright[9] is again lower than the author's result, the linear relation between $\log P$ and T^{-1} showing a smaller inclination compared with the author's. (Fig. 3). Plotting the experimental values of $\log P$ against T^{-1}, it is noticed in the author's measurement that there occurs a change in the linear relation between $\log P$ and T^{-1} at about 15°C and upward. Roughly speaking, the relation between $\log P$ and T^{-1} after this change goes almost parallel with that of Bright's. Also a simple dilatometric measurement revealed the occurrence of a change in the expansion coefficient of diphenylmethane at about 15°C. (Fig. 4). Although the nature of this transitional change is not clear as yet, it is likely that Bright missed it, putting too much weight on observed values of sublimation pressure above 15°C. The vapor pressure equation shown in Table III is, thus, valid for the temperature range below 15°C.

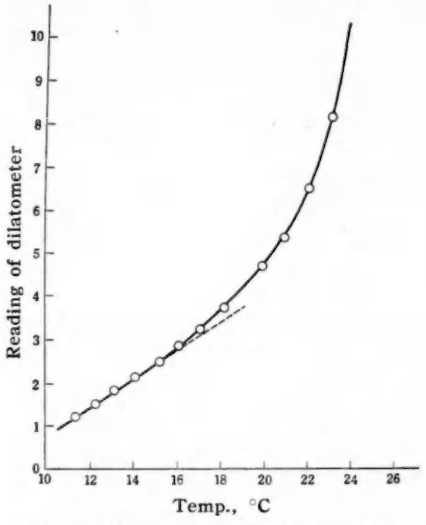

Fig. 4. Dilatometry of diphenylmethane. Reading of dilatometer is in an arbitrary scale.

Bright's[9] result on the sublimation pressure of dibenzyl deviates similarly from the author's as was seen in the two cases mentioned above: the vapor pressure equation and the heat of sublimation obtained by Bright are, $\log P = 9.86 - 3783/T$, $\Delta H = 17.3$ kcal./mol., while the author's are $\log P = 12.194 - 4386.0/T$ and $\Delta H = 20.07$ kcal./mol.

Of the other substances dealt with in this paper, mention should be made of the

TABLE XIV. VALUES OF THERMODYNAMIC FUNCTIONS

Compounds	ΔH_{obs} kcal./mol.	ΔH_{calc} kcal./mol.	$\Delta G^{298.2°K}$ kcal./mol.	ΔS cal./deg. mol.
	18.12±0.14	18.0	6.81±0.28	37.9±0.5
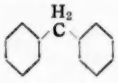	19.71±0.15	20.0	6.45±0.31	44.5±0.5
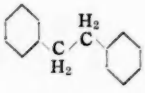	20.07±0.11	22.0	7.36±0.22	42.6±0.4
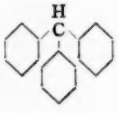	23.92±0.14	29.0	10.58±0.26	44.8±0.4
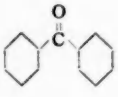	21.30 [3]	21.5	8.26 [3]	43.7 [3]
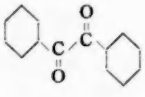	23.52±0.27	25.0	10.11±0.55	45.0±0.9
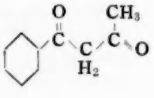	20.02±0.10	20.0	7.14±0.21	43.2±0.4
	15.84±0.54	15.5	5.61±1.12	34.3±1.9
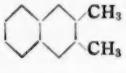	19.09±0.07	19.5	7.31±0.14	39.5±0.2
	20.07±0.09	19.5	7.40±0.18	42.5±0.3
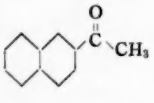	21.00±0.10	21.0	8.35±0.20	42.4±0.3
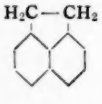	19.63±0.10	19.5	7.52±0.21	40.6±0.4
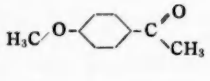	18.56±0.05	18.5	6.98±0.11	38.8±0.2

result of sublimation pressure of naphthalene. There are plenty of data on the sublimation pressure of naphthalene published already in literatures[11-13], but strangely none of them coincide with one another. The author's value of sublimation pressure lies between those of Bradley[11]* and Andrews[13], while ΔH=15.84 kcal./mol. by the author agrees well with Zilberman-Granovskaya's[12] value, ΔH=15.7 kcal./mol., and Wolf's[14] value, ΔH=15.9 kcal./mol. The differences between the various results must be due to different degrees of purity of the samples with which the determinations were made, and also due to the inaccuracy of the methods of determination.

The values of some thermodynamic functions of the substances derived from vapor pressure equations are shown in Table XIV.

Additivity of Lattice Energy

Inspection of the relation between the heats of sublimation and the molecular structures of the compounds listed in Table XIV suggests that an additivity rule may be applied to the lattice energies of these crystals, at least as a first approximation. Now let it be assumed that each constituent group of a molecule, such as methyl, carbonyl, phenyl, etc., makes a contribution to the lattice energy independently. Then, if we allot an appropriate energy to each group, it should be possible to get a "calculated lattice energy" of a compound in question. The third column of Table XIV shows the values of lattice energies thus calculated for compounds dealt with in this paper, with the following values of allotted lattice energies for constituent groups. (Table XV). Notwithstanding the approximate nature of the method of calculation, the agreement between observed and calculated values of lattice energies, i.e., ΔH_{obs} and ΔH_{calc}, is quite satisfactory, as can be seen in Table XIV. Disagreement noticed in a few cases, such as dibenzyl, triphenylmethane and benzil, can be ascribed to the bulky structure of the molecules which prevents the close approach of constituent groups to each other, thus decreasing the amount of contribution to the lattice energy to some extent.

Table XV. Allotment of lattice energies to groups

Groups	Energy kcal./mol.	Groups	Energy kcal./mol.
CH, CH_2, CH_3	2.0	O-CH_3	4.0
NH, NH_2	2.0	C_6H_5	9.0
OH	2.0	$C_{10}H_7$	15.5
C=O	3.5	*t*-Butyl	5.5

In Table XV, the value for phenyl group, 9.0 kcal./mol., was determined by dividing the heat of sublimation of biphenyl, 18.1 kcal./mol., by two: this value is very close to the heat of sublimation of benzene obtaind by Trieschmann, 9.2 kcal./mol.[15] The value for naphthyl group, 15.5 kcal./mol. is close to the average of the heat of sublimation of naphthalene determined by the author, Wolf[14], and Zilberman-Granovskaya[12]. As to the increment of lattice energy due to a methyl (or methylene) group, several investigators have published the following values: 2.3 kcal./mol. by Müller[16], 1.5 kcal./mol. by Inokuchi[17], 1.7~2.2 kcal. mol. by Moelwyn-Hughes[18], 1.1~1.7 kcal./mol. by Davies[19]. The author's value, 2.0 kcal./mol., is the average of the above values and those obtained by analyzing the data in Table XIV. The same value is assigned to amino and hydroxyl groups as that of a methyl group, because these molecules are all isoelectronic. The validity of assigning the same value to these groups will be confirmed in succeeding papers where the lattice energies of phenols, amides and amines will be discussed. Also Bondi and Simkin[20] have discussed this problem. The value for a carbonyl group, 3.5 kcal./mol., was obtained by analyzing the heats of sublimation of benzophenone, benzoylacetone, 2-acetylnaphthalene and some other compounds having a carbonyl group. The value for a *tert*-butyl group was derived from the heat of sublimation of 1,4-di*tert*-butylbenzene[21]. 4.0 kcal./mol. for

12) Zilberman-Granovskaya, *J. Phys. Chem.* (*U.S.S.R.*), **14**, 759 (1940):
log P=10.41−3429/T, ΔH=15.7 kcal./mol.

13) M. R. Andrews, *J. Phys. Chem.*, **30**, 1497 (1926):
log P=12.275−4000/T, ΔH=18.28 kcal./mol.

* Bradley's data:
log P=11.597−3783/T, ΔH=17.3 kcal./mol.

14) K. L. Wolf and H. Weghofer, *Z. physik. Chem.*, **B39**, 194 (1938).

15) H. G. Trieschmann, Dissertation, Kiel (1935).

16) A. Müller, *Proc. Roy. Soc.* (*London*), **A154**, 124 (1936).

17) H. Inokuchi, *J. Chem. Soc. Japan, Pure Chem. Sec.* (*Nippon Kagaku Zasshi*), **72**, 552 (1951).

18) E. A. Moelwyn-Hughes, "Physical Chemistry", Pergamon Press, London (1957), p. 682.

19) M. Davies, private communication.

20) A. Bondi and D. J. Simkin, *J. Chem. Phys.*, **25**, 1073 (1956).

21) E. R. Hopke and G. W. Sears, *J. Chem. Phys.*, **19**, 1345 (1951).

a methoxyl group was determined by subtracting the allotted lattice energies for methyl and carbonyl groups from the heat of sublimation of *p*-acetylanisole.

It must be admitted that the treatment of lattice energies of organic molecular crystals discussed above is quite rough and could not be applied to more complicated cases without further refinement. Still, an orthodox way of calculating lattice energies, such as by Slater-Kirkwood formula[4] or by other ways, does not necessarily give a satisfactory agreement between calculated and observed lattice energies, as has been pointed out by Seki and his collaborators[22]. Therefore, it would be helpful, at the present stage, to have an approximate way of estimating lattice energies of molecular crystals empirically, as is proposed in this paper. This procedure will be used later to get the energy of hydrogen bond in crystals of phenols, amides and amines.

22) S. Takagi, R. Shintani, H. Chihara and S. Seki, This Bulletin, **32**, 137 (1959).

Summary

Sublimation pressures of a number of organic molecular crystals were measured by a viscosity gauge. The heats of sublimation of these compounds were examined in relation to their molecular structures, and it was concluded that an additivity rule could be applied to the lattice energies of these crystals as a first approximation.

The author wishes to thank Professor M. Davies, the University of Wales, for informing the author about some of his results prior to publication. The cost of the work was partly defrayed by the financial support of the Ministry of Education to which the author's thanks are due.

Department of Chemistry
Faculty of Liberal Arts & Science
Shinshu University
Agata-machi, Matsumoto

Stress Relaxation of Thermo-Reversible Gels. Polyvinyl Alcohol—Congo Red—Water System

By Kiyoshi ARAKAWA

(Received June 1, 1959)

In the previous paper the author reported the result of the stress relaxation experiment made on the gel of the polyvinyl alcohol-glycerin-water system[1]. As another example of thermo-reversible gels of polymeric nature, the gel of the polyvinyl alcohol-congo red-water system is known, and several studies on the properties of the gel have been reported[2].

As a part of the series of rheological studies of thermo-reversible gels[1,3] a stress relaxation experiment has been attempted on the gel, and the result is reported in the present paper.

1) K. Arakawa, This Bulletin, **31**, 842 (1958).
2) C. Dittmar and W. J. Priest, *J. Polymer Sci.*, **18**, 275 (1955); N. Hirai, *J. Chem. Soc. Japan, Pure Chem. Sec.* (*Nippon Kagaku Zasshi*), **75**, 693 (1954); T. Danno, The 10th Annual Meeting of the Chemical Society of Japan, Tokyo, April. 1957.
3) K. Arakawa, *J. Chem. Soc. Japan, Pure Chem. Soc.* (*Nippon Kagaku Zasshi*), **80**, 133 (1959).

Experimental

Apparatus. — The apparatus to measure the relaxing stress produced in the specimen under a given strain is the same one as that used previously[1,3]. The chainomatic balance part of the apparatus is shown in Fig. 1. A specimen is compressed between a plate attached to a bar and a bottom plate connected to a screw gauge by the rotation of the gauge, which is graduated to 0.01 mm. The stress in the specimen is calculated from the vertical length of the suspended chain which is balancing automatically with the stress. The specimen is dipped in liquid paraffin, as was done in the preceding studies[1,3].

Sample. — A commercial sample of polyvinyl alcohol was purified by precipitation from aqueous solution. The amount of residual acetate groups in the sample was 1.5% by mole. The intrinsic viscosity $[\eta]_{30}$ was 0.96 100 cc./g., which was determined by a capillary viscometer. The viscosity-average molecular weight M_V was calculated to be 8.5×10^4 according to the formula by

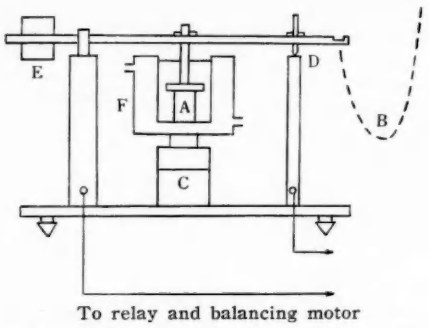

Fig. 1. Chainomatic balance relaxometer
A: specimen
B: chain
C: screw gauge
D: point contact
E: balancing weight
F: double jacket

A. Nakajima et al.[4] Congo red used was Merck's analytical grade chemical.

The preparation of specimens was as follows. A definite quantity of dried polyvinyl alcohol was mixed with dried congo red powder, the amount of which was adjusted to be accurately 1/10 of polyvinyl alcohol by weight (this weight ratio of congo red and polyvinyl alcohol was taken to be the same for all specimens used in the present study), and a calculated quantity of water was added to the mixture in a conical beaker. After being covered with liquid paraffin, the mixture was dissolved slowly by heating in a water bath. After complete dissolution the solution was poured into cylindrical moulds kept at about 85°C in a thermostat and was cooled down slowly to 50°C (the rate of temperature decrease: 5°C per hour), and then was aged at room temperature. After several days the specimens (diameter, 2 cm.; height, about 3 cm.) were taken out from the moulds, and were aged moreover at room temperature in liquid paraffin for about a month. The composition of the prepared specimens is described in Table I.

TABLE I. THE COMPOSITION OF GELS

Sample	Polyvinyl alcohol wt. %	Congo red wt. %
A	17.5	1.75
B	15.0	1.50

Samples A and B have typical rubber-like elasticity at ordinary temperature and make the sol-gel transition reversibly at about 80°C.

Results and Discussion

Stress Relaxation Data.—The data of stress relaxation of samples A and B are plotted in the form $(298/T)E_r$ vs. $\log t$, where $E_r=f/\gamma$ is relaxation Young's modulus; t time, and f stress, in Figs. 2a and 2b. The strain γ applied in the present experiment was 15% for all specimens. This value was in the range where the linear relation between stress and strain was almost maintained. These data are reduced to 25°C by multiplying E_r by a factor $298/T$.

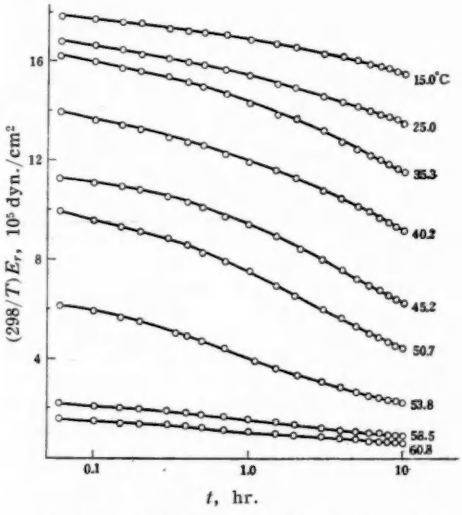

Fig. 2a. Reduced relaxation Young's modulus of 17.5% gel.

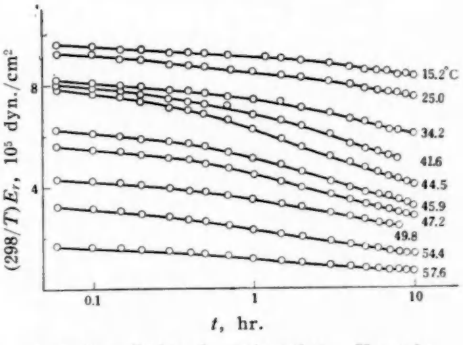

Fig. 2b. Reduced relaxation Young's modulus of 15% gel.

The master relaxation curve[5] at 25°C for each sample is obtained by means of arbitrary shift factors a_T. The curves,

4) A. Nakajima and K. Furutate, *Chem. High Polymers (Kobunshi Kagaku)*, **6**, 460 (1949).

5) J. D. Ferry, *J. Am. Chem. Soc.*, **72**, 3746 (1950); F. Schwarzl and A. J. Staverman, *J. Appl. Phys.*, **23**, 838 (1952); C. A. Dahlquist and M. R. Hatfield, *J. Colloid Sci.*, **7**, 253 (1952).

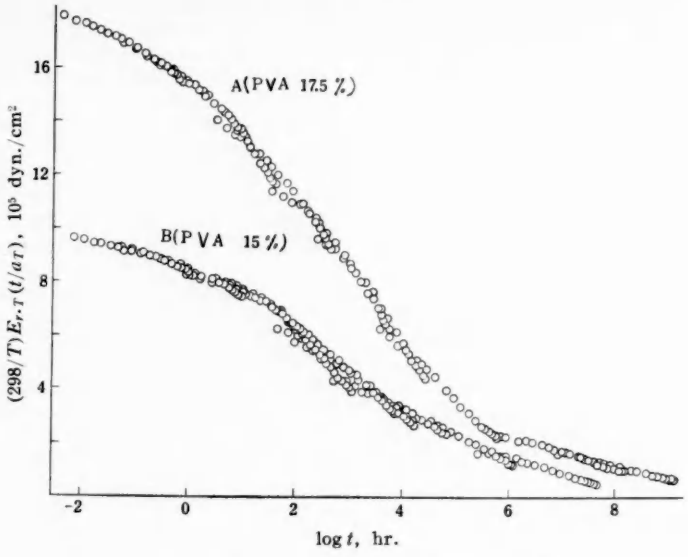

Fig. 3. Master relaxation curves at 25°C.

thus obtained, are plotted in Fig. 3. The superposition of each relaxation curve is seen to be fairly good.

Shift factors $\log a_T$ are plotted against $1/T$ in Fig. 4. It seems the $\log a_T$ vs. $1/T$ curve is approximately linear in the low temperature region, and that the deviation from linearity occurs at about 43°C. The apparent activation energy H_a which is calculated from the $\log a_T$ vs. $1/T$ curve is a constant value, 42 kcal., below 43°C. This value of H_a is smaller than that of the gel of polyvinyl alcohol, glycerin, and water system. The value of H_a increases with temperature above 43°C. This tendency differs from that observed in the polyvinyl alcohol-glycerin-water gel, but is similar to that observed in the hydrogel of agar-agar in which the deviation from linearity appears at about the same temperature, but the value of H_a below the temperature is much smaller*,[3].

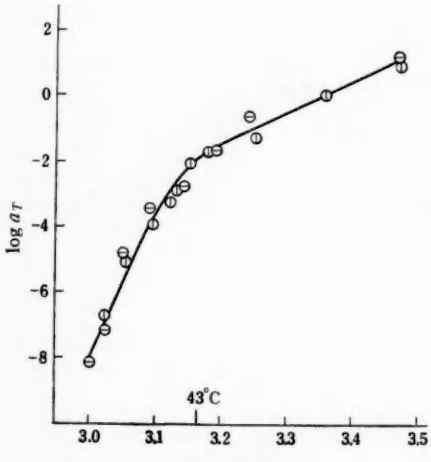

Fig. 4. Log a_T vs. $1/T$ relation.
⊖ Sample A
⊕ Sample B

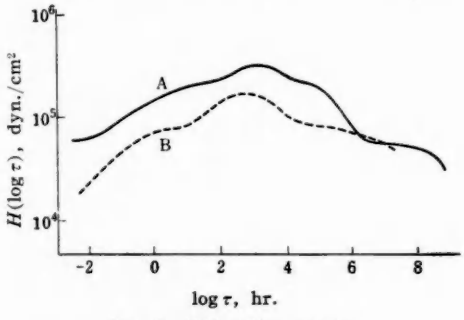

Fig. 5. Relaxation spectra

* In the hydrogels of agar-agar the superposition of each relaxation curve is not so good, except in the case of 2.6% gel, above ca. 40°C. The mechanical behavior of 2.6% gel was as described in the text. In the gels of the other concentration a similar tendency was seen, though exact master curves were not obtained.

As seen in the fact described above, the $\log a_T$ vs. T relation does not obey the equation of WLF form[6].

Distribution Functions of Relaxation Times.— The relaxation spectra $H(\log \tau)$ are shown in Fig. 5, which were calculated from the master relaxation curves shown in Fig. 3 by the second order approximation[7].

$$H\left(\log\frac{\tau}{2}\right)=2.303\left[E_r\left\{-\frac{\mathrm{d}\log E_r}{\mathrm{d}\log t}+\frac{1}{2.303}\frac{\mathrm{d}^2(\log E_r)}{\mathrm{d}(\log t)^2}+\left(\frac{\mathrm{d}\log E_r}{\mathrm{d}\log t}\right)^2\right\}\right]_{t=\tau}$$

Each curve in Fig. 5 is seen to exhibit the character of the box type region of the whole spectrum, which corresponds to the rubbery and fluid state of materials.

Each spectrum is similar in shape except at the long time end, and the spectrum for 15% gel is seen to conform to that for 17.5% gel when slid upwards and to the right.

From the above facts it seems to be possible that two curves shown in Fig. 3 are composed to a single curve approximately, but this reduction on concentration has turned out to need the multiplication factor $(C_0/C)^n$, where the value of n is 3.5~4 and C_0 is a reference concentration. This value of n is too large, being compared with the value, 2, reported previously by DeWitt et al.[8] on the solution of polyisobutylene. More data are required.

6) M. L. Williams, R. F. Landel and J. D. Ferry, *J. Am. Chem. Soc.*, **77**, 3701 (1955).
7) R. D. Andrews, *Ind. Eng. Chem.*, **44**, 707 (1952); F. Schwarzl and A. J. Staverman, *Physica*, **18**, 791 (1952).
8) T. W. DeWitt, H. Markovitz, F. J. Padden and L. J. Zapas, *J. Colloid Sci.*, **10**, 174 (1955).

Summary

Stress relaxation curves were obtained for the gels of the polyvinyl alcohol-congo red-water system in the temperature range, 15~60°C, by means of a chainomatic relaxometer. The molecular weight of polyvinyl alcohol was 8.5×10^4, and gels of 15.0 and 17.5% were used, where the concentration of congo red was adjusted to be 1/10 of that of polyvinyl alcohol. Master relaxation curves were obtained for each concentration over the range, 10^{-2}~10^9 hr, and relaxation spectra were calculated by the second order approximation. The following results were obtained.

1) The $\log a_T$ vs. T relation gives a single curve for two concentrations, and does not obey the equation of WLF form, Also it has characteristics similar to that of agar-agar gels.

2) The apparent activation energy is kept constant to be 42 kcal. below about 43°C, and above this temperature it sharply increases with temperature.

3) The reduction on concentration to a single composite relaxation curve seems to be possible in rough approximation.

The author is indebted to Mr. Morio Kamisho and Mr. Yoshio Daicho for their cooperation in carrying out the experiment.

Department of Chemical Industry
Faculty of Engineering
Shizuoka University
Oiwake, Hamamatsu

Infrared Studies of Polyvinyl Alcohol by Deuteration of its OH Groups

By Hiroyuki TADOKORO

(Received May 29, 1959)

In the previous paper[1] we have studied the density, the sorption of water vapor, and the infrared absorption spectrum of polyvinyl alcohol (PVA) films subjected to heat-treatments at different temperatures from the point of view of crystallinity, and have concluded as follows: (1) the degree of crystallinity determined by these methods is parallel unless the thermal decomposition is considerable, and (2) the 1141 cm^{-1} (8.76 μ)* band is a so-called "crystallization-sensitive" band[2-4]. Succeeding the previous work, we have carried out further studies on PVA by means of infrared spectrum, X-ray diffraction and density measurements in the hope of making some contribution to the studies of the crystallinity and fine texture[3] of high polymers.

The purpose of the present paper is to report some new information obtained by the results of deuteration of the OH groups of PVA.

We have made the infrared spectroscopic measurements of the deuterated PVA for the following purposes. The first is for the elucidation of the nature of the crystallization-sensitive band at 1141 cm^{-1}. As to the crystallization-sensitive band, a considerable number of reports have been published during these several years on polyethylene and many other polymers. Although some reasonable interpretations on the absorption mechanism of the crystallization-sensitive bands have been proposed in the cases of polyethylene, there is no conclusive one for the 1141 cm^{-1} band of PVA. The second purpose is for the assignments of the absorption bands in the region of 1500~800 cm^{-1}. There are already many publications on this problem[5-8], but it is not yet settled at all. The third is to test whether we can determine the crystallinity (or accessibilty) of PVA by means of the deuterium exchange method or not. In the case of cellulose, for instance, it is well known that the velocity of deuterium exchange reaction of the hydroxyl group in the amorphous region is much faster than it is in the crystalline region[9-11]. The fourth is to examine the fine structure of the OH stretching bands of the spectrum arising from the crystalline region, if the amorphous region is to be exclusively deuterated. Marrinan and Mann[11] have investigated the fine structure of the OH bands of various kinds of cellulose by the use of this method.

As to the infrared absorption spectrum of deuterated PVA, Ukita, Nishino and Kominami[12] and also Krimm, Liang and Sutherland[8] have reported quite independently. Ukita and his coworkers have recognized no appreciable change of the spectrum, except the new appearance of the broad band at 4.01 μ due to the OD stretching vibration, because of the low degree of deuteration in their case. Krimm and his coworkers have measured the spectrum of PVA-*d* (degree of deuteration: about 90%) in the region of 3600~400 cm^{-1}, and have obtained experimental results similar to ours. As the assignments of the absorption bands of polymers are generally very complicated problems, we have carried out other experiments such

1) H. Tadokoro, S. Seki and I. Nitta, This Bulletin, **28**, 559 (1955).

* Although the value 1146 cm^{-1} (8.74 μ) was used in the previous paper[1], 1141 cm^{-1} seems to be more precise according to the subsequent more accurate measurements.

2) J. B. Nichols, *J. Appl. Phys.*, **25**, 840 (1954).

3) I. Nitta and H. Tadokoro, *High Polymer (Kobunshi)*, **5**, 296, 345 (1956). (A review of the crystallinity of high polymers).

4) H. Tadokoro, *J. Chem. Soc. Japan, Ind. Chem. Soc. (Kogyo Kagaku Zasshi)*, **59**, 731 (1956). (A review of the application of the infrared spectroscopy for the study of the structure of high polymers).

5) H. W. Thompson and P. Torkington, *Trans. Faraday Soc.*, **41**, 246 (1945).

6) E. R. Blout and R. Karplus, *J. Am. Chem. Soc.*, **70**, 862 (1948).

7) A. Elliott, E. J. Ambrose and R. B. Temple, *J. Chem. Phys.*, **16**, 877 (1948).

8) S. Krimm, C. Y. Liang and G. B. B. M. Sutherland, *J. Polymer Sci.*, **22**, 227 (1956).

9) V. J. Frilette, J. Hanle and H. Mark, *J. Am. Chem. Soc.*, **70**, 1107 (1948).

10) K. E. Almin, *Svensk Paperstidn.* **55**, 767 (1952).

11) H. J. Marrinan and J. Mann, *J. Appl. Chem.*, **4**, 204 (1954); *Trans. Faraday Soc.*, **52**, 481, 487, 492 (1956); *J. Polymer Sci.*, **21**, 301 (1956).

12) J. Ukita, Y. Nishino and T. Kominami, *J. Chem. Soc. Japan, Ind. Chem. Sec. (Kogyo Kagaku Zasshi)*, **58**, 158 (1955).

TABLE I. SAMPLES

Samples	Conditions of heat-treatment	Density at 25°C (g./cc.)	Crystallinity (density method)
I	No heat-treatment	1.291_0	0.29
III	160°C, 15 min.	1.300_7	0.42

as infrared spectroscopic measurements of oriented PVA-*d* and of doubly oriented PVA[13,14], density measurements[15], etc., to get some useful data for this purpose.

Experimental

a) Polyvinyl Alcohol Samples.—Film specimens were prepared from the same starting material (PVA of average degree of polymerization: 1650) by the same method as that described already in the previous papers[1,16]. (See Table I). In the present work the films were cast on a polystyrene plate instead of a glass plate, because the most suitable thickness of the film for infrared measurements is about 7~10 μ, and it is difficult to strip off such a thin film from a glass plate.

The oriented film was prepared by stretching it by hand in one direction over a small flame until it could be stretched no more. Examination of the film between crossed polaroid sheets confirmed the orientation in the direction of stretching.

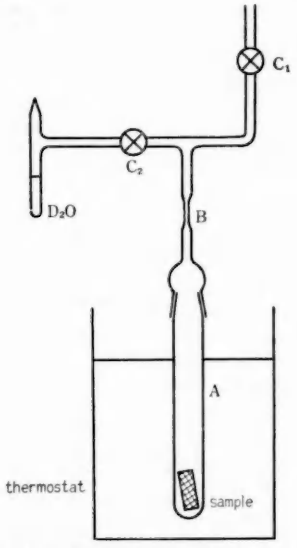

Fig. 1. Apparatus for deuteration.

b) Deuteration, Formalization and Infrared Measurements.—The deuteration of PVA was carried out by using 99.7% heavy water** in a vessel shown in Fig. 1. A PVA film (ca. 20 mm. ×30 mm.) put between the parts of folded stainless steel wire gauze (350 mesh), was inserted in a glass tube A, and was dried at 60°C for about 48 hr. under high vacuum (10^{-4} mmHg or below) by using a liquid air trap (stopcock C_1 being open, and C_2 being closed). After the drying was over, C_1 was closed, the temperature was lowered to room temperature, and then by opening C_2, the sample was equilibrated to the saturated vapor pressure of heavy water. After "being allowed to stand" for about 24 hr., the sample was dried again, and such procedures were repeated several times. At last the glass tube was sealed off at B. The measurements were carried out by putting the films between rock salt plates, with or without polychlorotrifluorocarbon oil (Difloil #3, kindly supplied by Osaka Kinzoku Kôgyô Co., Ltd.).

The oriented and deuterated PVA film for the measurement of dichroism could be prepared by successive procedures in a series of stretching, heat-treatment and deuteration.

Samples I and III were also subjected to formalization and then to deuteration. The formalization was carried out in an aqueous solution of sulfuric acid (200 g./l.), sodium sulfate (250 g./l.) and formaldehyde (40 g./l.) at about 50°C for 15 min. and 2 hr. for each sample. During the formalization treatment the film was held between the parts of a folded wire gauze of bronze (300 mesh) to be free from deformation.

Infrared absorption spectra were taken by using a Hilger H800 Recording Infrared Spectrophotometer with sodium chloride prism, and a Perkin-Elmer Model 21 Double Beam Recording Infrared Spectrophotometer with sodium chloride prism and silver chloride polarizer.

Results and Discussion

a) Deuteration.—The obtained spectra of PVA and of deuterated PVA are shown in Fig. 2a and Table II. The possible errors of the wave number are $\pm 10\,cm^{-1}$ and $\pm 5\,cm^{-1}$ in the regions of $4000 \sim 2000\,cm^{-1}$ and $2000 \sim 700\,cm^{-1}$, respectively. Thus, our spectral data shown in Fig. 2 and Table II are in substantial agreement with those obtained by Krimm et al.[6]

It is well known that OH or NH groups are easily converted into OD or ND by exchange reaction with heavy water, but CH groups are not converted easily unless

13) H. Tadokoro, S. Seki and I. Nitta, *J. Polymer Sci.*, **22**, 563 (1956).
14) H. Tadokoro, S. Seki, I. Nitta and R. Yamadera, ibid., **28**, 244 (1958).
15) H. Tadokoro, K. Kôzai, S. Seki and I. Nitta, ibid., **26**, 379 (1957).
** The product of Norsk Hydro-Electrisk Kvoelstofaktieselskab.
16) H. Tadokoro, S. Seki and I. Nitta, This Bulletin, **27**, 451 (1954).
17) Y. Nishino, J. Ukita and T. Kominami, *J. Chem. Soc. Japan, Ind. Chem. Sec.* (*Kogyo Kagaku Zasshi*), **58**, 159 (1955).
18) E. Nagai and S. Kuribayashi, *Chem. High Polymers* (*Kobunshi Kagaku*), **12**, 322, 368 (1955).
19) L. Glatt, D. S. Webber, C. Seaman and J. W. Ellis, *J. Chem., Phys.*, **18**, 413 (1950).

TABLE II. INFRARED SPECTRA AND VIBRATIONAL ASSIGNMENTS OF PVA AND PVA-*d*

PVA			PVA-*d*			Assignments[e]	
Frequency in cm^{-1}	Dichroism	Intensity	Frequency in cm^{-1}	Dichroism	Intensity	Previous work	This work
3340[a]		vs				ν(OH)	ν(OH)
2945	⊥	s	2945	⊥	s	$\nu_a(CH_2)$ (T, E, B, K)[d]	$\nu_a(CH_2)$
2910	⊥	s	2910	⊥	s	$\nu_s(CH_2)$	$\nu_s(CH_2)$
2840	⊥	sh	2840	⊥	sh	ν(CH) (K)	
			2470[a]		vs	ν(OD) (K)	ν(OD)
1440[b]	∥	s	1428	⊥	m	$\delta(CH_2)$ (T, B) δ(OH) or superposition of δ(OH) and $\delta(CH_2)$ (E) δ(CH+OH), 1428 cm^{-1} is $\delta(CH_2)$ (K)	superposition of $\delta(CH_2)$ and a coupling band (coupling of δ(OH) and 1383 cm^{-1} band of PVA-*d*). 1428 cm^{-1} band of PVA-*d* is $\delta(CH_2)$
1420[b]	⊥	s					
			1383	∥	s		w(CH) or $w(CH_2)$
1376	⊥	w	1376	⊥?	m	$\delta(CH_3$-C) (B) $w(CH_2)$ (K)	δ(CH)?
			1360	⊥	sh		
1326[c] 1315	⊥	m				hydrogen deformation (E) δ(CH+OH) (K)	coupling of δ(OH) and 1383 cm^{-1} band of PVA-*d*
			1256	⊥?	sh		
1232	∥	w	1230	∥	m	acetyl group (T, E) not to be acetyl group (B) w(CH) (K)	$w(CH_2)$ or w(CH)
1141	⊥	m	1148	⊥	s	associated with hydrogen-bond (Ni, Na) ν(C-O-C) (K) associated with oxygen-atom (E)	crystallization-sensitive band (see subsequent paper)
			1122	⊥	s		
1093	⊥	s				associated with oxygen-atom (T) ν(C-O) (B, E, K)	ν(C-O)
1083	∥	m	1083	∥	m		
			1049	⊥	s		ν(C-O)
			977	⊥	m		δ(O-D)
			930	⊥	sh		
913	⊥	w				$r(CH_2)$ (K)	skeletal or CH_2
890	⊥	vw					
849	⊥	m				ν(C-C) (K)	
			842	⊥	m		skeletal or CH_2
835	⊥	sh	825	⊥	sh		$r(CH_2)$
640[f]	∥	sh				w(OH) (K)	
610	⊥	m					
480	⊥	w				δ(C-O) (K)	
410	?	w				w(C-O) (K)	
360	⊥	w					

a) The ν(OH) band at about 3340 cm^{-1} shows no appreciable dichroism at the band maximum, but perpendicular and parallel nature at the higher frequency and lower frequency side, respectively, agreeing with the descriptions of Glatt et al.[19] and Krimm et al.[5] The ν(OD) band at about 2470 cm^{-1} was also found to show the same behavior.

b) The band at about 1430 cm^{-1} splits to 1440 and 1420 cm^{-1} in the polarized spectra because of the difference of their dichroism.

c) The band at about 1325 cm^{-1} has its absorption maximum at 1326 and 1315 cm^{-1} in the case of perpendicular and parallel radiation, respectively.

d) T: Thompson and Torkington[5], E: Elliott, Ambrose and Temple[7], B: Blout and Karplus[6], K: Krimm, Liang and Sutherland[8], Ni: Nishino, Ukita and Kominami[17], Na: Nagai and Kuribayashi[18].

e) ν: stretching, ν_a: antisymmetric stretching, ν_s: symmetric stretching, δ: bending, w: wagging, r: rocking.

f) The data in the region lower than 640 cm^{-1} was reproduced from the paper by Krimm et al.[8]

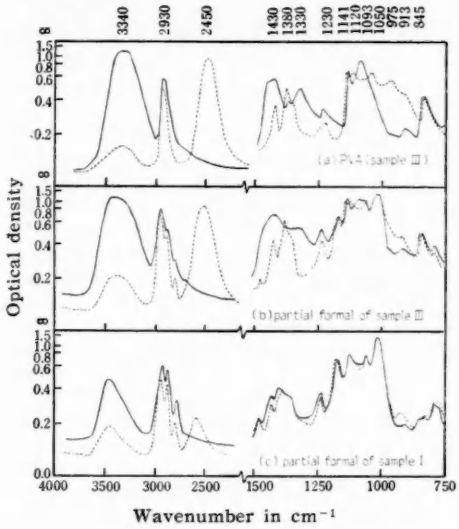

Fig. 2. Infrared spectra of (a) PVA, (b) partial formal of sample III and (c) that of sample I and their deuterated samples (broken line).

under some special conditions[20]. Thus, when PVA is brought into contact with heavy water, the following reaction will take place and the change of the structure will be detected in the infrared spectrum of the sample.

$$-(-CH_2-\underset{OH}{CH}-)_{\bar{p}} \xrightarrow{D_2O} -(-CH_2-\underset{OD}{CH}-)_{\bar{p}}$$

As a result of the deuteration, the intensity of the ν(O–H) band at 3340 cm^{-1} decreases and at the same time a new intense band appears at 2450 cm^{-1}. This latter band evidently corresponds to the ν(O–D) band. While the ν(C–H) band at 2940 cm^{-1} is not affected appreciably by deuteration, this band could be used as the standard for the intensity measurements. The diminution of the optical density of the ν(O–H) band referred to this C–H band, may be used as a measure of degree of deuteration. The extent of deuteration of the sample shown in Fig. 2a is found to be about 90% by this method of estimation.

Now, the deuterations for samples I and III of Table I were studied under various conditions. When the procedures of drying and of exposure to heavy water vapor were repeated alternately several times, both the samples were deuterated up to about 90% regardless of the degree of crystallinity. On the contrary, the extent of deuteration of nylon 6 which had undergone the same procedure as the PVA sample, was much lower than that of PVA. Moreover, the lower the degree of crystallinity of the sample of nylon 6 is, the higher is the extent of deuteration as is shown in Fig. 3. The same results have been reported on the celluloses as mentioned above[9-11].

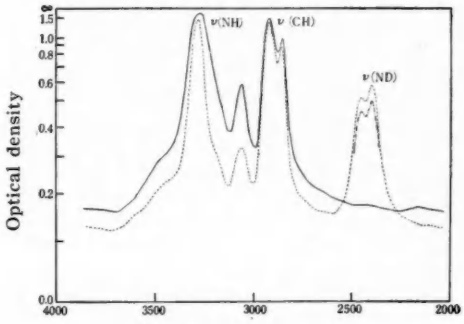

Fig. 3. Infrared spectra of nylon 6 (——) and deuterated nylon 6 (------): ——— sample subjected to heat-treatment.

In relation to these evidences, it will be quite interesting to examine whether the crystalline region of PVA, which is considered to be inaccessible to formalization[21,22], could be deuterated or not. The solid lines of Figs. 2b and 2c show the infrared spectra of samples I and III subjected to formalization. For sample I, the remarkable decrease of the intensity of the OH stretching band at 3340 cm^{-1} and its shift to the shorter wavelength side on formalization may indicate the high degree of formalization. However, for sample III the intensity of the OH stretching band decreases only to a slight extent. This result reconfirmed the fact that the crystalline region is not formalized appreciably as was reported previously by some authors[21,22]. The spectra of these partial formals after deuteration were also shown in the same figure with broken lines. This result indicates that the residual OH groups of the formal of sample III were

20) For example, M. Koizumi, Organic Deuterocompounds, "Advances in Organic Chemistry (Yûkikagaku no Shimpo)" Vol. II. Edited by M. Kotake and S. Akabori, Kyôritsu Shuppan Co. Ltd., Tokyo (1939), p. 27.

21) K. Hirabayashi and N. Fujimoto, *Chem. High Polymers (Kobunshi Kagaku)*, **7**, 159 (1950).

22) Y. Yoshioka and M. Nagano, ibid., **9**, 36 (1952).

deuterated up to about 84%. Thus, the crystalline region of sample III, which was not accessible to formalization, was found to be highly deuterated. These facts seem to show that the difference between the velocity of deuterium exchange in the crystalline region and that in the amorphous region, is considerable in the cases of nylon 6 and cellulose, while this difference is negligibly small in PVA. In this respect, the mechanism of the deuteration reaction of the crystalline region of PVA seems to be a very interesting problem.

b) Interpretation of the Spectra. — The infrared dichroism of the deuterated PVA is shown in Fig. 4, together with that of ordinary PVA for the purpose of comparison. This sample could be prepared by the successive procedures of stretching, heat-treatment and finally deuteration. This method of preparation is based upon the aforementioned remarkable fact that the crystalline region of PVA film even after subjected to heat-treatment can be easily deuterated by exposing it to D_2O vapor.

Although we can not make conclusive assignments of the absorption bands in the region of 1500~700 cm^{-1} at present, we may give here our tentative assignments on the main bands in this region. The band at about 1430 cm^{-1} was assigned by Thompson and Torkington[5] and also by Blout and Karplus[6] to a deformation mode of CH_2 group. On the other hand, Elliott, Ambrose and Temple[7] considered this band to be the δ(O–H), or to be the superposition of the δ(O–H) and the $\delta(CH_2)$ modes. However, this band should be a superposition of the CH_2 bending and some other band connected with hydroxyl group, or probably the O–H deformation, since the intensity of this band decreases sensitively on deuteration and there remains a sharp band which is certainly attributed to the CH_2 bending mode, because of its perpendicular nature. The perpendicular band at 1325 cm^{-1} should also be related to the hydroxyl group because of the intensity decrease on deuteration, whereas Elliott and his coworkers[7] merely referred this band to a hydrogen deformation mode. Just at the middle of the above-mentioned two bands, i. e., at 1380 cm^{-1}, a new intense and sharp band appears on deuteration. We have already suggested[23] that this fact is well interpreted by assuming that these two bands (1430 and 1325 cm^{-1}) are associated with the coupling of the δ(OH) and some other mode such as the CH deformation, and the coupling is removed on deuteration. Krimm and his coworkers[8] independently made a more or less similar interpretation on the results of deuterated PVA (no orientation), and concluded that these two bands come from the interaction between the δ(OH) and δ(CH) modes. However, we have found from the dichroic data with the oriented PVA-*d* that the new band at 1383 cm^{-1} has the nature of distinguished parallel dichroism, and there appear also two perpendicular bands at 1376 and 1361 cm^{-1}, superposed with the 1383 cm^{-1} band. Thus Krimm and his coworkers' assignment of the 1383 cm^{-1} band to δ(CH) can not explain the parallel dichroism of this band. The problem of the assignments of the bands in this region is very complex, but our suggestion in the previous paper[21] does not contradict the present experimental results***.

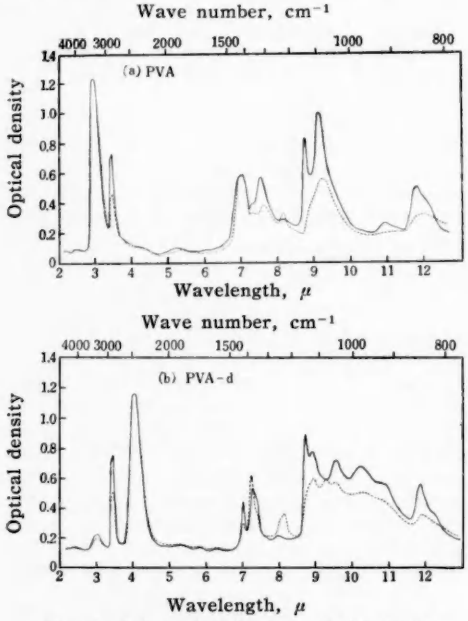

Fig. 4. Infrared dichroism of (a) PVA and (b) PVA-*d* (degree of deuteration ca. 92%): —— electric vector perpendicular to elongation: ------ electric vector parallel to elongation.

23) H. Tadokoro, S. Seki and I. Nitta, *J. Chem. Phys.*, **23**, 1351 (1955).

*** Possibile assignments will be that the 1383 cm^{-1} band is the w(CH) or the $w(CH_2)$[24], and 1376 cm^{-1} band the δ(CH).

24) I. Nakagawa, *J. Chem. Soc. Japan, Pure Chem. Sec.* (*Nippon Kagaku Zasshi*), **76**, 540 (1955).

The parallel band at 1230 cm^{-1} was reported to be associated with the residual acetyl group by Thompson et al.[5] and Elliott et al.[7] But later this assignment was shown to be inadequate by Blout and Karplus[6] from the experimental fact that this band is not removed by acid hydrolysis, although the 1256 cm^{-1} band in unpurified samples is removed simultaneously with the 1710 cm^{-1} band. From the facts that this band is not affected by deuteration and that it becomes intense on formalization with preserving the parallel dichroic nature, this band may be supposed to be $w(CH_2)$, although Krimm and his coworkers' assignment[8] to $w(CH)$ is also undeniable.

The 1148 cm^{-1} band of PVA-*d* is supposed to correspond to the 1141 cm^{-1} band of PVA, because of the distinct perpendicular dichroism. As to the assignment of this band, various interpretations have been proposed, and this seems to be one of the most interesting problems in the infrared studies of this substance. Detailed discussions of this band will be reported in subsequent paper.

The 1093 cm^{-1} band may be mainly associated to the ν(C–O) mode from its location, perpendicular dichroism and the reasonable wave number shift by deuteration, in accordance with the interpretations of Blout et al.[6], Elliott et al.[7], and Krimm et al.[8] The parallel band at 1083 cm^{-1}, superposing the 1093 cm^{-1} band, seems not to be affected by deuteration. On deuteration the 1093 cm^{-1} band disappears and three perpendicular bands appear at 1122, 1049 and 977 cm^{-1}. Of these three bands, the 1049 cm^{-1} band may be assigned to the ν(C–O), and 977 cm^{-1} band to the δ(O–D) tentatively from the consideration of the wave number ratios of the shifts on deuteration.

The perpendicular bands at 913 and 845 cm^{-1} are considered not to be directly associated with the OH group, because of the negligibly small effect of deuteration.

Finally, we wish to refer to the results of our infrared microspectroscopic measurement on the highly doubly oriented PVA sample[14]. In this experiment the measurements were made so that the direction of the polarized infrared beam was parallel to the direction of rolling (the same as that of the carbon zigzag chain). The spectra obtained in this experiment were partly reproduced in Fig. 5. The solid line represents the spectrum with the electric vector parallel to the rolled plane (i.e., the plane of the carbon zigzag chain), and the broken line that with the electric vector perpendicular to the rolled plane. It was found that the 913 and 845 cm^{-1} bands have weak pleochroism, and the latter is a superposition of two bands. The direction of the transition moment of the $r(CH_2)$ mode is perpendicular to the plane of the carbon zigzag chain. The 835 cm^{-1} band, the transition moment of which is in this direction as is evident from the curves in Fig. 5, may be considered as assigned to this mode. The assignment of the 913 cm^{-1} band to $r(CH_2)$ by Krimm et al.[8] is not consistent with our experimental result that the transition moment of this band is parallel to the plane of the carbon zigzag chain.

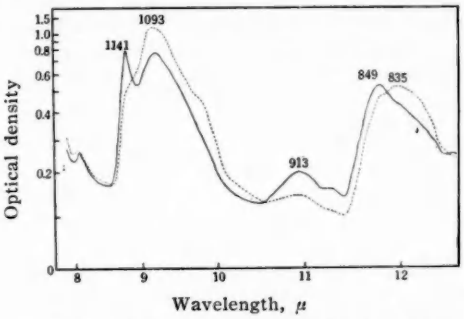

Fig. 5. Infrared spectra of highly doubly oriented PVA specimen[14]. The direction of the infrared beam is parallel to that of rolling.
—— electric vector ∥ rolled plane.
------ electric vector ⊥ rolled plane.

The author wishes to express his gratitude to Professor I. Nitta and Assistant Professor S. Seki, under whose guidance this research was carried out. He also expresses his sincere thanks to Professor T. Shimanouchi of the University of Tokyo for helpful advice and criticism, to Dr. T. Kanzawa and Mr. H. Kamio of Takeda Pharmaceutical Industries Co., Ltd. for preparing part of the charts of the infrared absorption spectra, and to Kurashiki Rayon Co., Ltd. for kindly giving him the PVA samples.

Department of Polymer Science
Faculty of Science
Osaka University
Nakanoshima, Osaka

Heats of Combustion and Formation of Lower Members of Methyl- and Ethyl-methoxypolysiloxanes

By Toshio TANAKA

(Received May 29, 1959)

The heats of combustion of lower members of polydimethylsiloxanes were measured by Thompson[1], and with the aid of the results, average values of bond energy terms for Si–O and Si–C bonds were found to be 117 and 64 kcal./mol., respectively. Of these energy values, the former seems to be too great and the latter somewhat too small, in comparison with those calculated from heats of formation of silica and carborundum. In fact, the Si–O bond energy term has been calculated to be 102 kcal./mol. as the reasonable value, from the heats of formation of methoxy-polysilanes and -polysiloxanes in the preceding paper[2].

In the present work, the heats of combustion of lower members of methyl- and ethyl-methoxypolysiloxanes represented by L_n and L'_2 have been measured, and thermal data derived therefrom have been discussed.

$$L_n:\quad CH_3O\left[\begin{array}{c}CH_3\\|\\Si\cdot O\\|\\OCH_3\end{array}\right]_n\cdot CH_3,\quad n=1\sim3$$

$$L'_2:\quad CH_3O\left[\begin{array}{c}C_2H_5\\|\\Si\cdot O\\|\\OCH_3\end{array}\right]_2\cdot CH_3$$

Experimental

Materials. — The preparation and the physical constants of the members of L_n [3] and L'_2 [4] used in the present work were already reported.

Calorimetry. — The apparatus and procedure used in the combustion experiment have been similar to that described elsewhere[2,5]. The calibration experiment of the calorimeter was carried out at 20°C using benzoic acid (39f) supplied from National Bureau of Standards, Washington, and its energy equivalent value was determined to be 2459 cal./deg. (relative mean deviation ±0.1%).

A thin walled glass ampoule[5] has been used for the purpose of making possible complete combustion of each member of L_n. The completeness of combustion has been ascertained by the method as described in the previous paper[5]. A few other techniques which cause organosilicon compounds to burn completely was reported[1,6]. It seems, however, that satisfactory combustion is not always attained even when these techniques are employed. In the experiment of L'_2, the techniques which are troublesome about the procedure have not been applied; a sample of about 0.4 g. has been weighed in a gelatine capsule, with a known heat of combustion, and the capsule has been vertically supported on a platinum combustion vessel by a platinum ignition wire, a piece of cotton being tied to it, which passes through two small holes at the top of capsule. The evaporation of L'_2 through the very small holes on the capsule has been neglected in quantity, because of its high boiling point (97°C/20 mmHg). This neglect has no influence on the experimental results of L'_2. After burning the sample by electrical ignition, carbon monoxide has not been identified by Winkler's reagent[7] in gaseous phase of bomb contents, and a bulky product, consisting of silica and an incomplete combustion product in a part, has been yielded on the combustion vessel. The incomplete combustion product contains amorphous carbon and, sometimes, a trace of carborundum, and these have been determined in quantity by the procedure described elsewhere[5]. Thermal corrections for carbon and carborundum have been calculated using the values of 7.84 cal./mg. (=32.8 joules/mg.)[9] and 6.86 cal./mg. for their heats of combustion, respectively. The latter value has been calculated from the figures of −26.7 kcal./mol. for the heat of formation of carborundum[10], and is that at standard constant volume process. The completeness of combustion in L'_2 has been found to be 98.5∼99.7% by the analysis of incomplete combustion product.

Results and Discussion

Four to six combustion experiments have been made with each liquid sample, and the results are shown in Table I.

1) R. Thompson, *J. Chem. Soc.*, **1953**, 1908.
2) T. Tanaka and T. Watase, This Bulletin, **28**, 258 (1955).
3) T. Tanaka, A. Tasaka, R. Ōkawara and T. Watase, *Technol. Repts. Osaka Univ.*, **7**, 193 (1957).
4) R. Ōkawara, This Bulletin, **28**, 360 (1955).
5) T. Tanaka, U. Takahashi, R. Ōkawara and T. Watase, ibid., **28**, 15 (1955).
6) S. Tannenbaum, S. Kaye and G. F. Lewenz, *J. Am. Chem. Soc.*, **75**, 3753 (1953).
7) L. W. Winkler, *Z. anal. Chem.*, **102**, 99 (1935).
8) T. Tanaka, *Technol. Repts. Osaka Univ.*, **8**, 437 (1958).
9) F. D. Rossini, "Experimental Thermochemistry", Interscience Publishers, Inc., New York (1956), p. 46.
10) F. D. Rossini et al., "Selected Values of Chemical Thermodynamic Properties", Natl. Bur. Standards, Washington (1952).

TABLE I. HEAT OF COMBUSTION AT CONSTANT VOLUME, cal./g.

Compound							Mean
L_1	5632	5629	5617	5609	—	—	5622
L_2	5213	5228	5221	5212	5219	—	5219
L_3	5083	5055	5074	5072	—	—	5071
L'_2	5875	5865	5903	5856	5891	5868	5876

The relative mean deviation in each run is somewhat high compared with modern precision measurements, but of sufficient precision for bond energy term purpose in view of the other uncertainties involved.

Table II is the summary of important thermal data of four organosilicon compounds, calculated from the results of combustion experiments. Notations in Table II are as follows: $-\Delta U_R$, the heats of combustion at standard constant volume process where the reactants are one atmospheric pressure; $-\Delta H_c$, the heats of combustion in isobaric process at one atmospheric pressure; $-\Delta H_f$, the heats of formation of liquid compounds under consideration from standard elements (gaseous H_2 and O_2, graphitic carbon and metallic silicon); $-\Sigma E$, the heats of formation of the gaseous compounds from monoatomic gases. These energy values, except that in the last column of Table II, have been calculated by the same method as that used in the preceding paper[2], and in the calculation of $-\Sigma E$, heats of vaporization have been estimated to be 7.9, 9.1, 10.3 and 9.5 kcal./mol. for L_1, L_2, L_3 and L'_2, respectively, from Trouton's rule.

Bond Energy Term. — According to the additive law of bond energy, the value ΣE obtained experimentally in such a way may also be expressed by the formula

$$\Sigma E = pE_{Si-O} + qE_{Si-C} + rE_{C-O} + sE_{C-H} + tE_{C-C} \quad (1)$$

where E represents the energy value of bond corresponding to each suffix, and the factors p, q, r, s and t the number of bonds in the molecule under consideration. The energy terms of C–O, C–H and C–C bonds are well known, and if it is assumed that each value is not varied with the change of molecule, the bond energy values of bonds concerning the silicon atom may be estimated by formula 1. The value of $-E\left[\begin{smallmatrix} & C & \\ O & -Si- & O \\ & O & \end{smallmatrix}\right]$ presented in the last column of Table II has been estimated in this manner, using 98.8, 83.2 and 83.2 kcal./mol. for C–H, C–C and C–O bond energy terms, respectively. The former two values have been calculated by the method of least squares from heats of formation of lower members (from ethane to hexane) in normal paraffin[11], other than methane, and the latter from the heat of formation of dimethylether[10] using the C–H bond energy obtained there. Two kinds of Si–O bond are contained in the molecules of L_n and L'_2; that of Si–O–CH_3 linkage and of Si–O–Si linkage. However, no energy difference between the two kinds of Si–O bond were observed in the preceding work on methoxy-polysiloxanes[2], and so these bonds will not be distinguished in the following discussion.

The $-E\left[\begin{smallmatrix} & C & \\ O & -Si- & O \\ & O & \end{smallmatrix}\right]$ in L_2 and L'_2 is in good agreement. However, this value increases with the polymer size of L_n, and further its energy difference between L_2 and L_3 is not so large as that between L_1 and L_2. This tendency has also been found in our recent investigation on heats of formation of methoxy end-blocked dimethylpolysiloxanes[12], and suggests that the $-E\left[\begin{smallmatrix} & C & \\ O & -Si- & O \\ & O & \end{smallmatrix}\right]$ may be close to a constant value as the polymer size increases*.

TABLE II. HEATS OF COMBUSTION AND FORMATION, AND BOND ENERGY, kcal./mol.

Compound	Mol. wt.	$-\Delta U_R$	$-\Delta H_c$	$-\Delta H_f$	$-\Sigma E$	$-E\left[\begin{smallmatrix} & C & \\ O & -Si- & O \\ & O & \end{smallmatrix}\right]$
L_1	136.23	766	767	227	1799	364
L_2	226.38	1181	1183	412	2847	368
L_3	316.54	1605	1608	589	3887	370
L'_2	254.43	1495	1498	422	3408	368

11) F. D. Rossini et al., "Selected Values of Physical and Thermodynamic Properties of Hydrocarbons and Related Compounds", Carnegie Institute of Technology, Pittsburgh, Pennsylvania (1953).

12) T. Tanaka, to be published in *J. Inorg. Nuclear Chem.*

* Such a tendency for bond energy will always be found in lower members of a homologous series; for example, in calculation of C-C bond energy from heats of formation of normal paraffin, assuming that C-H bond energy is constant in the members.

The heats of combustion of various alkylsilanes were already measured by Tannenbaum[6], and Si–C bond energy estimated therefrom[13]. There was found an interesting tendency; namely, that the Si–C bond energy decreased as the size of the alkyl group joined to the silicon atom increased. It will here be assumed for the convenience of discussion that Si–O bond energy in $Si(OCH_3)_4$ (103 kcal./mol.**), which is 1 kcal. lower than that in amorphous silica, is the normal value for its bond energy. Similarly, if Si–C bond energy calculated from the heat of formation of $Si(CH_3)_4$[6] is assumed to be its normal value, it may be estimated to be 71 kcal./mol. using the heats of atomization and the C–H bond energy adopted in the present work. This value for Si–C bond energy is 1 kcal. lower than that*** in carborundum, and seems to be reasonable for its normal bond energy. If such assumptions are accepted for the normal bond energies of Si–O and Si–C bonds, the calculated value for $-E\left[\begin{array}{c}C\\|\\O\text{–}Si\text{–}O\\|\\O\end{array}\right]$ results in 380 kcal./mol. under the additive law of bond energy, and is considerably higher than the observed value in L_3, not to speak of L_1, L_2 and L'_2. Such a deviation from the additive law of bond energy may be attributed to all of the bonds in the molecule under consideration. However, silicon atom has small electronegativity (1.8)[14] and its covalent radius is considerably larger than that of the carbon atom. Also it is well known that the silicon atom is, frequently, able to form a partially double bonding character with other atoms having lone-pair electron or electron donating power, by accepting the electron in its vacant *d*-orbital[15]. Considering these characteristics, the bonding orbital of the silicon atom seems to be liable to undergo any sort of distortion by the effect of neighboring groups.

The observed atomic distance of Si–O bond[16] is abnormally shorter than that (1.91 Å) expected from covalent radii, and this shortening has been considered to be due to the contribution of d_π-p_π bond character[17]. The π-bond character of each Si–O bond in structural unit, $\begin{array}{c}C\\|\\O\text{–}Si\text{–}O\\|\\O\end{array}$, of the molecules considered in this paper will be undoubtedly less than that in $\begin{array}{c}O\\|\\O\text{–}Si\text{–}O\\|\\O\end{array}$, being the structural unit of methoxy-polysiloxanes, considering the numbers of resonance structures between Si–O bonds in both the structural units. As the result, the energy value of Si–O bond in L_n and L'_2 will be supposed to be lower than that in methoxy-polysiloxanes. In this manner, the considerable lowering of bond energy should be expected in the case of methoxy end-blocked dimethylpolysiloxanes, $CH_3O[Si(CH_3)_2\cdot O]_n\cdot \begin{array}{c}C\\|\\O\text{–}Si\text{–}O\\|\\C\end{array}$, the structural unit being CH_3, and this expectation has been ascertained in the recent investigation on their lower members. This supposition on Si–O bond energy will correspond to the shortening of the silicon-halogen bond distance with the decrease of the number of halogen atoms attached to silicon[18].

Summary

1. The heats of combustion of lower members of methyl- and ethyl-methoxy-polysiloxanes have been measured at 20°C and constant volume, and the corresponding heats of combustion and formation in isobaric process have been calculated.

2. The bond energy term in structural unit of $\begin{array}{c}C\\|\\O\text{–}Si\text{–}O\\|\\O\end{array}$ has been calculated from the heat of formation, and it has been found that its value increases with the polymer sizes of the members. Finally, the $-E\left[\begin{array}{c}C\\|\\O\text{–}Si\text{–}O\\|\\O\end{array}\right]$ has been compared with

13) S. Tannenbaum, *J. Am. Chem. Soc.*, **76**, 1027 (1954).

** The Si-O bond energy has been calculated to be 103, 102 and 103 kcal./mol. from heats of formation of $Si(OCH_3)_4$, $Si_2O(OCH_3)_6$ and $Si_3O_2(OCH_3)_8$, respectively, using 98.8 and 83.2 kcal./mol., instead of 98.9 and 84.1 kcal./mol. adopted in the preceding paper[2], for C-H and C-O bond energies.

*** Calculated to be 72 kcal./mol. from heat of formation of carborundum[10].

14) O. Pritchard and H. A. Skinner, *Chem. Revs.*, **55**, 745 (1955).

15) For example, E. L. Reilly, C. Curran and P. A. McCusker, *J. Am. Chem. Soc.*, **76**, 3311 (1954).

16) 1.64±0.03 Å in $\left(O\begin{array}{c}(CH_3)_2\\|\\Si\text{–}O\\|\\Si\text{–}O\\|\\(CH_3)_2\end{array}\right)_2$Si, W. L. Roth and D. Harker, *Acta Cryst.*, **1**, 34 (1948); 1.66±0.04 Å in $[(CH_3)_2SiO]_3$, E. H. Aggarwal and S. H. Bauer, *J. Chem. Phys.*, **18**, 42 (1950); 1.64±0.03 Å in $Si(OCH_3)_4$, 1.63±0.05 Å in $((CH_3)_3Si)_2O$, see Ref. 18.

17) L. Pauling, *J. Phys. Chem.*, **56**, 361 (1952).

18) M. Yokoi, This Bulletin, **30**, 106 (1957).

that expected from the additive law of bond energy, and the lowering of bond energy in these molecules has been discussed in view of the resonance effect.

The author wishes to express his sincere thanks to Professor T. Watase for his gracious encouragement, Dr. R. Ōkawara for providing him with a part of the sample used in the present work, and Messrs. A. Tasaka and T. Ōtsuka for their aid during this experiment.

Department of Applied Chemistry
Faculty of Engineering
Osaka University
Miyakojima-ku, Osaka

Studies on the State of Formic Acid Adsorbed on Silica and Alumina by a Combined Method of Nuclear Magnetic Resonance and Infrared Absorption

By Kozo HIROTA, Kenji FUEKI, Kotaro SHINDO and Yasuo NAKAI

(Received June 6, 1959)

As reported already[1], formic acid is chemisorbed as the formate ion on several metallic powders (Ag, Cu, Ni, Rh, Pd, Pt and Zn), while the acid chemisorbed on silica does not dissociate[2]. However, it was found in the present study that the conclusion obtained in the case of silica can not be applied to alumina, especially in the case of low coverage of adsorption. Such a conclusion may be worthy to be reported, considering the fact[3] that the catalytic role of alumina is similar to that of silica rather than that of metals, e. g., these oxides have dehydrating activity in addition to dehydrogenating activity, contrary to the case of metals which have only dehydrogenating activity.

Experimental

Formic Acid.—The reagent of C. P. grade made by Edogawa Kagaku Kogyo Co. was repeatedly dehydrated by crystallization and then vacuum-distilled in the presence of anhydrous copper sulfate.

Silica.—Silica gel for chromatographic use made by Mallinkrodt Chemical Works was dehydrated at 300°C for 150 hr. It was confirmed by X-ray analysis that the amorphous structure of silica was not changed by dehydration. The specific surface area of the silica was found to be 520 m^2/g. by the BET method (adsorbate: nitrogen).

Alumina.—Alumina gel, precipitated by the reaction between aluminum nitrate and ammonia in aqueous solution, was dehydrated at 300°C for 50 hr. The specific surface area was found to be 310 m^2/g.

Measurement.—Formic acid was adsorbed on each adsorbent which was enclosed in a glass sample tube in vacuo. In the case of nuclear magnetic resonance measurement, a capillary tube filled with water as a standard substance was put in the center of the sample tube. The proton resonance spectra were obtained with a high resolution spectrometer (Varian V-4300B)* at a fixed frequency of 40 Mc/sec. The tube was always rotating around its axis during the measurement. The infrared spectra were obtained using the paste method[4], in which the sample was quickly mulled with Nujol, and a part of the sample was held between the plates of sodium chloride and then offered for measurement (apparatus: Hilger H800). During this procedure a small amount of formic acid may be lost in the atmosphere, but it was checked that this amount was small enough not to alter the conclusion. Taking such a situation into account, the coverage was conventionally designated by θ' instead of the true coverage θ in the case of samples used in infrared absorption measurement. Measurements were made at room temperature.

Results and Discussion

Proton Magnetic Resonance Absorption.—The proton resonace spectrum of formic acid

1) K. Hirota, K. Kuwata and Y. Nakai, This Bulletin, **31**, 861 (1958); K. Hirota, K. Kuwata and S. Asai, *J. Chem. Soc. Japan, Pure Chem. Sec.* (*Nippon Kagaku Zasshi*), **80**, 701 (1959).

2) K. Hirota, K. Fueki, K. Shindo and Y. Nakai, This Bulletin, **31**, 783 (1958).

3) G. M. Schwab and E. Schwab-Agallidis, *J. Am. Chem. Soc.*, **71**, 1806 (1949).

* In the preliminary report, the apparatus was referred to as Varian V-4310C, because some part of the apparatus is so named.

4) G. C. Pimentel, C. V. Gerland and G. Jura, *J. Am. Chem. Soc.*, **75**, 803 (1953).

adsorbed on silica is quite different from that in the liquid state, especially when the amount of adsorption is small, (e. g., $\theta=0.5$); only one signal**, corresponding to the hydrogen atom bonded to the carbon atom, appears as a broad one and, moreover, its position shifts by 33 cps to a higher magnetic field. However, as the coverage is increased up to 2.7, the signal becomes narrower in width and that of the hydrogen atom bonded to the oxygen atom also appears as a very broad one. Thus it may be concluded that the motion of hydrogen in the carboxyl group is fixed in the state of monomolecular adsorption, and such a restriction of the motion is relaxed gradually according as the adsorption layer is the upper. Furthermore, it is pointed out that the observed shifts may be mainly of apparent nature, and therefore, the effect of the magnetic susceptibility of bulk substance was taken into consideration. The chemical shifts, corrected for this effect[5], are shown in the last column of Table I. Though it seems that there is a relation between the amount of adsorbed formic acid and the chemical shift, it is too small for the meaning to be discussed in detail.

TABLE I. CHEMICAL SHIFT OF FORMIC ACID ADSORBED ON SILICA***
(Unit: cps)

δ_{ads}: Shift from reference (water)
δ_{meas}: Shift from liquid formic acid
δ_{cor}: Value to be corrected for bulk magnetic susceptibility
$\delta=\delta_{meas}-\delta_{cor}$: Chemical shift

θ	δ_{ads}	δ_{meas}	δ_{cor}	δ
0.5	97	33	26	7
1.1	100	30	25	5
1.7	103	27	23	4
2.7	109	21	19	2

On the other hand, we could not detect any appreciable signal for the formic acid adsorbed on alumina in the monomolecular state. This is probably due partly to the small amount of adsorption and partly to stronger interaction with alumina than with silica.

Furthermore, the difference in the adsorbed state between silica and alumina could be made clear by the infrared absorption measurement as shown below.

Infrared Absorption.—*Silica.*—In the case of silica two adsorption bands are observed at 3450 (broad) and 1620 cm^{-1}. Both bands may be ascribed to associated water on the surface[6]. However, the stretching band due to the isolated hydroxyl group on the silica surface[7] does not appear at 3749 cm^{-1}, probably being masked by the broad band at 3450 cm^{-1} [8].

Now, when formic acid is adsorbed on silica, new absorption bands appear at 1714 and 960 cm^{-1} in addition to the band near 3520 cm^{-1} (Fig. 1, Table II). The absorption band at 1714 cm^{-1} can be ascribed to

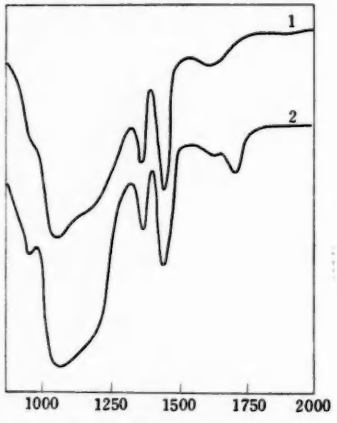

Fig. 1. Infrared spectrum of formic acid adsorbed on silica.
1: silica, 2: $\theta'=0.7$

the C=O stretching vibration, while the band at 960 cm^{-1} to the OH out-of-plane deformation vibration. Thus, it may be said that formic acid is adsorbed on silica in a non-dissociated state. The C=O stretching band shifts to lower frequency as compared to that of the monomer and also of the dimer. This band is rather similar in frequency to that of formic acid in the crystalline state. The same situation holds for the OH deformation band[9]. Considering these facts, it seems that the adsorbed formic acid forms hydrogen bonding not only to the silica surface, but also to each other, forming thus a two-dimensional net structure. Such a model

** The assignment of the signal was made by the use of deuteroformic acid HCOOD.

5) J. R. Zimmerman and M. R. Foster, *J. Phys. Chem.*, **61**, 282 (1957).

*** The resonance of proton bonded to the carbon atom is shown.

6) A. Chevet, *J. Phys. Radium*, **14**, 493 (1953).

7a) R. S. McDonald, *J. Am. Chem. Soc.*, **79**, 850 (1957); *J. Phys. Chem.*, **62**, 1168 (1958).

b) A. N. Terenin, N. G. Yaroslavskii, A. V. Karyakin and A. I. Sidorova, *Microchim. Acta*, 467 (1955).

8) K. Naito, presented at the Symposium on Infrared and Raman Spectra, Kyoto, October, 1958.

9) R. C. Millikan and K. S. Pitzer, *J. Chem. Phys.*, **27**, 1305 (1957); *J. Am. Chem. Soc.*, **20**, 3515 (1958).

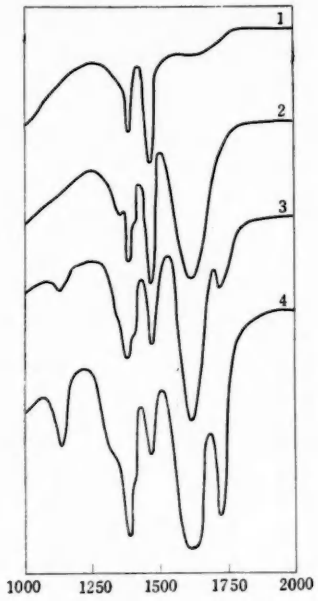

Fig. 2. Infrared spectrum of formic acid adsorbed on alumina.
1: alumina, 2: $\theta'=0.7$, 3: $\theta'=1.3$, 4: $\theta'=2.4$.

was already proposed in the case of the adsorption of water and ethanol on silica from the results of the dielectric measurement of these systems[10,11].

Alumina. — In the infrared spectrum of alumina, not only the absorption bands (3450 and 1620 cm^{-1}) of associated water on the surface, but also that (3760 cm^{-1}) of the isolated hydroxyl group are observed. When formic acid is adsorbed in a monomolecular layer, new absorption bands appear at 1344 and 1402 cm^{-1} besides 1620 cm^{-1} (strong), while the intensity of the band at 3450 cm^{-1} does not vary (Fig. 2, Table II). As the bands at 1344, 1402 and 1620 cm^{-1} can be assigned to the fundamental modes of vibration, ν_2, ν_5 and ν_4, of the formate ion[12], respectively, the state of formic acid adsorbed on alumina is similar to that on metals. However, when the amount of adsorbed formic acid is increased and a monomolecular layer is completed, new absorption bands appear at 1733 and 1124 cm^{-1}, and the band near 3520 cm^{-1} increases in intensity. These results show that non-dissociated formic acid can exist in the upper layer of adsorption on alumina.

TABLE II. SUMMARIZED RESULTS OF INFRARED ABSORPTION****

Adsorbent	θ' 0.3	0.7	1.3	2.4
Silica	1714	1714	1714	—
	960	960	960	—
Alumina			1733 (1705)	1733 (1705)
	1620 (1602)	1620 (1602)	1620 (1602)	1620 (1602)
	1402 (1377)	1402 (1377)	1402 (1377)	1402 (1377)
	1344 (1329)	1344 (1329)	1344 (1329)	1344 (1329)
			1124 (1100)	1124 (1100)

In short, it has been found that the adsorbed formic acid in a monomolecular layer exists as a dissociated or non-dissociated state, according as the adsorbent is alumina or silica. Such difference of state may be noteworthy, in the light of the fact that the catalytic activity of both oxides is similar, i. e., formic acid is dehydrated rather than dehydrogenated, in contrast with the overwhelmingly dehydrogenating activity of metallic powders. It seems, therefore, that there is no direct relation between the adsorbed state and the activated state of decomposition. Concerning this result further research is in progress.

Summary

The state of formic acid adsorbed on silica and alumina has been studied by a combined method of nuclear magnetic resonance and infrared absorption. The adsorbed formic acid in a monomolecular layer has been found not to be dissociated in the case of silica, but to be dissociated in the case of alumina.

A part of the expense for the present investigation has been defrayed from a grant given by the Ministry of Education, to which the authors' thanks are due.

Department of Chemistry
Faculty of Science
Osaka University
Nakanoshima, Osaka

10) M. Shimizu, *J. Chem. Soc. Japan, Pure Chem. Sec.* (*Nippon Kagaku Zasshi*), **78**, 21 (1957).
11) S. Kurosaki, T. Tsuchiya and R. Kawai, ibid., **78**, 1806 (1957).
12) Landolt-Börnstein, "Zahlenwerte und Funktionen", 1, 2. Teil, Springer, Berlin (1951), p. 237.

**** In this table, only the bands in low frequency region were shown. Values in parenthese were obtained by the measurement in which Nujol was not used.

Study on the Reductive Spinel—A New Spinel Formula AlN-Al_2O_3 instead of the Previous One Al_3O_4

By Goro YAMAGUCHI and Hiroaki YANAGIDA

(Received March 4, 1959)

It was proposed in the previous papers[1-3] that a lower valent aluminum ion Al^+ or Al^{2+} may exist in a spinel form Al_2O-$5Al_2O_3$ or Al_3O_4. L. M. Foster, however, suggested[4] that the spinel-like material contains nitride as its component and, therefore, the reducing ability is probably due to the nitride component.

In order to determine whether the reducing ability is due to the lower valent aluminum ion or to the nitride component, the chemical behaviors, the conditions of the formation, the magnetic susceptibility, the cell constant, and the density of the reductive spinel have been investigated.

Experimental

Synthesis of the Reductive Spinel.—Alumina and the reducing agent, aluminum or graphite, were mixed together and heated in the Tammann furnace (Fig. 1).

The X-ray diffraction patterns of the products were investigated at first, and the formation of the reductive spinel was confirmed with a number of methods as shown in Table I. The purity was confirmed also with the slow scanning X-ray diffraction recording.

Chemical Behaviors (Analysis of Nitrogen).—

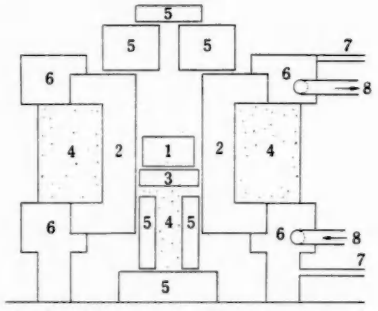

Fig. 1. Tammann furnace for the reductive spinel synthesis.
(1) sample, (2) graphite cylinder, resistance heater, (3) sintered alumina sample holder, (4) graphite powder, (5) refractory, (6) iron frame heater holder, (7) lead wire, (8) water, coolant.

The decomposition of the reductive spinel was tried by using the following reagents: (1) alkali or acid at room temperature; (2) PbO 90: B_2O_3 glass as a flux at 800°C in vacuo (Fig. 2); (3) air above 1000°C. The spinel employed in these experiments was confirmed not to show any X-ray diffraction pattern originating in crystalline aluminum nitride. The evolved gases in the

TABLE I. CONFIRMATION OF THE FORMATION OF THE REDUCTIVE SPINEL AND CHARACTERISTICS WHICH DISTINGUISH IT FROM OTHER SPINEL MgO-Al_2O_3 AND γ-Al_2O_3

Methods	Reductive spinel	$MgO \cdot Al_2O_3$	γ-Al_2O_3
1) X-ray diffraction recording (geigerflex, filtered Cu$K\alpha$ radiation) Scanning speed 4°2 θ per minute	Diffraction pattern of spinel structure Sharp peak	Diffraction pattern of spinel structure Sharp peak	Diffraction pattern of spinel structure Broad
2) X-ray diffraction recording Scanning speed 1/4°2 θ per minute	Unit cell dimension about 7.94 Å	Unit cell dimension about 8.06 Å	Unit cell dimension about 7.89 Å
3) Observation of Becke's line; comparison with the refractive index 1.74 of CH_2I_2	>1.74	<1.74	<1.74
4) Observation of weight increase above 1000°C through heating in air	Increase	—	—

1) G. Yamaguchi, *J. Electrochem. Soc. Japan* (*Denki-Kagaku*), **14**, 106 (1946).
2) G. Yamaguchi, *J. Ceram. Assoc. Japan* (*Yogyo Kyokai Shi*), **61**, 549 (1953); *Ceram. Abstr.*, **33**, 87*e* (1954); *Chem. Abstr.*, **48**, 3652*b* (1954).
3) G. Yamaguchi, This Bulletin, **23**, 89 (1950).
4) Private communication from Dr. L. M. Foster (ALCOA).

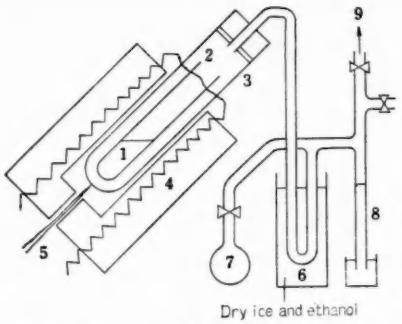

Fig. 2. Apparatus for nitrogen analysis.
(1) sample and flux, (2) silica tube, (3) transparent silica tube, (4) heater, (5) thermo-couple, (6) condenser, (7) gas sample flask, (8) pressure gauge, (9) vacuum pump.

decomposition process were analyzed by a mass-spectrometer.

Other Properties of the Spinel.—The magnetic susceptibility was measured by the Gouy method. The applied magnetic field was 8500 or 13000 gauss.

The mean dielelectric constant of the system of the spinel and air was measured. The frequency applied was 1 MC. The size of the spinel was 60~80 in Tyler mesh. Its packing ratios were from 0.48 to 0.53.

Results

Formation of the Reductive Spinel.—The reductive spinel can be formed through reduction of alumina in a reductive atmosphere above 1650°C, but in vacuo, alumina evaporates. The best procedure in the present study is as follows: (1) mixing 0.2 g. of graphite with 5 g. of γ-alumina thoroughly; (2) heating it at 1700°C for 2 hr. in the Tammann furnace through which only a little air can pass; (3) quenching it. When the reduction of alumina is insufficient α-alumina remains, whereas crystalline aluminum nitride is isolated when the reduction has proceeded too far.

Chemical Behaviors.—The decomposition of the reductive spinel by acid or alkali can not be noticed at room temperature. Products of the reaction between the reductive spinel and the glass as a flux were lead metal and nitrogen gas. The volume of the emitted nitrogen gas corresponds to 85% of the calculated value from the formula of AlN-Al_2O_3. The volume of nitrogen gas was fluctuated because of the difficulties of complete fusing. The emitted gas moved the flux to a lower temperature part. The sample increased in weight by 6.90% when it was kept in air above 1000°C, and turned into α-alumina.

Other Properties.—The observed magnetic susceptibility was $\chi = -0.34\times10^{-6}$/g. The dielectric constant was calculated to be 23.8. The refractive index 1.80 was also calculated from data[3]. Then, the ionic refraction of nitrogen N^{3-} in the reductive spinel should be 4.30. This calculation was made by the Lorentz-Lorenz equation. The unit cell dimension is 7.940 Å (in spinel structure $Fd3m$), and the density is 3.78 g./cc.

Discussion

The synthetic experiments show that the presence of nitrogen is inevitable in the conditions of the formation of the reductive spinel, and alumina turns into aluminum suboxide and evaporates in vacuo[5]. Emission of nitrogen gas and the weight increase of the reductive spinel through oxidation lead us to conclude that the reducing ability is due to the nitride component. The weight increase by 6.90% corresponds approximately to that of AlN-Al_2O_3 by 6.95%. The magnetic susceptibility shows an absence of lower valent aluminum ion Al^{2+}. The ionic refraction of nitrogen ion 4.30 in the spinel structure is only 1.14 times larger than that of oxygen ion 3.77[3]. This shows that the ionic radii of nitrogen ion is not much greater than that of oxygen ion. The density 3.78 g./cc. and the cell dimension 7.940Å are coincident with a spinel formula AlN-Al_2O_3.

Summary

A compound between aluminum oxide and aluminum nitride can be produced in a reductive atmosphere above 1650°C.

A new spinel formula AlN-Al_2O_3 should be adopted instead of the previous one Al_2O-$5Al_2O_3$ or Al_3O_4.

The physical constants of AlN-Al_2O_3 are as follows: crystal structure $Fd3m$, $Z=8$, $a=7.940$ Å; density 3.78 g./cc.; dielectric constant 23.8; refractive index 1.80; magnetic susceptibility -0.34×10^{-6}/g.

Department of Applied Chemistry
Faculty of Engineering
The University of Tokyo
Hongo, Tokyo

5) R. Kiyoura and T. Sata, *J. Ceram. Assoc. Japan (Yogyo Kyokai Shi)*, **66**, 44 (1958).

*The Molecular Structure of the Monomer and the Dimer of Acrylic Acid**

By Takeshi UKAJI

(Received June 2, 1959)

Acrylic acid is known as an important source of some highly polymeric products, however its molecular structure has been left unsolved.

Recent electron diffraction study[1] of the monomer of formic and acetic acids has indicated that the two distances between the carbon atom and oxygen atoms in carboxyl group are not the same. This result essentially agreed with the structure of the monomer of formic acid of the electron diffraction sector-photometer method proposed by Karle and Karle[2]. Furthermore, various data[3] on the conjugated system show that the C–C single bond distance between two double bonds is shorter than its normal distance of 1.54 Å.

The present investigation was undertaken for the purpose of clarifying the stereochemical structure of acrylic acid, and also to elucidate the question as to what changes may occur on association of the monomer of the acid.

Experimental

Acrylic acid was prepared by hydrolysis of commercial grade methyl acrylate. On careful distillation of the acid, a fraction boiling at 50~51°C/20 mmHg was collected.

Electron diffraction photographs were taken according to the usual manner using a camera reported in the previous paper[4] (camera distance, ca. 9 cm., electron wavelength, 0.056~0.063 Å, determined by gold foil). The diffraction pattern were visually measured to the extent of ca. 70 of q-values.

Interpretation of Diffraction Patterns and Results

The well known formula for the calculation of the theoretical intensity curves are as follows:

$$I_{(q)}=\sum_i\sum_j \frac{Z_iZ_j}{r_{ij}} \exp(-a_{ij}q^2) \sin\frac{\pi}{10}qr_{ij}$$

$$q=(40/\lambda)\sin(\theta/2),\quad a_{ij}=(\pi^2/200)\ <\Delta r_{ij}^2>$$

where r_{ij} is the distance between the i-th and j-th atom, λ the electron wavelength, θ the scattering angle, Z_i the atomic number of i-th atom, and $<\Delta r_{ij}>$ the mean square amplitude of r_{ij}. The exponential term is omitted as a first approximation, i. e., $\exp(-a_{ij}q^2)=0$.

Monomer of Acrylic Acid. — To obtain the monomer of the acid, a fine nozzle through which its vapor flowed out was heated at 170~200°C by a spiral nichrome wire. No available data concerning the thermal equilibrium between the dimer and monomer of the vapor of this acid have appeared in literature. Also the temperature of the nozzle was controlled to obtain diffraction patterns different from those of the dimer. Some photographs were taken and these were then carefully compared with that of the dimer of the acid. In the regions of 20~30 of q-values, a remarkable change was observed in these patterns. Eight satisfactory photographs were obtained.

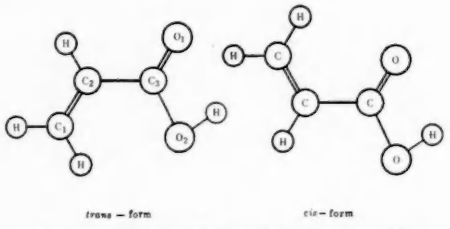

Fig. 1. Schematic model showing the *trans*- and *cis*-forms of acrylic acid.

It is assumed that all the atoms in this molecule are coplanar, and that the C-H distance and ∠CCH are 1.08 Å and 120°, respectively. The hydrogen atom in OH group was neglected, because its contribution to the total theoretical intensity curve was small. The parameters C_1=C_2, C_2-C_3, C_3=O_1 and C_3-O_2 used in the calculation of theoretical intensity curves, were varied from 1.32 to 1.45 Å, from 1.40 to 1.54 Å, from 1.18 to 1.24 Å and from 1.32 to 1.50 Å in steps of 0.02 or 0.03 Å, respectively, while the angles of $C_1C_2C_3$, $C_2C_3O_1$ and $O_1C_3O_2$ were varied from 110 to 130°, from 110 to 130° and from 110 to 135° in steps of 2 or 3°, respectively. In Fig. 2, the solid lines are the theoretical intensity curves of *trans*-form, and the chain lines are of *cis*-form.

*Presented partly at the Symposium on Structural Chemistry, Fukuoka, Nov. 22, 1957.

1) J. Karle and L. O. Brockway, *J. Am. Chem. Soc.*, **66**, 574 (1944).

2) I. Karle and J. Karle, *J. Chem. Phys.*, **22**, 43 (1954).

3) P. W. Allen and L. E. Sutton, *Acta Cryst.*, **3**, 46 (1950).

4) T. Yuzawa and M. Yamaha, This Bulletin, **26**, 414 (1953).

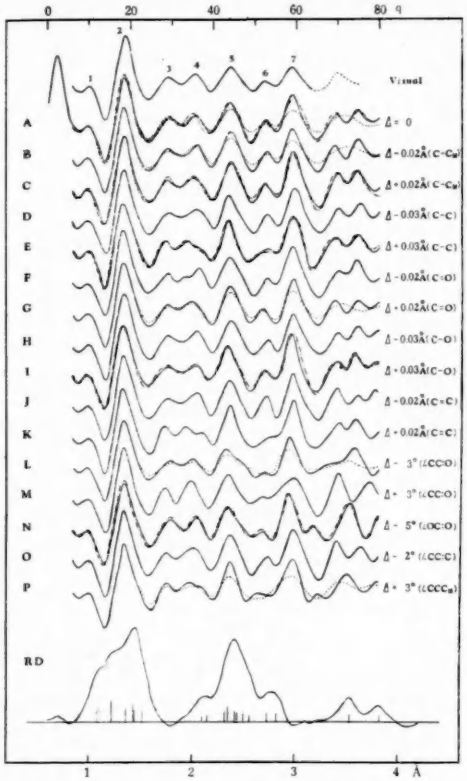

Fig. 2. Visual, theoretical intensity curves and radial distribution curve for acrylic acid. The notations on the right hand side of this figure show that the models deviate from the most probable model, for example, $\Delta=0$ is the most probable model which has the parameter as follows: C–H, 1.08; C=C, 1.36; C–C, 1.44; C=O, 1.22; C–O, 1.43 Å; $\angle C:CH=\angle C:CC=\angle CC:O$, 120° and $\angle OC:O$, 125°.

The effect of thermal vibration on the theoretical curves was examined, the vibration factors a's listed in Table I being used, and the curves including these effects were shown in the dotted lines in the same figure.

A careful comparison was made between the visual and theoretical intensity curves. Curve A is in the best agreement with the visual one. The curves of several other models resemble the visual one, but they differ from it in some features. The 4th, 5th and 6th maxima of curve B shift outward, while in curve C the 3rd and 4th maxima shift inward. Curves D and E are taken for the purpose of ascertaining the limit of acceptability for C=O distance, both curves being in good agreement with the visual one in all respects, except for the small displacement of the positions of the 3rd, 4th and 6th maxima. Likewise curves F and G are used to show the limit for C–O distance. These curves are also rejected because of the disagreement with the visual curve in the range $q>45$. In curve H, the 4th and 6th maxima shift outward, while in curve I the 3rd and 5th maxima shift outward, while in curve I the 3rd and 5th maxima shift inward. Curves J and K are taken as typical ones for models which have values accepted as borderline: the features of these curves in the range $q>50$ disagree with the visual curve. In curve L, the 4th minimum and the 7th maxima both shift inward, while the 4th and 5th maximum shift outward. Curves M and N are shown as the acceptable limit for the angle $C_1C_2C_3$. In curve M, the 6th and 7th maxima shift outward greatly, on the other hand, in curve N the positions of the 5th maximum and minimum shift inward.

As shown in Fig. 2, the theoretical curves of the *trans*- and *cis*-forms remain almost unchanged in all features. Therefore, we could not distinguish the difference between the *trans*- and *cis*-configurations of this molecule.

From the above considerations, model A is regarded as the most acceptable one, while the others are all accepted as borderline fits. Seven models are selected from them, and their q_C/q_O values are summarized in Table II.

TABLE I. APPROXIMATE VIBRATION FACTORS a_{ij} USED IN CALCULATION FOR THE MONOMER AND DIMER OF ACRYLIC ACID

a_{ij}	Atom pairs	
	Monomer	Dimer
0	C_1=C_2, C_2–C_3, C_3=O_1, C_3–O_2	C_1=C_2, C_2–C_3, C_3=O_1, C_3–O_2
0.00010	$O_1'\cdots C_2$, $O_2'\cdots C_2$	$O_1'\cdots C_2$, $O_2'\cdots C_2$
0.00015	C–H, $O_1'\cdots O_2$, $C_1'\cdots C_3$	C–H, $O_1'\cdots O_2$, $C_1'\cdots C_3$
0.00020	$C'\cdots H$, $O_2''\cdots C_1$	$C'\cdots H$, $O_2''\cdots C_1$
0.00035	$O_1''\cdots C_1$	$O_1''\cdots C_1$
0.00040		OH···O'
0.00060		$O_1\cdots O_1'$, $O_2\cdots O_2'$, $O_1\cdots C_3'$, $O_2\cdots C_3'$, $C_3\cdots C_3'$
0.00080		$O_1\cdots C_2'$, $O_2\cdots C_2'$, $C_3\cdots C_2'$, $C_2\cdots C_2'$, $O_1\cdots C_1'$, $O_2\cdots C_1'$
0.00100		$C_3\cdots C_1'$, $C_2\cdots C_1'$, $C_1\cdots C_1'$

TABLE II. q_C/q_O VALUES FOR ACRYLIC ACID

Feature Max.	Feature Min.	q_O	q_C/q_O Model A	C	D	F	G	I	M	Wt.
1		10.37	0.984	0.964	0.945	0.984	0.964	0.984	0.984	1
	1	14.25	0.983	0.983	0.983	0.969	0.982	0.976	0.982	1
2		19.06	0.995	0.971	0.984	0.979	0.997	0.976	0.984	2
	2	24.34	0.998	1.017	1.018	0.998	0.998	0.994	1.007	2
3		29.53	0.999	0.958	0.992	0.999	0.974	0.974	0.999	4
	3	32.48	0.998	0.939	0.970	0.964	0.959	0.985	0.978	2
4		35.57	1.001	0.984	1.012	1.006	0.990	0.984	0.998	4
	4	40.57	0.993	0.998	0.986	0.990	0.974	0.992	0.986	2
5		45.35	1.000	0.979	0.995	1.006	1.003	0.985	0.999	4
	5	49.08	1.006	0.993	1.007	1.011	1.009	1.007	1.006	1
6		52.38	1.004	1.008	1.012	0.998	1.009	1.016	1.016	2
	6	56.15	0.996	1.002	0.996	0.988	0.997	1.011	1.000	1
7		60.04	1.003	1.004	0.999	0.983	1.020	1.002	1.016	1
Wt. mean			0.998	0.981	0.995	0.994	0.989	0.988	0.996	
Wt. mean dev.			0.004	0.023	0.014	0.010	0.015	0.016	0.008	

The radial distribution curve for this molecule (RD curve in Fig. 2) was calculated using the following equation:

$$rD_{(r)} = \sum_{q=1}^{q_{max}} I_{(q)O} \exp(-bq^2) \sin \frac{\pi}{10} qr$$

where $I_{(q)O}$ is the intensity read from the visual curve. The value of b was determined by setting the $\exp(-bq^2) = 0.1$ at $q=70$. The curve shows that the first peak corresponds to the C-H, C_1-C_2, C_2-C_3, C_3-O_1 and C_3-O_2 distances, the second to the C'···H, C_1'···C_3, O_1'···O_2, O_1'···C_2 and O_2'···C_2 distances, the third to the O_2''···C_1 and fourth to the O_1''···C_1 distance, respectively. Owing to the complex nature of the peaks, no attempt was made to resolve them. It is found, however, that the positions determined from the most probable model agree fairly well with the peaks observed in this radial distribution curve.

The following values are obtained for the structure of the monomer of acrylic acid: C_1-C_2=1.36±0.02 Å; C_2-C_3=1.44±0.03 Å; C_3-O_1=1.22±0.02 Å; C_3-O_2=1.43±0.03 Å; $\angle C_1C_2C_3$=120±2°; $\angle C_2C_3O_1$=120±3°; $\angle O_1C_3O_2$=125±5°.

Dimer of Acrylic Acid. — It was assumed that the association of acrylic acid was the hydrogen bond coupling of two single molecules of the same type as in the case of formic and acetic acids, that the two planar acrylic acid molecules were coplanar, and also that the C_2, C_3, C_2' and C_3' atoms were laid on the same axis (as shown in Fig. 3). Many parameters were involved, so that the complete analysis on the molecular structure of the dimer of this acid would be very laborious. Therefore, some of the parameters of the most probable model obtained from

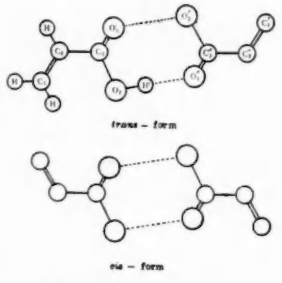

Fig. 3. Schematic model showing the skeletons and the numbering of atoms of the dimer of acrylic acid.

the above-mentioned analysis of monomer of this acid were assumed to be as follows: C-H, C_1-C_2, $\angle C_2C_1H$ and $\angle C_1C_2C_3$ are assumed to be 1.08, 1.36 Å, 120 and 120°, respectively. Then the other parameters determining the structure C_2-C_3, C_3-O_1 and C_3-O_2 distances were varied from 1.40 to 1.50 Å, from 1.18 to 1.24 Å and from 1.30 to 1.43 Å in steps of 0.02 or 0.03 Å and O-H···O separation was varied from 2.65 to 2.80 Å with the same increment, while the angles of $\angle C_2C_3O_1$ and $\angle O_1C_3O_2$ were varied from 110 to 130° and from 120 to 135° in steps of 2 or 3°, respectively.

Some of the intensity curves are shown in Fig. 4. In this figure, the solid lines are the theoretical intensity curves of the *trans*-form, and the chain lines are of the *cis*-form. The effect of thermal vibration factors listed in Table I being used, the curves including these effects are shown in a dotted line in the same figure.

Curve E is in the best agreement with the visual one. In curve A, the 3rd and 4th maxima shift inward, while in curve B these maxima shift outward. A comparison of curves C and D, which possess 0.02 Å longer and shorter parameters, respectively, for C_3-O_1 distance, show that there are remarkable changes of the features

TABLE III. q_C/q_O VALUES FOR THE DIMER OF ACRYLIC ACID

Feature		q_O	q_C/q_O Model				Wt.
Max.	Min.		E	B	G	K	
1		12.28	1.005	0.915	0.968	0.982	1
	1	14.30	1.008	1.015	1.028	0.969	1
2		18.45	1.001	0.995	1.011	0.995	2
4		35.53	0.998	0.991	0.986	0.949	3
	4	40.24	1.005	0.989	1.025	1.016	2
5		45.18	1.000	1.022	1.014	0.999	3
	5	49.32	0.997	1.015	0.983	0.997	1
6		51.86	1.005	1.022	1.016	0.995	2
	6	55.45	0.989	0.996	0.997	0.983	1
7		60.48	1.009	1.011	1.011	1.007	1
Wt. mean			1.001	1.002	1.005	0.988	
Wt. mean dev.			0.005	0.017	0.016	0.017	

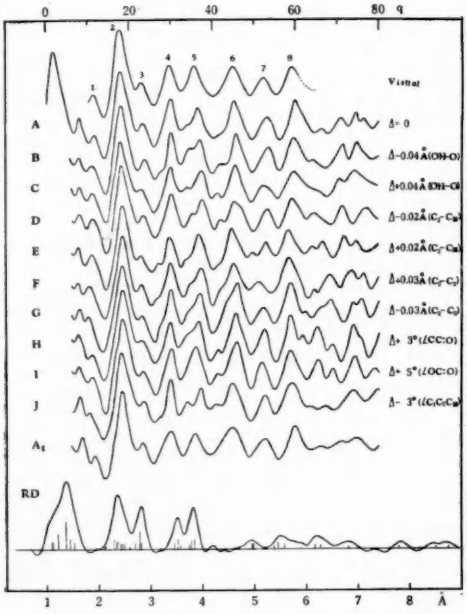

Fig. 4. Visual, theoretical intensity curves and radial distribution curve for the dimer of acrylic acid.
The notations on the right hand side of this figure show that the models deviate from the most probable model, for example, $\Delta=0$ is the most probable model which has the parameter as follows; C–H, 1.08; C=C, 1.36; C–C, 1.44; C=O, 1.22; C–O, 1.36 Å; ∠C:CH=∠C:CC=∠CC:O, 120°; ∠OC:O, 1.25° and OH···O distance, 2.76 Å.

in the region of 20 to 30 q-values. Curve F differs from E, the former possessing a parameter of an OH···O distance which is 0.04 Å longer than in the latter; and curve G differs from E, the former possessing the same distance by 0.04 Å shorter. These curves disagree with the visual one in the positions of the 3rd and 4th maxima. In curves H and I, remarkable differences from the visual one are found in features between 20 and 30 of q-values and in positions of 3rd and 4th maxima. Curves J and K were examined for the purpose of ascertaining the limit of acceptability for C_2-C_3 distance, both curves being in good agreement with the visual one in all respects, except the 3rd and 6th maxima.

The radial distribution curve for the dimer of acrylic acid is shown in Fig. 2 (RD curve). The positions determined from the most acceptable model (shown in vertical lines in this curve) fairly well agree with the peaks observed in this radial distribution curve. A relatively small peaks is found at 2.76 Å corresponding to the separation across the bridge O–H···O.

The structure determined for the dimer of acrylic acid, which is in agreement with the quantitative results (q_C/q_O values in Table III), is as follows: C_1=C_2=1.36 Å (assumed); C_2–C_3=1.44±0.03 Å; C_3=O_1=1.22±0.02 Å; C_3–O_2=1.36±0.03 Å; ∠$C_1C_2C_3$=120° (assumed); ∠$C_2C_3O_1$=120±3°; ∠$O_1C_3O_2$=125±5°; O–H···O=2.76±0.04 Å.

Discussion

The C=O and C–O distances in acrylic acid are the same as those observed in several interesting structural studies of the carboxyl group on formic and acetic acids. Therefore, no differences between a saturated and an unsaturated substituent attached to the carboxyl group could be found in this work.

Moreover, the C=C, C–C and C=O distances and the valence angles in this

molecule generally agree with the corresponding bond lengths and valence angles of acrolein[5] and acrylyl chloride[6] which are obtained by electron diffraction studies. Bond shortening and bond elongation of C–C and C=C bonds in conjugated molecules were plausibly explained by the delocalization of π-electron. As a matter of fact, it may be considered that the order of conjugation in this molecule is the same as that calculated on acrolein by C. A. Coulson[7].

In the dimer, the C–O bond becomes 0.07 Å shorter than that in the monomer, while the C=O bond remains unchanged. Within the limits of accuracy of this work, the circumstances are the same as in the case of association of formic and acetic acids. Several investigations show that the heat of dimerization of some carboxylic acids is of the order of 13~18 kcal./mol. The C–O bond shortening may be attributed for considerable part to the formation of a ring by two carboxyl groups across the hydrogen bridges.

The author wishes to express his sincere gratitude to Professor A. Kotera and Mr. M. Igarashi of Tokyo University of Education for their kind guidance and encouragement throughout this work, and for the free use of the apparatus located at their university. Thanks are also due to Professor J. Kurahashi and Dr. T. Takeshima of this university for their helpful advice.

Department of Chemistry
Faculty of Science
Ibaraki University, Mito

5) H. Mackle and L. E. Sutton, *Trans. Faraday Soc.*, **47**, 691 (1951).
6) T. Ukaji, This Bulletin, **30**, 737 (1957).
7) C. A. Coulson, *Trans. Faraday Soc.*, **42**, 106 (1946).
8) O. Z. Foz and J. Marcills, *Chem. Abstr.*, **44**, 8716*b* (1950); J. J. Fox and A. E. Martin, *Trans. Faraday Soc.*, **36**, 397 (1940); F. H. MacDougall, *J. Am. Chem. Soc.*, **63**, 3420 (1941).

---

*The Molecular Structure of the Monomer and the Dimer of Methacrylic Acid**

By Takeshi UKAJI

(Received June 2, 1959)

It has been commonly recognized that the derivatives of acrylic acid which have a methyl group on the α-carbon atom are reactive than the one having no substituent. Theoretical and structural explanation of this chemical fact seems not yet to have been given. The present work is directed to clarifying the stereochemical structure of methacrylic acid, and also to elucidate the question concerning the changes which may occur on the introduction of the methyl group into the α-position of the acid and on the association of the monomeric acid.

Experimental

Methacrylic acid was prepared by hydrolysis of commercial grade methacrylate. On careful distillation of the acid, a fraction boiling at 75~76°C/20 mmHg was collected. It was stocked over hydroquinone.

The electron diffraction photographs were taken according to the usual manner using a camera reported in the previous paper[1] (camera distance, ca. 9 cm.; electron wavelength, 0.053~0.061 Å, determined by calibration with gold foil). The experimental technique concerning the photographs of the monomer of this acid was essentially the same in the case of the monomer of acrylic acid. The diffraction pattern was visually measured to an extent of ca. 70 of q-values.

Interpretations of Diffraction Patterns and Results

For the calculation of theoretical intensity curves, the authorized formula[3b] was used. The thermal vibration factor is omitted as a first approximation.

Monomer of Methacrylic Acid.—To examine if the temperature of the present experiment is sufficient for the thermal dissociation of the acid, some photographs were taken and these were carefully compared with that of the dimer of this acid. A remarkable change was observed

* Presented partly at the Symposium on Structural Chemistry, Fukuoka, Nov. 22, 1957.
1) T. Yuzawa and N. Yamaha, This Bulletin, **26**, 414 (1953).

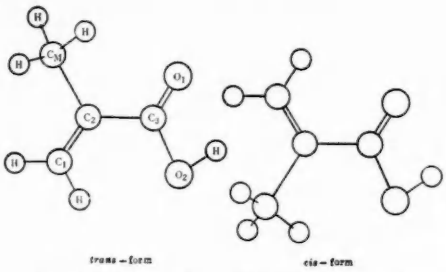

Fig. 1. Schematic model showing the *trans*- and *cis*-forms of methacrylic acid.

in the feature at about 23 of q-values in these patterns. Six satisfactory photographs were obtained.

On the basis of foregoing information[2,3], it is assumed that all the carbon and oxygen atoms in this molecule are coplanar, and that the C-H bond distance in the methyl group is 1.10 Å, in which each hydrogen atom forms tetrahedral configuration, and the C-H distance and ∠CCH in methylene group are 1.08 Å and 120°, respectively. The hydrogen atom in the hydroxyl group was neglected for the same reason as that described in the previous paper[3b]. The parameters C_1=C_2, C_2-C_3, C_3=O_1, C_3-C_2 and C_2-C_M (in methyl group), used in the calculation of theoretical intensity curves, were varied from 1.32 to 1.45 Å, from 1.40 to 1.54 Å, from 1.18 to 1.24 Å, from 1.32 to 1.50 Å and from 1.40 to 1.54 Å in steps of 0.02 or 0.03 Å, while the angles of $C_1C_2C_3$, $C_3C_2C_M$, $C_2C_3O_1$ and $O_1C_3O_2$ were varied from 110 to 130°, from 110 to 130°, and from 110 to 135° in steps of 2 or 3°, respectively.

In Fig. 2, the solid lines are descriptive of the theoretical intensity curves of the *trans*-form, and the chain lines those of the *cis*-form. The effect of thermal vibration (the factors are listed in Table I) was then examined and the curves including these effects were shown in the dotted lines in the same figure.

A careful comparison was made between the visual and theoretical intensity curves. Curve A is in the best agreement with the visual one. The curves of several other models quoted in this figure also resemble the observed intensity curve, but they differ from it in the features of some maxima and minima. Curves B and C agree with the visual one in all features, except for the position of the 4th maximum. While in curves D and E, the positions of the 3rd minimum and the 4th maximum and minimum, and the feature of the 6th peak differs from the visual curve. Curves F, G, H and I are taken for the purpose of ascertaining the limit of acceptability for C_3=O_1 and C_3-O_2 distances; these curves are in good agreement with the observed one in all features, except for the positions of the 4th and

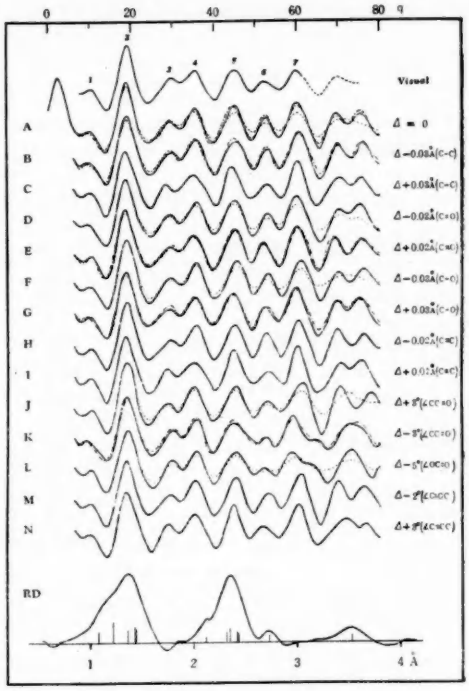

Fig. 2. Visual, theoretical intensity curves and radial distribution curve for methacrylic acid. The notations on the right hand side of this figure show that the models deviate from the most probable model, for example, Δ=0 is the most probable model which has the following parameters; C-H=1.08, C_M-H (in methyl group)=1.10, C=C=1.36, C-C=1.44, C=C=1.22, C-O=1.43 Å, ∠CC_MH=109.5°, ∠C:CH=∠C:CC=∠CCC=∠CC:O=120° and ∠OC:O=125°.

6th maxima. In curves J and K, the positions of the 4th maximum and the intensity relations of the 6th peak are different from those of the visual one. Curves L and M are used to examine the limit of angle $C_2C_3O_1$. These curves are rejected because of the disagreement with the visual one in the range of q>45. Curves from N to P show the acceptable limit of the angles of $O_1C_3O_2$, $C_1C_2C_3$ and $C_2C_3C_M$, respectively. These curves have small differences in the positions and features of the 3rd minimum, the 4th and the 6th maximum.

The theoretical intensity curves of the *trans*- and the *cis*-forms remain almost unchanged throughout all the features. Therefore, we could not distinguish between the *trans*- and *cis*-configuration of this molecule.

From the above considerations, model A is regarded as the most acceptable one, while others are all accepted as on the borderline.

2) T. Ukaji, This Bulletin, **32**, 1266 (1959).
3) (a) H. Mackle and L. E. Sutton, *Trans. Faraday Soc.*, **47**, 691 (1951). (b) T. Ukaji, This Bulletin, **30**, 737 (1957).

TABLE I. APPROXIMATE VIBRATION FACTORS USED IN CALCULATION FOR THE MONOMER AND DIMER OF METHACRYLIC ACID

Values of factor	Atom pairs	
	Monomer	Dimer
0	C_1=C_2, C_2–C_3, C_3–C_M, C_3=O_1, C_3–O_2	C_1=C_2, C_2–C_3, C_2–C_M, C_3=O_1, C_3–O_2
0.00010	$O'_1\cdots C_2$, $O'_2\cdots C_2$, $C'_1\cdots C_M$, $C'_3\cdots C_M$, $C'_1\cdots C_3$	$O'_1\cdots C_2$, $O'_2\cdots C_2$, $C'_1\cdots C_M$, $C'_3\cdots C_M$, $C'_1\cdots C_3$
0.00015	C–H, C_M–H (in methyl group), $O'_1\cdots O_2$	C–H, C_M–H (in methyl group), $O'_1\cdots O_2$
0.00020	$C'_2\cdots$H, $C'_2\cdots$H (in methyl group)	$C_2\cdots$H, $C'_2\cdots$H (in methyl group)
0.00035	$O_2''\cdots C_1$, $O_1''\cdots C_M$	$O_2''\cdots C_1$, $O_1''\cdots C_M$
0.00040	$O_1''\cdots C_1$	$O_1''\cdots C_1$, OH$\cdots$O′
0.00060	$O_2''\cdots C_M$	$O_2\cdots C'_M$, $O_1\cdots O_1'$, $O_2\cdots O'_2$, $O_1\cdots C'_3$, $O_2\cdots C'_3$, $C_3\cdots C_3'$
0.00080		$O_1\cdots C'_2$, $O_2\cdots C'_2$, $C_3\cdots C'_3$, $O_1\cdots C'_1$, $O_2\cdots C'_1$, $C_3\cdots C'_M$, $O_1\cdots C'_M$, $O_2\cdots C_M$
0.00100		$C_3\cdots C'_1$, $C_2\cdots C'_1$ $C_1\cdots C'_1$, $C_1\cdots C'_M$, $C_2\cdots C'_M$
0.00120		$C_M\cdots C'_M$

TABLE II. q_C/q_O VALUES FOR METHACRYLIC ACID

Feature		q_O	q_C/q_O Model							Wt.
Max.	Min.		A	B	E	G	H	M	N	
1		10.44	0.982	0.986	0.982	0.977	0.987	0.982	0.977	1
	1	14.06	0.996	0.982	0.982	0.996	0.996	0.996	0.982	1
2		18.66	0.997	0.994	0.993	0.993	0.997	0.993	0.989	2
	2	24.27	1.001	1.009	1.009	1.009	1.009	1.001	1.003	2
3		29.02	1.004	1.004	0.982	0.999	1.004	1.009	1.020	4
	3	32.41	1.009	1.003	0.941	0.964	1.003	0.957	0.957	2
4		35.74	0.996	1.007	0.951	0.972	1.002	0.968	1.021	4
	4	39.21	1.002	1.005	1.000	1.005	1.014	0.992	1.002	2
5		44.00	1.000	1.007	0.995	1.005	1.006	0.994	0.989	3
	5	49.30	0.998	0.999	0.999	0.992	1.004	0.999	1.008	2
6		52.25	1.005	1.014	1.014	0.995	1.019	0.993	0.991	1
	6	55.02	0.999	1.009	1.004	0.999	1.007	0.967	0.985	1
7		58.96	1.001	1.001	1.005	1.006	0.997	1.009	0.986	1
Wt. mean			1.001	1.003	0.984	0.992	1.003	0.989	0.998	
Wt. mean dev.			0.004	0.007	0.020	0.012	0.006	0.014	0.016	

Seven models are selected from them, and their q_C/q_O values are summarized in Table II. The structural information deduced from the values of averages and the average deviations of q_C/q_O ratios is consistent with the above correlation analyses.

The RD curve in Fig. 2 is the radial distribution curve for this molecule. In this curve, the first peak corresponds to the C–H, C_M–H (in methyl group), C_1=C_2, C_2–C_3, C_2–C_M, C_3=O_1 and C_3–O_2 distances, the second, third and fourth to the $C'\cdots$H, $C'_2\cdots$H, $O'_1\cdots C_2$, $O'_2\cdots C_2$, $C'_1\cdots C_M$, $C'_3\cdots C_M$, $C'_1\cdots C_3$, $O''_2\cdots C_1$ and $O''_1\cdots C_M$, the fifth to the $O''_1\cdots C_1$ and the sixth to the $O''_2\cdots C_M$ distances, respectively. The interatomic distances determined from the most probable model (shown in vertical lines in this RD curve) are in good agreement with the peaks observed in this radial distribution curve.

The following values are obtained for the structure of the monomer of methacrylic acid: C_1=1.36±0.02 Å; C_2–C_3=1.44±0.03 Å; C_2–C_M=1.52±0.02 Å; C_3=O_1=1.22±0.02 Å; C_3–O_2=1.43±0.03 Å; $\angle C_1C_2C_3$=120±2°; $\angle C_3C_2C_M$=120±3°; $\angle C_2C_3O_1$=120±3°; $\angle O_1C_3O_2$=125±5°.

Dimer of Methacrylic Acid.—The circumstances of the association of methacrylic acid is assumed to be the same as in the case of the dimer of acrylic acid. The complete analysis on the molecular structure of the dimer of this acid may be very laborious because of the inclusion of so many parameters. Therefore, some parameters of the most probable model of the

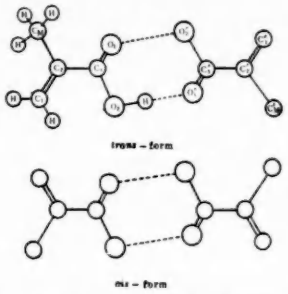

Fig. 3. Schematic model showing the skeletons and the numbering of atoms of the dimer of methacrylic acid.

monomer of this acid obtained from the above analysis were assumed to be as follows: C-H (in methyl group), C_M-H (in methyl group), C_1=C_2, C_3=O_1, $\angle C_2C_1H$, $\angle C_2C_MH$, $\angle C_1C_2C_3$, $\angle C_2C_3O_1$ and $\angle O_1C_3O_2$ were taken to be 1.08 Å, 1.10 Å, 1.36 Å, 1.22 Å, 120°, 109.5°, 120°, 120° and 125°, respectively. In the thirty models examined in this analysis, the parameters C_2-C_3, C_2-C_M and $C_1C_2C_M$ were varied from 1.40 to 1.50 Å, from 1.45 to 1.54 Å and from 110 to 130°, respectively.

Some of the theoretical intensity curves are shown in Fig. 4. These curves are representative of the theoretical intensity curves of the *trans*-form, and those of the *cis*-form are omitted in this figure for the reason that few differences are found between them. Curve A is in the best agreement with the visual one, and has parameters described in the notations of Fig. 4. In curves B and C, the 5th and 6th maxima have some different features from the visual curve; the position of the 7th maximum shifts outward in the former curve and the same maximum

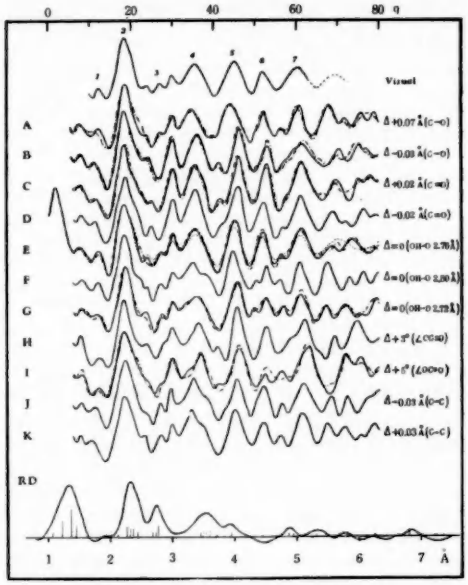

Fig. 4. Visual, theoretical intensity curves and radial distribution curve for the dimer of methacrylic acid. The notations on the right hand side of this figure show that the models deviate from the most probable model, for example, Δ=0 is the most probable model which has the following parameters; C-H=1.08, C_M-H (in methyl group)=1.10, C=C=1.36, C-C=1.44, C=O=1.22, C-O=1.36 Å, $\angle$C : CH=$\angle$C : CC=$\angle CCC_M$=$\angle$CC : O=120°, $\angle CC_MH$=109.5°, $\angle$OC:O=125° and OH···O=2.75Å.

TABLE III. q_C/q_O VALUES FOR THE DIMER OF METHACRYLIC ACID

Feature		q_O	q_C/q_O Model					Wt.
Max.	Min.		A	C	E	G	J	
1		11.35	1.007	0.978	0.965	0.951	0.933	1
	1	14.21	1.002	0.993	0.999	0.968	0.968	1
2		17.86	1.003	0.994	1.011	1.025	1.008	1
	2	21.65	1.000	0.998	0.995	1.016	1.025	1
3		23.02	1.000	0.991	0.984	0.995	1.021	2
	3	26.41	0.983	0.985	0.962	1.003	0.996	2
4		29.63	1.006	1.012	0.996	1.012	1.006	4
	4	32.57	0.998	0.998	0.996	0.998	0.981	3
5		35.65	1.005	1.036	1.023	1.035	1.014	2
	5	40.23	0.998	0.989	0.997	0.994	0.982	1
6		44.77	1.002	1.014	0.994	1.026	0.999	2
	6	49.15	1.005	1.001	0.983	1.001	1.000	1
7		52.28	1.010	0.997	1.002	0.999	1.006	1
	7	55.51	1.006	0.999	0.999	0.991	0.993	1
8		59.05	1.005	1.004	0.986	0.999	1.001	1
Wt. mean			1.001	1.002	0.993	1.004	0.994	
Wt. mean dev.			0.005	0.011	0.012	0.015	0.014	

shifts inward in the latter. Curves D and F are taken for the purpose of ascertaining the limit of acceptability for C_2–C_M distance, both curves being in good agreement with the visual one in all the positions of maxima and minima; however, small peaks and shoulders appear among them. In curve F, the 3rd minimum and 7th and 8th maxima shift inward and the 5th maximum outward, while in curve G, the 5th and 6th maxima shift outward. In curves H and I, the 4th and 5th minima and 6th maximum have different positions, but in curve J small peaks appear between the 4th and 5th and 6th maxima. Curve A shows the effect of thermal vibration on curve A, using the vibration factors listed in Table I.

The radial distribution curve for the dimer of methacrylic acid is shown in Fig. 4 (RD curve). The curve shows that the positions and their relative height of peaks determined from the most probable model (as shown in vertical lines) agree fairly well in general with the peaks observed in this radial distribution curve.

The structure of the dimer of methacrylic acid, which is in agreement with the quantitative results in Table III, is determined as follows: C_2–C_M=1.52±0.02 Å, $\angle C_1C_2C_M$=120±3° and O_1–H···O_2 separation 2.75±0.04 Å; and all other parameters are the same as in the dimer of acrylic acid.

Discussion

The C_1=C_2, C_2–C_3, C_3=O_1 and C_3–O_2 distances and the valence angles of $C_1C_2C_3$, $C_2C_3O_1$ and $O_1C_3O_2$ in this molecule are essentially the same as the corresponding bond lengths and valence angles of acrylic acid which is obtained in a previous paper[2]. The C_2–C_M distance in this molecule is shorter than the normal C–C single bond distance 1.54 Å. This bond shortening is explained by the term hyperconjugation. The result of the theoretical calculation by Coulson and Crawford[4] shows that the bond compression energy of C–C single bond, from 1.54 to 1.52 Å, is 0.13 kcal./mol. In our preliminary calculation by a simple MO method** (neglecting overlap integral) acrylic and methacrylic acid, the values of bond order and free valence are shown schematically as follows:

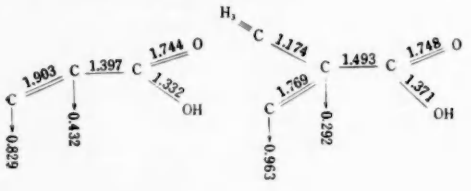

When the values obtained here of the bond order and the bond lengths were treated following the method of Mulliken and others[5], the results compared favorably with the criterion regarding the bond order and the bond lengths which included the idea of hyperconjugation of them (the values concerned with C=C and C–C of acrylic acid, C=C, C–C and C–C_M (in methyl group) of methacrylic acid). In the above figure, the comparison of free valence shows that methacrylic acid has a tendency to possess somewhat greater sensibility than acrylic acid in radical reaction.

In the dimer of this acid, the circumstances are the same as in the case of the association of acrylic acid.

The author wishes to express his sincere gratitude to Professor A. Kotera, Mr. M. Igarashi and Mr. M. I'Haya of Tokyo University of Education for their kind guidance and encouragement throughout this work, and for the free use of the

4) C. A. Coulson and V. A. Crawford, *J. Chem. Soc.*, **1953**, 2052.

** The well-known LCAO molecular orbital treatment is conducted as follows: the effect of the σ electron, assumed to be constant, is neglected, and the π-electrons are considered, as an approximation, to occupy the molecular orbital formulated below.

$$\Psi_i = \sum_{r=1}^{n} c_{ir}\phi_r$$

Then, we have the equatin:

$$(\alpha_r - E)C_r + \sum_{s \neq r} (\gamma_{rs} - S_{rs}E)C_s = 0$$

$$(r = 1, 2, \cdots\cdots, n)$$

in which α is the coulomb integral, E's the energies of LCAO MO's, γ_{rs} the exchange integral and S_{rs} the overlap integral. The details of the calculations of the lower energy levels of these molecules and the empirical parameters adopted are essentially the same as in the case of the calculation of hyperconjugation by I'Haya except for the parameters assigned of oxygen atoms which are: α_O(carbonyl oxygen)=α_C+2.0 and α_O(carboxyl oxygen)=α_C+1.5. Here α_C is the coulomb integral of the carbon atom. According to Coluson's*** definition, the charge density (q_r) of π-electron on the atom r and the bond order (p_{rs}) of the bond between atoms r and s are given by the following equations:

$$q_r = 2\sum_i C_{ir}^2$$

$$q_{rs} = 2\sum_i C_{ir} \cdot C_{is}$$

where the summations are taken overall occupied MO's.

The calculation of the free valence F_r at atom r in a molecule followed the definition formulated by Coulson****

$$F_r = N_{\max} - N_r$$

The values of $N_{\max}$ is $3+\sqrt{3}$ and the N_r is

$$N_r = 3 + \sum_i p_{rs}$$

in which p_{rs} is the π-bond order of the r-s bond, where s is adjacent to r atom.

*** C. A. Coulson, *Proc. Roy. Soc.* (*London*), **A169**, 413 (1939).

**** C. A. Coulson, *Discussions Faraday Soc.*, **2**, 9 (1947).

5) R. S. Mulliken et al. *J. Am. Chem. Soc.*, **63**, 41 (1941).

apparatus located at their university. Thanks are also due to Dr. T. Takeshima of this university for his helpful advice.

Department of Chemistry
Faculty of Science
Ibaraki University, Mito

*The Molecular Structure of Methyl Acrylate and Methyl Methacrylate**

By Takeshi UKAJI

(Received June 2, 1959)

Investigations of methyl formate and methyl acetate by electron diffraction have been reported[1], but no information seems to have been proposed regarding the stereochemical structure of methyl acrylate and methyl methacrylate which are important materials for high polymeric products.

In the present work, structural studies on methyl acrylate and methyl methacrylate by the electron diffraction method are undertaken to determine the most probable location of the methyl group of ester in these two compounds and to inspect the effect of hyperconjugation on the C–C single bond between the methyl group and the α-carbon atom in methyl methacrylate.

Experimental

Samples were purified by careful distillation. Methyl acrylate, b. p. 84.5~85.5°C. Methyl methacrylate, b. p. 100~101°C. These were stocked over hydroquinone.

The electron diffraction photographs were taken in the usual manner using a camera similar to the one reported in the previous paper[2] (camera distance, ca. 9 cm., electron wavelength, 0.059~0.063 Å, determined by calibration with gold foil). Fifteen satisfactory photographs were obtained in the case of methyl acrylate and eight in the case of methyl methacrylate. The diffraction patterns were visually measured to an extent of about $q=80$ in both cases.

Interpretation of Diffraction Patterns and Results

For the calculation of theoretical intensity curves, the authorized formula[3] was used. The exponential term of the formula is omitted as a first approximation.

Methyl Acrylate.—In the models of this molecule only four parameters are changed. In these the C_3–O_2 distance in carboxyl bond is varied from 1.32 to 1.45 Å in steps of 0.02 or 0.04 Å, and the O_2–C_4 distance in methoxyl bond from 1.40 to 1.50 Å with the same increments. The angle of $C_3O_2C_4$ of methoxyl group varied from 105 to 130° in steps of 5° and the angle between $C_3O_2C_4$ plane and the plane composed of the other atoms in the molecule is varied from 0 to 60°. The other parameters of this molecule were assumed to be those of the most probable model of acrylic

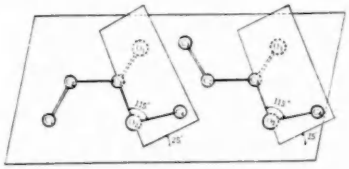

Fig. 1. Schematic models showing the skeletons and the numbering of atoms of methyl acrylate. The left model is *trans*-form and the right *cis*-form.

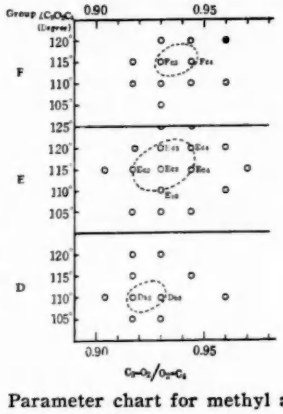

Fig. 2. Parameter chart for methyl acrylate.

* Partly presented at the 9th Annual Meeting of the Chemical Society of Japan, Kyoto, April, 1956.

1) A survey of the results of electron diffraction through 1949 is found in the tabulation by P. W. Allen and L. E. Sutton, *Acta Cryst.*, **3**, 46 (1950).

2) T. Yuzawa and M. Yamaha, This Bulletin, **26**, 414 (1953).

3) P. A. Shffer, V. Schomaker and L. Pauling, *J. Chem. Phys.*, **14**, 659 (1946).

4) T. Ukaji, This Bulletin, **32**, 1266 (1959).

acid[9]. Careful comparison was made between the visual intensity curve and the theoretical ones.

Fig. 2 shows the parameter chart for this molecule. The groupings of the models in the following discussions are made according to the qualitative similarity of the theoretical intensity curves. Groups D, E and F correspond to the models of which methyl groups are inclined by 20, 25 and 30°, respectively, to the molecular plane, and others are all rejected because of the disagreement with the visual curve.

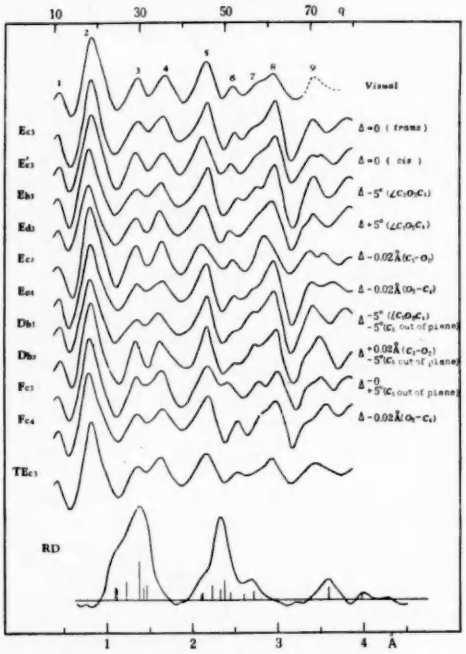

Fig. 3. Visual, theoretical intensity curves and radial distribution curve for methyl acrylate. The notations on the right hand side of this figure show that the models deviate from the most probable model, for example, $J=0$ is the most probable model which has the following parameters; C_1–H =1.08, C_3–H (in methyl geoup)=1.10, C_1=C_2 =1.36, C_2–C_3=1.44, C_3=O_1=1.22, C_3–O_2=1.36, O_2–C_4=1.46 Å, $\angle C_2C_1H=\angle C_1C_2C_3=\angle C_2C_3O_1$ =120°, $\angle O_2C_4H$ (in methyl ester group)= 109.5°, $\angle O_1C_3O_2=125°$, $\angle C_3O_2C_4=115°$ and C_4 atom is 25° out of plane configuration.

Of curves of the *trans*-form of the models E_{c2}, E_{b3}, E_{c3}, E_{d3} and E_{c4}, curve E_{c3} is in excellent agreement with the visual curve in all respects (Fig. 2). Curve E'_{c3} is taken as the typical one of which the model has a *cis*-configuration as regards C_1=C_2 and C_3=O_1. No remarkable discrepancies in the positions of maxima, minima and their intensity relations of the theoretical intensity curves are found throughout this work between the *trans*- and *cis*-configurations. Therefore, that of the *cis*'s of all the other models are omitted in Fig. 3. Curves E_{c3}, E_{b3}, E_{d3} and E_{c4} are given in order to show the limits of acceptability for the positions and relative intensities of the 5th, 6th and 8th maxima, and of the acceptable range of shapes of the 7th shelf. All curves with 4th maximum and minimum shifting inward and with the resolution of the 7th shelf greater than that in curve E_{b3} were rejected. Curve E_{d3} was the lower limit of acceptability for the 4th, 5th and 6th maxima shifting inward and for the prominence of the 7th shelf.

Curves D_{b2} and D_{b3} are given as acceptable curves of the D group. The height of the 5th maximum is slightly increased in both curves, and that of the 3rd maximum in the D_{b2} curve decreased, but that in D_{b3} increased. These discrepancies are not regarded as sufficient to justify the rejection of these models, and both models are considered to be acceptable borderline ones.

Of models in the F group, curves F_{c3} and F_{c4} are taken as representative ones. The features of the 6th maximum and the 7th shelf are both accepted as the limit of permission.

The effect of the thermal vibration on the theoretical curve was then examined. The vibration factor is listed in Table I. Curve TE_{c3} is a representative one showing this effect on the theoretical curve calculated from model E_{c3}. This curve has the same feature in all respects as the visual one has.

From the above considerations, model E_{c3} may be regarded as the most acceptable one, while the others are all accepted as borderline cases. The q_C/q_O values of these eight models are summarized in Table II. The weighing for each feature is indicative of its reliability in comparison with theoretical curves. Low weighing is given to the inner features, because these have generally been found to give less satisfactory agreement than do those at somewhat greater q values. Features for which reproducible measurements could not be obtained are also given lower weights. To the features farther out are assigned relatively low weights.

TABLE I. APPROXIMATE VIBRATION FACTORS USED IN THE CALCULATION FOR METHYL ACRYLATE

Factors	Atom pairs
0.00008	for C_3=O_1 and C_1=C_2
0.00012	for C_3–O_2, C_4–O_2 and C_2–C_3
0.00015	for $O_1'\cdots O_2$, $C_2'\cdots O_1$, $C_2'\cdots O_2$ and $C_1'\cdots C_3$
0.00030	for C–H, $O_1'\cdots C_4$ and $C_1'\cdots O_2$
0.00040	for $C'\cdots$H, $O_2'\cdots$H, $C_2''\cdots C_4$ and $C_1''\cdots O_1$
0.00045	for $C_1'''\cdots C_4$

TABLE II. q_C/q_O VALUES FOR METHYL ACRYLATE

Feature			q_C Model							
Max.	Min.	q_O	E_{c4}	E'_{c3}	E_{b3}	E_{d3}	E_{c2}	E_{c4}	D_{b3}	F_{c3}	Wt.
1		11.70	0.992	1.000	0.983	0.983	0.992	0.992	0.992	0.983	1
	1	14.25	0.986	0.986	0.976	0.975	1.013	0.990	0.983	0.997	1
2		18.70	1.003	1.000	0.974	0.979	1.000	1.005	0.974	1.000	2
	2	24.81	0.992	1.017	1.008	1.008	1.019	1.015	1.003	1.003	1
3		29.56	1.001	0.990	1.014	0.998	0.998	1.008	1.011	0.988	2
	3	32.55	0.999	1.004	0.984	0.984	0.992	0.999	0.968	0.992	1
4		36.00	1.000	0.992	0.979	0.976	0.987	1.000	0.967	0.981	2
	4	40.50	0.993	0.978	0.976	0.981	0.993	1.002	0.956	0.993	1
5		45.67	1.001	0.986	1.012	0.990	0.990	1.007	1.007	1.009	2
	5	49.44	1.011	0.995	1.011	0.995	1.011	1.011	1.005	1.001	1
6		52.20	1.001	0.990	1.019	0.983	1.002	1.006	—	0.978	1
	6	54.73	0.987	0.989	1.003	0.982	1.015	0.996	—	0.996	1
7		(57.50)	1.000	1.008	0.992	—	—	1.000	0.988	1.008	0
8		61.84	1.002	0.996	0.999	0.990	0.963	1.001	0.996	1.011	1
	8	66.15	0.997	0.998	1.002	0.998	1.005	1.001	0.998	1.008	1
Wt. mean			0.998	0.994	0.994	0.986	0.997	1.003	0.987	0.996	
Av. dev.			0.006	0.011	0.017	0.016	0.013	0.018	0.022	0.011	

TABLE III. APPROXIMATE VIBRATION FACTORS USED IN THE CALCULATION FOR METHYL METHACRYLATE

Factors	Atom pairs
0.00008	for C_1–O_1 and C_1–C_2
0.00012	for C_3–O_2, C_4–O_2, C_2–C_3 and C_2–C_5
0.00015	for $C_1'\cdots O_2$, $O_1'\cdots C_2$, $O_2'\cdots C_2$ and $C_3'\cdots C_4$
0.00018	for $C_1'\cdots C_3$, $C_3'\cdots C_5$ and $C_1'\cdots C_5$
0.00030	for C–H, $O_1'\cdots C_4$, $O_1''\cdots C_5$ and $O_2''\cdots C_1$
0.00040	for $C_2'\cdots H$, $O_2'\cdots H$, $O_1''\cdots C_1$, $O_2''\cdots C_5$ and $C_1'''\cdots C_4$
0.00050	for $C_4'''\cdots C_5$

TABLE IV. q_C/q_O VALUES FOR METHYL METHACRYLATE

Feature			q_C/q_O Model					
Max.	Min.	q_O	I	II	III	IV	V	Wt.
1		10.43	1.030	1.004	1.015	0.992	1.045	1
	1	14.26	1.013	0.982	0.978	0.972	0.982	1
2		18.08	0.999	1.013	0.999	1.001	1.006	2
	2	24.72	0.983	0.996	0.992	1.021	0.992	1
3		29.23	0.975	1.004	0.989	1.016	0.987	2
	3	32.18	0.988	1.011	0.979	0.995	0.979	1
4		35.80	0.987	1.002	0.978	0.957	0.971	2
	4	39.52	0.992	0.995	0.998	0.942	0.975	2
5		41.75	1.029	1.007	—	0.958	—	1
	5	43.08	1.010	1.015	—	0.963	—	1
6		45.05	1.021	1.021	1.011	1.003	0.999	2
	6	49.00	1.031	1.004	1.005	1.010	1.020	1
7		57.03	0.995	0.999	1.007	0.988	0.993	2
	7	59.59	1.002	0.993	1.006	0.987	0.974	1
8		61.41	1.023	1.003	1.014	0.989	0.998	1
	8	66.52	1.015	0.992	0.995	1.015	0.993	1
9		71.10	1.009	0.997	1.005	1.019	0.985	1
	9	75.03	0.999	0.984	0.999	1.010	0.973	1
Wt. mean			1.003	1.002	0.997	0.989	0.991	
Av. dev.			0.014	0.010	0.014	0.026	0.018	

The radial distribution function for this molecule is calculated by the use of the following equation, (RD curve in Fig. 3):

$$rD_{(r)}=\sum_{q=1}^{q_{max}} I_{(q)O}\exp(-bq^2)\sin\frac{\pi}{10}qr$$

where $I_{(q)O}$ is the intensity read from the visual curve. The value b is determined by setting $\exp(-bq^2)=0.1$ at $q=80$. The curve shows that the first peak corresponds to the C–H, C_3–O_1, C_2–C_3, C_3–O_2 (in carboxyl) and O_2–C_4 (in methoxyl) distance, the second and the third to the nonbonding atom pairs, i. e., $C'\cdots H$, $O'_2\cdots H$, $O_1'\cdots O_2$, $O_1'\cdots C_2$, $O_2'\cdots C_2$, $C_1'\cdots C_3$, $C_1'\cdots O_2$ and $C_2''\cdots C_4$, the fourth to the $C_1''\cdots O_1$, and the fifth to the $C_1'''\cdots C_4$, respectively. Owing to the complex nature of the peaks, no attempt was made to resolve the distances. It may be noted, however, that the position determined from the most acceptable model agrees fairly well with the peaks observed in this radial distribution curve.

The results obtained from the examination of theoretical intensity curves and the visual ones are as follows.

Assumption: C–H=1.08 Å, C–H (in methyl group)=1.10 Å, C_1–C_2=1.36 Å, C_2–C_3=1.44 Å, C_3–O_1=1.22 Å, $\angle CCH=\angle C_1C_2C_3=\angle C_2C_3O_1=120°$, $\angle O_1C_3O_2=125°$ and $\angle O_2C_4H=109.5°$ (in methyl group).

Results: C_3–O_2 (in carboxyl)=1.36±0.02 Å, O_2–C_4 (in methoxyl)=1.46±0.02 Å, $\angle C_3O_2C_4=115\pm5°$ and out-of-plane angle of methyl group is 25±5°.

Methyl Methacrylate.—On account of the many parameters involved, a complete analysis on the molecular structure of methyl methacrylate may be very laborious. The present analysis was based upon the following assumption: C–H (in methylene group)=1.08 Å, C–H (in methyl group) =1.10 Å, the hydrogen atoms in two methyl groups have tetrahedral configuration, C_1–C_2= 1.36 Å, C_2–C_3=1.44 Å, C_3–O_1=1.22 Å, C_3–O_2 (in carboxyl)=1.36 Å, O_2–C_4 (in methoxyl)=1.46 Å, $\angle C_2C_1H=\angle C_1C_2C_3=\angle C_2C_3O_1=120°$, $\angle O_1C_3O_2=125°$, $\angle C_3O_2C_4=115°$ and the C_4 atom is inclined by 25° to the molecular plane. Therefore, in the models examined in this work, only two parameters are changed; the C_2–C_5 distance between C_5 atom of methyl group and α-carbon atom is varied from 1.45 to 1.54 Å in steps of 0.02 or 0.03 Å and the angle of $C_5C_2C_3$ from 110 to 130° in steps of 2 or 3°.

The theoretical intensity curves which are calculated through the above mentioned equation are carefully compared with the visual one. In Fig. 5, visual and theoretical intensity curves and also the radial distribution curve are shown. Curve B is the most acceptable one, and curves A and from C to E can be considered to show the limit of acceptability for the resolution and

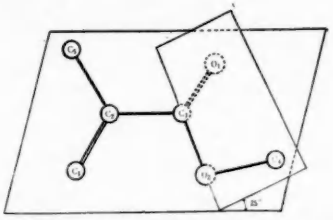

Fig. 4. Schematic model showing the skeleton and the numbering of atoms of methyl methacrylate. This model shows the *trans*-form.

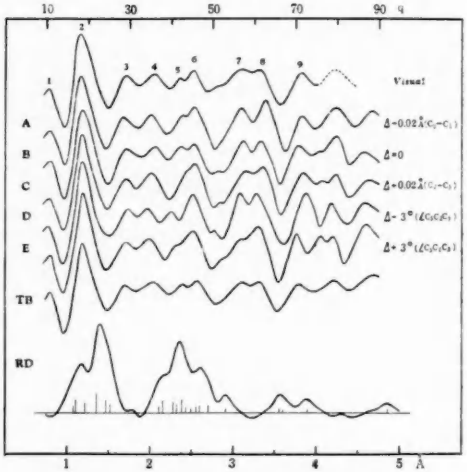

Fig. 5. Visual, theoretical intensity curves and radial distribution curve for methyl methacrylate. The notations on the right hand side of this figure show that the models deviate from the most probable one, for example, $\Delta=0$ is the most probable model which has the following parameters; C_1–H=1.08, C_4–H=C_5–H=1.10, C_1=C_2=1.36, C_2–C_3=1.44, C_3=O_1=1.22, C_3–O_2=1.36, O_2–C_4 =1.46 Å, $\angle C_2C_1H=\angle C_1C_2C_3=\angle C_2C_3O_1=120°$, $\angle C_2C_5H=\angle O_2C_4H=109.5°$, $\angle O_1C_3O_2=125°$, $\angle C_3O_2C_4=115°$ and C_4 atom is 25° out of plane configuration.

for the relative intensities of the 7th and 8th maxima and the feature of the 5th shelf. Curve TB shows the effect of thermal vibration. The thermal vibration factors examined in this case are listed in Table III. The q_C/q_O values of these models are summarized in Table IV. The weighing of these features followed the same consideration as in the case of methyl acrylate.

The radial distribution curve (RD curve in Fig. 5) is drawn according to the above equation. The value of b is determined by setting $\exp(-bq^2)=0.1$ at $q=90$. The curve shows that the positions determined from the most acceptable model agree

well with the peaks observed in this radial distribution curve.

The results obtained from the above analyses in this molecule are as follows.

Assumption: All parameters of the most probable model of methyl acrylate were assumed, and the C_5 atom in the methyl group was coplanar, H atoms in this group were of tetrahedral configuration and C_5–H bond lengths were 1.10 Å.

Results: C_2–C_5 = 1.52±0.02 Å and $\angle C_5C_2C_3$ = 129±3°

Discussion of the Results

The results obtained from electron diffraction investigation of acrylic acid generally agree with the corresponding bond lengths and valence angles of acrolein and acetic acid which were obtained by electron diffraction study by Sutton et al.[5] and by Brockway et al.[6] On the basis of the above reason, it was assumed that the skeletons of methyl acrylate and methyl methacrylate were of the same dimension as in the case of acrylic acid.

Unfortunately, no data have appeared which make possible the valid comparison of the C=C, C–C and C=O distances in these esters with those in other compounds. However, the configuration of the methyl group in methyl acrylate agrees with that of methyl acetate. The values for the $C_3O_2C_4$ angle (115±5°) and for the out-of-plane configuration (25±5°) obtained in this work do not differ significantly from the values reported for methyl acetate.

Regarding methyl methacrylate, the value of C_2–C_5 distance obtained here is comparable with the recent value obtained by Keidel and Bauer[7] in the case of toluene, and with the results of I'Haya's theoretical calculation on hyperconjugation[8] of the methyl group in ethylacetylene.

The author wishes to express his sincere thanks to Professor A. Kotera and Mr. M. Igarashi of Tokyo University of Education for their kind guidance and encouragement throughout this work. Thanks are also due to Dr. T. Takeshima of this university for his helpful advice.

Department of Chemistry
Faculty of Science
Ibaraki University, Mito

5) H. Mackel and L. E. Sutton, *Trans. Faraday Soc.*, **47**, 691 (1951).
6) J. Karle and L. O. Brockway, *J. Am. Chem. Soc.*, **66**, 574 (1944).
7) F. A. Keidel and S. H. Bauer, *J. Chem. Phys.*, **25**, 1218 (1956).
8) Y. I'Haya, This Bulletin, **28**, 369 (1955).

SHORT COMMUNICATIONS

The Glass Transition Temperatures of Various Kinds of Polyethylenes

By Kōji TANAKA

(Received August 18, 1959)

It is well known that various physical properties of polyethylene are considerably affected by the chain branching. According to C. A. Sperati et al.[1], for instance, short chain branching controls crystallinity, and long chain branching the viscoelastic properties of the molten polymer and the ultimate strength of the solid.

The author performed an experiment in order to know whether chain branching affects the glass transition temperature or not.

Samples used in this investigation are Marlex 50, Ziegler type polyethylene, and eight kinds of high-pressure polyethylene which are different in their molecular weights, melt index and numbers of short and long chain branchings. These high-pressure samples were provided by courtesy of E. I. du Pont de Nemours and Company. Marlex 50 and Ziegler were commercial polymers. In Table I are shown molecular parameters for these high-pressure polyethylenes. For Marlex 50 and Ziegler these data were not available hitherto, but since the number of short chain branchings was found for

1) C. A. Sperati, W. A. Franta and H. W. Starkweather, Jr., *J. Am. Chem. Soc.*, **75**, 6127 (1953).

the two materials in the paper by R. C. Rempel et al.[2], those were adopted for reference. These are 0.15 and 0.25 for Marlex 50 and Ziegler, respectively. Prior to a series of measurements these ten samples were sufficiently crystallized by thermal treatment.

TABLE I. MOLECULAR PARAMETERS[a] FOR HIGH-PRESSURE POLYETHYLENES

Sample	Melt index	$Mn \times 10^{-3}$	Nc[b]	Nw[c]
A	0.2	34	1.6	20
B	2.1	32	1.6	18
C	2.1	21	2.2	27
D	2.1	18	3.0	34
E	3.8	20	1.6	13
F	2.0	50	2.0	18
G	1.8	27	0.6	10
H	1.6	12	3.2	29

a) These data were determined at E. I. du Pont de Nemours and Company according to the method described in *J. Am. Chem. Soc.*, **75**, 6110 (1953).

b) Short chain branching index in CH_3 groups per 100 CH_2 groups.

c) Long chain weight average number of branch points per molecule[3].

Measurements were carried out by volume dilatometry[4]. As confining liquid mercury and absolute alcohol were used for the run above $-40°C$ and for that from $-70°C$ to room temperature, respectively. A Dewar vessel containing toluene was used as a bath. Cooling and heating of the bath were conducted at the rate of 0.3°C per min. by throwing dry ice and inserting nichrom wire into the bath.

Glass transition temperature, T_g, was determined from intersection of two straight lines on the volume-temperature curve and from discontinuity of the curve obtained by plotting the volume-temperature derivatives as a function of temperature.

Glass transition temperatures obtained from this experiment were plotted as a function of the short chain branching index (Fig. 1). From the figure it seems that the glass transition temperature of these samples lowers proportionally with the increase of the short chain branchings, though Marlex and Ziegler appear to deviate somewhat from this tendency. Then the relation between the glass

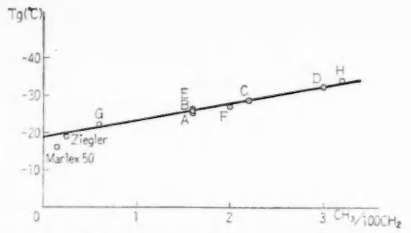

Fig. 1. Glass transition temperatures of various polyethylene samples different in their short chain branching index.

transition temperature and the short chain branching index of these high-pressure polyethylenes was led to the following equation:

$$T_g = -4.6\ \mathrm{Nc} - 18.7$$

On the other hand, long chain branching does not appear to affect the glass transition temperature so much as short chain branching does.

The author thanks Professor M. Takeda for many helpful suggestions and discussion.

Department of Chemistry
Tokyo College of Science
Shinjuku-ku, Tokyo

2) R. C. Rempel, H. E. Weaver, R. H. Sands and R. L. Miller, *J. Appl. Phys.*, **28**, 1082 (1957).

3) B. H. Zimm and W. H. Stockmayer, *J. Chem. Phys.*, **17**, 1301 (1949).

4) N. Bekkedahl, *J. Research Natl. Bur. Standards*, **42**, 145 (1949).

Studies on Organic Catalytic Reactions. I

By Ken-ichi WATANABE

(Received October 3, 1959)

It is interesting to study the application of metallic catalysts to new organic reactions beyond the customary catalytic reactions. Various reactions of organic compounds may be accelerated with the aid of catalysts and subsequently some new catalytic reactions are expected to be found. In this paper, general aspects of hydrolysis of aromatic nitriles and esters with nickel catalysts—mainly the Urushibara nickel catalyst[1]— are reported, and reactions of aromatic halogen compounds with the catalyst are also described.

When aromatic nitriles were refluxed with water in the presence of the catalyst, they were found to be hydrolyzed to the

1) Y. Urushibara and S. Nishimura, This Bulletin, **27**, 480 (1954).

TABLE I. HYDROLYSIS OF BENZONITRILE WITH URUSHIBARA NICKEL CATALYST

Benzonitrile g.	U-Ni-B g.	Solvent cc.	Time hr.	Products, g. Amide	Amine	acid	Remarks
5	4	Water 80	11	4.2 (73%)	0.4	+	
5	4	Ethanol 60	9	0.6 (11%)	4.0	+	
10	8	Ethanol 100	8	3.6 (19%)	3.6	+	Recovered 0.1 g.
10	8	Dioxane 100	12	4.0 (34%)	1.5	−	Recovered 0.4 g. White crystals m.p. 220°C

corresponding acid amides in fairly good yields even though the reaction medium was neutral to litmus. The hydrolysis was generally stopped at the amide stage and very small amounts of acids were obtained. Further hydrolysis of amides to acids could not be observed even when the amides were treated again with a newly prepared catalyst. Small quantities of nitriles were hydrogenated to amines by hydrogen absorbed on the nickel catalyst. Some factors, effective for the reaction, were examined in regard to the kind of catalyst, promoter or poison, solvent and duration of refluxing. In most of the reactions, the Urushibara nickel was used as the catalyst, and representative results of the experiments with benzonitrile are shown in Table I. Stabilized nickel catalysts (K. S. Y. Catalysts)[2] were also used in some experiments, and similar results could be observed.

Among the varieties of the Urushibara catalyst, U-Ni-B was the most advantageous for the hydrolysis; U-Ni-A[3], BA[4], AA[5] and U-Cu-B were not so admirable because some undesirable side reactions were induced. When precipitated nickel prepared from nickel chloride and zinc dust was used in place of the Urushibara catalyst, the product was found to be a complex of a primary amine and zinc, which can be decomposed to the amine by treating with alkali. Zinc powder by itself did not show any catalytic activity for hydrolysis.

As for the reaction solvents, water, ethanol, dioxane and *n*-butanol were used, and water was proved to be the most excellent of all as shown in Table I. A small quantity of thiophene or pyridine was added to the U-Ni-B catalyst in order to examine specific behavior as a promoter for the catalyst. However, they were of no use but rather gave an unfavorable effect.

The hydrolysis of the nitrile group was also observed in *p*-tolunitrile, *o*-nitrobenzonitrile and benzyl cyanide, yielding the appreciable amounts of the corresponding amides. On the contrary, hydrolysis of ethyl benzoate hardly proceeded with the same method, and benzoic acid could scarcely be obtained.

On the other hand, some aromatic halogen compounds were treated with the nickel catalyst in the same procedure mentioned above. Chlorobenzene, bromobenzene and iodobenzene were mainly dehalogenated to bezene along with a small quantity of biphenyl, although the reaction velocity of chlorobenzene was very slow compared with those of the others. When a small quantity of thiophene was added to the catalyst in the reaction of bromobenzene, alternative obscure reaction occurred yielding an unidentifiable oily product of a high boiling point. Reactions of nitro or amino derivatives of halogenobenzenes were more complicated. Among the reactions of this series, remarkable result was obtained with benzyl chloride. When benzyl chloride was refluxed with U-Ni-B in ethanol, a Wurtz type reaction was observed and bibenzyl was obtained in a good yield (above 70%). However, when the mixture was refluxed for a long time, the production of bibenzyl was accompanied with the formation of a highly boiling oil.

As the results of the studies on these catalytic reactions, it was found that amides are obtained from nitriles without acidic or alkaline hydrolysis, and that bibenzyl is obtained from benzyl chloride without sodium metal. These reactions are simple in procedure, and the yields of products are fairly good when the reactions are carried out under suitable conditions. The details of these experiments and discussion will be published in a following paper.

2) T. Yamanaka et al., *J. Sci. Res. Inst.*, **51**, 168 (1957); **52**, 143, 224 (1958).
3) Y. Urushibara, S. Nishimura and H. Uehara, This Bulletin, **28**, 446 (1955).
4) K. Hata, S. Taira and I. Motoyama, ibid., **31**, 776 (1958).
5) K. Hata, K. Watanabe and H. Watanabe, ibid., **32**, 6 (1959).

The author wishes to express his hearty thanks to Professor Kazuo Hata for his kind advice.

Department of Chemistry
Faculty of Science
Tokyo Metropolitan University
Setagaya-ku, Tokyo

The New Synthetic Method of β-Acetyl-butyrolactone

By Yoshihiko Nishizawa

(Received October 3, 1959)

B. R. Baker[1] has prepared β-acetyl-butyrolactone (II) from itaconic acid half ester or dimethyl methoxy-succinate. This method, however, gave a very poor yield and β-acetyl-butyrolactone (II) was only isolated as 2,4-dinitrophenylhydrazone derivative.

The present author found that β-acetyl-butyrolactone (II) is synthesized in a smooth way from diethyl acetyl-succinate[2] (I) according to the following equation[3].

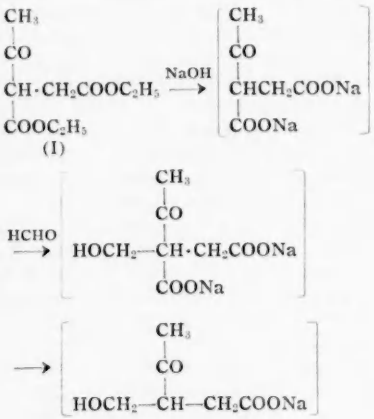

(I)

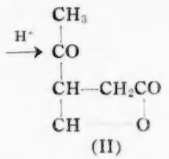

(II)

One hundred and eight grams (0.5 mol.) of diethyl acetyl-succinate (I) (b. p. 140~142°C/14 mmHg, n_D^{16} 1.4380) were added to 480 ml. of 10% sodium hydroxide aqueous solution at 0°C and left for twenty four hours at room temperature (ca. 15~20°C). After the oil was dissolved completely, the aqueous solution was neutralized with 30% sulfuric acid to pH 8~8.2 and then 20 g. of sodium bicarbonate and 54 ml. of 37% formaline were added. After the mixture was allowed to stand overnight at room temperature, acidified with 30% sulfuric acid and extracted continuously with ether. The ether layer was dried with anhydrous sodium sulfate and then ether was evaporated. The residual oil was distillated under the diminish pressure; yield, 28.0 g. (43.8%), b. p. 140~143°C/6 mmHg, n_D^{31} 1.4600.

Anal. Found: C, 55.98; H, 6.41. Calcd. for $C_6H_8O_3$: C, 56.24; H, 6.29%.

2,4-Dinitrophenylhydrazone; m. p. 191~192°C (recrystallized from acetic acid).

Anal. Found: C, 46.61; H, 3.70; N, 18.20. Calcd. for $C_{12}H_{12}O_6N_4$: C, 46.76; H, 3.92; N, 18.18%.

The 2,4-dinitrophenylhydrazone was soluble in sodium bicarbonate aqueous solution and the mixed melting point with the authentic 2,4-dinitrophenylhydrazone[1] was not depressed.

The author is much indebted to Mr. S. Kitamura for his earnest assistance and wishes to express his thanks to his coworkers for the microanalysis.

Sumitomo Chemical Co., Ltd.
Osaka Works
Konohana-ku, Osaka

1) B. R. Baker, *J. Org. Chem.*, **17**, 116 (1952).
2) C. Rach, *Ann.*, **231**, 35 (1886).
3) Y. Nishizawa, Japan. Pat., No. 254,740.